MEASUREMENTS OF THE NEUTRON ANGULAR FLUX SPECTRUM IN GRAPHITE

A.E. Profio, et al

General Dynamics
San Diego, California

October 1966

31

GENERAL ATOMIC

DIVISION OF GENERAL DYNAMICS

DASA Report No. 1933
GA-7470

MEASUREMENTS OF THE NEUTRON ANGULAR FLUX SPECTRUM IN GRAPHITE

ANNUAL REPORT

October 30, 1966

281

GENERAL ATOMIC

DIVISION OF

GENERAL DYNAMICS

JOHN JAY HOPKINS LABORATORY : PURE AND APPLIED SCIENCE

P.O. BOX 608, SAN DIEGO, CALIFORNIA 92112

DASA Report No.
GA-7470

MEASUREMENTS OF THE NEUTRON ANGULAR FLUX SPECTRUM IN GRAPHITE

ANNUAL REPORT

Work done by:

H. M. Antunez
J. H. Audas
G. K. Houghton
A. E. Profio
G. E. Rogers
J. L. Russell, Jr.
T. G. Williamson

Report written by:

A. E. Profio
H. M. Antunez
T. G. Williamson

Project 543
Defense Atomic Support Agency
Contract DA-49-146-XZ-482

October 30, 1966

ABSTRACT

Measurements of the neutron angular flux spectrum in graphite have been made to provide a standard of comparison for neutron penetration calculations. The configuration approximated a point, fission-like source in an infinite medium. The spectrum from 0.002 eV to 15 MeV was measured with an accuracy of ±10% to ±20%, and resolution of ≤10%, by the pulsed-source, time-of-flight method. The source spectrum and other characteristics were also measured. Spectra were obtained at angles from 0° to 60° and penetrations to 66 cm. In addition, dieaway measurements, indium subcadmium and epicadmium flux traverses, sulfur and aluminum threshold foil traverses, and a threshold foil spectrum measurement were made. Procedures, apparatus, and results are described in detail so that others can evaluate our results and use them to test transport codes and input approximations. Comparison of the time-of-flight data with a preliminary discrete-ordinates calculation indicates fairly good agreement except for detail in the carbon resonance region, where the flux oscillates strongly. Both calculations and experiment indicate the intermediate spectrum for $r > 20$ cm from the source is not $1/E$ as usually assumed. Low energy foil activation and time-of-flight results are consistent, but threshold foils give poor results.

CONTENTS

CONTENTS (Contd.)

LIST OF FIGURES

LIST OF FIGURES (Contd.)

LIST OF FIGURES (Contd.)

LIST OF TABLES

LIST OF TABLES (Contd.)

1. INTRODUCTION

The purpose of this research project was to measure the neutron angular flux spectrum in graphite, to provide a standard of comparison for neutron penetration calculations. The geometry was made very simple, approximating a point source in an infinite medium. The spectrum from 0.002 eV to 15 MeV was measured with good accuracy and energy resolution by the pulsed source, time-of-flight method. The source spectrum and other characteristics were measured to avoid any ambiguity in this regard. Procedures, apparatus, and results are reported in detail so that others may evaluate our results and use them to test transport codes and input approximations.

In addition to the time-of-flight measurements described in Section 2, we measured the thermal neutron flux dieaway and derived a mean emission time correction, which is discussed in Section 3. Spatial distributions of thermal, indium resonance, and fast neutron fluxes were measured with foils, and threshold foils were irradiated for comparison with the time-of-flight spectra. This work is reported in Section 4.

Although the research was primarily experimental, preliminary calculations were made as described in Section 5. Results are discussed and compared, and conclusions and recommendations given, in Section 6.

The target is discussed in more detail in Appendix A, and the tabulated time-of-flight spectra are listed in Appendix B.

2. TIME-OF-FLIGHT EXPERIMENT

2.1 PRINCIPLES OF THE TIME-OF-FLIGHT METHOD

In the time-of-flight method, the neutron energy and angular distribution are measured by extracting a collimated beam from the experimental assembly at the desired position and angle, and measuring the time-of-flight over a fixed, known distance (50 meters in this experiment). Time-zero is defined by pulsing the neutron source. The pulsed neutron source in our experiments is a depleted uranium target bombarded by 28-MeV electrons from the linear accelerator. The electrons generate bremsstrahlung, which in turn produces a broad spectrum of fast neutrons by the (γ, n) and (γ, F) reactions. Neutron emission is coincident with, and proportional to, the electron current pulse, and the length of the current pulse is always made small compared to the flight time of the fastest neutron detected. For measurements in a large experimental assembly, however, a small correction is made for the mean emission time, i.e., the average time for a source neutron to slow down and diffuse to the point where it enters the collimated beam to the detector.

The neutrons are detected in any one of three counters, depending on the energy. A proton-recoil organic liquid scintillator is used for high energies (0.5-15 MeV). A boron capture detector is used from 200 eV to 1.5 MeV. A bank of BF_3 counters is used below 200 eV. The arrival of the neutron is timed by a fast discriminator, and hence the speed and energy are measured with good resolution. However, to convert counting rate to flux it is necessary to divide by the neutron detection efficiency at that energy. The absolute efficiencies of our detectors have

been accurately measured and calculated, so that it is possible to report angular fluxes with good precision. All measurements are normalized to a standard source intensity by activation of monitor foils in a reproducible geometry.

Two graphite assemblies were investigated in this experiment. The fast and intermediate spectrum measurements by the time-of-flight method were made in a 152 cm x 152 cm x 132 cm block, which allowed for measurements at angles up to 60° to the radius vector by displacement of the stack as explained in the following section. Thermal spectrum measurements and foil activations were made in a smaller block, 112 cm x 112 cm x 132 cm. Since the beam was always extracted in the horizontal plane (at 0° or 90° to the long axis) this size was sufficient, and it had a shorter dieaway time constant than the larger assembly.

2.2 THE FAST SPECTRUM ASSEMBLY

Measurements of the neutron angular flux spectrum from 200 eV to 15 MeV were made in the graphite assembly illustrated in Fig. 2.1. The assembly was designed to be effectively infinite, i.e., large enough that the measured flux was insensitive to the location of the boundaries. The measured flux can thus be compared with one-dimensional or infinite-medium calculations. The criterion for effectively infinite behavior was to locate the target (source) and measurement points some three mean free paths from the nearest boundary. In Fig. 2.2 the total mean free path of graphite at density $\rho = 1.64$ g/cm^3 is plotted against energy. The largest mean free path is about 20 cm and it approaches a constant 2.5 cm at lower energies. In the configuration of Fig. 2.1 the target was located 56 cm from the edge, which was believed to be acceptable. The measurement points, as we shall see later, were at least 66 cm from the sides and top, and all, except the last 6° measurement position, were more than 46 cm from the end of the block.

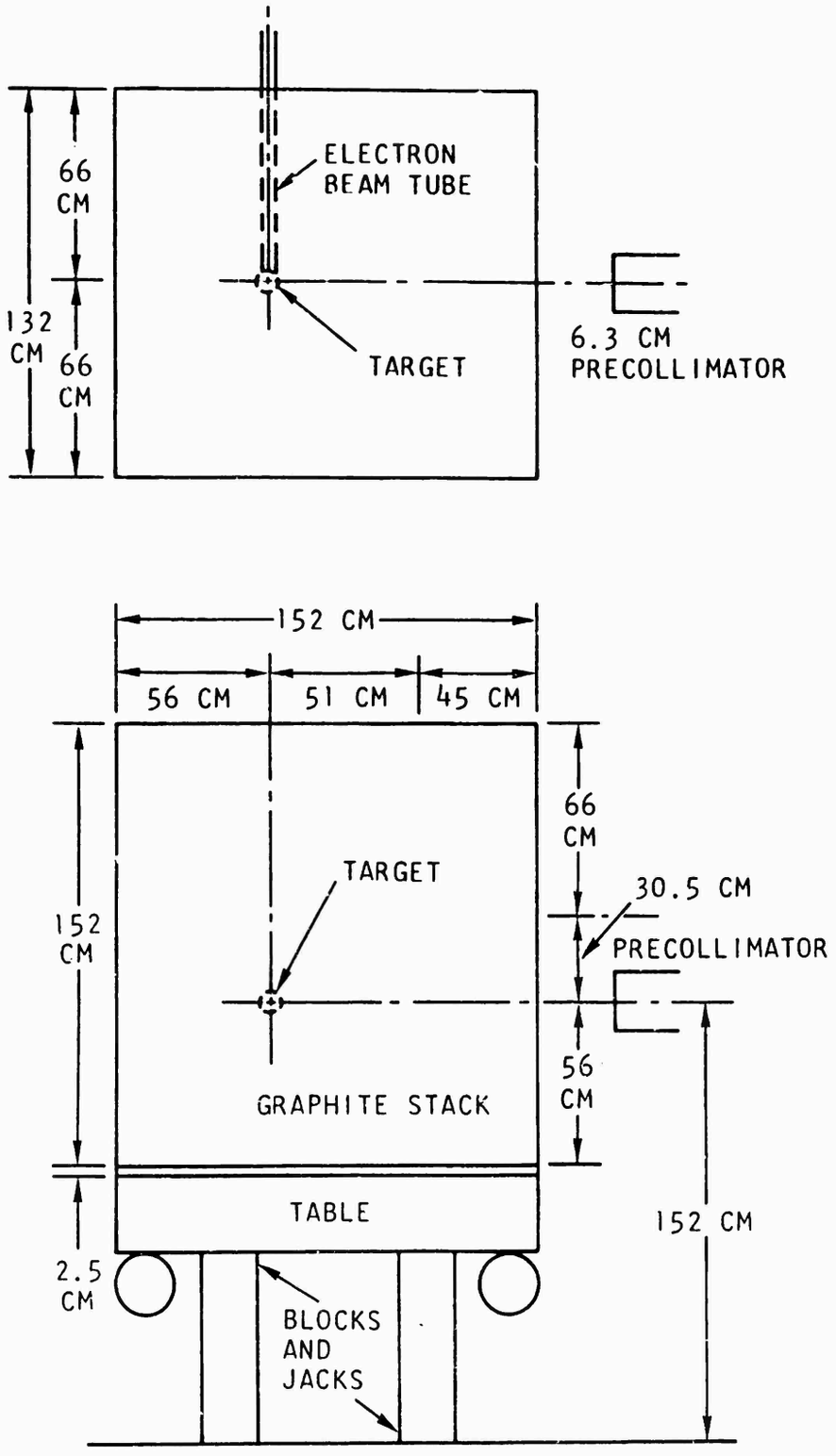

Fig. 2.1--Dimensions of the graphite fast spectrum assembly

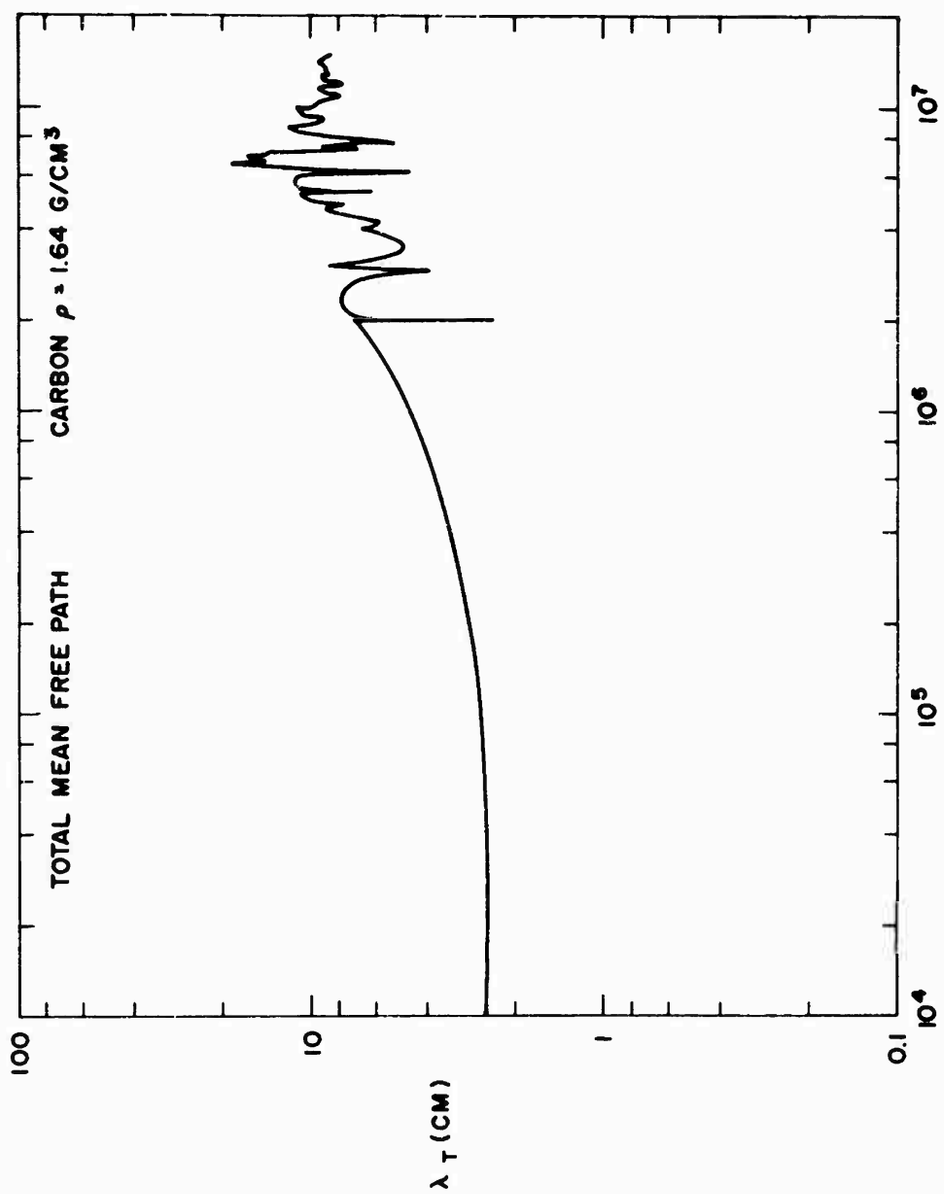

Fig. 2.2--Total mean free path in graphite

As a further aid to the design, the fast neutron angular flux spectrum in spherical geometry was obtained from P_3, S_{16} GAPLSN[1] calculations. Effective cross sections for 10 energy groups from 0.8 to 14.9 MeV were obtained from an infinite-medium GAM-II[2] calculations. For these preliminary calculations the 3.81-cm radius target was centered in a 7.62-cm radius cavity. The calculated angular flux in a 37.62-cm radius sphere is given in Fig. 2.3, and in a 52.62-cm radius sphere in Fig. 2.4. The curves are labeled by the nominal penetration in graphite (15, 30 or 45 cm), and the angle to the radius vector. The spectrum at 30 cm increases only by 30% or less upon adding the 15 cm of graphite, which implies that even less than three mean free paths is probably sufficient for infinite medium conditions. The 0^o flux, which is mostly uncollided, is unaffected by the additional material, indicating that 0^o measurements could be made as close to the boundary as desired.

The magnitude of the calculated fluxes when compared to earlier measurements in CH_2[3] indicated that no difficulty should be experienced in making measurements to a 45-cm penetration in graphite. Actually, one 0^o measurement was made at 61 cm. The relatively small change in flux at 30 cm, with and without the additional graphite, implied that the much smaller perturbation due to a probe hole of reasonable size should be acceptable, at least for energies above 0.8 MeV. The earlier measurements in CH_2 were made on the surface with our standard 6.3-cm diameter collimator. To maintain a reasonable counting rate at equal attenuations, we decided to use this collimator for the fast and intermediate spectrum measurements. The collimation requires a 7.62-cm diameter hole for extracting a neutron beam from the interior of an assembly. In the thermal neutron spectrum measurements a smaller collimator and a 3.81-cm diameter hole were used.

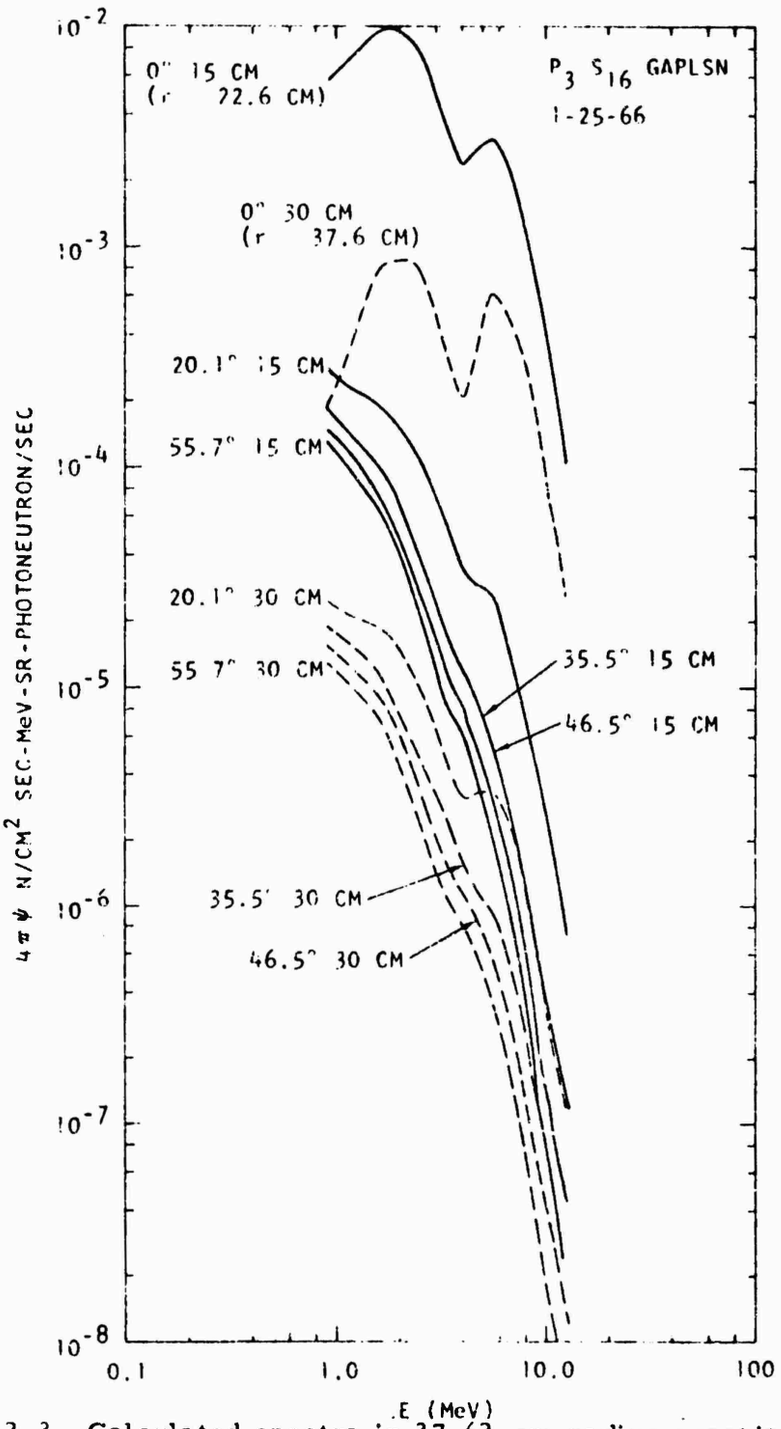

Fig. 2.3--Calculated spectra in 37.62-cm radius graphite sphere

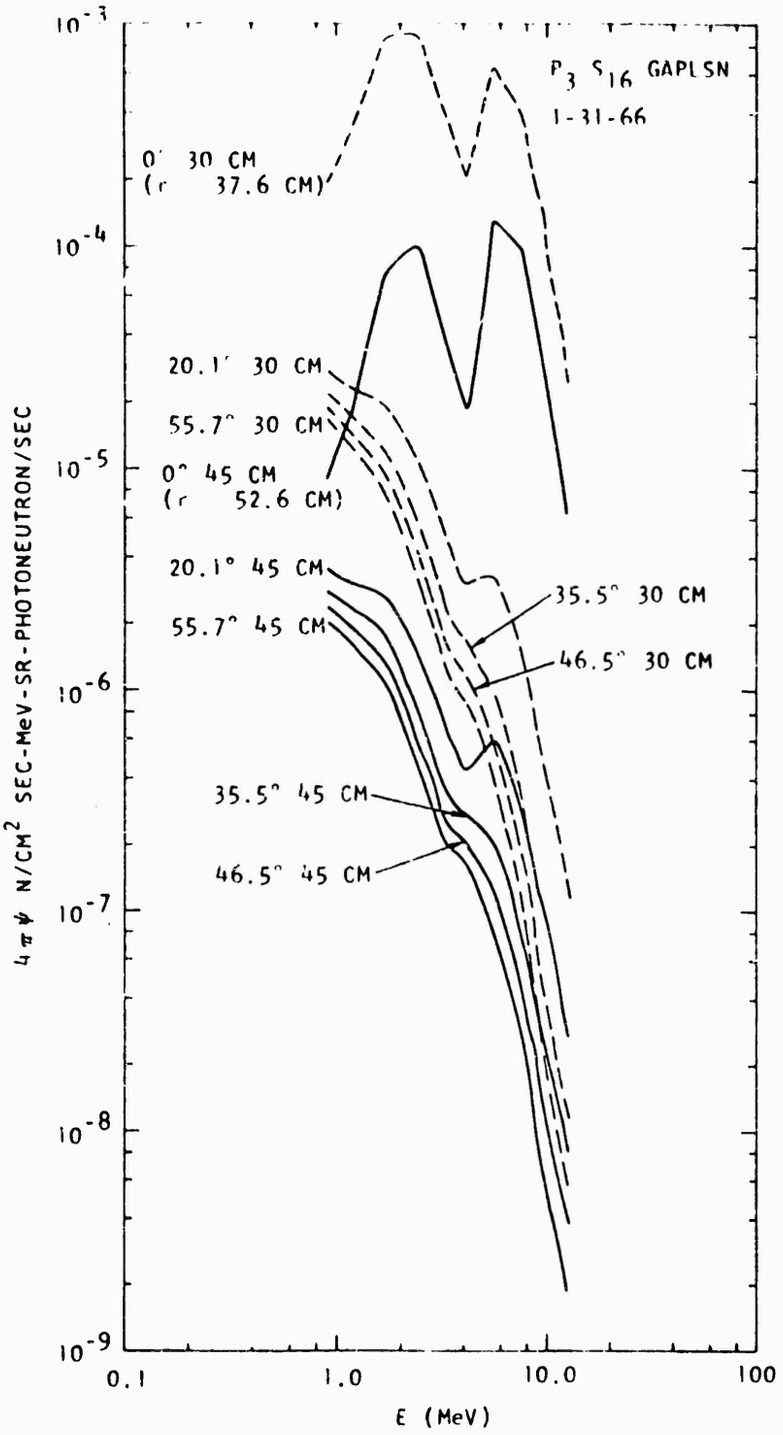

Fig. 2.4--Calculated spectra in 52.62-cm radius graphite sphere

The graphite stack was made of machined 4.000 in. x 4,000 in. (10.16 cm x 10.16 cm) stringers and it was convenient to build on this module in the vertical dimension. The angular distribution was to be measured over several angles from 0^{o} to 60^{o}, and the spatial distribution at suitable intervals up to at least 45 cm penetration. Although at one time the target was to be located in a 7.62-cm radius spherical cavity, we later decided to make the air gap smaller and centered the target in a 4.45 cm radius cavity. The angles and radii measured are shown in Fig. 2.5. From the results in Appendix A, spherical symmetry could be assumed (isotropic target and infinite medium), hence the off-zero angular measurements were made by lowering the entire graphite stack past the fixed precollimator (Fig. 2.1) in 10.16-cm increments. This required bending the electron beam downward a few degrees and tilting the target slightly for alignment on the beam. The assembly was aligned on the collimator axis by a transit and cross hairs on the precollimator and 16-meter station window of the flight path, and by plumb lines.

About 22,000 kg of reactor-grade graphite were borrowed for the experiment. The measured density was 1.65 ± 0.01 g/cm^3. The results of a spectroscopic analysis (General Atomic samples 15537 and 15538) are given in Table 2.1. Activation analysis for oxygen gave 580 ± 40 ppm (General Atomic service order 5672, April 12, 1966). Gravimetric analysis for hydrogen (General Atomic chemistry department) revealed 10 ppm. Although these impurities should have very little effect on the spectrum, we decided to bake out all the graphite to remove any excessive moisture which had not been detected in the analysis of samples. After baking a sample at 100^{o}C for four hours the hydrogen content was reduced to 6 ppm, and after 24 hours it was 2-3 ppm. The graphite stringers were baked in batches for 24 hours at over 100^{o}C. The graphite does absorb a small amount of moisture from the air, since it is not practical to hermetically seal the stack. This should have little effect on the neutronics, but could be included in calculations if desired.

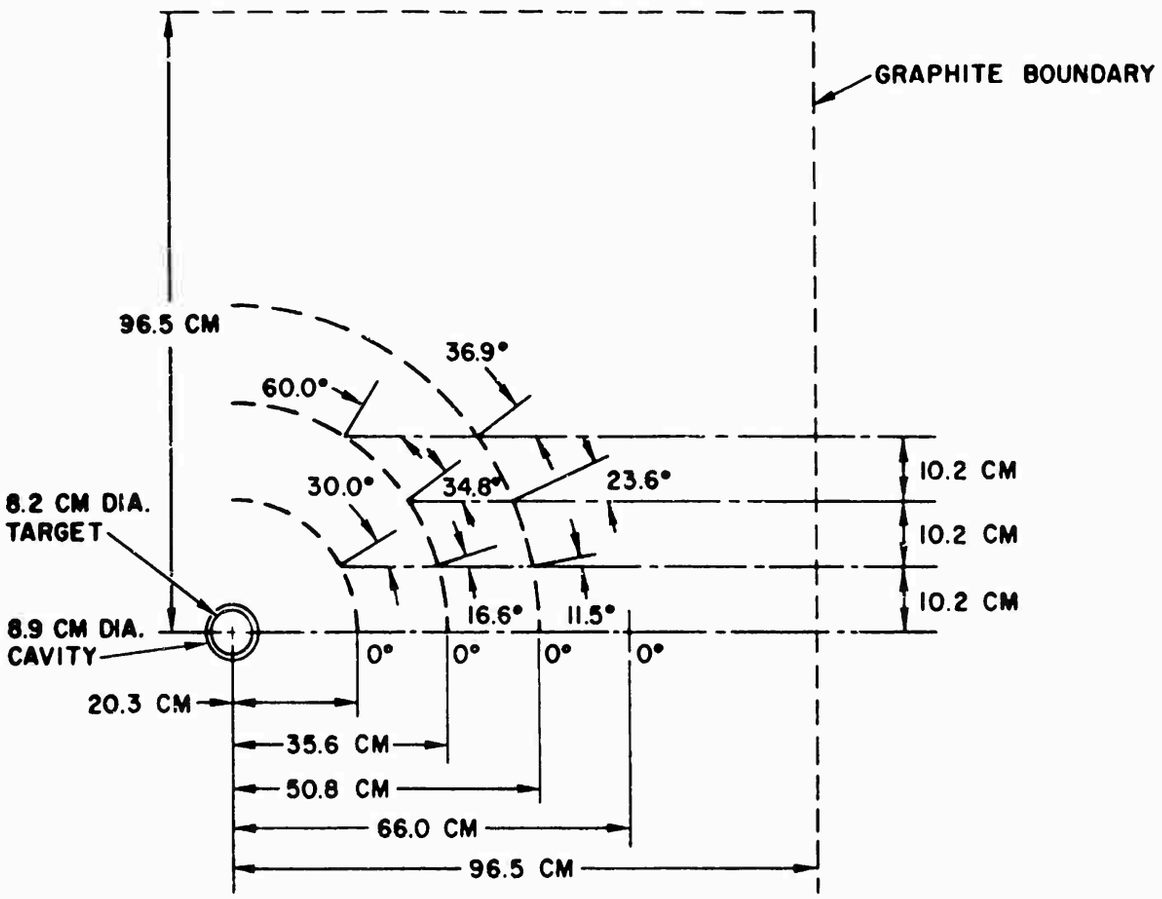

Fig. 2.5--Angles and radii of measurements

Table 2. 1

SPECTROSCOPIC ANALYSIS OF GRAPHITE (ppm)

Ag	< 1	Mo	< 10
Al	< 4	Na	< 1
As	< 40	Nb	< 100
Au	< 5	Ni	< 8
B	< 0.5	P	< 100
Ba	< 1	Pb	< 40
Be	< 1	Pd	< 10
Bi	< 4	Pt	< 6
Ca	< 10	Rb	< 2
Cd	< 20	Rh	< 20
Co	< 10	Ru	< 10
Cr	< 60	Sb	< 10
Ce	< 10	Si	< 8
Cu	< 100	Sn	< 4
Fe	< 6	Sr	< 10
Ga	< 6	Ta	< 60
Ge	< 40	Te	< 8
Hf	< 40	Th	< 10
Hg	< 8	Ti	< 4
In	< 20	Tl	< 40
Ir	< 40	V	< 4
K	< 1	W	< 60
Li	< 1	Zn	< 6
Mg	< 1	Zr	< 1
Mn	< 2		

Figure 2.6 is a cutaway drawing of the graphite stack with the target in place and the probe hole opened for a 0^{o} measurement. The drawing indicates the stacking only schematically, since 30.5 cm to 91.4 cm long stringers were used, and joints were staggered in more than one direction to eliminate streaming cracks. In the most critical area, the neutron beam extraction probe holes, alternate rows of stringers were stacked horizontally and vertically. Since the stringers are machined to a flatness and straightness tolerance of 0.0127 cm, and since the only possible opening is at the intersection of the horizontal and vertical joints, streaming should be negligible. The top of the probe-area graphite assembly was bridged with long graphite stringers to enable the probe area graphite to be removed without having to restack a major portion of the pile. This left a slight gap, estimated at 0.05 cm average; however, it was located well above the measurement points and should not affect the results.

The different radii and corresponding angles of measurement were reached by adding or removing graphite plugs machined to the proper angles and lengths. The plugs are 7.62 cm in diameter and fit quite snugly into the probe hole. In one measurement, the innermost 30.5-cm of the probe hole was fitted with graphite sleeves stopping the diameter down to 3.81 cm, to test for probe hole perturbation. Figure 2.7 is a photograph of the probe area graphite, spaced to show the construction, with a selection of plugs in the foreground. The four columns on the left do not have plugs. All but one stringer in each column is solid. One stringer with a 7.62-cm diameter hole in the proper location is moved about to extend the probe hole to the surface. With the plug and stringer arrangement, there are no holes left other than the one needed for the neutron beam extraction in that particular measurement.

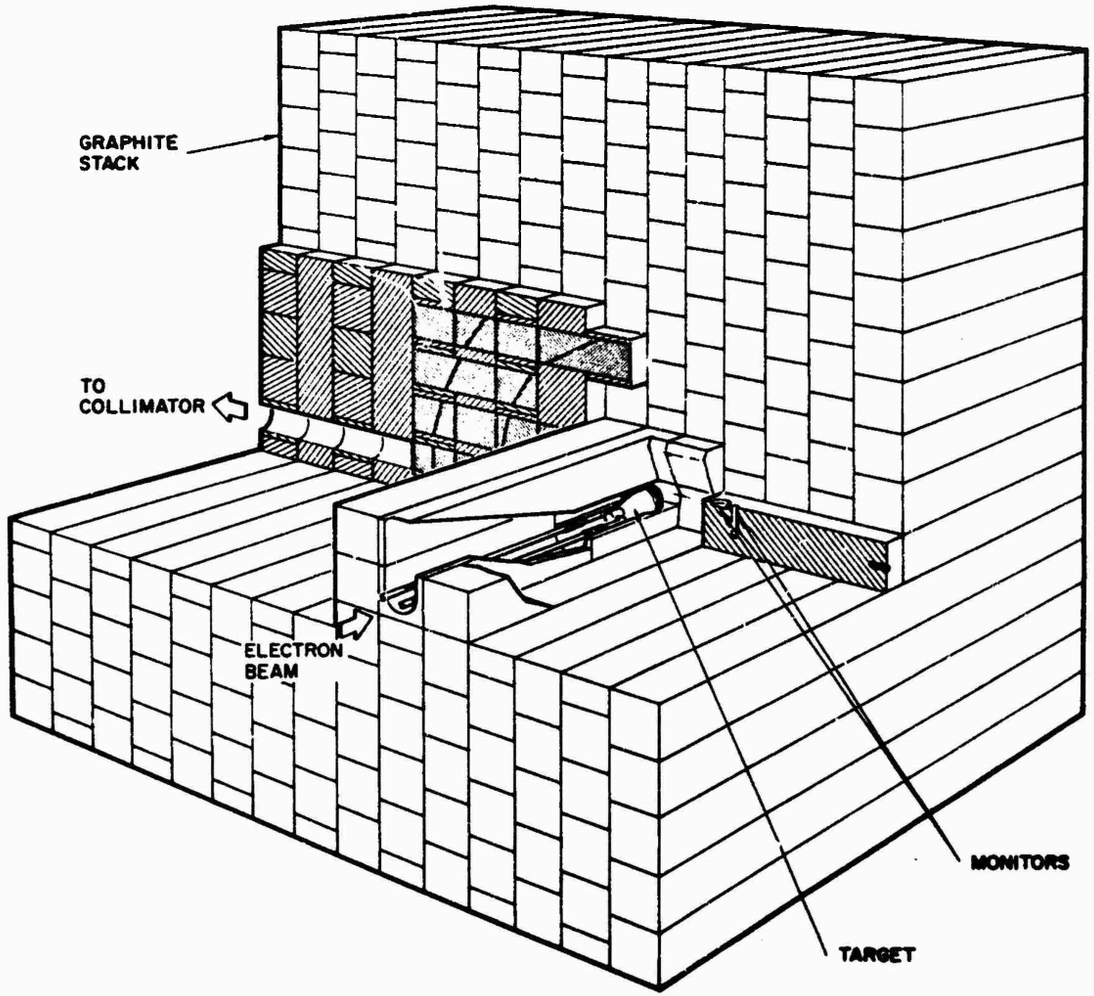

Fig. 2.6--Cutaway view of the graphite fast spectrum assembly

Fig. 2.7--Graphite probe hole assembly

The water-cooled, depleted uranium target was located in the 8.9-cm diameter cavity as shown in Fig. 2.8. One side of the stringer containing the cavity has been moved aside to permit the target sphere to be seen. The target was fitted with inlet and outlet water tubes long enough to extend outside the stack, where they made a right-angle bend and connected to the coolant water hoses. The target is completely welded except for one brazed joint at the snout, minimizing the possibility of water leakage into the graphite. The target was vacuum tested and water pressure and flow tested before use. As a further precaution against wetting, the target was bagged in a thin polyethylene film. The water circulating system was equipped with low-level and low-flow interlocks to shut down the Linac and the water pump in case of trouble. An electrical conductivity leak detector was installed under the target and inside the bag to sound an alarm in case of water leakage. The leak detector consisted of a strip of absorbent paper with two copper ribbons taped to one side. Insulated leads were taken to a remote amplifier, relay, and bell assembly designed and built by P. L. Phelps of the Linac electronics staff. A single drop of water, or anything which reduces the resistance across the ribbons to less than 60,000 ohms, is sufficient to trip the alarm. Fortunately, no leakage was experienced in the entire experiment.

The 28-MeV electron beam from the linear accelerator was brought through a 0.005-cm thick stainless steel window brazed to the end of a 3.18-cm diameter tube sealed to the Linac vacuum system. The window was cooled by a stream of dry compressed air. The beam then traveled about 23 cm through air to the bottom of the reentrant hole in the target. The beam was deflected, both horizontally and vertically, by electromagnets, and focused by magnetic quadrupole lenses. To monitor the position and size of the electron beam, we painted the target opening with a fluorescent material, and viewed the beam spot glow

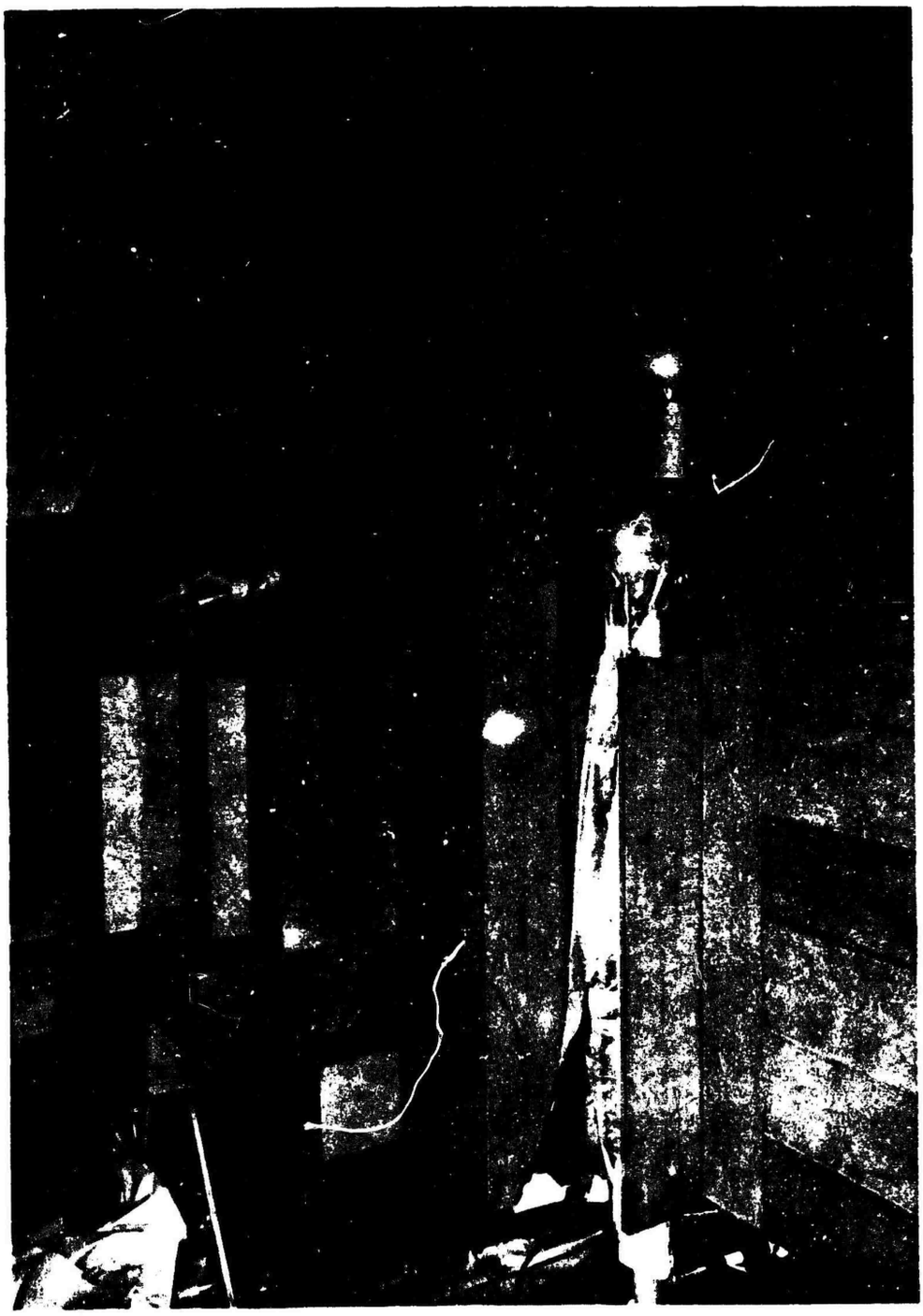

Fig. 2.8--Target in graphite

with a closed-circuit TV camera and mirror. A small light bulb with rheostat control was installed to provide enough light for initial focusing of the camera. The graphite was cut away just enough to clear the water tubes and electron beam tube, but this provided a sufficient opening for the TV camera sight line. Figure 2.9 is a photograph of the fast spectrum assembly from the Linac side, showing the support table with its electrically-powered jacks and the electron beam tube and target water lines. The occasional damaged graphite stringers visible were used only at the surface.

The Linac operator observed on an oscilloscope the pulsed current from the electrically-insulated target. However, this current is related in an unknown way to the neutron output, because of variable resistance to ground (e.g., in the water lines), and drifts in spot position and beam energy. Thus the integrated target current, in this experiment, may not give a reliable normalization to a standard source intensity from run to run. Instead, we irradiated a 1.5-in. (3.81 cm) diameter by 0.375-in. (0.952 cm) thick standard sulfur pellet (supplied and beta-counted by E.G.G., Inc., Goleta, California) and a 1.59-cm diameter by 3.81-cm long aluminum rod, in the monitor stringer shown in Fig. 2.6. The sulfur pellet was held in a hole 1.27-cm deep and 3.18-cm from the center to end of the stringer; the center of the sulfur was 19.1 cm from the center of the target. The aluminum rod was held in a hole 7.32-cm deep and 6.40-cm from the center to the end; the center of the aluminum rod was 21.9 cm from the center of the target. The measurements were reduced to a standard intensity as given by the sulfur pellet, while the aluminum activity served as a check.

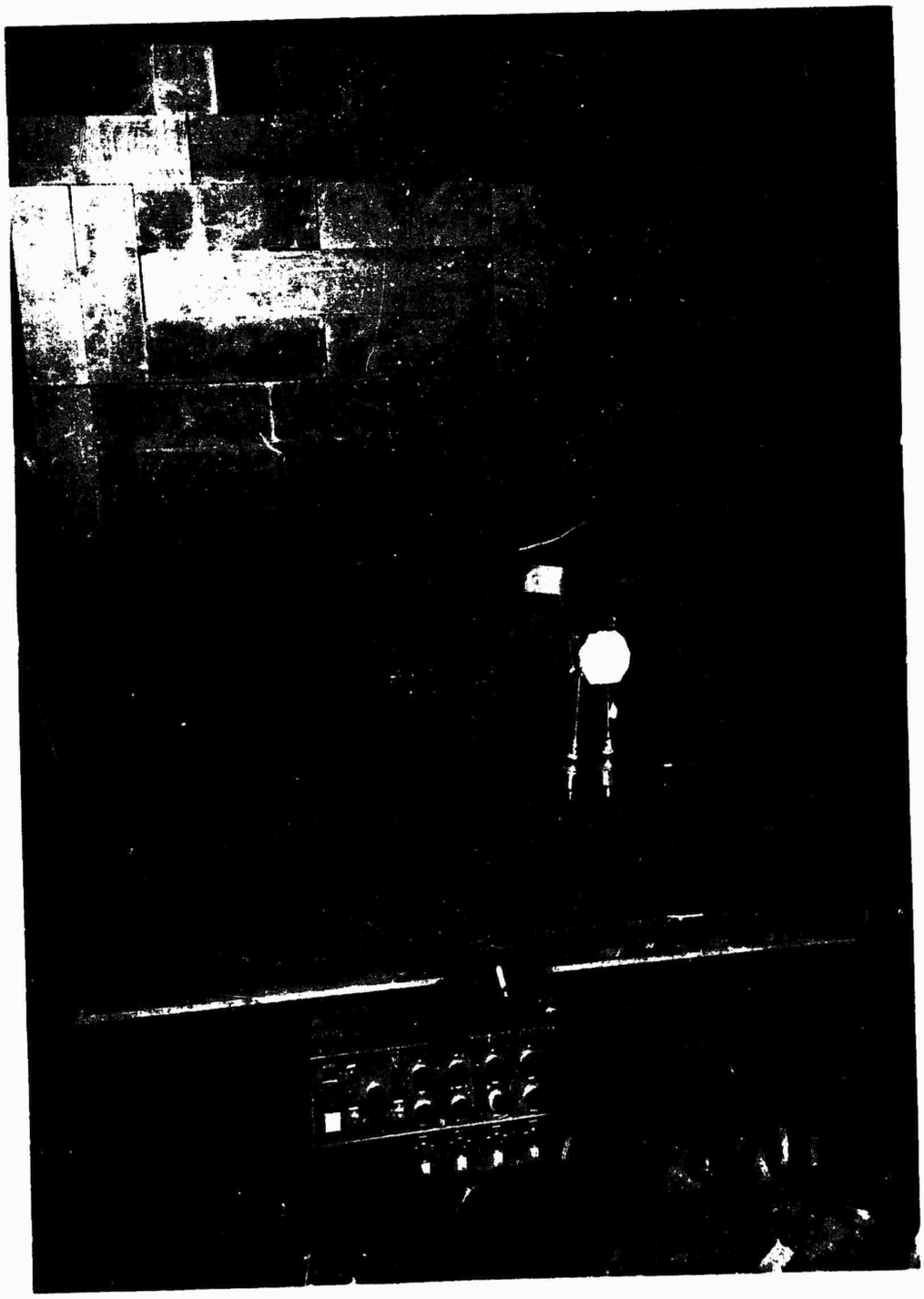

Fig. 2.9--Fast spectrum assembly

2.3 THE THERMAL SPECTRUM ASSEMBLY

Measurements of the neutron angular flux spectrom from 0.002 to 200 eV were made in the graphite assembly shown in Fig. 2.10. Foil flux plots, threshold foil irradiations, and thermal neutron flux dieaway experiments were also made in this assembly. Since the low energy flux should be nearly isotropic, measurements were made in the horizontal plane only at 0° and 90° to the long axis of the stack, as seen in Fig. 2.10. Since we wanted to measure at the same radii as in the fast spectrum experiment, and wanted to maintain the target and monitors in approximately the same geometry, the length of the stack was left at 152 cm. However, a truly infinite medium could not be achieved in the unpoisoned graphite, where the slowing down length to indium resonance is about 43 cm and the diffusion length about 50 cm. Furthermore, to achieve good energy resolution, we had to reduce the thermal neutron dieaway time constant to about 2000 μsec by making the transverse dimension 112 cm. The target was located symmetrically and since most so-called infinite-medium calculations can include a buckling factor, truly infinite medium conditions were considered not to be essential.

Part of the graphite from the fast spectrum assembly was restacked into the thermal spectrum assembly, recut as necessary. Alternate layers were criss-crossed. The sixth layer contained the target in its cavity, the special pieces for the water tubes, electron beam tube, and TV viewing space, the monitor foil stringer, and the stringers with 3.81-cm diameter probe holes. Holes not needed for a particular measurement were filled with closely fitting graphite plugs, usually 15.2 cm long. Figure 2.11 is a photograph of the graphite for the sixth layer, except for the target assembly stringers, as arranged for the 0° measurements. The plugs shown were used in the indium flux plots and have a small depression in the end to hold the foil. In the time-of-flight experiment, plugs were inserted to make measurements at 20.3 cm,

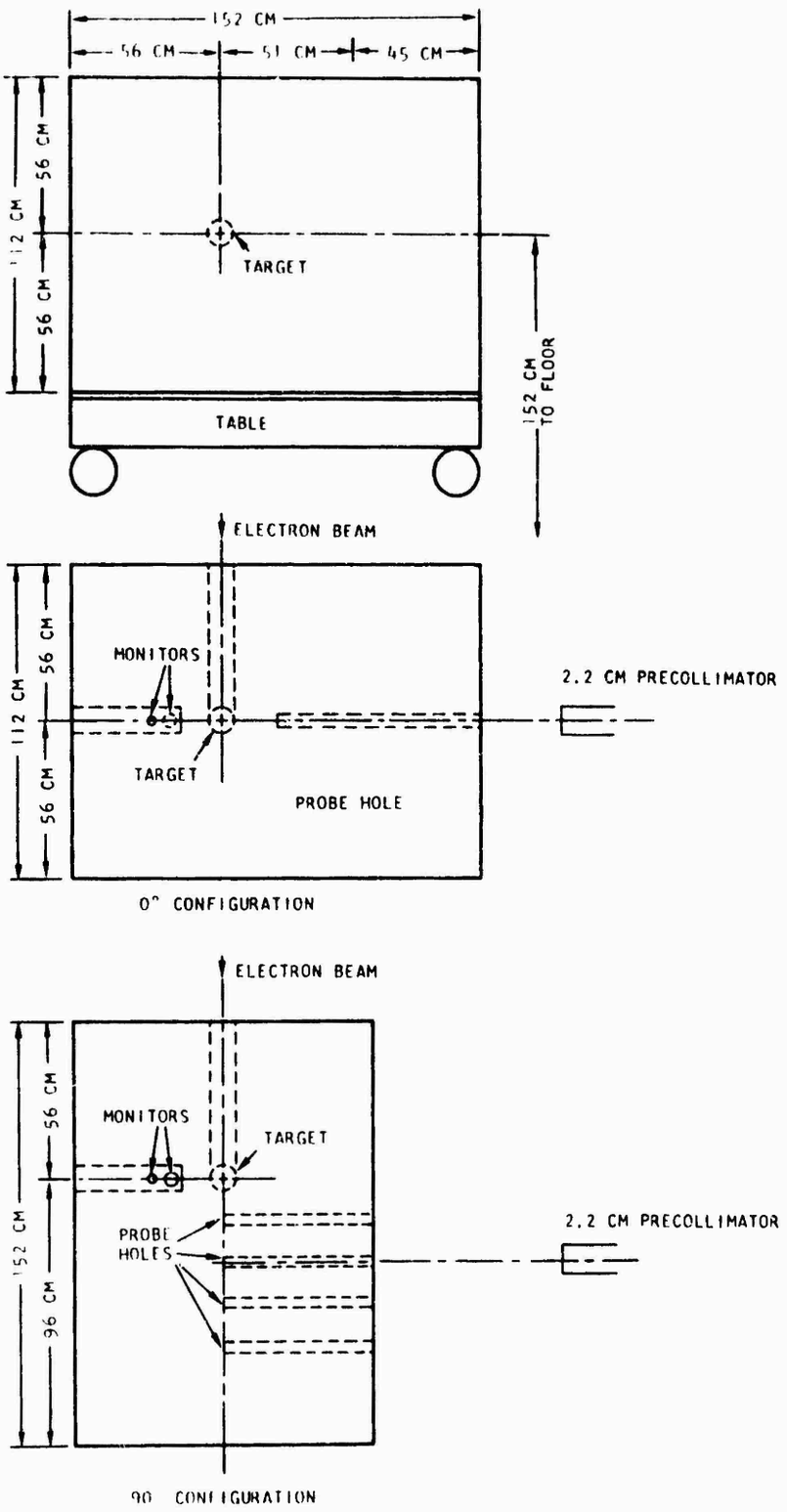

Fig. 2.10--Dimensions of the thermal spectrum assembly

Fig. 2.11--Sixth layer, 0^{o} measurements

35.6 cm, 50.8 cm, or 66.0 cm from the center of the target. The arrangement for a 90° measurement at 20.3 cm from the center of the target, on the centerline, is shown in Fig. 2.12. To make measurements at the other distances the stringer with the hole was exchanged with the appropriate solid stringer.

The thermal neutron boundary conditions were defined by covering the stack with 0.32 cm of borated polyethylene and 0.051 cm of cadmium. The new universal-motion table was used for this assembly, with the graphite stacked on a bed consisting of a 1.27-cm thick sheet of aluminum, the cadmium, the borated polyethylene, and a 0.32-cm thick sheet of aluminum. The final assembly, seen from the side opposite the Linac, is shown in Fig. 2.13.

2.4 THE PULSED NEUTRON SOURCE

The pulsed neutron source consists of a nominal 3-in. (7.6 cm) diameter depleted uranium target, water-cooled, irradiated by the pulsed electron beam from the General Atomic three-section L-band linear accelerator. Since the target was developed for use on several projects, it has been described in a separate report, which is included as Appendix A. The linear accelerator facility is shown in Fig. 2.14, and general characteristics of the accelerator are summarized in Table 2.2.

Typical accelerator pulse conditions were 28 MeV, 0.02 μsec pulse width, 360 pps, and peak pulse currents up to ~ 1 ampere in the fast spectrum measurements with the liquid scintillation detectors. For the intermediate (200 eV--1.8 MeV) spectrum measurements with the boron capture detector, the repetition rate was reduced to 180 pps and the pulse width increased to 0.05 or 0.1 μsec. However, the photomultiplier tube (and

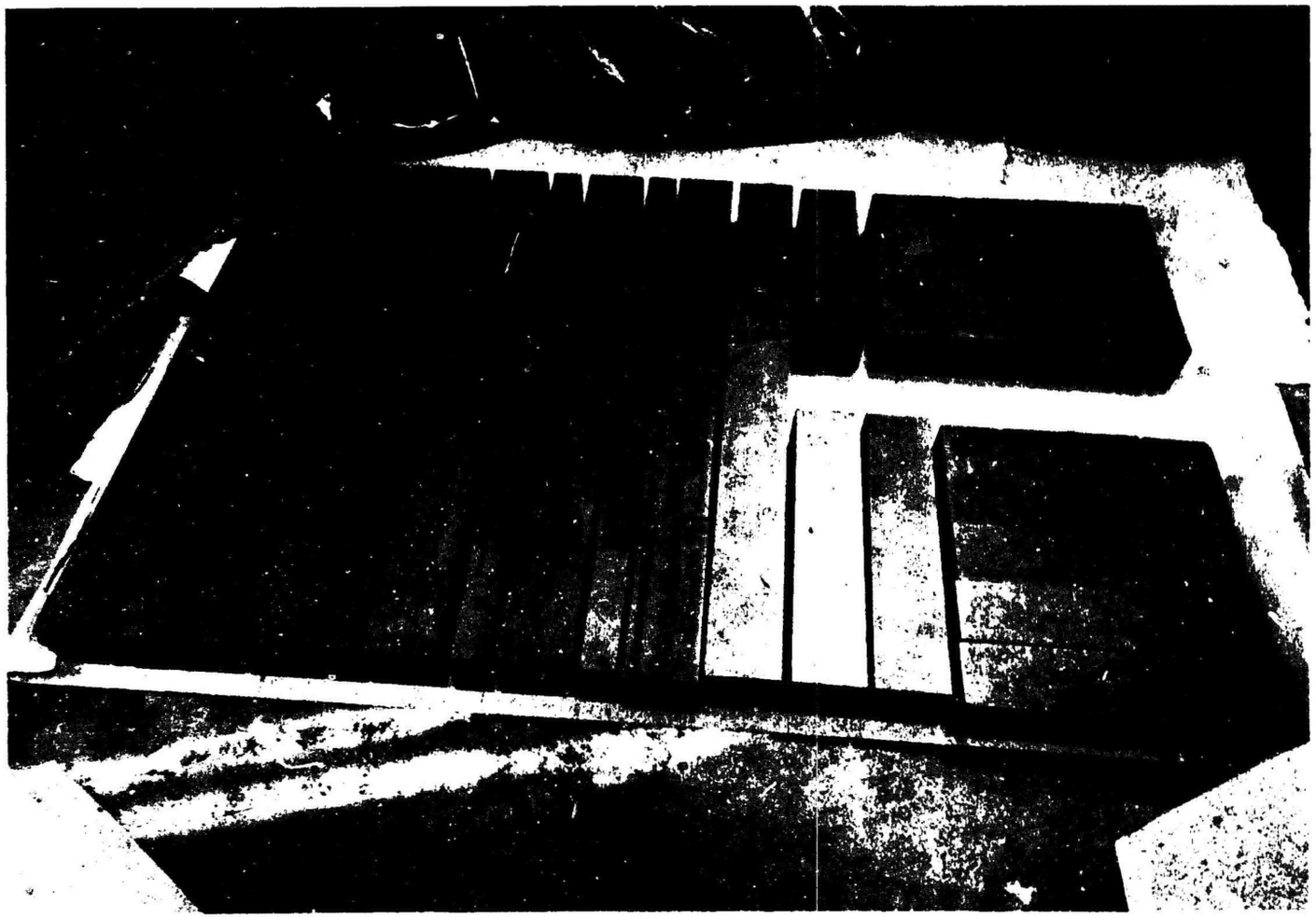

Fig. 2.12--Sixth layer, 90° measurements

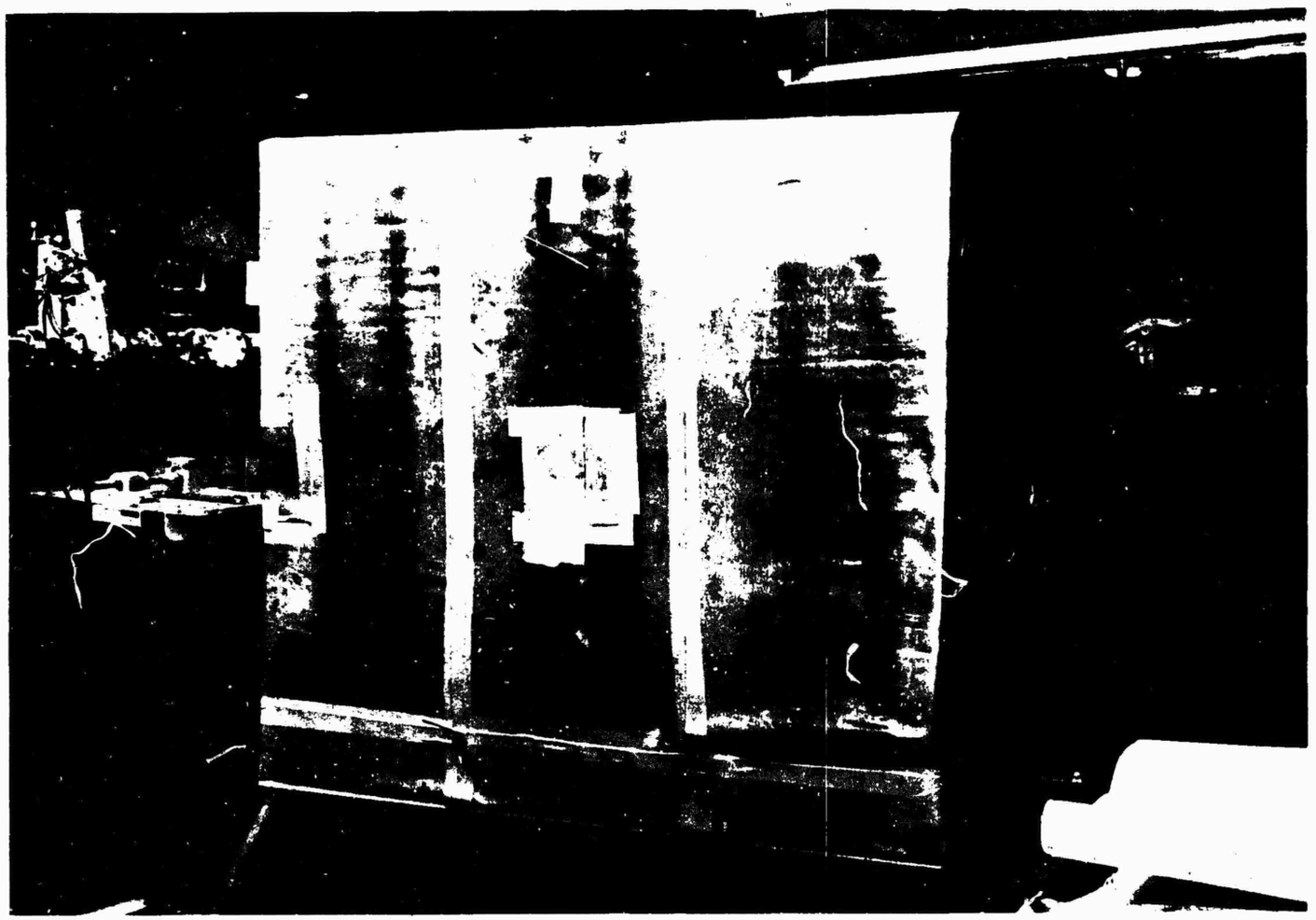

Fig. 2.13--Thermal spectrum assembly

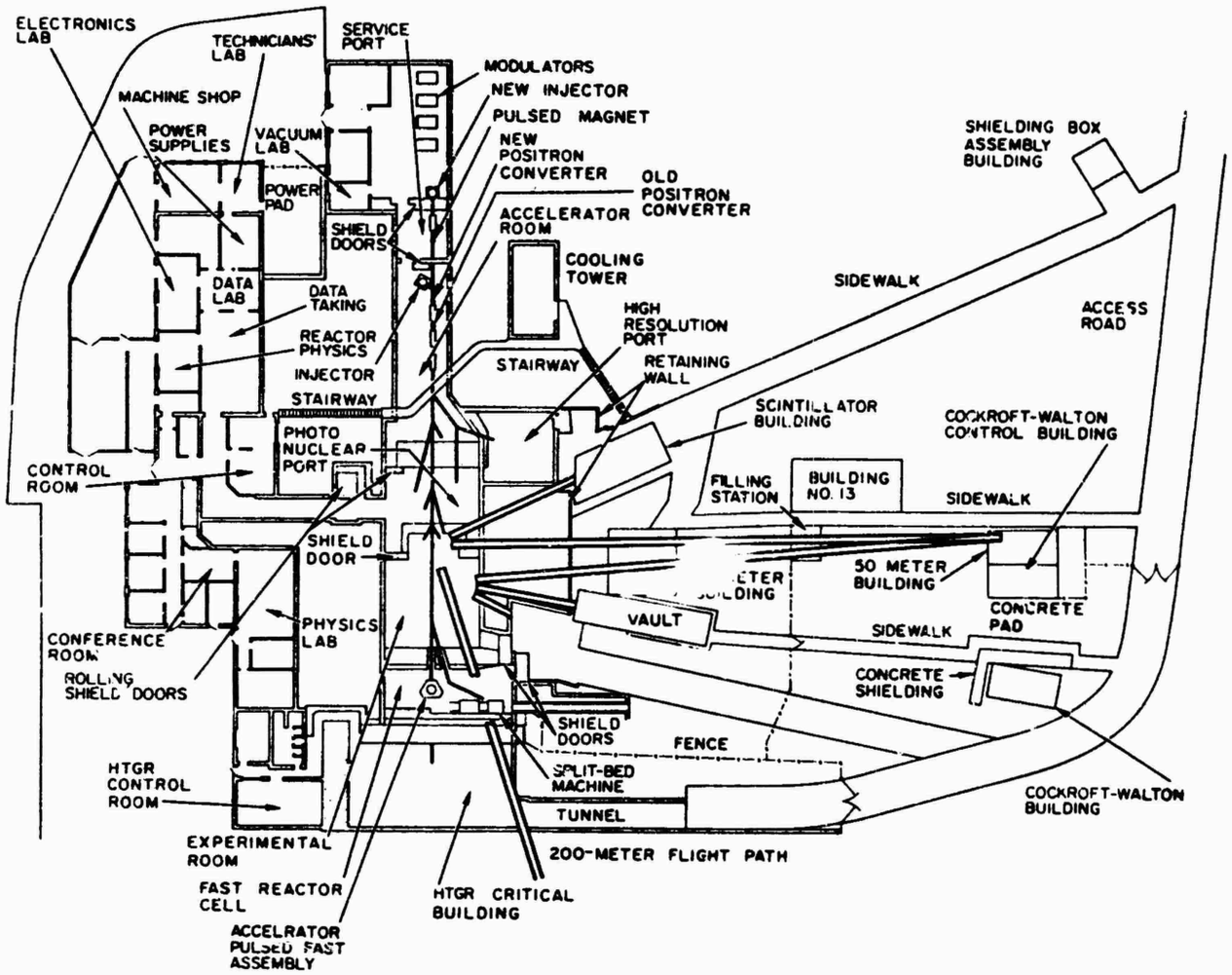

Fig. 2.14--General Atomic Linear Accelerator Facility

Table 2.2

ELECTRON LINEAR ACCELERATOR, 45 MeV L-BAND

OPERATING CHARACTERISTICS

Microwave frequency, Mc	1300
Number of accelerator waveguides	3
Energy range, Mev	1 to 45
Beam energy at maximum efficiency, Mev	25
Peak beam current at maximum efficiency, ma	500-700
Rated average power, kw:	
At 8 Mev	4
At 20 Mev	12
At 25 Mev	13.6
At 30 Mev	12
At 40 Mev	4
Maximum peak beam current, ma (pulses longer than 0.5 μsec	700
Maximum peak beam current, ma (pulses shorter than 0.5 μsec	2000
Beam pulse lengths, μsec	0.01 to 4.5
Pulse repetition rates per second:	
At 5 μsec	1, 7.5, 15, 30, 60, 120, 180
At 2.5 μsec	360
At 0.5 μsec and shorter	720
Energy spectrum, ΔE/E full width, half maximum	~3%

OUTPUT CHARACTERISTICS

Approximate electron dose at one foot	10^5-10^6 rads/burst
Electron dose rate at one foot during burst	10^{10}-10^{11} rads/sec
Approximate gamma dose at one foot	10^2 rads/burst
Gamma ray dose rate at one foot during burst	10^7 -10^8 rads/sec
Approximate neutron yield, near fission spectrum	10^{11} neutrons/burst
Maximum neutron yield rate during burst	10^{17} neutrons/sec
Sustained neutron yield rate	10^{13} neutrons/sec
Positron energy, Mev	3 to 30
Maximum positron yield during burst, amperes	10^{-8} to 3×10^{-7}
Approximate sustained positron yield, amperes	10^{-11} to 3×10^{-10}
Energy resolution, ΔE/E full width	2%
Monoenergetic gamma-ray source, Mev	3 to 30
Maximum photon yield during burst, forward direction	10^9/sec
Sustained photon yield, forward direction	10^6/sec
Energy resolution, ΔE/E full width	2%

RF pulse on the Linac) were gated on at a 360 pps rate so that background could be measured midway between the neutron bursts. For the thermal spectrum measurements with BF_3 counters the pulse width was 2 to 4.5 μsec and the repetition rate was 7.5 pps.

2.5 NEUTRON DETECTORS AND ELECTRONICS

The 5.08 cm x 5.08 cm NE211 liquid scintillation detector and the 12.7 cm x 12.7 cm NE213 liquid scintillation detector are described in a separate report,[4] which also discusses the measured and calculated efficiency, G(E) counts/neutron incident. The G(E)'s used in reducing the graphite experiments are listed in Tables 2.3 and 2.4. Figure 2.15 is a block diagram of the electronics as used in the fast spectrum measurements in graphite. The linear channel, with the timing discriminator in coincidence, is used to set the bias of the discriminator. In the actual time-of-flight experiment, the discriminator stops the time-analyzer ramp, which is started by the injector trigger pulse. The injector trigger pulse fires the accelerator, and after being delayed by 0.4 μsec, gates the phototube on after the bremsstrahlung has reached and passed the detector. The phototube remains on for about 120-150 μsec. Time zero is obtained from the channel in which the bremsstrahlung is recorded (with the tube temporarily gated on during the bremsstrahlung arrival period), corrected for the flight time of the photons. The fast neutron time distribution was taken in 512 channels, each 31.25 nanoseconds wide. Since the analyzer can accept only one signal pulse per ramp, a counting rate loss correction is necessary. To keep the correction small, the Linac current is adjusted so that the data counts are 10-20% or less of the injector trigger pulses, or less than about 4000 cpm at the 360 pps repetition rate. Background is obtained from the average counting rate after some 10 μsec, corresponding to neutron energies below the bias of the detector.

Table 2.3

EFFICIENCY OF THE 5.08 CM DETECTOR AT 0.040 COBALT BIAS, COUNTS/NEUTRON INCIDENT[4]

Energy (eV)	G(E)
1.4400+07	1.6300-01
1.2800+07	1.6500-01
1.1000+07	1.7100-01
9.4000+06	1.8000-01
8.1200+06	1.8900-01
7.0000+06	2.0500-01
5.9700+06	2.2500-01
5.0000+06	2.4500-01
3.9600+06	2.7300-01
3.5000+06	2.8600-01
2.9800+06	3.0900-01
2.4000+06	3.2900-01
1.9100+06	3.5000-01
1.5600+06	3.7000-01
1.2500+06	3.7700-01
9.4600+05	3.7000-01
8.5000+05	3.5900-01
7.6000+05	3.3900-01
7.0000+05	3.1900-01
6.5000+05	2.9600-01
6.0000+05	2.6200-01
5.5800+05	2.0000-01
5.3200+05	1.7000-01
5.0000+05	1.3100-01
4.6800+05	1.0000-01
4.2900+05	7.0000-02
4.0000+05	5.3000-02
3.6300+05	3.5000-02
3.3500+05	2.4000-02
3.0000+05	1.5000-02
2.7200+05	1.0100-02

Table 2.4

EFFICIENCY OF THE 12.70 CM DETECTOR
AT 0.046 COBALT BIAS, COUNTS/NEUTRON INCIDENT[4]

Energy (eV)	G(E)
1.4400+07	4.2200-01
1.1000+07	4.2700-01
9.0000+06	4.6100-01
7.0000+06	5.1500-01
5.0000+06	5.8300-01
4.0000+06	6.1800-01
3.0000+06	6.6500-01
2.0000+06	7.0900-01
1.5000+06	7.1700-01
1.2500+06	7.1700-01
1.0000+06	6.8100-01
8.0000+05	5.8600-01
6.0000+05	3.9500-01
5.0000+05	2.7300-01
4.0000+05	8.8000-02
3.5000+05	4.5000-02
3.0000+05	2.8000-02
2.5000+05	1.7000-02
2.0000+05	7.0000-03
1.8000+05	2.0000-03
1.7000+05	1.0100-03

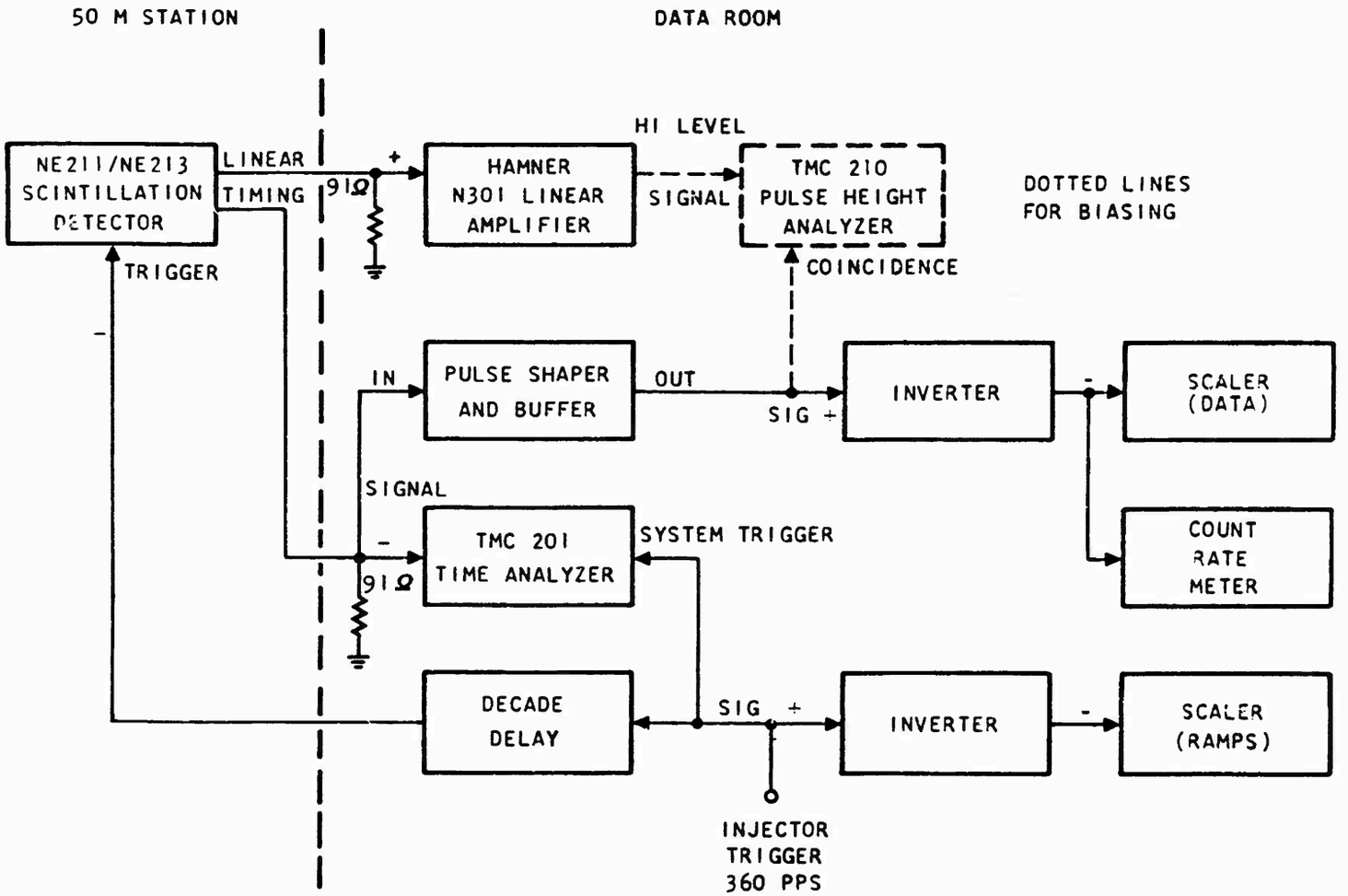

Fig. 2.15--Block diagram of electronics for NE211 and NE213 scintillation detectors

The intermediate neutron energy detector consists of a NE226 liquid scintillator counting capture gamma rays from a disk of boron carbide-loaded paraffin wax. The detector and its efficiency calibration are discussed in Ref. 5, and the G(E) used in the graphite data reduction is given in Table 2.5. Figure 2.16 is a block diagram of the electronics as used in the graphite experiment. The linear channel is the same as for the NE211 and NE213 detectors, except that a separate preamplifier is used. Two time analyzers were operated simultaneously to obtain data and inter-pulse background. The TMC211 analyzer accumulated data in 1,024 channels each 0.250 μsec wide (in the LC oscillator mode; discriminator should be set to 8). The 256-channel RCL analyzer has a special unit built at General Atomic with 16 μs time channel width. Thus it accumulated data and background out to 4096 μsec. However, the photomultiplier tube is gated on twice in each 1/180 pps (period = 5555 μsec). At a few tenths of a microsecond after the bremsstrahlung burst, it is gated on for about 500-600 μsec. After a 3000-μsec delay, it is gated on again for the same interval. A 3000-μsec flight time at 50 meters corresponds to neutrons of 1.5 eV energy. A boron-10 filter was inserted in the flight path at 16 meters to absorb neutrons below about 10 eV. Thus the background measured should be mostly ambient and long dieaway-time gamma rays. The gate trigger arrangement shown in Fig. 2.17 was used during most of the experiment. However, the 0^{o} measurement at 20.3 cm, which was made first, had the Linac RF pulsed at 360 pps, giving a trigger to gate the photomultiplier tube at 2778 μsec intervals.

The thermal neutron detector used in this experiment was a bank of thirty-six enriched boron trifluoride proportional counters filled to 70 cm pressure. The "36 BF_3" bank and its efficiency calibration are discussed in Ref. 6. The G(E) used in the data reduction of the graphite experiment is listed in Table 2.6. The electronic setup for the time-of-flight measurement is shown in Fig. 2.17. Two time-analyzers

Table 2.5

EFFICIENCY OF THE BORON CAPTURE DETECTOR 10/14/66 COUNTS/NEUTRON INCIDENT[5]

Energy (eV)	G(E)	Energy (eV)	G(E)
1.0001+02	6.3600-03	4.0000+05	7.2700-03
2.0000+02	6.3800-03	4.1000+05	7.0500-03
5.0000+02	6.4000-03	4.1500+05	6.9800-03
1.0000+03	6.4300-03	4.2000+05	6.9100-03
3.0000+03	6.4500-03	4.2500+05	6.9000-03
5.0000+03	6.4700-03	4.3000+05	6.9200-03
1.0000+04	6.4900-03	4.3500+05	6.9600-03
3.0000+04	6.5200-03	4.4000+05	7.0200-03
4.0000+04	6.5250-03	4.6000+05	7.2800-03
5.0000+04	6.5350-03	4.8000+05	7.5000-03
5.5000+04	6.5400-03	5.0000+05	7.8000-03
6.0000+04	6.5500-03	5.2000+05	7.9800-03
6.5000+04	6.5600-03	5.3000+05	8.0100-03
7.0000+04	6.5800-03	5.4000+05	8.0300-03
8.0000+04	6.6300-03	5.5000+05	8.0500-03
9.0000+04	6.6900-03	5.6000+05	8.0400-03
1.0000+05	6.7500-03	5.7000+05	8.0350-03
1.1000+05	6.8100-03	5.8000+05	8.0250-03
1.4000+05	7.0200-03	6.0000+05	8.0000-03
1.7000+05	7.2200-03	6.2000+05	7.9700-03
1.9000+05	7.3000-03	6.6000+05	7.8900-03
2.0000+05	7.3500-03	7.0000+05	7.8000-03
2.3000+05	7.4300-03	7.4000+05	7.7200-03
2.5000+05	7.4700-03	7.8000+05	7.6500-03
2.7000+05	7.5000-03	8.2000+05	7.5600-03
2.9000+05	7.5200-03	8.6000+05	7.4900-03
3.0000+05	7.5300-03	9.0000+05	7.4200-03
3.3000+05	7.5400-03	9.4000+05	7.3700-03
3.5000+05	7.5500-03	9.8000+05	7.2900-03
3.6000+05	7.5400-03	1.2000+06	6.9400-03
3.7000+05	7.5300-03	1.4000+06	6.5900-03
3.7500+05	7.5250-03	1.6000+06	6.2100-03
3.8000+05	7.5200-03	1.8000+06	5.8800-03
3.8500+05	7.4500-03	2.0000+06	5.5800-03
3.9000+05	7.3800-03	2.1000+06	5.5000-03

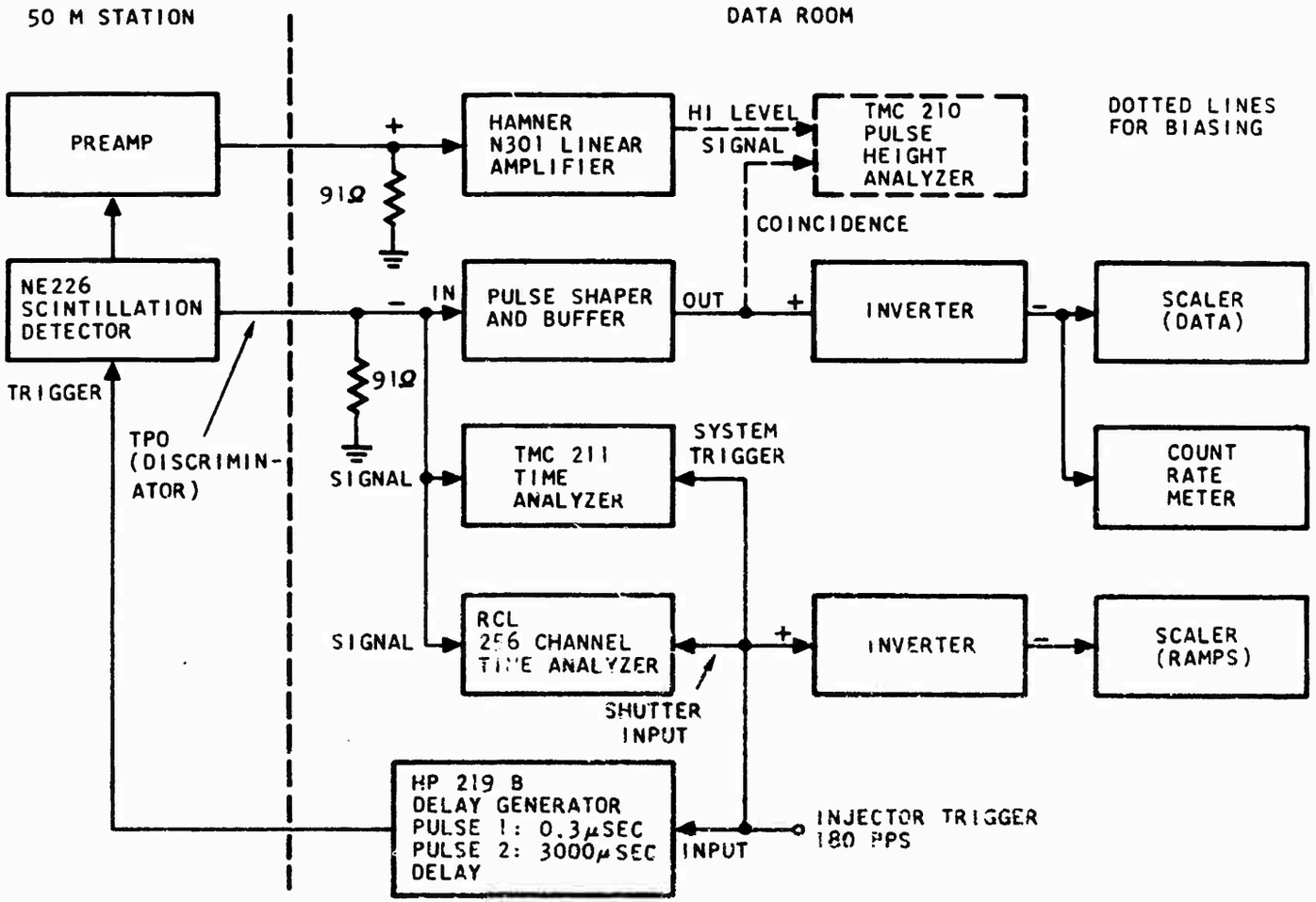

Fig. 2.16--Block diagram of electronics for the B_4C-CH_2-NE226 scintillation detector

Table 2.6

EFFICIENCY OF THE 36 BF_3 BANK 1/9/67
G(E) COUNTS / NEUTRON INCIDENT[6]

Energy (eV)	G(E)	Energy (eV)	G(E)
1.0010-03	9.5400-01	1.5000-01	4.7700-01
1.5000-03	8.9100-01	2.0000-01	4.2900-01
2.0000-03	8.7800-01	3.0000-01	3.7000-01
3.0000-03	8.4100-01	4.0000-01	3.5800-01
4.0000-03	8.0600-01	6.0000-01	3.5700-01
4.5000-03	8.0000-01	8.0000-01	3.1500-01
5.0000-03	7.9900-01	1.0000+00	2.9200-01
5.5000-03	7.9100-01	1.5000+00	2.7300-01
6.0000-03	7.8100-01	2.0000+00	2.6000-01
6.5000-03	7.7200-01	3.0000+00	2.4600-01
7.0000-03	7.5600-01	4.0000+00	2.3400-01
7.5000-03	7.5300-01	6.0000+00	2.1800-01
8.0000-03	7.4700-01	8.0000+00	2.1000-01
9.0000-03	7.1300-01	1.0000+01	2.0300-01
1.0000-02	6.5900-01	1.5000+01	1.8900-01
1.3000-02	6.5500-01	2.0000+01	1.8100-01
1.6000-02	6.2200-01	3.0000+01	1.7100-01
1.9000-02	6.0300-01	4.0000+01	1.6400-01
2.2000-02	5.8100-01	6.0000+01	1.5400-01
2.5000-02	5.6100-01	8.0000+01	1.4700-01
3.0000-02	5.6200-01	1.0000+02	1.4100-01
3.5000-02	5.5100-01	1.5000+02	1.3300-01
4.0000-02	5.3000-01	2.0000+02	1.2600-01
4.5000-02	5.2800-01	3.0000+02	1.1700-01
5.0000-02	5.1900-01	4.0000+02	1.1100-01
5.5000-02	5.1700-01	6.0000+02	1.0100-01
6.0000-02	5.0200-01	8.0000+02	9.3600-02
7.0000-02	4.8700-01	1.0000+03	8.9600-02
8.0000-02	4.8600-01	1.5000+03	7.8700-02
9.0000-02	4.6700-01	2.0000+03	7.0900-02
1.0000-01	4.6200-01		

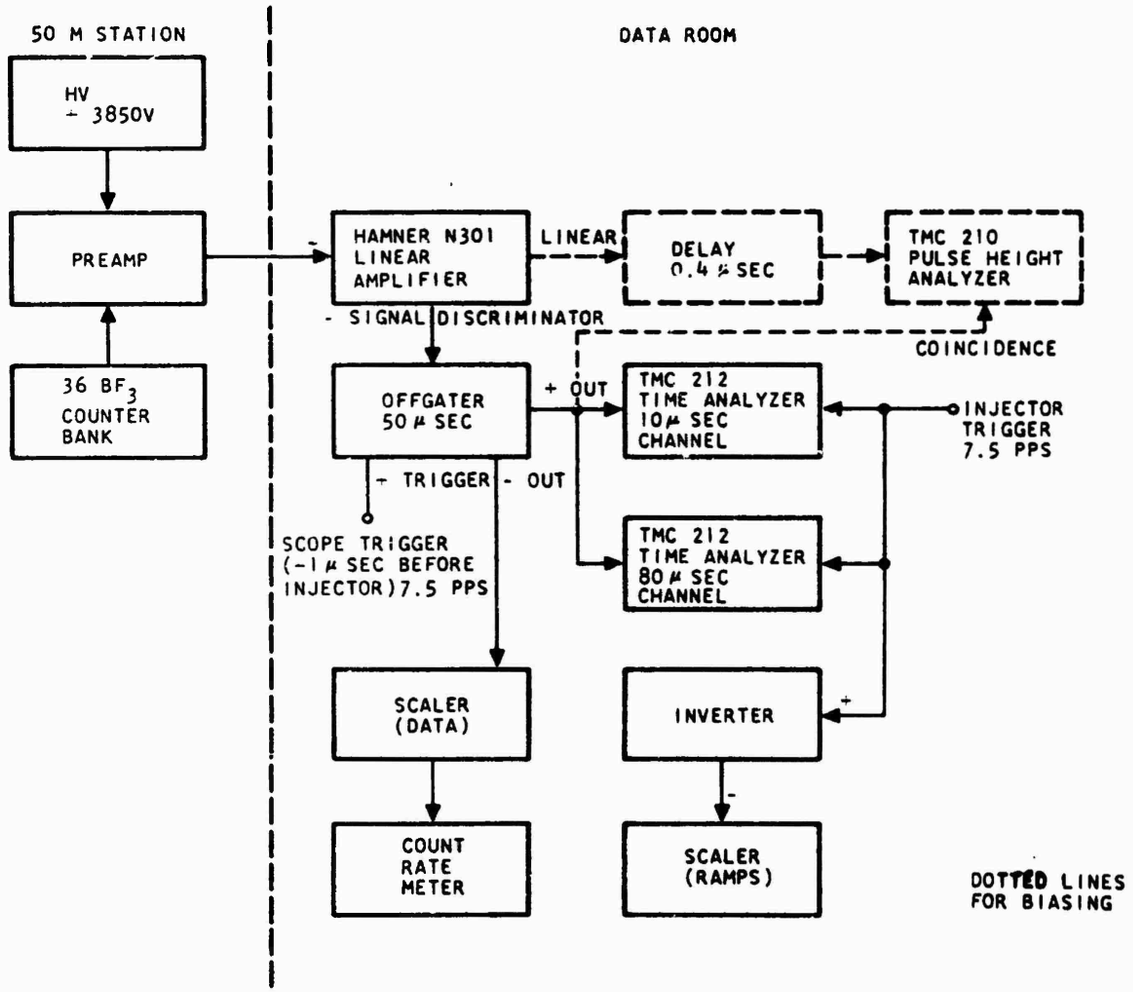

Fig. 2.17--Block diagram of the electronics for the BF_3 detector

were used, with different channel widths, to provide good time resolution at the higher energies while covering the entire thermal energy range with the wider channels. Background for each BF_3 detector measurement was obtained in a separate run with a neutron absorber installed at the bottom of the 3.81-cm diameter probe hole. The absorber was a 3.81-cm diameter by 3.18 cm long, thin-wall (0.06 cm) aluminum cylinder filled with 93% enriched boron powder.

2.6 COLLIMATION AND FLIGHT PATH

The fast and intermediate spectrum measurements were made on a 50-meter flight path. The flight path consists essentially of a precollimator, collimators at 16 m and 32 m, a shielded detector at 50 m, and large diameter steel drift tubes evacuated to rough vacuum with mechanical pumps. Most of the fast and intermediate spectrum measurements were made with a 3.0 in. (7.62 cm) diameter probe hole in the graphite and a 2.5 in. (6.35 cm) I. D. precollimator. This configuration is shown in Fig. 2.18. One intermediate spectrum measurement, at 60° and 35.6 cm radius, was made with a 1.5 in. (3.81 cm) diameter probe hole and the 0.87 in. (2.21 cm) I. D. precollimation system shown in Fig. 2.19. The precollimators and inserts are made of mild steel tubes filled with a mixture of lead dust, boric acid, and epoxy resin. The 16 m and 32 m collimators are made of hydrated boric acid backed by 10.16 cm of lead. Tests have shown that stray background with these systems is much less than ambient. The neutrons pass through Mylar windows on the drift tubes. For certain measurements, as described later, a 3.144-cm thick x 30.5 cm x 30.5 cm filter of depleted uranium may be inserted at the 16 m position. For other measurements a B^{10} filter (Fig. 2.20) may be inserted in the flight path.

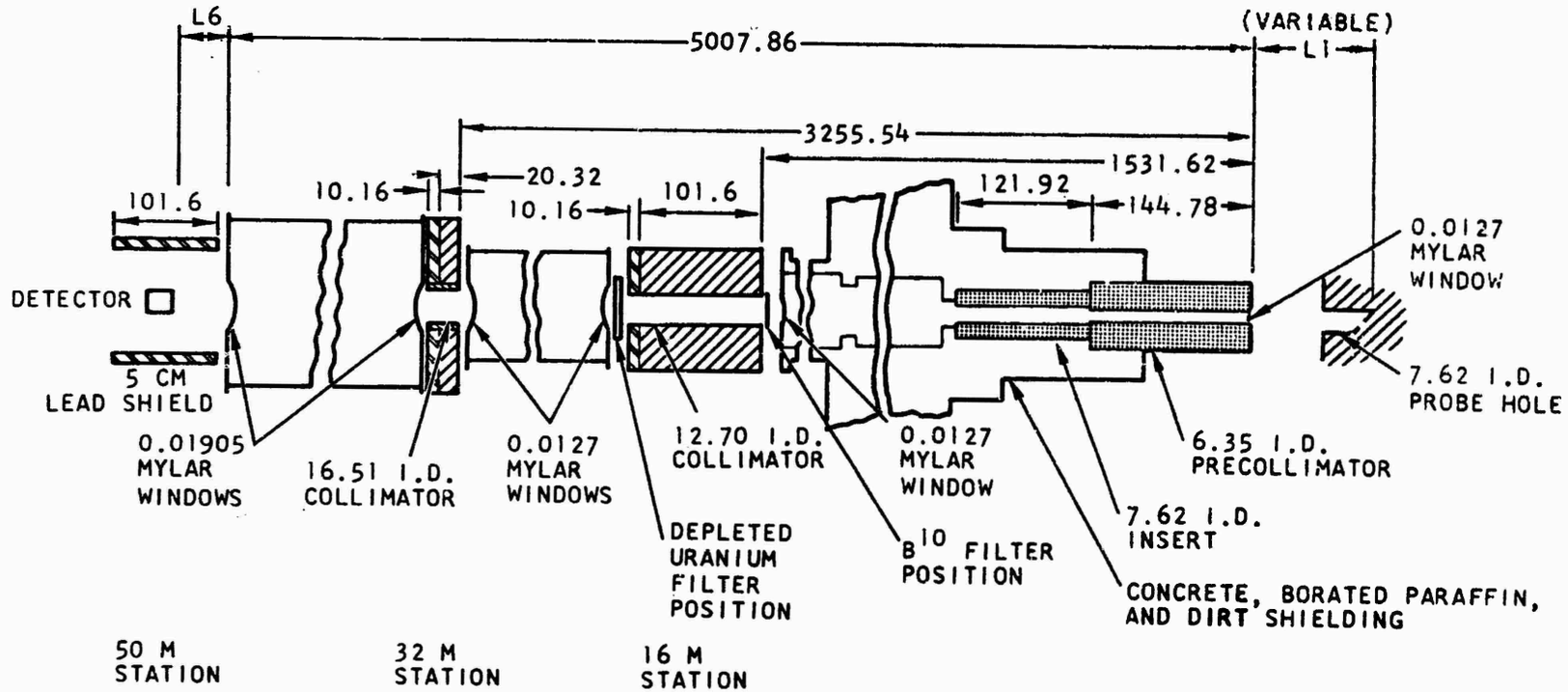

L6 = 35.56 FOR NE213, NE226 DETECTORS (END)
= 55.88 FOR 2 INCH NE211 DETECTOR (CENTER)
(DIMENSIONS IN CM)

Fig. 2.18--Fifty-meter flight path, 6.35 cm precollimator

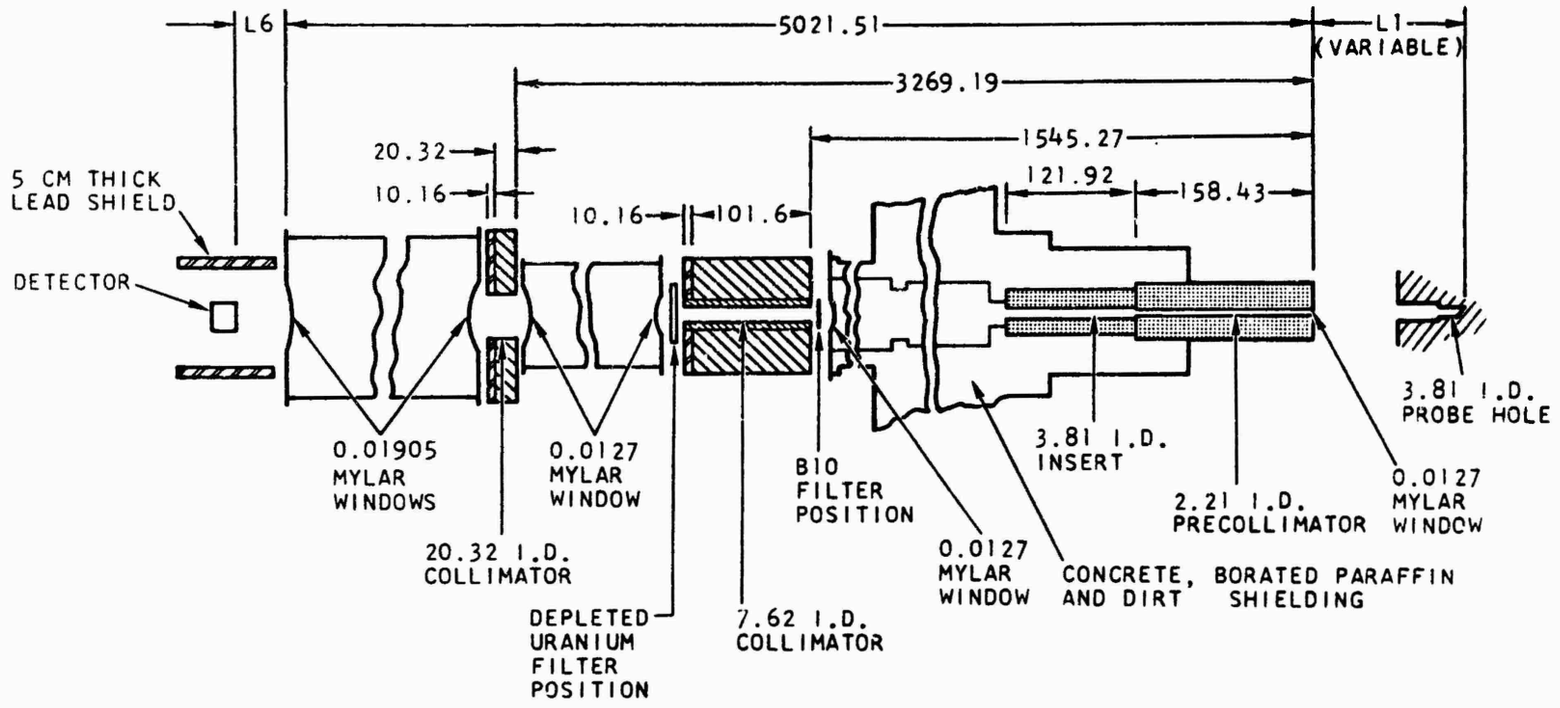

L6 = 35.56 FOR 5 INCH NE213, NE226 DETECTORS (END)
= 55.88 FOR 2 INCH NE211 DETECTOR (CENTER)

(DIMENSIONS IN CM)

Fig. 2.19--Fifty-meter flight path, 2.21 cm precollimator

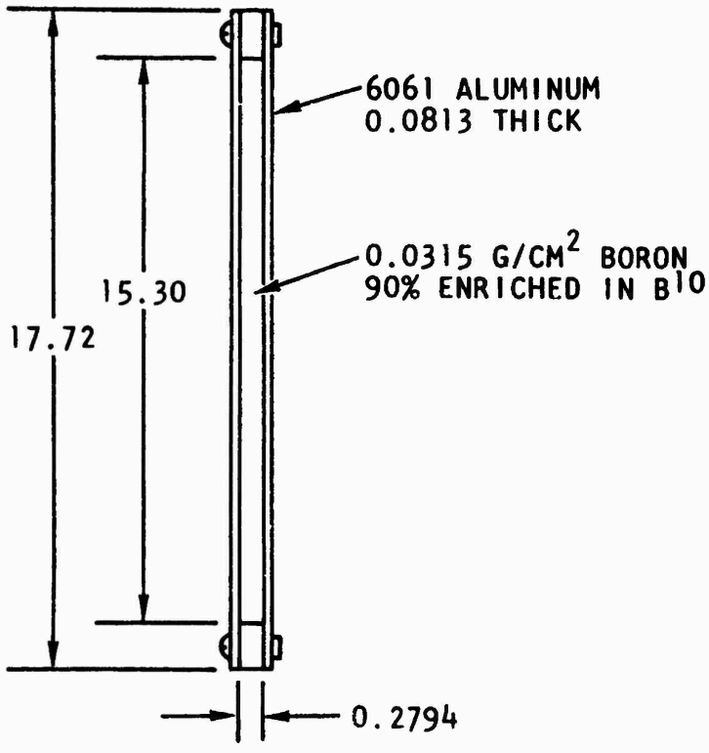

(DIMENSIONS IN CM).

Fig. 2.20--B^{10} filter

Thermal neutron spectrum measurements were made with the 36 BF_3 bank at 50 meters and the collimation system shown in Fig. 2.21.

To reduce the counting rate per unit energy, C(E) counts/sec eV, to angular flux per unit energy, $\psi(E)$ n/cm^2 sec sr eV, we use

$$\psi(E) = \frac{C(E)}{G(E)\, T(E) \frac{A_d}{L^2} \eta A_s} \qquad (2.1)$$

where,

$G(E)$ = intrinsic efficiency, counts/neutron incident

$T(E)$ = flight path transmission

A_d = detector area, cm^2

L = flight distance, cm

A_d/L^2 = solid angle, steradian

ηA_s = efficiency of the collimation system times the reference viewed area perpendicular to the beam, cm^2.

The collimation efficiency is defined as the counting rate with the collimators in place, divided by the counting rate without the collimators. It has been calculated for our geometries by the CAP code.[7] The geometry for CAP calculations is shown in Fig. 2.22. Neutrons are emitted from the disk source, diameter d_s, which is located at the bottom of the probe hole, and is assigned the area A_s of the probe-hole cross section. The other possible limiting apertures are included as d_2, d_3, etc., ending with the detector as the last aperture. The thickness of the collimators are indicated by t_1, t_2, etc. The distances of the entrance apertures of the collimators from the outside face of the experimental assembly are defined by the z coordinates. The z_1 distance and the depth of the probe hole, ℓ, depend on the location of the

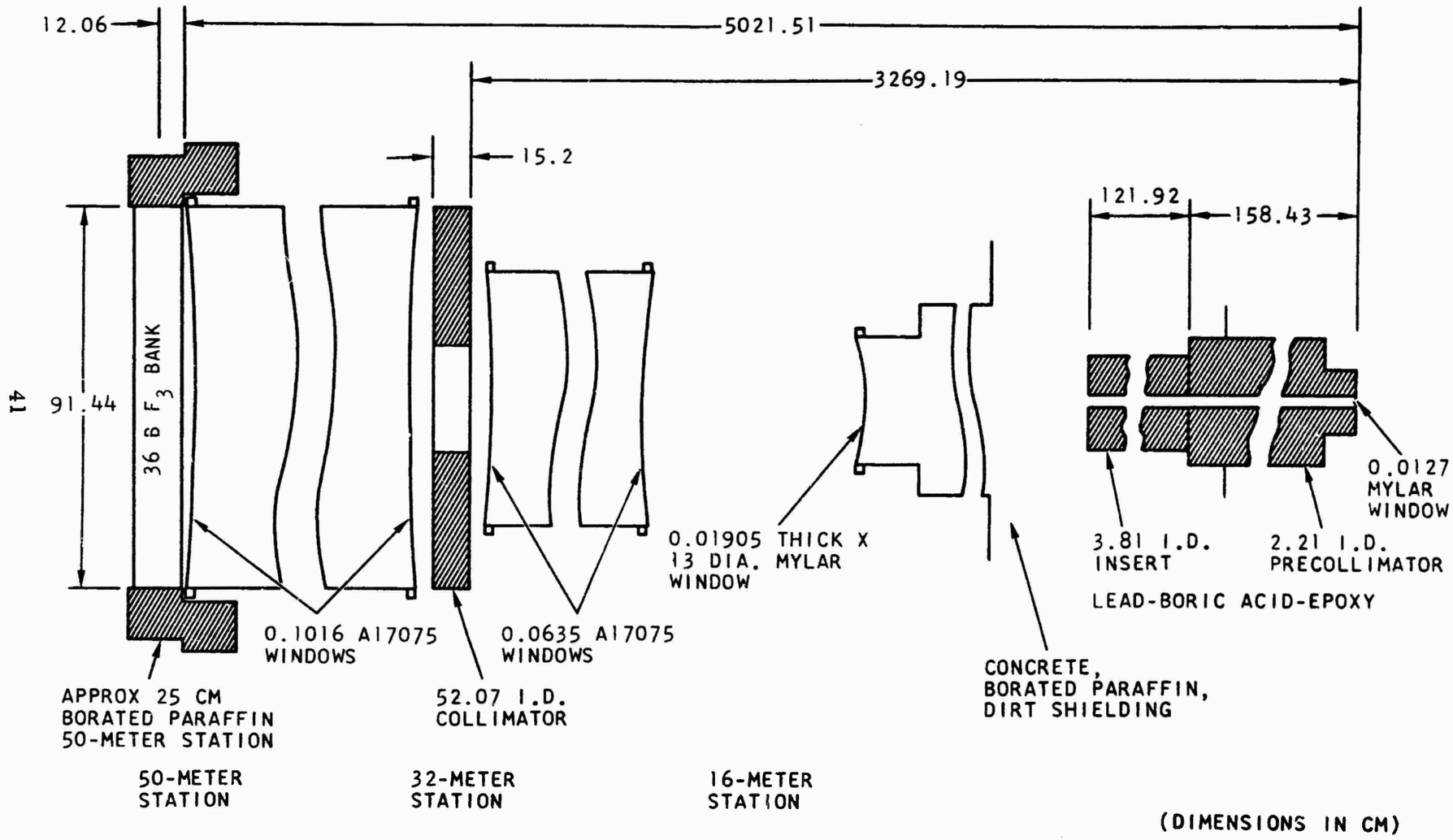

Fig. 2.21--Collimation system for the BF_3 detector measurements

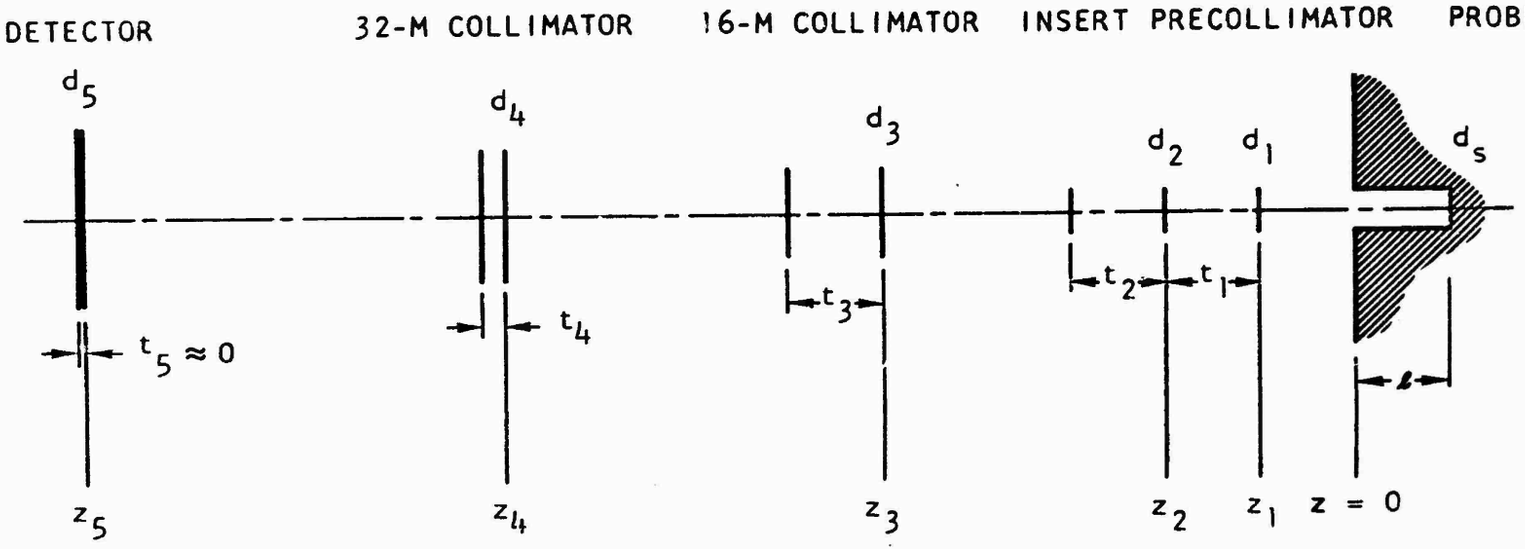

DETECTOR	d_5 CM	A_d CM^2	PRECOLLIMATOR d_1 CM	d_s CM	A_s CM^2
NE211	5.08 × 5.08	25.81	2.21	3.81	11.40
NE213	12.70	126.68	6.35	7.62	45.60
NE226	19.05	285.02			
BF_3	91.44	6566.90			

Fig. 2.22--Geometry for collimation analysis

measurement. The other distances can be found from Figs. 2.18, 2.19, and 2.21. The source (probe hole) and detector diameters and areas are indicated in Fig. 2.22 and the collimator diameter and areas in Figs. 2.18, 2.19, and 2.21. The CAP program traces rays from small discrete areas on the source to the detector, computes the efficiency for each area, and then computes an average efficiency η of the whole system.

The results of the collimation efficiency calculations and the overall geometrical factor $(A_d/L^2)\,\eta\,A_s$ are listed in Table 2.7 for the angles and radii in the graphite experiments. Factors in parenthesis are interpolated from other CAP calculations.

A study was made to determine the sensitivity of η to the alignment of the source, collimators, and detector with the collimation axis. It was found that a 2.54-cm displacement of the detectors resulted in no change in η, and we believe that our alignment was always within this figure. A 2.54-cm displacement of the 16-meter collimator (for the fast and intermediate spectrum runs) resulted in a 30% decrease in η. However, we believe the 16-m collimator was always aligned to within ± 0.1 cm. A 2.54-cm displacement of the 32-meter collimator (for the thermal spectrum runs) resulted in no change in η.

The collimator efficiency was found to be fairly sensitive to misalignment of the source, especially for the BF_3 bank. In addition, with sufficient misalignment, the flux from the walls of the probe hole or even the outer surface of the assembly will contribute, a most undesirable condition. On the other hand, the probe hole diameter is made as small as practical, to reduce the perturbation of the flux in the assembly. With the transit and cross hairs on the precollimator and probe hole, we believe we can align the probe hole to ± 0.1 cm. This amount of misalignment has an effect of less than 0.5% using the NE211, NE213 or boron detector (NE226 scintillator). The geometry factor for the BF_3 bank, however, is reduced by 4%. Thus with this detector, which does not lie within

Table 2.7

GEOMETRICAL FACTORS*

Radius cm	Angle	Detector	Precollimator	A_d/L^2	η	$\frac{A_d}{L^2}\eta A_s(10^{-5})$
20.3	0^o	NE211	6.35	1.02×10^{-6}	0.691	3.21×10^{-5}
	0^o	NE226	6.35	11.22	0.691	35.35
	0^o	BF_3	2.21	258.5	0.134	39.49
	30^o	NE213	6.35	4.99	(0.686)	15.61
	30^o	NE226	6 35	11.22	(0.691)	35.35
	90^o	BF_3	2.21	258.5	(0.134)	39.49
35.6	0^o	NE211	6.35	1.02	0.691	3.21
	0^o	NE213	6.35	4.99	0.686	15.61
	0^o	NE226	6.35	11.22	0.680	34.79
	0^o	BF_3	2.21	258.5	0.135	39.78
	17^o	NE213	6.35	4.99	(0.686)	15.61
	17^o	NE226	6.35	11.22	(0.680)	34.79
	35^o	NE213	6.35	4.99	(0.686)	15.61
	35^o	NE226	6.35	11.22	(0.680)	34.79
	60^o	NE213	6.35	4.99	(0.686)	15.61
	60^o	NE226	6.35	11.22	(0.680)	34.79
	60^o	NE226	2.21	11.22	0.309	3.95
	90^o	BF_3	2.21	258.5	(0.134)	39.49
50.8	0^o	NE213	6.35	4.99	0.686	15.61
	0^o	NE226	6.35	11.22	0.679	34.74
	0^o	BF_3	2.21	258.5	0.134	39.49
	12^o	NE213	6.35	4.99	(0.686)	15.61
	12^o	NE226	6.35	11.22	(0.679)	34.74
	24^o	NE213	6.35	4.99	(0.686)	15.61
	24^o	NE226	6.35	11.22	(0.679)	34.74
	37^o	NE213	6.35	4.99	(0.686)	15.61
	37^o	NE226	6.35	11.22	(0.679)	34.74
	90^o	BF_3	2.21	258.5	(0.134)	39.49
66.0	0^o	NE213	6.35	4.99	0.686	15.61
	0^o	NE226	6.35	11.22	0.681	34.84

*An average z_1 = 31.4 cm and average L = 5138 cm (BF_3) or 5146 cm (NE211, 213, 226) were used for these factors. The exact L was used for the time-of-flight to energy conversion. The ℓ length was 76.2 cm at 20.3 cm radius, 61.0 at 35.6, 45.8 at 50.8, and 30.6 cm radius. A_s = 45.60 cm^2 for 6.35 cm collimator (7.62 cm diameter probe hole); A_s = 11.40 cm^2 for 2.21 cm collimator (3.81 cm diameter probe hole).

the collimated beam as do the others, normalization errors of several percent may be expected due to unavoidable alignment errors. It should be noted also that most of the fast and intermediate spectrum measurements were made by interchanging detectors while leaving the collimators and assembly unchanged at a given radius and angle. Thus although the absolute over-all detection efficiency may be affected slightly by misalignment, the relative normalization should not be affected, provided the detectors were reinstalled each time to within 2.54 cm of the collimation axis.

Transmission of neutrons through the flight path is calculated as $T(E) = \exp\left(-\sum_i N_i \sigma_i(E) t_i\right)$ where i refers to the material, N the nuclear density, σ the total cross section, and t the thickness. The materials considered are air at 50% relative humidity, Mylar, the 3.144 cm of depleted uranium (0.22 wt % U^{235}) and its 0.02-cm total thickness of polyethylene wrapping (replaced by 3.1 cm of NTP air when removed) and the B^{10} filter when it is used. For the thermal spectrum measurements some of the Mylar windows were replaced by aluminum windows. The total equivalent thickness of air at NTP, including the residual air in the drift tubes, on the fifty-meter flight path, has been calculated as 214.9 cm (without filters) plus the distance from the detector to the drift tube, the distance from the precollimator to the bottom of the probe hole, and the equivalent thickness of air at the pressure existing in the precollimator-to-16 m section (about 42 cm). The cross sections of Al metal, H, O, N, and C are usually included along with Al and enriched B when needed. The reference nuclear densities are given in Table 2.8. For convenience the nuclear densities of H and O are taken as those in air at NTP (293 K, 1 atm). The factors for multiplying the thickness (cm) of Mylar and polyethylene to convert the equivalent thickness in air at NTP are also given in the table. The nuclear density of carbon in Mylar is tabulated. The factor for converting from polyethylene is also given.

Table 2.8

REFERENCE NUCLEAR DENSITIES IN FLIGHT PATH

Material	N (nuclei/cm^3)	Factor for Mylar	Factor for Polyethylene
U	4.73×10^{-2}	---	---
H	6.48×10^{-7}	5.36×10^{4}	1.219×10^{5}
O	1.092×10^{-5}	1.589×10^{3}	---
N	3.93×10^{-5}	---	---
C	4.34×10^{-2}	---	91
Al	6.03×10^{-2}	---	---
B	6.73×10^{-2}	---	---

The total cross sections for uranium were obtained from

	BNL 325 Supplement 2 and AWRE 7963, for
hydrogen	Gammel, BNL 325, and UCRL 5226, for
oxygen	KAPL-M-6452, for
nitrogen	BNL 325 Supplement 2 and UCRL 5226;
carbon	BNL 325 Supplement 2 and KFK 120;
aluminum 7075	BNL 325 2nd edition and Supplement 2, GA 5884;
aluminum 6061	BNL 325 2nd edition and Supplement 2, GA 5884;
boron	From BNL SCISRS TAPE and BNL 325 2nd edition.

The transmission of the flight path with the 6.35 cm precollimator and no filters, at r = 35.6 cm, 0^{o} is plotted in Fig. 2.23. The transmission is nearly unity and should be accurate to ± 3%. The total cross section of depleted uranium (.22 wt % U^{235}) is given in Table 2.9. The computed transmission of the depleted uranium filter with its polyethylene wrapping is plotted in Fig. 2.24 (200 eV to 15 MeV). The transmission correction is large, especially at the lower energies. The estimated accuracy is ± 12% from 200 eV to 100 keV and ± 6% from 100 keV to 15 MeV. The resonances at a few keV had to be included to avoid spurious oscillations in the graphite spectrum. The transmission of the enriched boron filter including its aluminum windows is plotted in Fig. 2.25. Accuracy in the 200 eV-15 MeV range is estimated at ± 5%, except at the aluminum resonances. The transmission of the flight path with aluminum (and Mylar) windows and no filters, as in the thermal spectrum measurements at r = 35.6 cm, 0^{o}, is plotted in Fig. 2.26 from 0.001 eV to 400 eV. Accuracy is estimated at ± 3%.

2.7 SOURCE NEUTRON MONITORS

All experimental spectra are normalized to a standard target intensity by dividing by a number proportional to the activity of a foil irradiated in a reproducible geometry. The graphite experiments used standard sulfur pellets, 3.81 cm in diameter by 0.95 cm thick (18 gm), supplied by Edgeton, Germeshausen and Grier, Inc., and counted by them at their Goleta, California laboratory. The beta-activity from the $S^{32}(n, p)P^{32}$ reaction, with an effective threshold of 3 MeV and effective cross section of 300 mb, is scintillation-counted at least three times and the decay-corrected data analyzed, after making sure the correct half-life (14.3 days) is observed. Decay is corrected to the midpoint of the exposure interval. Exposures are typically 1 to 3 hours. Calibration is obtained from a Cockcroft-Walton accelerator exposure (D-T neutrons) monitored with an associated particle counter. Over-all systematic accuracy is specified at ± 10%. However, we have been informed by

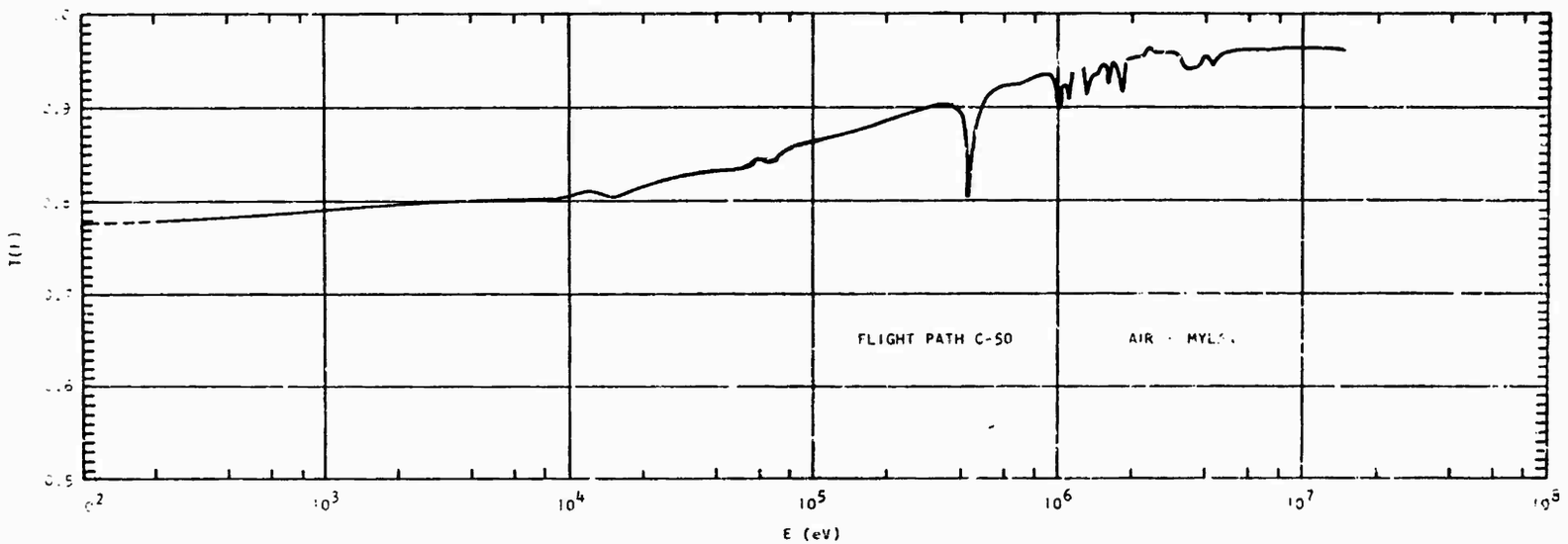

Fig. 2.23--Transmission of the fifty-meter flight path (Air + Mylar)

Table 2.9

TOTAL CROSS SECTION OF DEPLETED URANIUM

Energy (eV)	σ_T(b)	Energy (eV)	σ_T(b)
1.5000+07	5.9100+00	6.0000+04	1.2400+01
1.4000+07	5.7400+00	5.0000+04	1.2690+01
1.3000+07	5.5700+00	4.0000+04	1.2970+01
1.2500+07	5.5000+00	3.0000+04	1.3250+01
1.2000+07	5.4700+00	2.0000+04	1.3540+01
1.1750+07	5.4600+00	1.0000+04	1.4000+01
1.1500+07	5.4700+00	9.0000+03	1.4300+01
1.1000+07	5.5000+00	8.0000+03	1.5000+01
1.0500+07	5.5500+00	7.5000+03	1.5000+01
1.0000+07	5.6500+00	7.0000+03	1.5000+01
9.5000+06	5.7800+00	6.5000+03	1.5000+01
9.0000+06	5.9200+00	6.0000+03	1.5000+01
8.5000+06	6.1100+00	5.5000+03	1.5000+01
8.0000+06	6.3000+00	5.0000+03	1.5000+01
7.5000+06	6.5000+00	4.5000+03	1.5000+01
7.2500+06	6.6600+00	4.4000+03	1.5000+01
7.0000+06	6.8100+00	4.3000+03	1.5300+01
6.7500+06	6.9700+00	4.2000+03	1.5500+01
6.5000+06	7.1100+00	4.1500+03	1.6000+01
6.2500+06	7.2500+00	4.1000+03	2.0000+01
6.0000+06	7.3800+00	4.0000+03	1.8000+01
5.7500+06	7.5000+00	3.9000+03	1.6500+01
5.5000+06	7.6200+00	3.8000+03	1.5000+01
5.2500+06	7.7300+00	3.7000+03	1.5000+01
5.0000+06	7.8100+00	3.6000+03	1.5400+01
4.7500+06	7.8000+00	3.5500+03	1.6500+01
4.5000+06	7.9400+00	3.5000+03	1.6500+01
4.2500+06	7.9800+00	3.4500+03	1.5000+01
4.0000+06	7.9900+00	3.4000+03	1.5000+01
3.5500+06	7.9900+00	3.3000+03	1.5500+01
3.4500+06	7.9800+00	3.2000+03	1.6000+01
3.2500+06	7.9500+00	3.1000+03	1.6500+01
3.0000+06	7.9000+00	3.0000+03	1.6000+01
2.7500+06	7.8500+00	2.9500+03	1.5800+01
2.5000+06	7.7500+00	2.9000+03	1.6000+01
2.2500+06	7.6300+00	2.8500+03	1.6500+01

Table 2.9 (Continued)

Energy (eV)	σ_T(b)	Energy (eV)	σ_T(b)
2.0000+06	7.4800+00	2.8000+03	1.6000+01
1.7500+06	7.3000+00	2.7000+03	1.5300+01
1.5000+06	7.1000+00	2.6500+03	2.1500+01
1.4000+06	6.9000+00	2.5000+03	1.7500+01
1.3000+06	6.8100+00	2.4000+03	1.5500+01
1.2000+06	6.8000+00	2.3500+03	1.4500+01
1.1000+06	6.8700+00	2.3000+03	1.5200+01
1.0000+06	6.9400+00	2.2000+03	1.7500+01
9.0000+05	7.0700+00	2.1000+03	1.2000+01
8.0000+05	7.2100+00	2.0000+03	1.5000+01
7.0000+05	7.3900+00	1.9500+03	1.7700+01
6.0000+05	7.5800+00	1.9000+03	1.6000+01
5.0000+05	7.8200+00	1.8800+03	1.2500+01
4.5000+05	7.9800+00	1.8000+03	1.4500+01
4.0000+05	8.1600+00	1.7000+03	1.3500+01
3.5000+05	8.4000+00	1.6000+03	1.5500+01
3.0000+05	8.7000+00	1.5500+03	1.3500+01
2.7000+05	8.9400+00	1.5300+03	1.2500+01
2.4000+05	9.2300+00	1.5000+03	1.4000+01
2.1000+05	9.5000+00	1.4200+03	1.2700+01
1.8000+05	9.9900+00	1.3800+03	1.6000+01
1.5000+05	1.0490+01	1.3200+03	1.3500+01
1.2000+05	1.1030+01	1.2400+03	1.5500+01
1.0000+05	1.1450+01	1.2000+03	1.5500+01
9.0000+04	1.1690+01	1.1000+03	1.5500+01
8.0000+04	1.1910+01	1.0500+03	1.5500+01
7.0000+04	1.2160+01	1.0000+03	1.5500+01

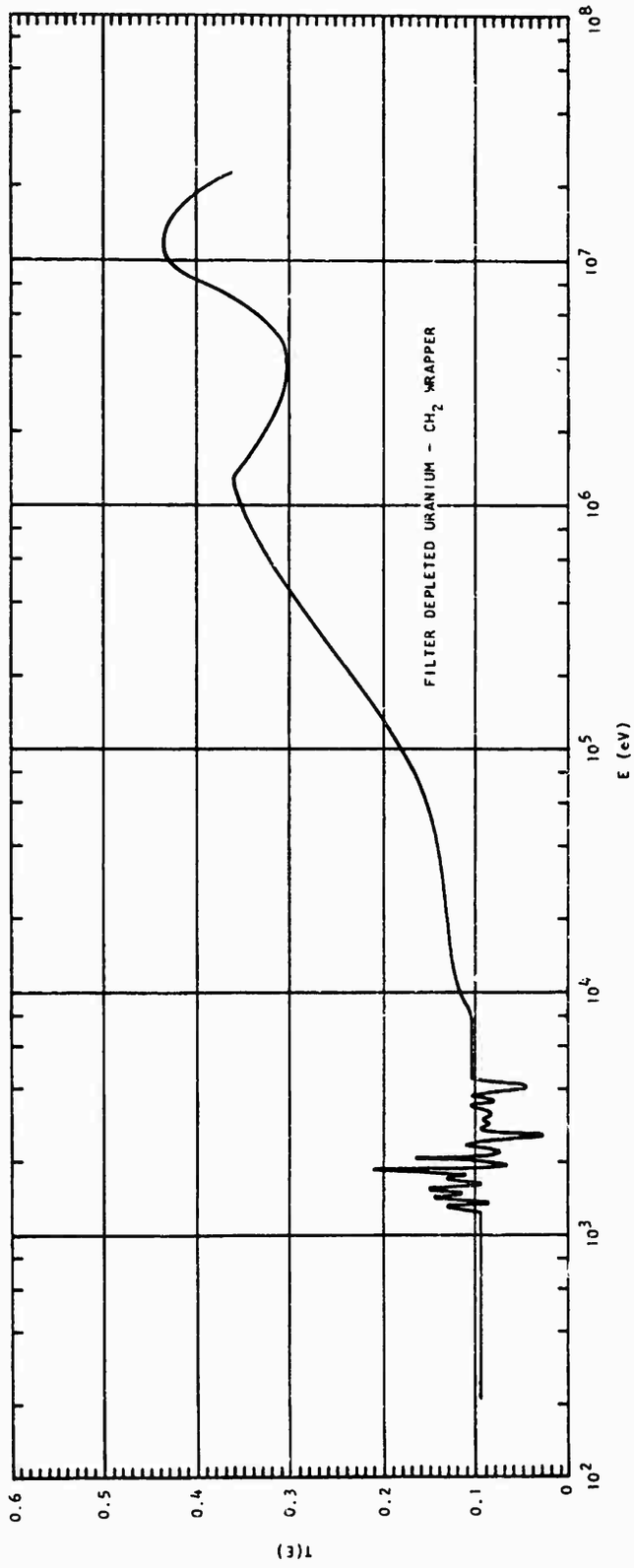

Fig. 2.24--Transmission of the depleted uranium filter

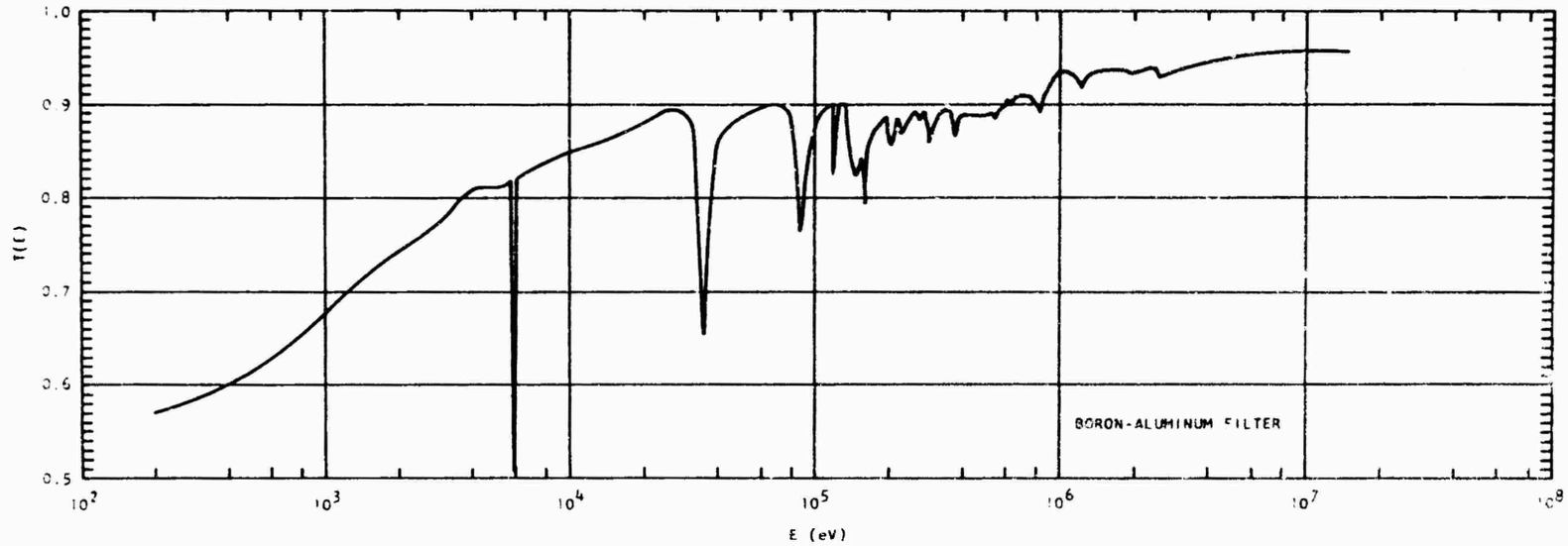

Fig. 2.25--Transmission of the boron-aluminum filter

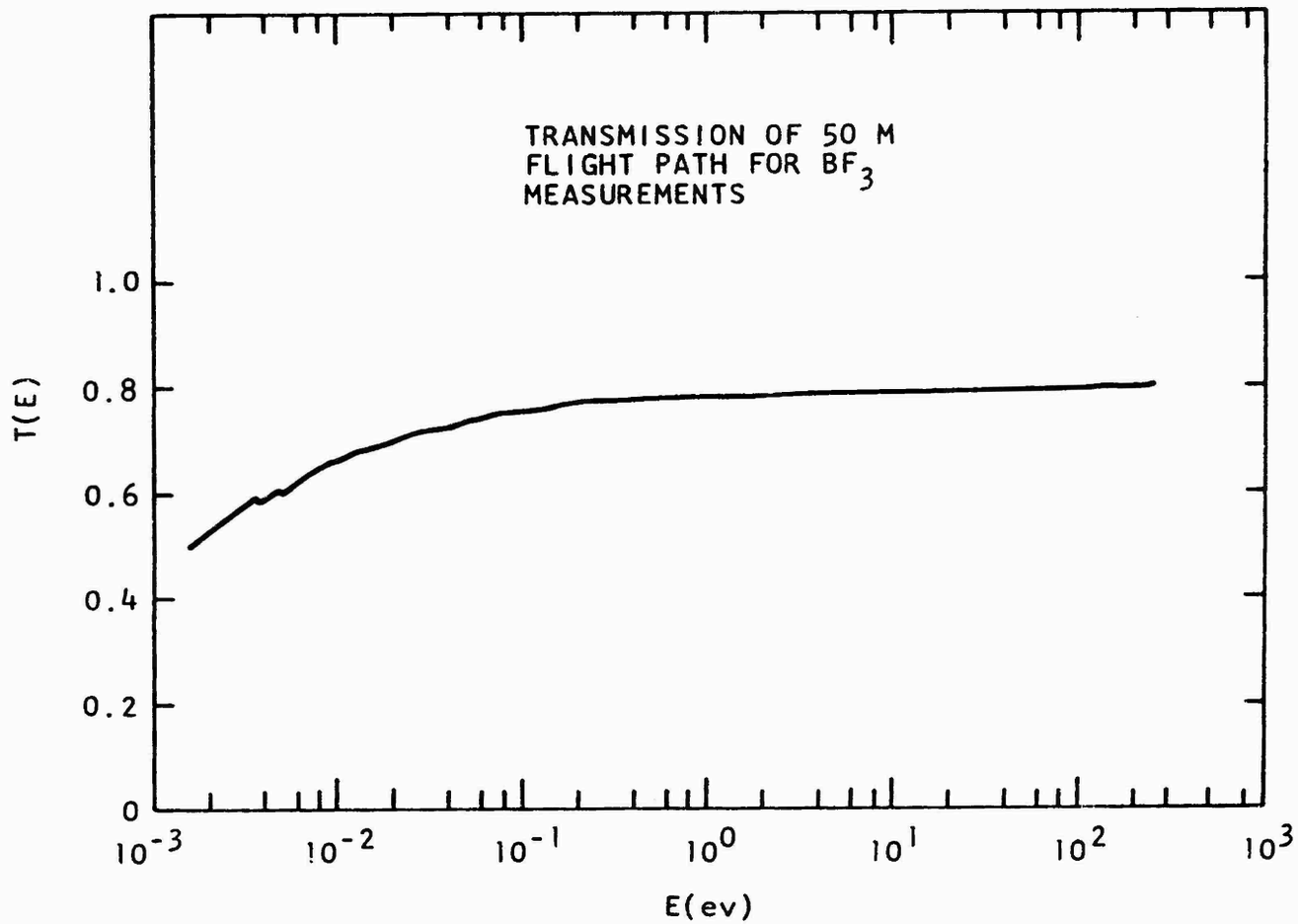

Fig. 2.26--Transmission of the flight path for the BF_3 measurement

E.G.G. that the relative activation of foils measured within a 3-month period is accurate to about 1%, taking into account the systematic error due to counter drift. Statistical errors in counting are in addition to this and are quoted along with the fluence, nvt n.cm^{2} > 3 MeV based on the standard cross section.

As a backup in case of loss of the sulfur normalization, we also exposed and counted at General Atomic an aluminum rod 1.59 cm in diameter and 4.45 cm long (in the fast spectrum assembly) or a 1.28 cm diameter by 0.00254 cm thick copper foil held at the lower end of a similar aluminum rod (in the thermal spectrum assembly). We found that the activity counted in the aluminum appeared to be mostly due to impurities, probably copper, hence we changed to copper foils in the later experiments.

A cross section of the monitor foil stringer and its relation to the target is shown in Fig. 2.27 and the sulfur monitor results are listed in Tables 2.10 and 2.11.

2.8 DATA REDUCTION AND RESULTS

The graphite spectrum measurements are summarized in Tables 2.10 and 2.11.

The data is obtained as counts per time channel vs channel number. First the data is reduced with the code HECTO.[5] Briefly, the code performs the following operations. The flight time corresponding to the middle of the time channel is calculated and converted to energy from

$$E(eV) = \frac{5.2268 \times 10^{-7} L^2}{(t-t_0)^2} \qquad (2.2)$$

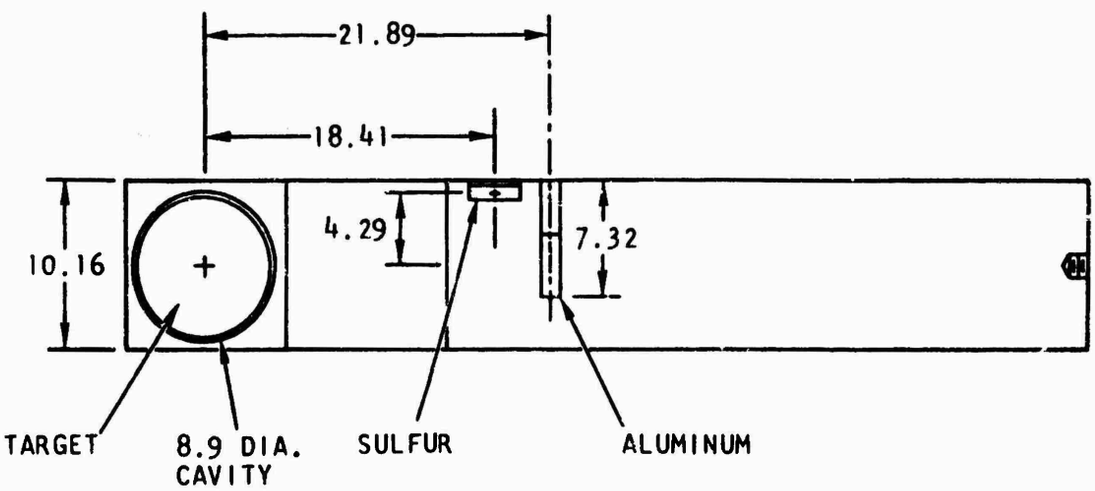

(DIMENSIONS IN CM)

Fig. 2.27--Monitor geometry

Table 2.10
SUMMARY OF FAST AND INTERMEDIATE
SPECTRUM MEASUREMENTS

Date	Run	Radius	Angle	Precoll.	Detector	Filter	Burst (nsec)	S Monitor	Monitor M
5-17	001	20.3	0°	6.35	NE226	U+B^{10}	100	1.00±.01(10)	1000.
	002	20.3	0°	6.35	NE211	U	20	1.20±.01(10)	1200.
	003	35.6	0°	6.35	NE211	U	20	4.91±.08(10)	4910.
5-20	001	35.6	0°	6.35	NE213	U	20	5.46±.05(9)	546.
	002	35.6	0°	6.35	NE226	U+B^{10}	50	5.21±.03(10)	5210.
	003	50.8	0°	6.35	NE226	U+B^{10}	50	1.17±.01(11)	11700.
	004	50.8	0°	6.35	NE213	U	20	3.18±.01(10)	3180.
5-21	005	66.0	0°	6.35	NE213	U	20	4.32±.04(10)	4320.
	006	66.0	0°	6.35	NE226	U+B^{10}	50	4.62±.03(10)	4620.
	008	35.6	60°	6.35	NE226	B^{10}	100	9.47±.01(10)	9470.
	009	35.6	60°	6.35	NE226	U+B^{10}	100	2.85±.01(10)	2850.
	010	35.6	60°	6.35	NE213	U+B^{10}	50	4.67±.01(10)	4670.
5-24	001	35.6	60°	2.21	NE226	B^{10}	100	9.50±.07(10)	9500.
	002	50.8	37°	6.35	NE226	B^{10}	100	9.04±.04(10)	9040.
	003	50.8	37°	6.35	NE213	None	20	2.7 ±.1 (10)	2700.
5-27	001	20.3	30°	6.35	NE213	None	20	4.5 ±.1 (9)	450.
	002	20.3	30°	6.35	NE226	B^{10}	50	5.32±.02(9)	532.
	003	20.3	30°	6.35	NE226	U+B^{10}	50	6.80±.02(10)	6800.
	005	35.6	17°	6.35	NE226	B^{10}	100	3.30±.01(10)	3300.
	006	35.6	17°	6.35	NE213	None	20	1.47±.01(10)	1470.
	007	50.8	12°	6.35	NE213	None	20	2.86±.01(10)	2860.
	008	50.8	12°	6.35	NE213	U	20	6.59±.02(10)	6590.
	009	50.8	12°	6.35	NE226	B^{10}	100	1.02±.01(11)	10200.
5-28	010	35.6	35°	6.35	NE226	B^{10}	100	8.69±.03(10)	8690.
	011	35.6	35°	6.35	NE213	None	20	3.38±.02(10)	3380.
	012	35.6	35°	6.35	NE213	U	20	3.27±.02(10)	3270.
	013	50.8	24°	6.35	NE213	U	50	9.48±.03(10)	9480.
	014	50.8	24°	6.35	NE226	B^{10}	100	1.23±.01(11)	12300.

Table 2.11

SUMMARY OF BF_3 THERMAL SPECTRUM MEASUREMENTS

Date	Run	Radius	Angle	Background Plug	Burst μsec	S Monitor	M Monitor
7-22	001	50.8	0°	out	2.0	1.88±.01 (10)	1880
	002	50.8	0°	in	2.0	1.52±.03 (10)	1520
	003	35.6	0°	out	1.0	9.4 ±.2 (9)	940
	004	35.6	0°	in	1.0	8.87 ±.09 (9)	887
	005	20.3	0°	out	0.5	4.9 ±.1 (9)	490
	006	20.3	0°	in	0.5	4.4 ±.1 (9)	440
7-25	001	50.8	90°	out	2.0	1.52±.01(10)	1420
	002	50.8	90°	in	2.0	1.89±.01(10)	1890
7-26	003	50.8	90°	out	4.5	3.10±.01(11)	--
	004	35.6	90°	out	1.2	1.11±.01(10)	1110
	005	35.6	90°	in	1.2	1.21±.01(10)	1210
	006	20.3	90°	out	0.4	2.36±.08(9)	--
7-28	001	20.3	90°	in	0.4	2.79±.03(9)	279
	002	20.3	90°	out	0.4	2.63±.07(9)	263

where L is the flight distance (cm), t is in milliseconds, and t_0 is the zero-time, including any mean emission time and detection time delay. The counts are corrected for deadtime and the deadtime corrected background is subtracted from the data. The number of neutrons per eV is found from the relationship $C(E)\Delta E = C(t)\Delta t_c$ where Δt_c is the channel width. Then C(E) is divided by S(E) = G(E) T(E), where G(E) is the intrinsic detection efficiency already discussed and T(E) the flight path transmission. We now have N'(E), the number of neutrons per eV which would be incident on the detector if T = 1, versus E. To normalize to the source intensity and the length of irradiation, the published output is

$$N(E) = \frac{N'(E)}{M} \qquad (2.3)$$

where M is a number proportional to the time-integrated irradiation (the fluence given by the sulfur pellet in the graphite experiment).

In addition to the channel-by-channel reduced data, the code groups and prints the average N(E) in several adjacent channels, the first grouping to satisfy an energy resolution criterion specified by the experimenter. This may be either $\Delta E/E$ = constant, or $\Delta E/E$ proportional to $E^{1/2}$, which corresponds to the case when the time uncertainty Δt is fixed, since the flight time t is proportional to $E^{-1/2}$. Further grouping is done if the average N(E) does not meet a second criterion, viz. the statistical error DELTA(N)/N less than a specified value. The statistical error includes the statistical error in the background.

The quantity of interest is the angular flux $\psi(\underline{r}, E, \underline{\Omega})$, the number of neutrons at position $\underline{r}$, per eV, per steradian, per second, which cross a 1 cm^2 area perpendicular to the direction $\underline{\Omega}$. The number of neutron incident on the detector (for T = 1), per eV, is

$$N'(E) = t_R \iint \psi(\underline{r}, E, \underline{\Omega})\, d\Omega dA \qquad (2.4)$$

where t_R is the run time. The dependence on t_R and on the source intensity S n/sec, is removed by referring to the number of monitor counts

$$M = kSt_R \qquad (2.5)$$

where k is a calibration constant. The angular flux can be removed from the integral by considering an average value, and

$$\iint d\Omega dA = \frac{A_d}{L^2}\, \eta\, A_s \qquad (2.6)$$

the geometrical factor discussed in Section 2.6 and listed in Table 2.7. Final results for N(E) divided by $(A_d/L^2)\eta A_s$ are given in Appendix B. Thus all experimental results are reduced to angular flux per unit sulfur monitor fluence.

The 0° fast neutron spectra are plotted in Fig. 2.38 for the different radii. The boron detector spectra are not plotted because they must be corrected further for background, as discussed later. The 0° thermal neutron spectra (BF_3 detector) are plotted in Fig. 2.29 and the 90° spectra in Fig. 2.30.

The spectrum from 200 eV to 10 MeV at r = 20.3 cm, 30° is plotted in Fig. 2.31. The spectra at r = 35.6 cm and the various angles are plotted in Fig. 2.32 from 200 eV to 10 MeV, except at 0°. The high energy spectra at r = 50.8 cm are similarly plotted in Fig. 2.33.

Additional measurements and discussion of all results are included in Section 6.

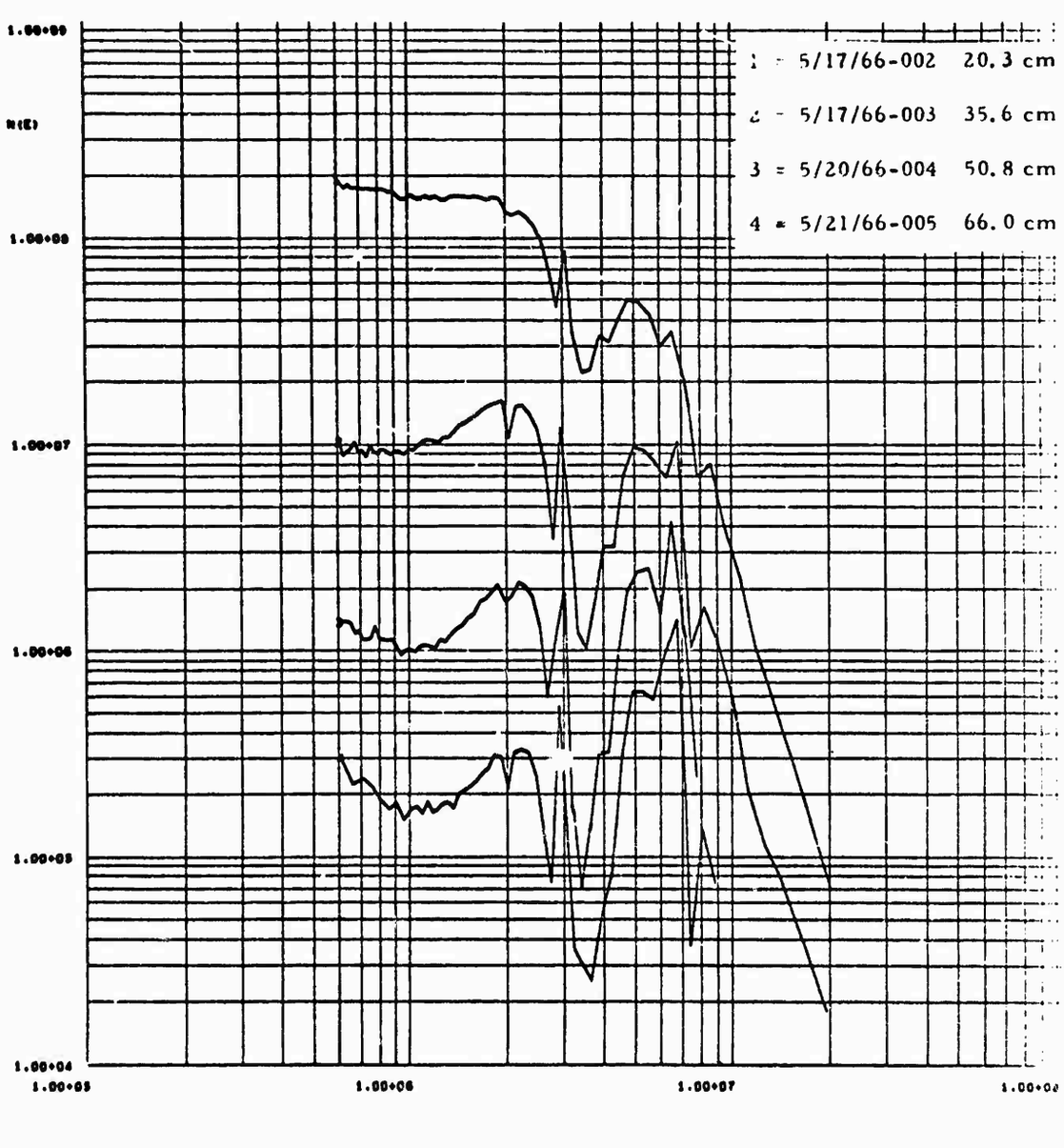

Fig. 2.28--Fast neutron spectra at 0^{o} vs radius

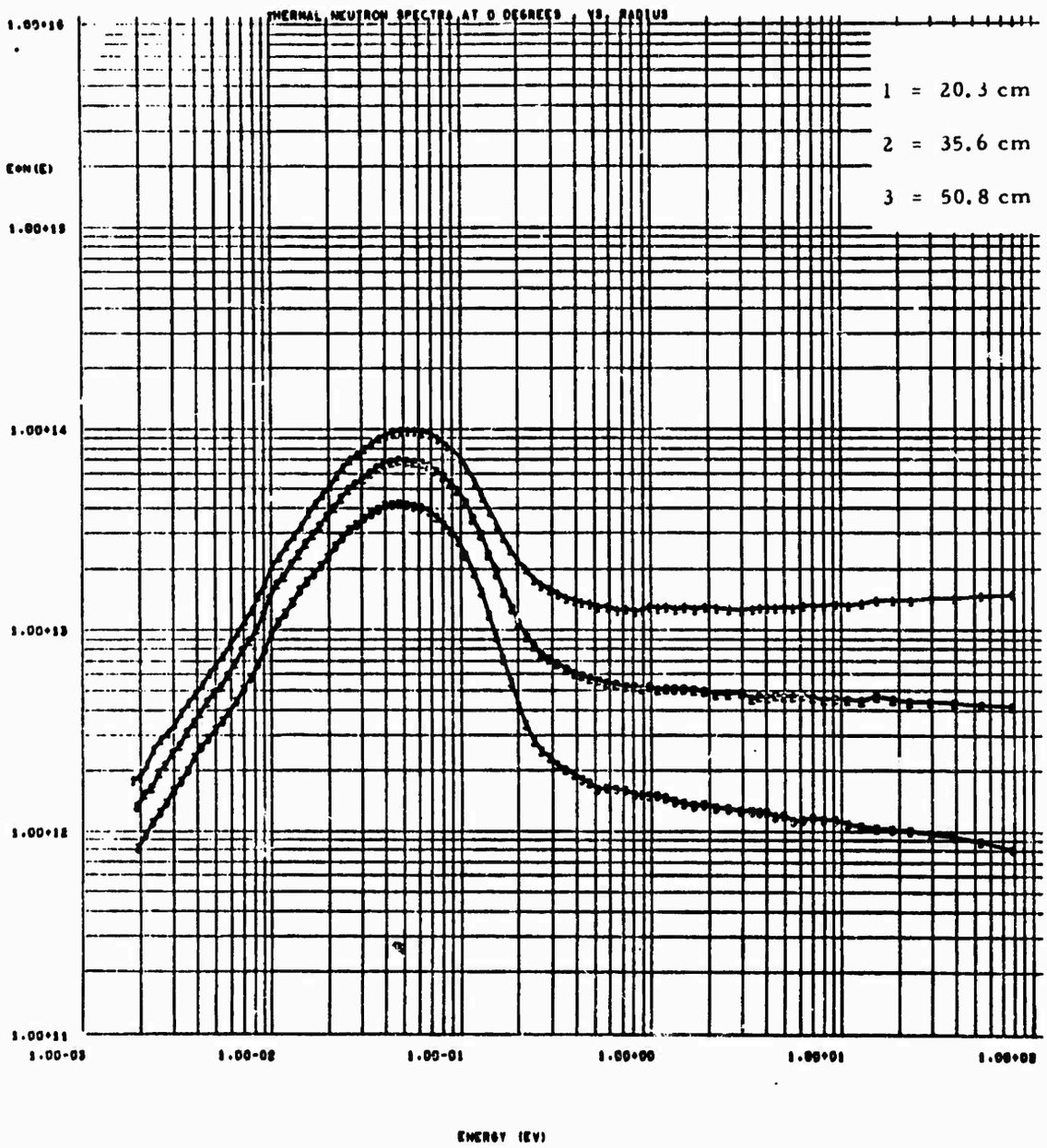

Fig. 2.29--Thermal neutron spectra at 0° vs radius

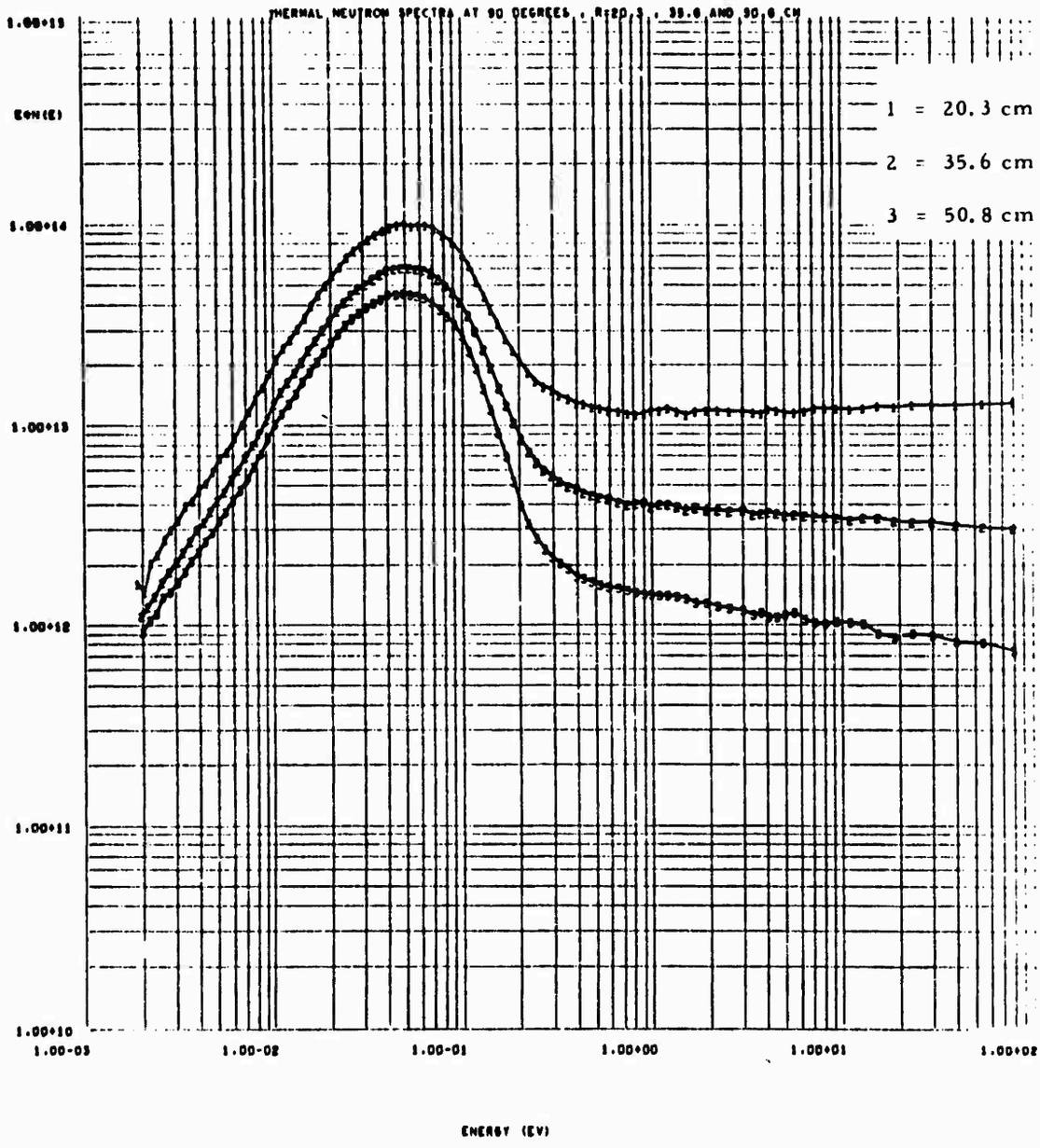

Fig. 2.30--Thermal neutron spectra at 90° vs radius

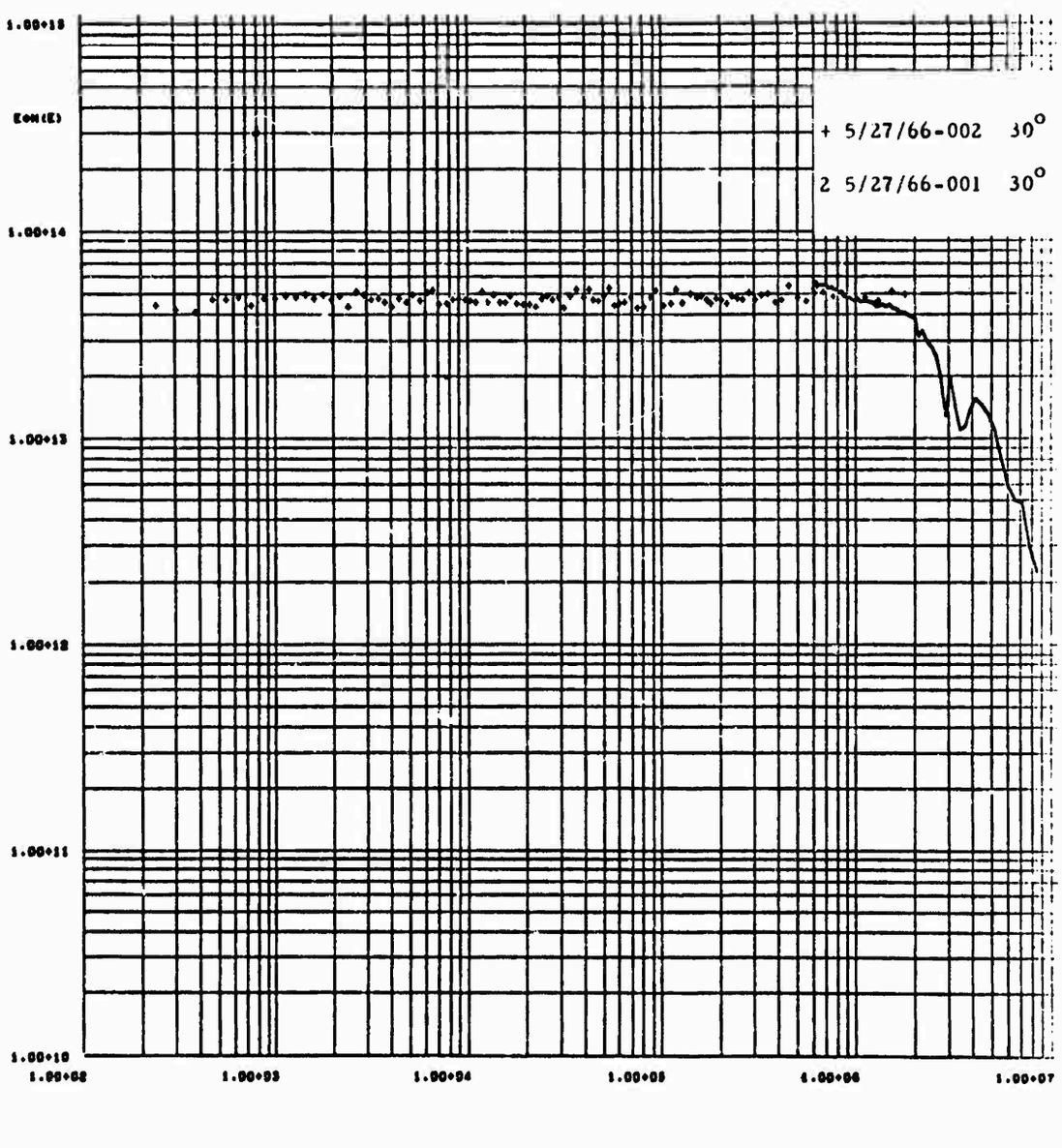

Fig. 2.31--High energy spectrum at 20.3 cm

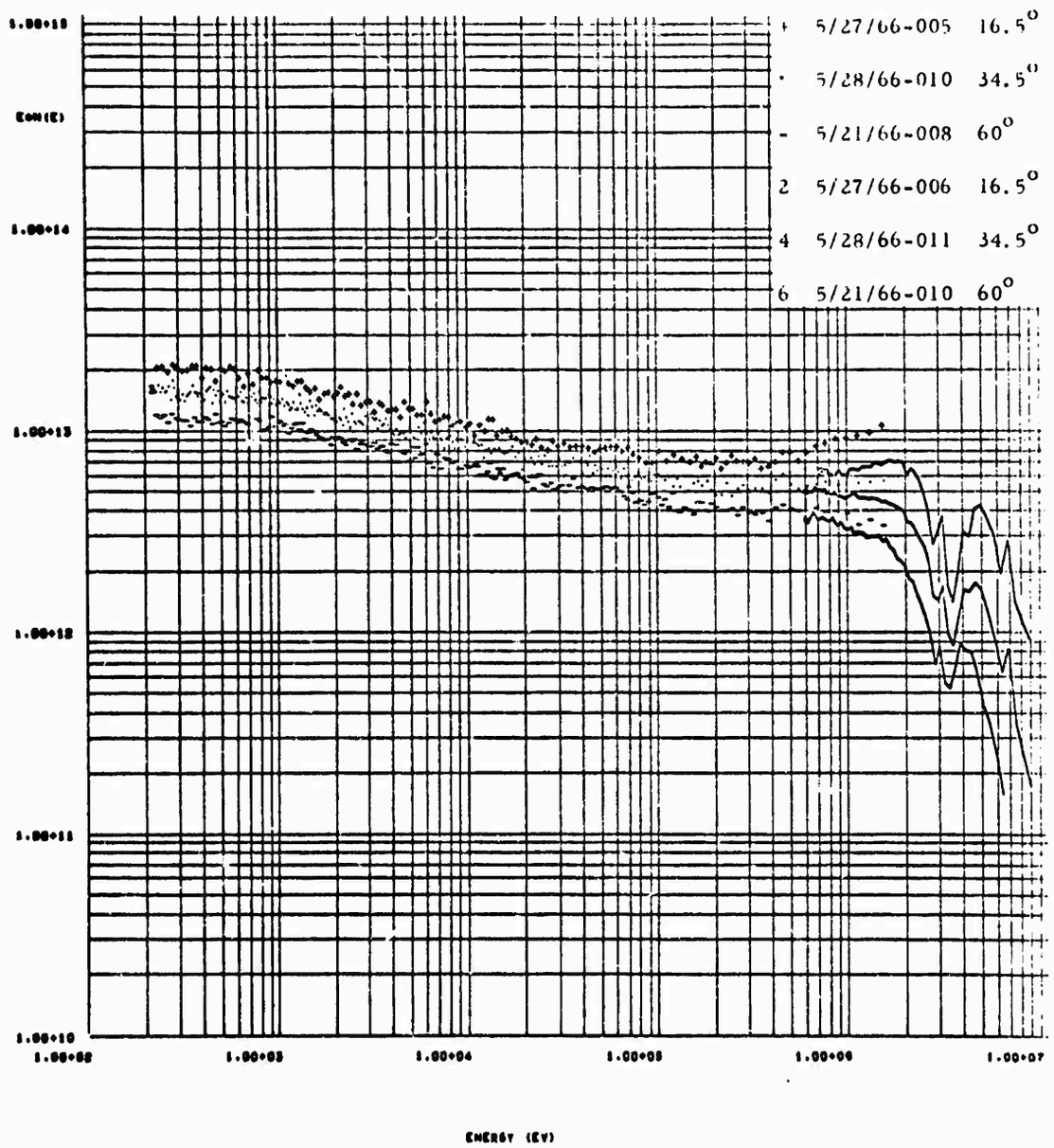

Fig. 2.32--High energy spectra at r = 35.6 cm

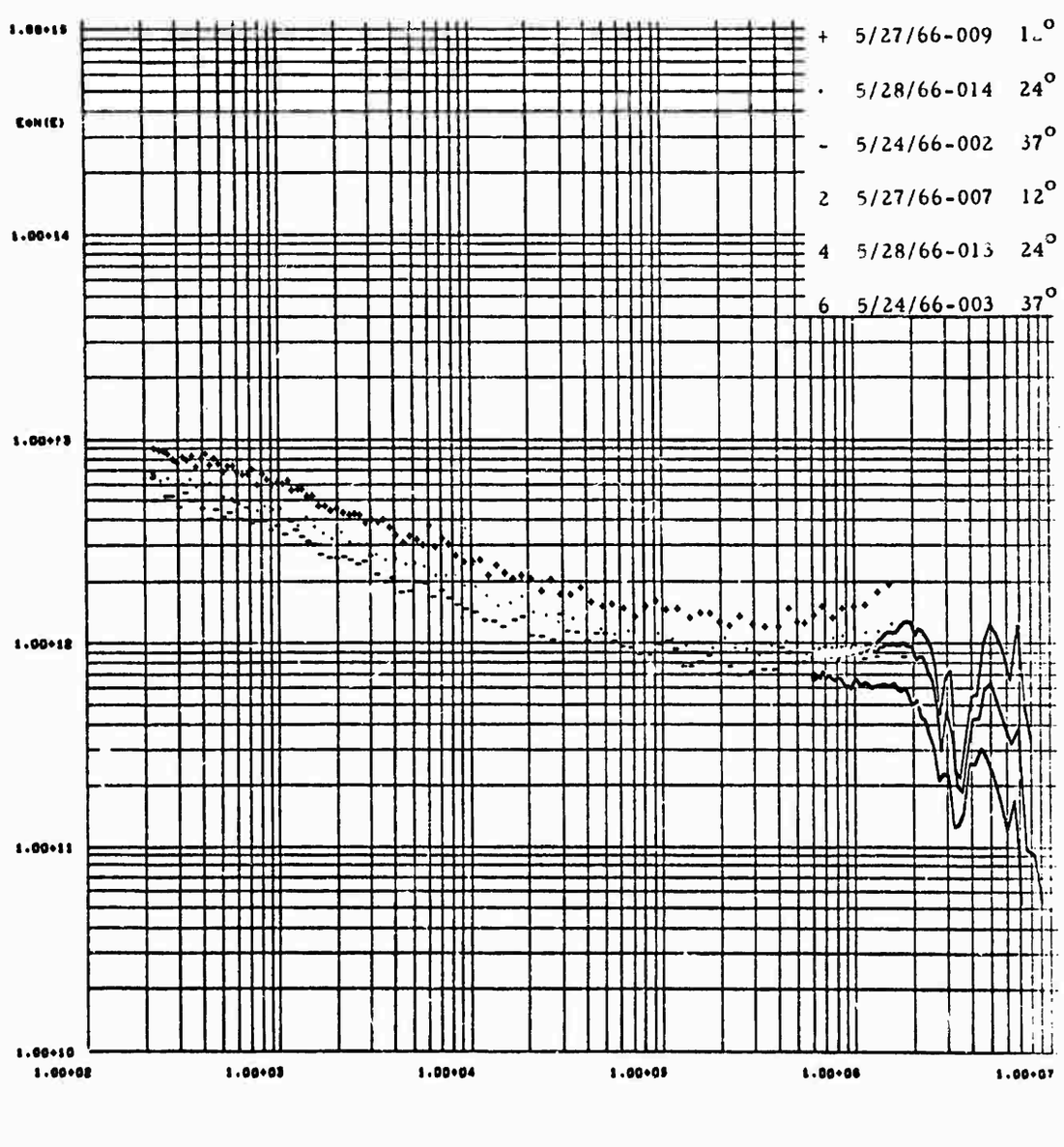

Fig. 2.33--High energy spectra at r = 50.8 cm

3. DIEAWAY EXPERIMENT AND MEAN EMISSION TIME

In our large, unpoisoned graphite stack, the mean emission time (MET) of thermal neutrons is quite long. For a pure fundamental mode the MET approaches, at certain energies, 0.15 times the neutron time of flight (T-O-F) for a 50-m flight path. In off-center measurement positions the ratio can easily be as high as 0.25 (cf. Fig. 3.1). Thus a 10% error in the determination of the MET will result in an error of up to 5% in the neutron energy assigned to a certain time channel, and the error further distorts the measured spectrum when reducing the data with a detector sensitivity curve shifted in energy. (A 10% error in the determination of the MET is not unlikely since it changes very rapidly with energy precisely in the .1 eV region, where MET/TOF is largest.) For these reasons, a careful determination of the MET was undertaken in the present experimental program. As a byproduct, information about the time spread of the neutron emission was obtained, which was applied to evaluate the energy resolution of the measured spectra.

The MET was determined at the positions of the T-O-F measurements by the following steps:

1. Measurements of the neutron dieaway
2. Approximate modal analysis of the results
3. Evaluation of the absorption cross section
4. Calculation of the slowing down time with the continuous slowing down model.
5. Calculation of the migration time (mean value and standard deviation) for the fundamental mode by the time moments method with the GATHER-II code (101 groups for energies from 1.55 eV down).

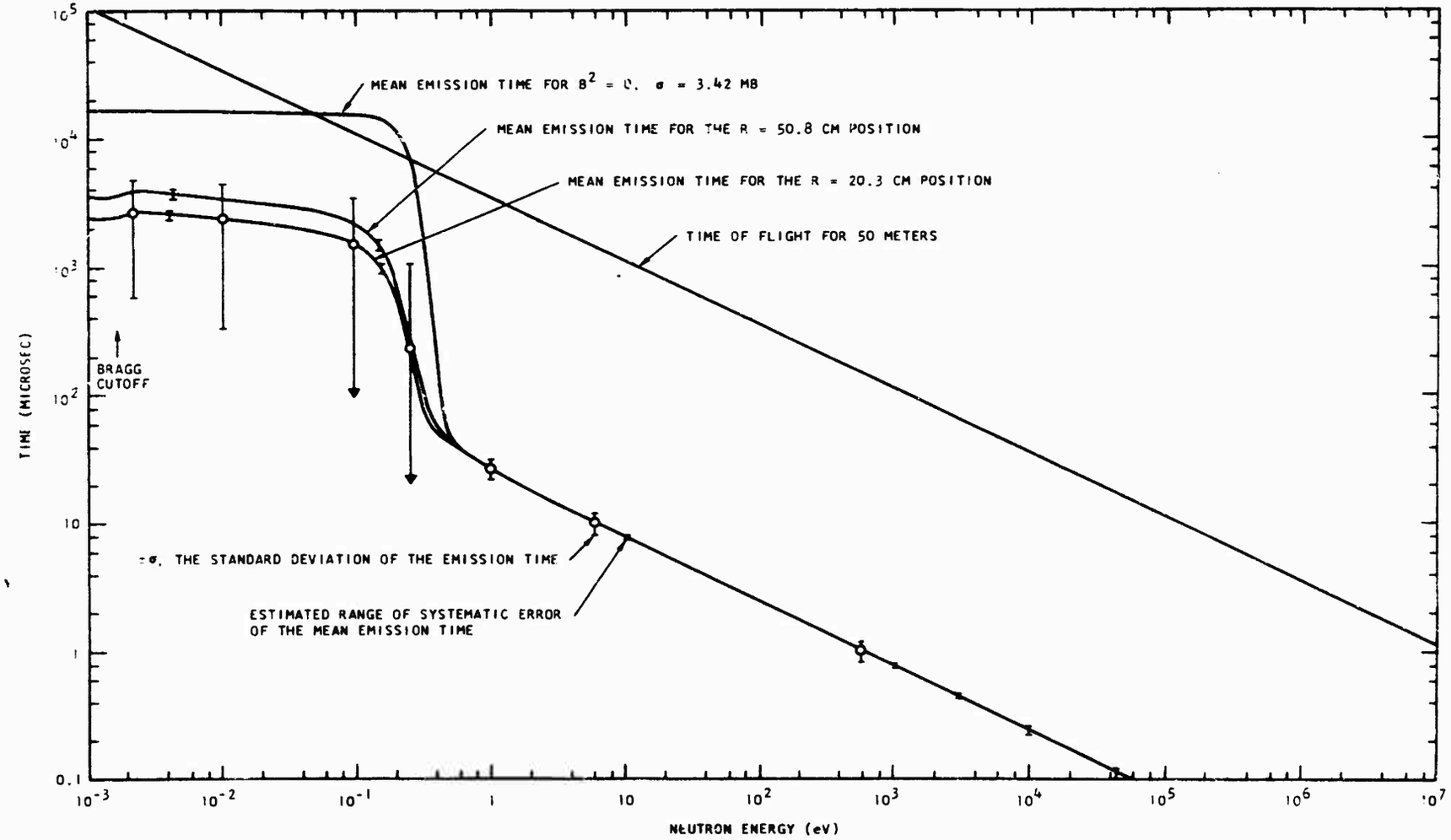

Fig. 3.1--Emission and flight times

6. Evaluation of the spatial dependence of the MET.

3.1 NEUTRON DIEAWAY MEASUREMENTS

The time dependence of the thermal neutron population was measured at the four locations in the graphite stack where neutron spectrum measurements were made (20.3 cm, 35.6 cm, 50.8 cm, and 66 cm radius). The graphite stack setup was the same as for the 90° spectrum measurements. In every case the detector was located against the bottom wall of the 3.81 cm diameter reentrant hole. A block diagram of the electronics used is shown in Fig. 3.2. The detector was a 0.63-cm diameter, 2.5 cm active length fission chamber internally coated with U^{235}. It is well known that the practical U^{235} thickness limitation on these detectors is imposed by the fission fragment range. Even a "thick" 2 mg U_3O_8/cm^2 detector has a negligible effect due to self-shielding on the energy dependence of its thermal neutron sensitivity: 1% on radially incident 0.002 eV neutrons. The discriminator was set in the valley in the pulse height spectrum between the noise and the fission fragment pulses. The time distributions of the pulses after the Linac burst, obtained with a TMC 1024-cnannel analyzer, are shown in Fig. 3.3. Ten μsec channels were used with a 10-μsec lapse between channels to allow for storage in the computer memory. The time analyzer was started by the injector trigger of the Linac (t = 0), coincident with the electron burst. The leading edge of the first channel occurs 18 μsec thereafter.

The Linac pulse repetition rate was increased to 30 pps; in the thermal spectrum measurements it had to be lower to avoid pulse overlap due to the long TOF of the lower energy neutrons. In all the runs the electron burst width was very short, 20 nsec or less; the electron energy was the same as in the T-O-F runs, 28 MeV, and the current was low enough to keep the deadtime count losses below 1% in all the time channels used for the decay constant computation.

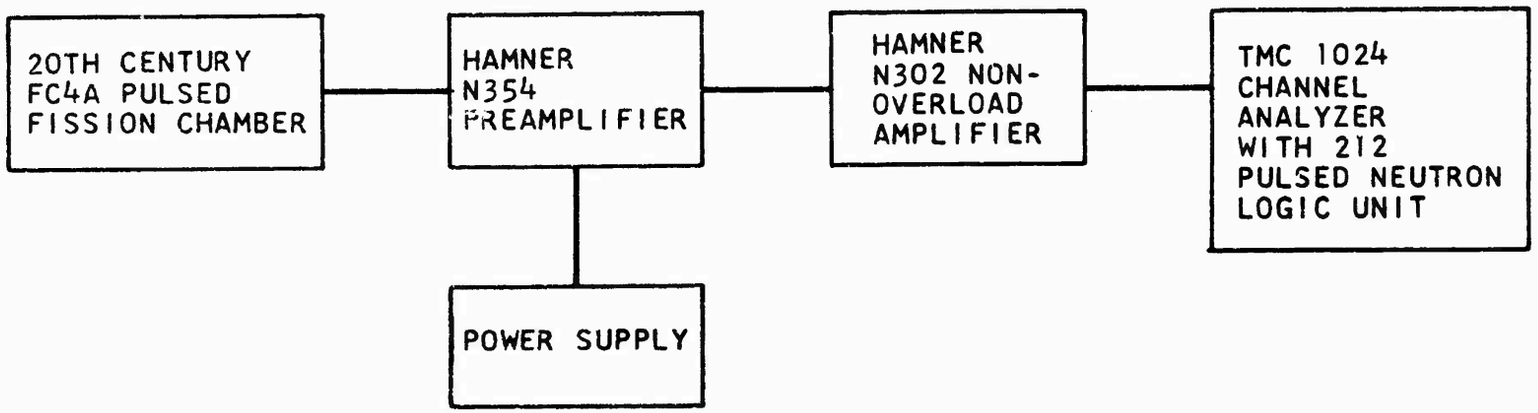

Fig. 3.2--Electronics for the dieaway measurements

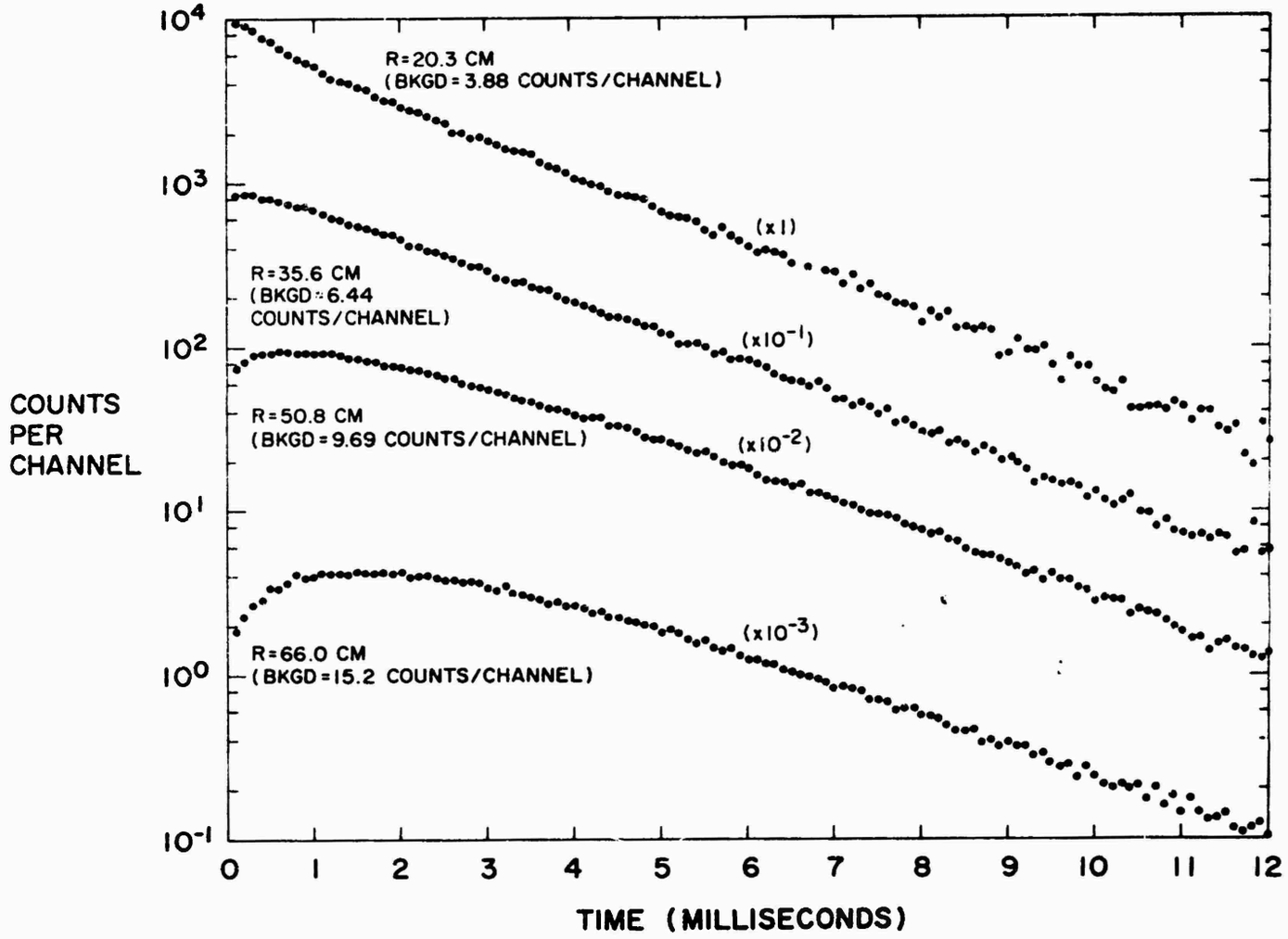

Fig. 3.3--Neutron dieaway measurements

A constant background for every run (which includes counts from neutrons from previous bursts) was determined at long times after the Linac pulse, and subtracted from the data.

3.2 APPROXIMATE MODAL ANALYSIS OF THE RESULTS

The time distribution of the U^{235} fission detector count rate

$$C(t) = k \int_E \sigma_f(E)\varphi(E,t)dE \simeq k' \int_E \frac{1}{v}\varphi(E,t)dE = k'n(t)$$

is seen to be approximately (except for non 1/v behavior of $_f(E)$) proportional to the thermal neutron population n(t). The data were analyzed with the code GAPS.[9] The least-squares fit to

$$C(t) = C_o e^{-\lambda t} \qquad (3.1)$$

resulted in the values shown in Table 3.1 for λ, its standard deviation σ_λ, and C_o, for different ranges of time after the Linac burst. It is worth noting that the λ values in our experiment are well below $(\nu\Sigma)_{min}$ = 2600 sec^{-1}[10], or even $(\nu\Sigma)_{min}$ = 1000 sec^{-1} for graphite,[8] and that the waiting times after the Linac burst are safely above the recommended value of 2 msec.[12, 13]

To thoroughly understand the position and time dependence of the λ values, a qualitative picture was drawn of the contributions of the first four "longitudinal" modes (those along the 152 cm axis), according to the source and detector positions in the graphite assembly (see Fig. 3.4). Along the 112 cm axes, the source and detector are centered, so that only the fundamental and higher odd modes will be present.

The constancy of λ in the 20.3 cm radius position, after 2.8 msec, shows that only the first longitudinal mode is observed there at long times. Hence, λ_{111} (i.e., the value of λ for the 111 mode) is taken as (478.4±1.3) sec^{-1}.

Table 3.1

EXPONENTIAL FIT PARAMETERS FOR C(t)

Position	Time range msec	λ sec^{-1}	σ sec^{-1}	λ^{-1} msec	C_0
20.3 cm, 90°	2.8 to 12	478.4	1.3	2.090	7578.
	2.8 to 4.9	475.6	4.4	2.103	7823.
	4.9 to 7.8	460.6	5.1	2.171	6818.
	7.8 to 12.	481.1	7.6	2.079	7692.
35.6 cm, 90°	3. to 12.	452.7	1.2	2.209	11745.
	3. to 4.8	428.2	4.8	2.336	10635.
	4.8 to 7.4	444.2	5.4	2.251	11390.
	7.4 to 12.	483.0	4.3	2.070	15093.
50.8 cm, 90°	5.5 to 12.	453.6	1.6	2.204	27431.
	5.5 to 7.6	424.5	5.7	2.356	22748.
	7.6 to 9.6	459.0	6.5	2.179	29145.
	9.6 to 12.	488.4	9.4	2.048	38605.
66.0 cm, 90°	5.8 to 11.2	433.2	2.2	2.308	17309.
	5.8 to 8.2	411.4	5.1	2.431	14961.
	8.2 to 11.2	444.5	6.4	2.250	19133.

This value, with the λ_{tr} and Σ_a calculated as described in Section 3.3, results in

$(\lambda_{111})^{-1} = 2.09$ msec $\quad (\lambda_{131})^{-1} = 0.58$ msec $\quad (\lambda_{133})^{-1} = 0.34$ msec

$(\lambda_{211})^{-1} = 1.37$ msec $\quad (\lambda_{231})^{-1} = 0.51$ msec $\quad (\lambda_{233})^{-1} = 0.31$ msec

$(\lambda_{311})^{-1} = 0.87$ msec $\quad (\lambda_{331})^{-1} = 0.42$ msec $\quad (\lambda_{333})^{-1} = 0.28$ msec

$(\lambda_{411})^{-1} = 0.57$ msec $\quad (\lambda_{431})^{-1} = 0.34$ msec $\quad (\lambda_{433})^{-1} = 0.24$ msec,

where the first subindex corresponds to the longitudinal mode.

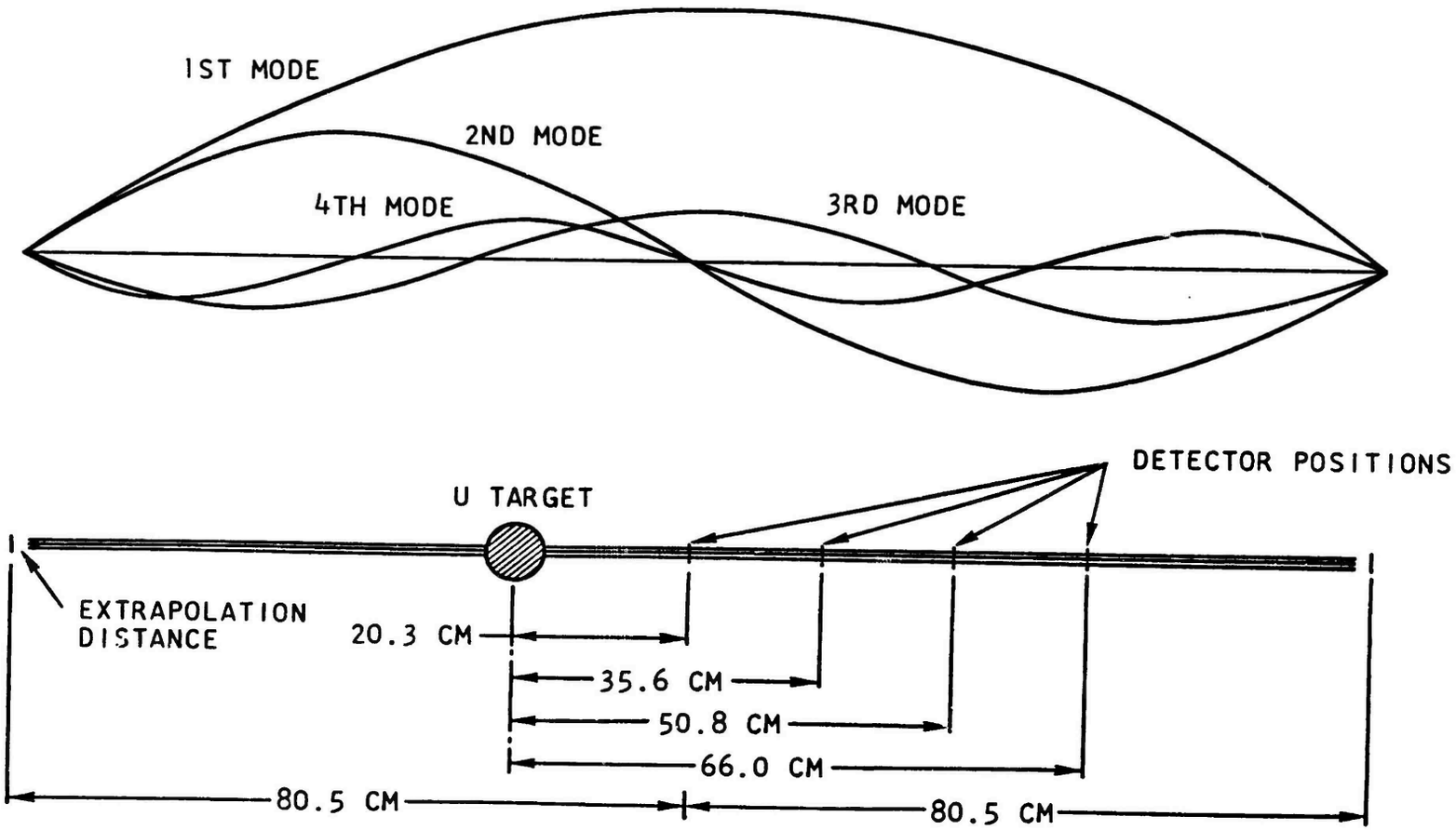

Fig. 3.4--Qualitative picture of the contributions of the first four axial modes

The preceding qualitative and numerical information suggested analyzing the dieaway at 35.6 cm, 50.8 cm, and 66.0 cm radius in terms of two longitudinal (z-axis) modes, thus

$$n(z,t) = c_{111}e^{-\lambda_{111}t}\cos B_{111}z + c_{211}e^{-\lambda_{211}t}\cos B_{211}z \qquad (3.2)$$

where B_{111} and B_{211} are the square-roots of the buckling for the two modes (calculated from the extrapolated dimensions). At 35.6 cm and 50.8 cm the dieaway eventually reaches the fundamental (first) mode and the coefficient c_{111} can be evaluated. Subtracting the counting rate that follows the first mode decay from the total counting rate at early times, we can evaluate c_{211}. Then at intermediate times the difference between the measured counting rate and that calculated from Eq. 3.2 is a measure of the accuracy of the two-mode description. Table 3.2 gives the results. The measured counting rates at each radius are normalized for convenience. The differences between calculated and measured values are sufficiently small to indicate the adequacy of the two-mode analysis for times greater than 3 msec (35.6 cm) or 5.5 msec (50.8 cm).

At 66.0 cm the dieaway reached background before the pure first mode was established. In this case the separation into modes was accomplished by taking $c_{211}/c_{111} = 0.50$, the same as at 35.6 cm. (The ratio should be constant, but at 50.8 cm it was 0.46, since the two-mode description is not exact.)

Table 3.2

COMPARISON OF TWO-MODE DESCRIPTION OF THERMAL NEUTRON POPULATION DIEAWAY WITH MEASURED VALUES

R = 35.6 cm

Time (msec)	Measured	First mode	Second mode	1st and 2nd modes	Difference %
3.0	65.8	76.2	-10.7	65.5	0
4.8	29.9	-	-	29.5	-1
7.4	9.4	-	-	9.0	-4
12.0	1.00	-	-	1.03	3

R = 50.8 cm

Time (msec)	Measured	First mode	Second mode	1st and 2nd modes	Difference %
5.5	19.8	22.8	-3.0	19.8	0
7.6	8.1	-	-	7.85	-3
9.6	3.23	-	-	3.08	-5
12.0	1.00	-	-	1.00	0

R = 66.0 cm

Time (msec)	Measured	First mode	Second mode	1st and 2nd modes	Difference %
5.8	10.2	12.5	-2.3	10.2	0
8.2	3.82	-	-	3.62	-5
11.2	1.00	-	-	0.92	-8

3.3 EVALUATION OF THE ABSORPTION CROSS SECTION

As usual, the absorption cross section of the graphite could not be computed to the needed degree of precision from chemical analysis. It was therefore calculated from the expression for the fundamental mode decay constant λ_{111} on pages 215 and 220 of Ref. (14).

$$\lambda_{111} = \overline{v\Sigma_a} + (\overline{Dv})_o B^2 - CB^4 + FB^6 + \ldots \qquad (3.3)$$

where:

B^2 is the geometrical (fundamental mode) buckling,

C is the diffusion cooling constant,

F is the coefficient of the third degree term in the polynomial approximation for $\lambda_{111} = \lambda_{111}(B^2)$,

$\overline{v\Sigma_a}$ is the average value of the product $v\Sigma_a$, which is independent of the spectrum unless Σ_a does not depend on energy as 1/v,

$\overline{(Dv)_o}$ is the average value of the product Dv for a Maxwellian neutron distribution with a temperature equal to the temperature of the moderator.

$\lambda_{111} = 478.4 \pm 1.3 \text{ sec}^{-1}$ (from Section 3.2).

The density of our graphite was taken to be (1.66) gcm^{-3}, and the measurements were made at 25°C, i.e., for $\bar{v} = 2.50 \times 10^5 \text{ cm sec}^{-1}$.

A value of $\lambda_{tr} = 2.50$ cm was used, obtained by reducing to the density of our graphite the average of Tables 3.10 and 3.12 of Ref. (15). From this extrapolation distance $\epsilon = 1.77$ cm, and $B^2 = .001890 \text{ cm}^{-2}$. Then, using the values appropriate to our temperature, density, and buckling range,

1. $\Sigma_a = (38.2 \pm 2.5) \times 10^{-5} \text{ cm}^{-1}$ with $(\overline{Dv})_o$ and C from the three parameter analysis of Ref. 12.
2. $\Sigma_a = (38.2 \pm 2.5) \times 10^{-5} \text{ cm}^{-1}$ with $(\overline{Dv})_o$, C and F from the four parameter analysis of Ref. 12.
3. $\Sigma_a = (39.2 \pm 1.5) \times 10^{-5} \text{ cm}^{-1}$ with $(\overline{Dv})_o$ and C from the three parameter analysis of Ref. 13.

A value of $\Sigma_a = (38.8 \pm 2.5) \times 10^{-5} \text{ cm}^{-1}$ was chosen. (Note that with the value of D = 0.833 cm, this corresponds to a diffusion length L = 46.4 cm. At 0.025 eV, $\sigma_a = 5.3 \pm 0.4$ mb compared to pure carbon $\sigma_a = 3.4 \pm 0.2$ mb. The difference may be explained by 0.25 mb absorption due to nitrogen in the pores, 0.85 mb from 1 ppm boron, and about 0.15 mb equivalent from neutrons absorbed in the target.

3.4 CALCULATION OF THE SLOWING-DOWN TIME

In the energy region well above thermal, where no upscattering is possible, the leakage effect was neglected for the calculation of the slowing-down time. This is a usual and justified assumption, since for carbon and for our fission-type source spectrum:

1. There is practically no inelastic scattering below 4.43 MeV, the first excited state of C^{12} (the first excited state of C^{13}, 1.11% in abundance, is 3.09 MeV).

2. Since $\alpha = 0.716$ all neutrons which have slowed down to energy E have at least suffered (except for inelastic scattering) one collision at an energy $E' \leq E/\alpha < 1.4\ E$; and since the cross sections are very smooth below 2 MeV down to the thermal region, the leakage probabilities do not vary appreciably within all the possible histories which can lead a neutron to have energy E.

Hence, the average time for a neutron to slow down to energy E is not affected by the dimensions of the graphite stack to a good approximation.

The mean slowing-down time was calculated then for pure elastic scattering in an infinite medium with the formula from page 172 of Ref. (14) with a correction for the velocity v_Q corresponding to the average neutron source energy, taken as 2 MeV:

$$\langle t_E \rangle = \frac{A(A+2)}{(A+\frac{2}{3})\bar{\Sigma}_s}\left(\frac{1}{v} - \frac{1}{v_Q}\right) \tag{3.4}$$

where $\bar{\Sigma}_s$ is the average macroscopic scattering cross section.

The value of the ratio of the standard deviation of t_E to $\langle t_E \rangle$ is independent of E. From the same source:

$$\frac{\sigma}{\langle t_E \rangle} = \left[\frac{(A+4)(A+\frac{2}{3})}{(A+2)^2} - 1\right]^{1/2} \tag{3.5}$$

For graphite, $\sigma/\langle t_E \rangle = 0.185$ gives a measure of the relative dispersion in the time of moderation to energy E.

The calculation with Eq. (3.4) was performed for the energy range between the average source energy (2 MeV) and the source energies for the GATHER-II calculation discussed in Section 3.5.

Estimated ranges for systematic errors are as follows:

Above	1	MeV	± 100%
	0.5	MeV	± 50%
	0.25	MeV	± 25%
	0.1	MeV	± 15%
	30	keV	± 10%
	10	keV	± 8%
	3	keV	± 5%
Below	1	keV	± 3%

In the first few values, the main source of error lies in not having considered the energy distribution of the source neutrons. In the others, the error is attributed to the uncertainty of the $\bar{\Sigma}_s$ calculation. However, the mean emission time in this range is small compared to the time-of-flight (cf. Fig. 3.1), and there are other more important sources of error.

3.5 CALCULATION OF THE MIGRATION TIME FOR THE FUNDAMENTAL MODE

The principles of the time moments method for the calculation of migration times are described elsewhere.[16] The code GATHER-II, incorporated into the code GGC-II,[17] was used to calculate the neutron flux and its first and second time moments, $\langle t \rangle$ and $\langle t^2 \rangle$, as a function of energy, in the P_0 approximation. The code worked on 101 energy points from 1.55 to 0.001 eV with cross sections from the "BE 92PT GASKET" tape for:

1. Graphite at 300°K (the temperature in our experiment was actually 298.2°K) including scattering data from Ref. (18).

2. A 1/v absorber, no scattering, to account for the excess of σ_a for the graphite used in the measurements over σ_a for graphite in the tape. The energy dependence of the different values of σ_a was taken into account in assigning an atom density to this absorber.

The buckling $B^2 = 0.001890\ cm^{-2}$ (from Section 3.3) was used. The source term was calculated by the code, assuming a 1/E epithermal flux. No appreciable difference in computer running time was observed when using a flux guess $\varphi = 1$ or the output of a previous similar problem.

The first time moment calculated by the code, plus the slowing-down time to the source energy, is the MET as a function of energy for the fundamental mode. Since the source is spread over several energy groups between 1.55 and 1.15 eV $\cong \alpha$ (1.55 eV), a weighted average of the corresponding mean slowing down times was used.

The standard deviation of the emission time, $\sigma_{em} = \sqrt{\langle t^2 \rangle - \langle t \rangle^2}$, and the ratio of the standard deviation to the MET and TOF was determined for a few energy values with the results shown in Table 3.3. The high values of this ratio in the 0.15 eV region seriously limit the energy resolution in that area. However, this only happens to such a degree in unpoisoned graphite measurements, and then the spectrum is smooth. Obviously, when a poison is present, the emission time, and hence σ are very much shortened; and for a fixed flight path length σ_{em}/TOF is smaller and the energy resolution considerably improved.

Table 3.3

STANDARD DEVIATION OF THE EMISSION TIME
FOR THE FUNDAMENTAL MODE

Energy eV	σ_{em} msec	σ_{em} MET	σ_{em}/TOF
0.0022	2.16	0.77	.028
0.010	2.07	0.84	.058
0.095	1.93	1.18	.168
0.130	1.82	1.38	.184
0.150	1.72	1.55	.187
0.170	1.58	1.78	.184
0.200	1.31	2.24	.164
0.245	0.84	3.21	.117
0.305	0.374	3.91	.058
0.995	0.005	0.18	.001

3.6 SPATIAL DEPENDENCE OF THE MEAN EMISSION TIME

Before choosing the method for describing the spatial dependence of the MET, let us consider the consistency of the two sets of data available:

1. The "calculated" $\bar{t}$ as a function of energy from the GATHER-II code, as discussed in Section 3.5. These values are based on the geometrical buckling in the fundamental mode of our graphite stack, and on a Σ_a resulting from the measured dieaway constant λ_{111}, as discussed in Sections 3.2 and 3.3. It should be recalled that GATHER-II is an infinite-medium code, and it furnishes the flux and its time-moments for a pure spatial mode in the P_o approximation.

2. The "measured" time-dependent flux, energy-integrated by the detector, as a function of position.

In order to compare the two sets of data, the "calculated" first time moment (the MET) was averaged in energy with the corresponding flux calculated by GATHER-II, multiplied by the U^{235} fission cross section

as the weighting function. The resulting energy-averaged MET is given in the first line of Table 3.4. The following four lines show the effect on the energy-averaged MET of varying several parameters in its calculation.

The "measured" energy-averaged MET (also designated by <MET>) for each of the four detector locations includes contributions from several spatial modes. The values listed in Table 3.4 were computed by properly integrating the time distributions plotted in Fig. 3.3. In the last line of the table, the value of $(\lambda_{111})^{-1}$ is considered to be the <MET> for a pure fundamental mode.

There is a discrepancy of 7% between the 1.95 msec from the first line of the "calculated" <MET> and the 2.09 msec of the last line for the "measured" <MET>. Several possible reasons for the discrepancy were investigated:

1. It would be inconsistent to use the graphite absorption cross section from the "BE 92P7 GASKET" tape, instead of the diffusion-cooling corrected cross section as measured in our stack. However, it is worth noting that if the GASKET cross section were used, it would bring the "calculated" value to within 1% of the "measured" value.

2. A reduction in the buckling of 1% (corresponding to increasing all three extrapolated dimensions of the stack by 0.5 cm) would increase the "calculated" value by only 1%.

3. A reduction of the diffusion coefficient by 1% would have the same effect.

4. Use of $\varphi(E)v^{-1}$ as weighting function instead of the proper one would increase the "calculated" value by 1%.

Examination of the dieaway experiment showed that:

1. As explained in Section 3.1, the self-shielding effect of the detector is negligible.

Table 3.4

MEAN EMISSION TIME VALUES AVERAGED IN ENERGY

"Calculated" Values, Integrated from GATHER II MET(E) Plus Slowing Down Time (Fundamental Mode)

$B^2(cm^{-2})$	$\sigma_a(.025\ eV)$ (mbarn)	Weight function	⟨MET⟩ (msec)
.001890[a]	5.33[a]	$\varphi(E)\sigma_f(E)$	1.95
.001890[a]	4.65[b]	$\varphi(E)\sigma_f(E)$	1.99
.001890[a]	3.42[c]	$\varphi(E)\sigma_f(E)$	2.07
.001875	3.42[c]	$\varphi(E)\sigma_f(E)$	2.09
.001890[a]	4.65[b]	$\varphi(E)v^{-1}$	1.97

"Measured" Values, Integrated from the Time Distribution of Pulses (Die Away Measurements)

Position	Modes contributing (cf. Fig. 3.3)	⟨MET(R)⟩ (msec)
R = 20.3 cm	Odd modes	1.99
R = 35.6 cm	All modes	2.36
R = 50.8 cm	All modes	2.87
R = 66.0 cm	All modes	3.36
-------	Pure fundamental mode: $\lambda_{111})^{-1}$	2.09

[a] Measured value

[b] Measured value, not corrected for diffusion cooling

[c] From BE 92 PT GASKET tape

2. The uncertainty in the position of the detector has a negligible effect on the fundamental mode dieaway constant determination (see Section 3.2).

3. About 7% of the neutron captures in the graphite stack occur in the target assembly (see Section 6.2) but the effect of this extra absorber is already taken into account in the calculations in a first approximation. In fact, Σ_a results from a measurement made in the stack as it is.

As a consequence of this analysis, we believe the small discrepancy between the two values can be attributed to:

1. The use of $(\lambda_{111})^{-1}$ as the "measured" value of the $\langle MET \rangle$ for a pure fundamental mode. This is equivalent to assuming that such a mode is excited for thermal neutrons instantaneously after the Linac burst:

$$\langle MET \rangle_{111} = \frac{\int_0^\infty \varphi_{111}(t)\, t\, dt}{\int_0^\infty \varphi_{111}(t)\, dt} ;$$

$$\frac{\int_0^\infty e^{-\lambda_{111} t}\, t\, dt}{\int_0^\infty e^{-\lambda_{111} t}\, dt} = \frac{1}{\lambda_{111}} \qquad (3.6)$$

Note that by extrapolating $\varphi(t)$ for $t \to 0$ in the r – 20.3 cm data, it can be estimated that

$$\langle MET \rangle_{111} \simeq 1.02\, (\lambda_{111})^{-1} \qquad (3.7)$$

Actually, the asymptotic value (2.09 msec), measured after thermalization has been completed, is not the same as the GATHER-II "calculated" value, which includes a contribution from epithermal neutrons (from the slowing-down source), and which decreases the energy-averaged MET.

2. The approximate nature of the models used to compute Σ_a from λ_{111} and to calculate the time-moments with GATHER-II.

Since a more exact analysis would be time-consuming, and since our primary purpose was to obtain a fairly small correction to time-of-flight data, we decided to normalize the MET values from GATHER-II to the experimental values for the different measurement positions. Assuming space-energy separability, this also counts for the spatial dependence of the MET.

It was observed in a GATHER-II calculation for $B^2 = 0$ that the MET does not differ appreciably from the $B^2 = .001890\ cm^{-2}$ values above 0.5 eV. Hence, the correction for position-dependence was made only for energies below 0.5 eV. (MET = 0.04 msec for that energy.) A linear correction was made:

$$MET(E, R) = 0.04\ msec + [MET(E, GATHER\text{-}II) - 0.04\ msec] \frac{\langle MET(R) \rangle}{1.95\ msec} \qquad (3.8)$$

with $\langle MET(R) \rangle$ from Table 3.4. The resulting MET(R, E) values are compiled in Table 3.5 (where the first four lines are written in the usual floating point notation, e.g., +06 means 10^6).

The systematic errors of MET(R, E) are estimated to be within ± 8%. This accounts for the observed difference between "calculated" and "measured" <MET> for the fundamental mode and for the error resulting from detector positioning which is at most ± 3%; and for the assumed space-energy separability. The resulting relative errors in the neutron energy are not larger than 2.2% in the 20.3 cm, and 3.2% in the 50.8 cm radius position; and this for the energy of the most unfavorable MET/TOF, which is approximately 0.1 eV (see Fig. 3.1).

The energy resolution limitation of these thermal spectrum measurements in unpoisoned graphite is mainly due to the standard deviation of the emission time as discussed in Section 3.5.

Table 3.5

MEAN EMISSION TIME AS A FUNCTION OF NEUTRON ENERGY FOR THREE DIFFERENT POSITIONS IN THE THERMAL SPECTRUM GRAPHITE STACK

E(eV)	2.	+06	1.	+06	5.	+05	2.5	+05	1.11	+05	6.25	+04	4.
MET(msec)	0.0	-06	14.6	-06	29.8	-06	42.4	-06	67.6	-06	92.1	-06	116.
E(eV)	2.78	+04	2.04	+04	1.56	+04	1.233	+04	1.	+04	6.95	+03	5.1
MET(msec)	138.	-06	162.	-06	186.	-06	215.	-06	235.	-06	282.	-06	332.
E(eV)	3.91	+03	3.09	+03	2.5	+03	1.6	+03	1.11	+03	816.		625.
MET(msec)	377.	-06	426.	-06	475.	-06	608.	-06	717.	-06	841.	-06	961.
E(eV)	494.		400.		330.		278.		237.		204.		156.
MET(msec)	1086.	-06	1201.	-06	1327.	-06	1452.	-06	1577.	-06	1692.		.00193
E(eV)	123.3		100.		69.5		51.		39.1		30.9		25.
MET(msec)	.00218		.00242		.00291		.00341		.0039		.00439		.00487
E(eV)	16.		11.1		8.16		6.25		4.94		4.		3.3
MET(msec)	.00609		.00731		.00853		.00976		.01098		.0122		.01342
E(eV)	2.78		2.37		2.04		1.55		1.45		1.36		1.28
MET(msec)	.01464		.01587		.01709		.0214		.0222		.0231		.024
E(eV)	1.21		1.15		1.1		1.06		1.03		1.01		.995
MET(msec)	.0249		.0258		.0266		.027		.0274		.0276		.028
E(eV)	.98		.965		.95		.935		.92		.905		.89
MET(msec)	.0282		.0284		.0287		.0289		.0291		.0294		.0297
E(eV)	.875		.86		.845		.83		.815		.8		.785
MET(msec)	.0299		.0302		.0305		.0308		.0312		.0315		.0318
E(eV)	.77		.755		.74		.725		.71		.695		.68
MET(msec)	.0322		.0325		.0329		.0333		.0337		.0342		.0346
E(eV)	.665		.65		.635		.62		.605		.59		.575
MET(msec)	.0351		.0356		.0361		.0366		.0372		.0377		.0383

E(eV)	.56	.545	.53	.515	.5	.485	.47
MET R = 20.3 cm(msec)	.0390	.0397	.0404	.0411	.042	.0429	.0439
MET R = 35.6 cm(msec)	.0390	.0397	.0404	.0411	.0423	.0434	.0447
MET R = 50.8 cm(msec)	.0390	.0397	.0404	.0411	.0428	.0442	.0457
E(eV)	.455	.44	.425	.41	.395	.38	.365
MET R = 20.3 cm(msec)	.0451	.0463	.0477	.0494	.0514	.0541	.0577
MET R = 35.6 cm(msec)	.046	.0475	.0492	.0511	.0536	.0568	.0611
MET R = 50.8 cm(msec)	.0473	.0491	.0512	.0536	.0565	.0604	.0656
E(eV)	.35	.335	.32	.305	.29	.275	.26
MET R = 20.3 cm(msec)	.0627	.0695	.0794	.0937	.1144	.1443	.1866
MET R = 35.6 cm(msec)	.0669	.075	.0868	.1037	.1283	.1638	.214
MET R = 50.8 cm(msec)	.0728	.0826	.0969	.1176	.1476	.1908	.2519
E(eV)	.245	.23	.215	.2	.19	.18	.17
MET R = 20.3 cm(msec)	.246	.324	.425	.545	.638	.734	.836
MET R = 35.6 cm(msec)	.284	.377	.497	.64	.75	.864	.985
MET R = 50.8 cm(msec)	.337	.45	.596	.771	.904	1.043	1.19
E(eV)	.16	.15	.14	.13	.123	.116	.109
MET R = 20.3 cm(msec)	.940	1.045	1.148	1.249	1.313	1.379	1.441
MET R = 35.6 cm(msec)	1.108	1.233	1.356	1.476	1.552	1.63	1.703
MET R = 50.8 cm(msec)	1.341	1.493	1.642	1.788	1.88	1.976	2.065
E(eV)	.102	.095	.088	.081	.074	.067	.06
MET R = 20.3 cm(msec)	1.502	1.56	1.617	1.673	1.727	1.781	1.834
MET R = 35.6 cm(msec)	1.776	1.844	1.913	1.979	2.042	2.107	2.17
MET R = 50.8 cm(msec)	2.153	2.236	2.32	2.4	2.478	2.557	2.633
E(eV)	.055	.05	.045	.04	.035	.03	.025
MET R = 20.3 cm(msec)	1.872	1.911	1.954	1.997	2.045	2.098	2.156
MET R = 35.6 cm(msec)	2.215	2.261	2.312	2.363	2.421	2.483	2.552
MET R = 50.8 cm(msec)	2.687	2.744	2.805	2.868	2.938	3.014	3.097
E(eV)	.02	.016	.013	.01	.008	.007	.006
MET R = 20.3 cm(msec)	2.222	2.281	2.326	2.405	2.461	2.491	2.534
MET R = 35.6 cm(msec)	2.63	2.701	2.754	2.848	2.914	2.949	3.001
MET R = 50.8 cm(msec)	3.193	3.279	3.343	3.458	3.539	3.582	3.644
E(eV)	.005	.004	.003	.0022	.0015	.001	
MET R = 20.3 cm(msec)	2.567	2.604	2.67	2.744	2.407	2.485	
MET R = 35.6 cm(msec)	3.040	3.084	3.162	3.251	2.85	2.942	
MET R = 50.8 cm(msec)	3.692	3.746	3.841	3.948	3.461	3.573	

4. ACTIVATION EXPERIMENT

4.1 INDIUM FOIL TRAVERSES

Indium foils, bare and cadmium covered, were irradiated in the graphite assembly to determine the spatial distribution of the thermal and resonance neutron flux. The buckling and approximate values of the thermal diffusion length and the neutron age were also derived. Gold foils were exposed at one point and analyzed by E. G. and G. to give the absolute magnitude of the thermal neutron flux.

The indium foils used were those numbered 23 through 157 in the Linac foil set. The foils are of an indium aluminum alloy which contains 12.7 ± 2% weight percent indium. Each foil is 0.0254 ± 0.000762 cm thick by 0.635 ± 0.00508 cm in diameter (specified by the supplier, Dresser Products, Inc., Great Barrington, Massachusetts) and has a mass of about 0.0220 ± 0.0008 gm (This number was not calculated but estimated from a table of foil weights which is in the possession of J. M. Neill of General Atomic.) Because of the consistency of the foil masses, no weight corrections were made to the counting data.

The cadmium covers were 0.9525 cm diameter by 0.05588 cm thick. Each cover consisted of a cup, with a slight indentation to hold the foil, and a flat cover. The bare, or uncovered, foils were placed between aluminum discs to avoid contamination of the foils by the cellophane tape used to hold them in place (Scotch Magic Tape).

A plan view of the graphite stack showing the locations at which the flux was mapped is shown in Fig. 4.1. In the Z direction a 3.81-cm diameter hole was drilled and cylindrical graphite plugs 10.16 cm long were made to slide in this hole. Indentations 0.95 cm in diameter and

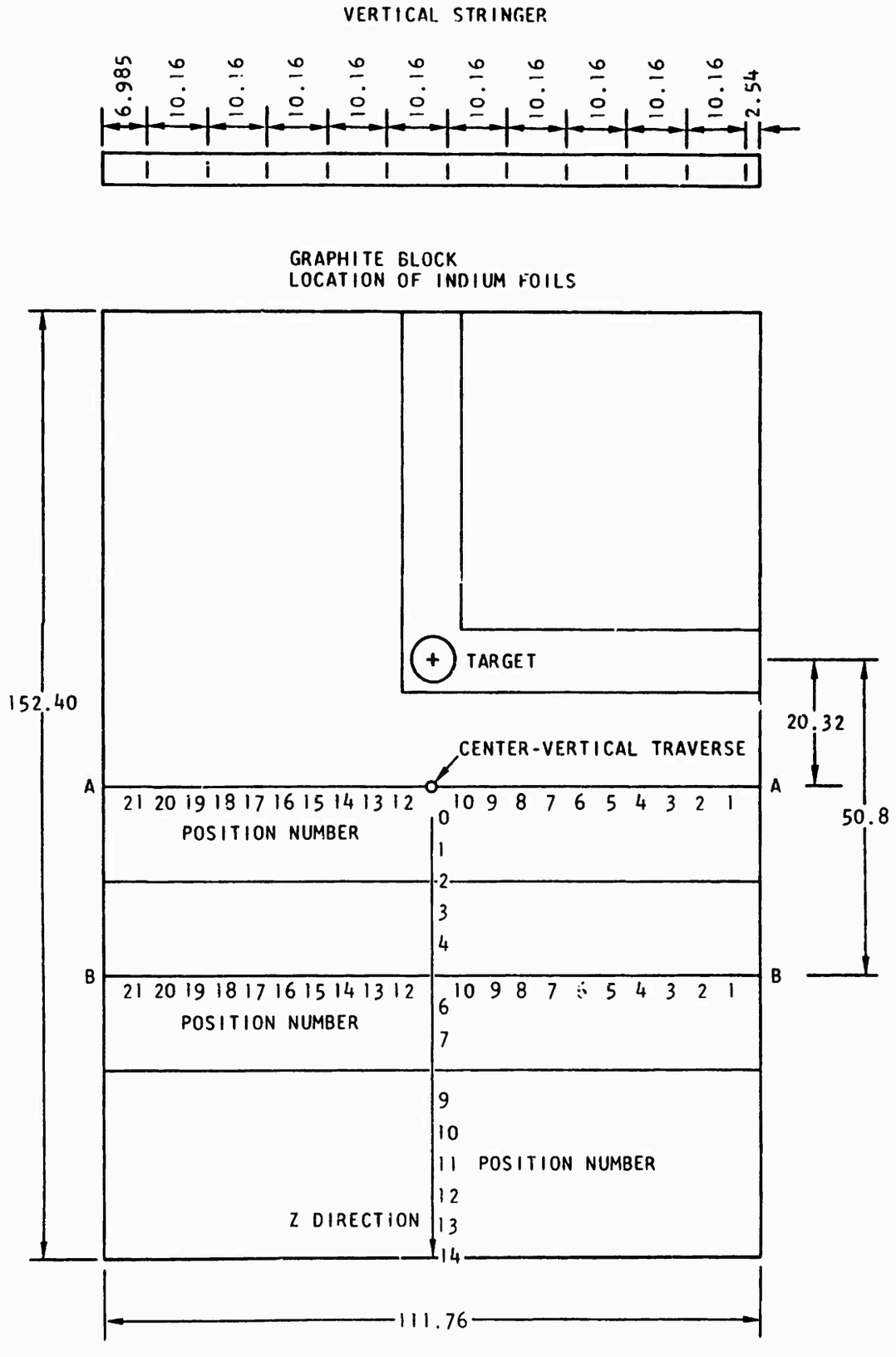

Fig. 4.1--Indium foil locations

0.318 cm deep were machined in the center of one face of each plug to hold the foils and their covers. During each irradiation the separation between foils was at least 10.16 cm. A 5.08 cm long cylindrical spacer was placed in one end of the hole on alternate runs so the neutron distribution could be mapped at 5.08 cm intervals.

For the AA and BB horizontal traverses, 10.16 cm cubes, with an indentation machined in one face to receive the foils, were used. These blocks were slightly undersized so they would slide through the stack and could be loaded simply by pushing one in after another. A spacer 5.08 cm thick was also available so the distribution could be mapped at 5.08 cm intervals.

A 2.461 cm diameter graphite rod was made to fit in a vertical hole through the center of the stack. The foils were placed in 0.318 cm slots milled in the rod at 10.16 cm intervals as shown in Fig. 4.1. For one run, the first slot was 2.54 cm from the bottom of the graphite block; for the succeeding irradiation the rod was turned over so that the first foil was 6.985 cm from the bottom. In this way the vertical distribution was mapped an approximately 5 cm intervals.

For all runs the foils were exposed for ten minutes as measured by a stop watch. The Linac was operated at 28 MeV with a beam current of 400 mA, 7.5 pulses per second, and a burst width of 0.2 μsec. Copper and indium foils were placed in reproducible positions during each run as flux monitors. The indium monitors were used to normalize each run rather than the copper because of the higher counting rates obtained.

After irradiation each foil was placed in a numbered plastic vial 1.59 cm diameter by 2.54 cm tall and counted in either a 5.08 x 5.08 cm NaI well crystal or on a 5.08 x 5.08 cm solid NaI crystal. In the latter case a plastic collar was fitted over the crystal to hold the vial, so that each could be counted in reproducible geometry. The bias on each counter was set at about 350 kilovolts (well crystal) or 200 kilovolts (solid crystal). The average background of the flat crystal was about 380 counts per

minute with the Linac on and 100 cpm with it off. The indium monitor foils were counted several times with each counter to establish a ratio so that all counts could be normalized to the well counter. Each foil was counted at least twice for one minute intervals. The data for each foil were then corrected for decay using a half-life of 54.42 minutes (John Neill's decay tables), averaged to give a single count for each foil, corrected to a common counter, and corrected by the monitor foils to give the flux distributions.

Most of the activations resulted in counting rates greater than 10,000 cpm, giving better than 1% statistics. However, some of the counts, particularly for the cadmium-covered foils far from the source, had higher errors. Some typical errors, representing one standard deviation, as calculated from counting statistics alone are given with the data tabulated in Table 4.1 to 4.4. The data are plotted in Figs. 4.2, 4.3, and 4.4, except for the BB horizontal traverse which had poor statistics in the cadmium-covered activity.

The good cadmium-covered indium data were plotted against the square of the distance from the source, on semilog paper. A straight line was drawn through the points at intermediate distances from the source. An age of 303 cm^2 was obtained from the slope. This may be compared with an age of 294 cm^2 for fission neutrons derived from adjusting to 1.65 g/cm^3 density the age reported on page 128 of Ref. 15.

Both horizontal and vertical traverses were taken to test for the possibility of a perturbation due to the heavy support table. However, both thermal (subcadmium) flux traverses are symmetrical and can be fitted with a cosine using an extrapolation distance of 1.77 cm from Section 3.3. The transverse buckling so obtained is then

$$B_1^2 = 2\left(\frac{\pi}{111.76 + 2(1.77)}\right)^2 = 1.484 \times 10^{-3}\ cm^{-2}$$

Although the experiment was not designed for a precision measurement of the diffusion length, it is interesting to calculate an approximate L

Table 4.1

INDIUM HORIZONTAL TRAVERSE (AA)

Distance From center (cm)	Bare Foil Counts/min.	Cd-Covered Counts/min.	Difference	Cadmium Ratio
0		81719		
5.08	236090 ± < 1%	86367 ± < 1%	149733	2.74
10.16	228000	76055	151945	3.00
15.24	200390	68512	131878	2.94
20.32	167617	51672	115845	3.24
25.40	147706	39997	107709	3.70
30.48	125870	25864	100006	4.85
35.56	92376	22247	70129	4.15
40.64	68365	16500	51865	4.14
45.72	44309 ± ~ 1.5%	9298	35011	4.77
50.80	24480	5502 ± ~ 3%	18978	4.44
55.88	7256	1000	6256	7.3

Table 4.2

INDIUM HORIZONTAL TRAVERSE (BB)

Distance From center (cm)	Bare Foil Counts/min.	Cd-Covered Counts/min.	Difference	Cd Ratio
0	72673			
5.08	68816	7913	60903	8.70
10.16	67245	5493	61752	12.24
15.24	65232	5841	59391	11.17
20.32	63747	3189	60558	20.09
25.40	58893	3154	55739	18.67
30.48	54216	1646	52570	32.94
35.56	48246	1101	47145	43.82
40.64	41679	927	40752	44.96
45.72	33392	212	33180	157.51
50.80	25918	770	25148	33.66
55.88				

Table 4.3

INDIUM VERTICAL TRAVERSE

Distance From Bottom of Stack (cm)	Bare Foil Count/min.	Cd-Covered Counts/min.	Difference	Cd Ratio
2.54	18044	3609	14435	5.0
6.98		6567		
12.70	53667	13573	40094	3.96
17.14	79691	14652	65039	5.40
22.86	94650	25950	68700	3.65
27.30	131482	35914	95568	3.66
33.02	150191	48069	102122	3.13
37.46	175584	66642	108942	2.64
43.18	198615	76684	121931	2.59
47.62	210226	81244	128982	2.59
53.34	216812	88472 ± < 1%	128340	2.46
63.50	216628	86039	139589	2.52
67.94	204073	73009	132064	2.81
73.66	165805	58766	107039	
78.10	157463	45813	37471	
83.82	119837	35590	84247	3.37
88.26	104619	22289	82330	4.70
93.98	70222	14905	55317	4.70
98.42	59400	10203	49197	4.70
104.14	31859 ± ~ 1.5%	4617 ± 3.5%	27242	6.90
108.58	18422	3585	14837	5.10

Table 4.4

INDIUM Z DIRECTION TRAVERSE

Distance From Center of Source (cm)	Bare Counts/min.	Cd-Covered Counts/min.	Difference	Cd Ratio
25.40	199,913 ± < 1%	64,605 ± < 1%	135,300	3.1
30.48	170,960	45,141	125,820	3.8
35.56	Au Foil			
40.64	96,127	20,510	75,617	4.7
45.72	85,090	12,052	73,040	7.1
50.80	60,907	7,011	53,896	8.6
55.88	47,915	6,741	41,174	7.1
60.96	31,555	3,976	27,579	7.9
66.04	31,490	2,470	29,020	12.8
71.12	22,647	1,208	21,439	18.8
76.20	16,341	1,551 - ± ~ 4%	14,790	10.5
81.28	11,798	424	11,374	27.8
86.36	8,459	691	7,768	12.2
91.44	4,075	204	3,871	19.8
96.52	2,575 ± ~ 2.5%	245 ± ~ 10%	2,330	10.5

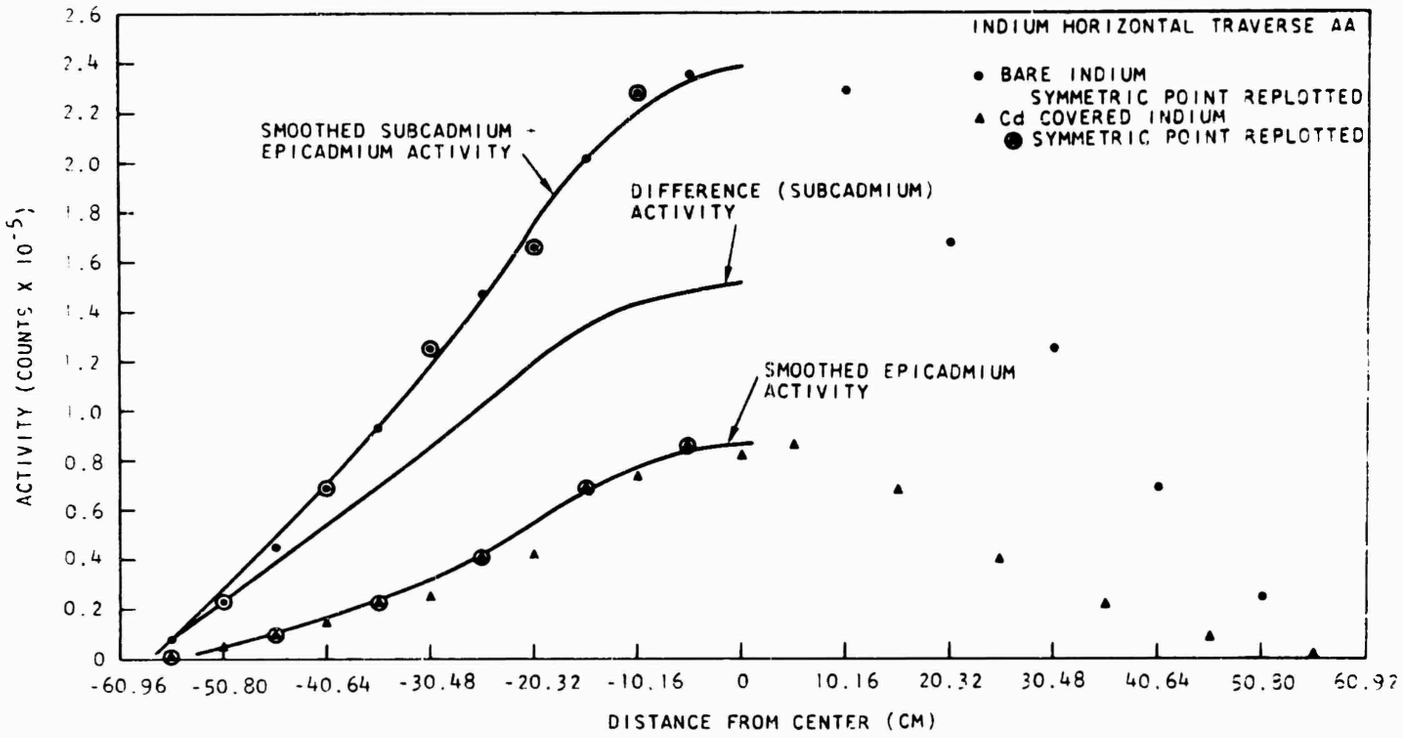

Fig. 4.2--Indium traverse in horizontal AA direction

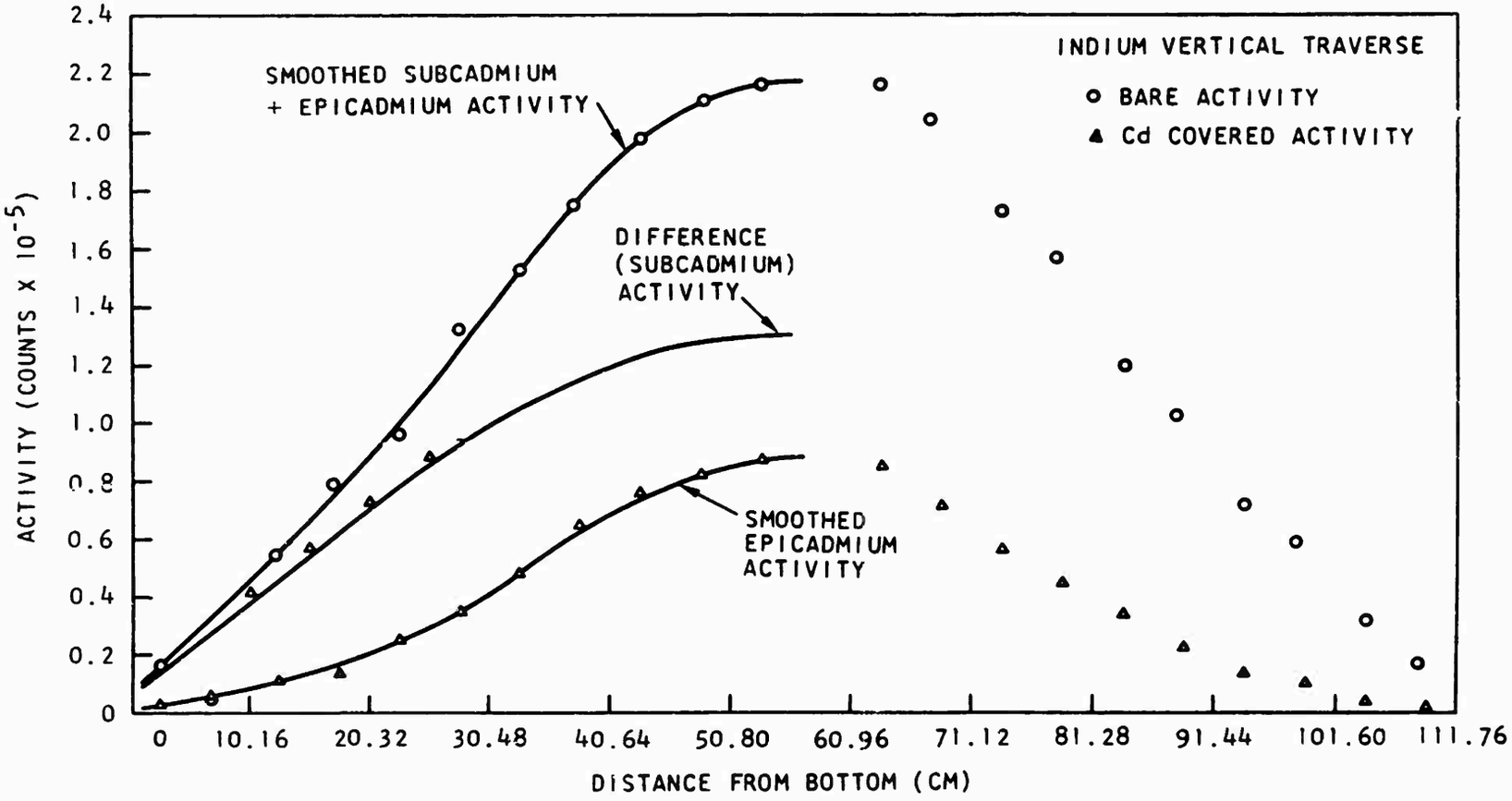

Fig. 4.3--Indium traverse in vertical direction

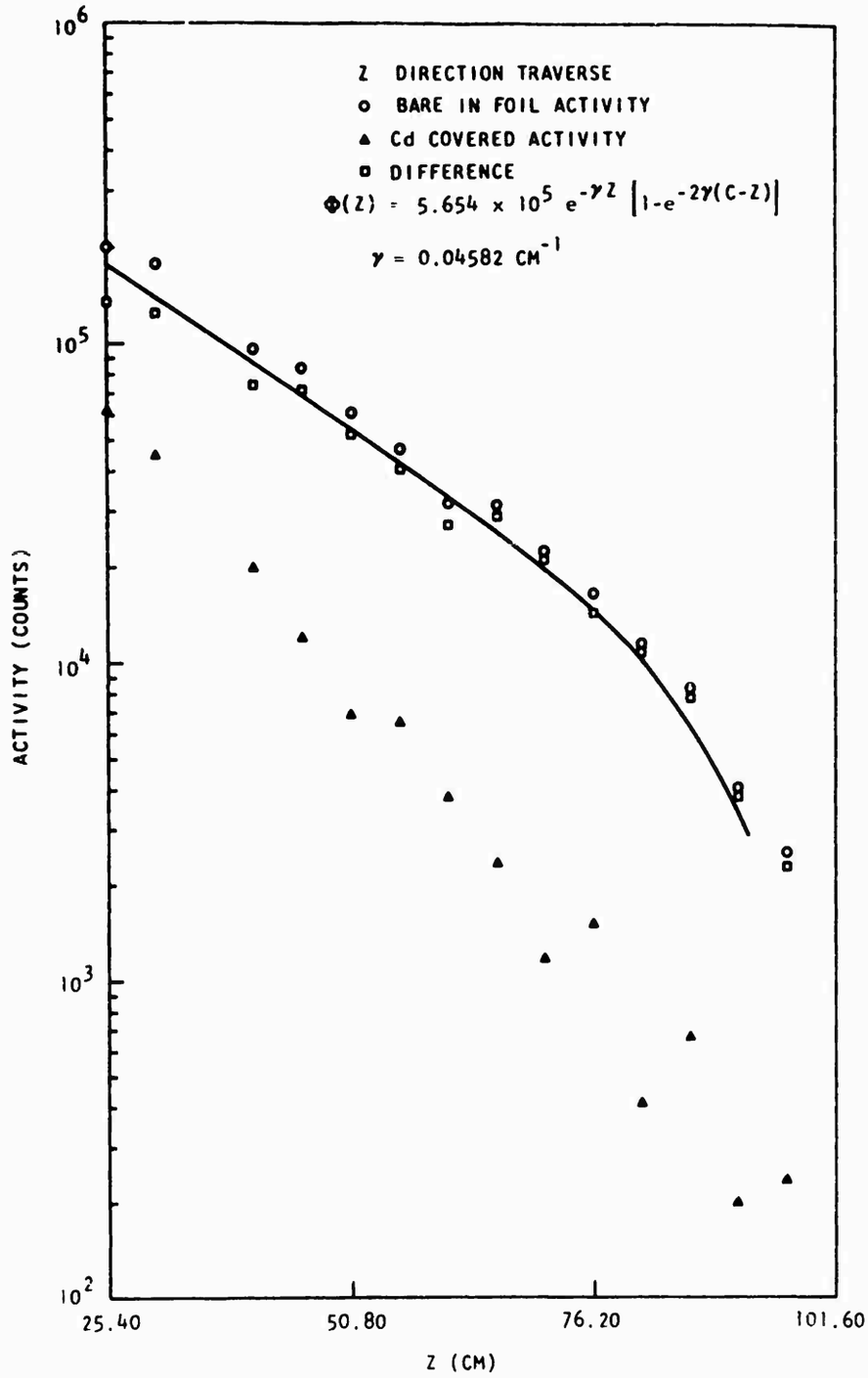

Fig. 4.4--Indium traverse in Z direction

from the data available. The thermal neutron flux not too near the source should be fit by

$$\varphi_{th}(z) = \varphi_o(z)e^{-\gamma z}\left[1-e^{-2\gamma(c-z)}\right] \qquad (4.1)$$

where the factor in brackets is the end correction and c the boundary in the Z-direction. The diffusion length is related to γ by

$$\frac{1}{L^2} = \gamma^2 - B_\perp^2 \qquad (4.2)$$

As a first trial the points far from the end were fit to an exponential to get a trial γ. The points were then corrected by the factor in brackets and refit by a single exponential to give $\gamma = 0.04582\ cm^{-1}$, hence $L \approx 40$ cm. However, $1/L^2$ is a small difference between two large numbers. A diffusion length of 50 cm would be obtained if γ were only 6% smaller.

Bare and cadmium-covered gold foils were exposed for ten minutes during two of the indium foil runs at a position 35.56 cm from the source in the Z direction. The foils were analyzed by E.G. and G for the absolute neutron fluence. The results are bare foil, $1.00 \pm 0.01 \times 10^{10}$ n/cm^2, cadmium-covered foil, $9.6 \pm 0.2 \times 10^8$ n/cm^2. For a 10-minute exposure this corresponds to a thermal neutron flux of 1.507×10^7 n/cm^2-sec. The absolute thermal neutron flux was then inferred from the fit to the indium foil distribution (Eq. 4.1), and tabulated in Table 4.5. However, the point at 20.32 cm lies below the fitted curve. Recommended values are listed in the third column.

The run in which the absolute thermal flux was measured was monitored with sulfur pellet 7S49. In order to improve counting statistics, this pellet was irradiated in three more ten-minute runs on 7/22/66. The neutron yield, as monitored by individual In-Al foils for each run, varied

Table 4.5

THERMAL NEUTRON FLUX

Distance From Source (cm)	Φ_{th} (n/cm^2-sec) Exponential Fit	Recommended Value
20.3	3.04×10^7	1.78×10^7
35.6	1.507×10^7	1.507×10^7
50.8	0.74×10^7	0.74×10^7
66.0	0.35×10^7	0.35×10^7

between 93% and 98% of the yield in the run with the gold foil. The total fluence measured by 7S49 was $1.3 \pm 0.1 \times 10^9$ nvt, E > 3 MeV. Corrected to the average fluence in the four runs, the sulfur monitor gave $3.3 \pm .3 \times 10^8$ nvt (E > 3 MeV) compared to 9.04×10^9 nvt thermal flux measured by the gold foils at 35.6 cm. Hence unit sulfur monitor fluence corresponds to 27.4 n/cm^2 thermal at 35.6 cm.

4.2 SULFUR AND ALUMINUM FOIL TRAVERSES

Sulfur and aluminum foils were exposed at positions 20.3, 35.6, 50.8, and 66.0 cm from the source (along the Z-direction) to compare the fast neutron attenuation as measured by foil activation with that measured by time of flight. The reactions used were $^{32}S(n, p)^{32}P$ with a threshold of about 3 MeV and $^{27}Al(n, \alpha)^{24}Na$ with a threshold of about 8 MeV. The sulfur pellets were 0.965 cm thick by 3.81 cm diameter, with a mass of 18 grams, and were obtained from and analyzed by E.G. and G.

The aluminum foils used were 2.54 cm in diameter with a mass of 0.036 gms. These foils were stacked 10 to a package and covered with cadmium before irradiation. After irradiation each package was gamma counted with a 5.08 cm x 5.08 cm NaI crystal biased at about 200 keV. They were counted for five minutes at various times until the activity was decaying on a 15-hour half life. The measured counts are plotted in

Fig. 4.5. Each count after 15 hours was multiplied by $e^{\lambda t}$, with $\lambda = \frac{0.693}{15}\ hr^{-1}$, to give the equivalent activity at time of removal from the irradiating flux. These numbers were averaged and are represented on Fig. 4.5 by the intersection of the 15-hour decay lines with the count axis. The shorter-lived activity was not identified, but may be a 2.58-hour activity from manganese impurity.

The background for these five-minute intervals was about 1800 counts which gives a counting error of 2.4%. Since the net number of counts is the difference between a higher number of counts (with a correspondingly smaller error) and the background, the error in the net counts must be at least this large. At most it will be $\sqrt{2(2.4)^2} = 3.4\%$. The activity calculated at $\lambda = 0$ is the average of several numbers with about a 3% deviation so this number itself will have a standard deviation of the order of 3% from counting statistics alone.

Several of the individual aluminum foils were weighed and the weights averaged. The mass of each ten-foil packet used in the experiment is 0.36 ± 0.01 gm which will contribute another 3% uncertainty in the final data. The number of nuclei used in the data reduction was 0.8037×10^{22}.

The counting efficiency of the detector was obtained by counting a calibrated Na-24 source made by the General Atomic chemistry division. This source had an initial activity of 1.73 μcuries at 12:00 noon July 25, 1966. It was counted in one-minute intervals for several half-lives. Counts were fit by least-squares to find the measured counting rate at the time of calibration.

The measured aluminum activity was corrected for nonsaturation during irradiation and counter efficiency, and divided by the number of atoms of Al-27 to obtain the saturated activity per atom (or nucleus). The results are tabulated in Table 4.6 and the activities times $4\pi r^2$ are listed in Table 4.7 and plotted in Fig. 4.6.

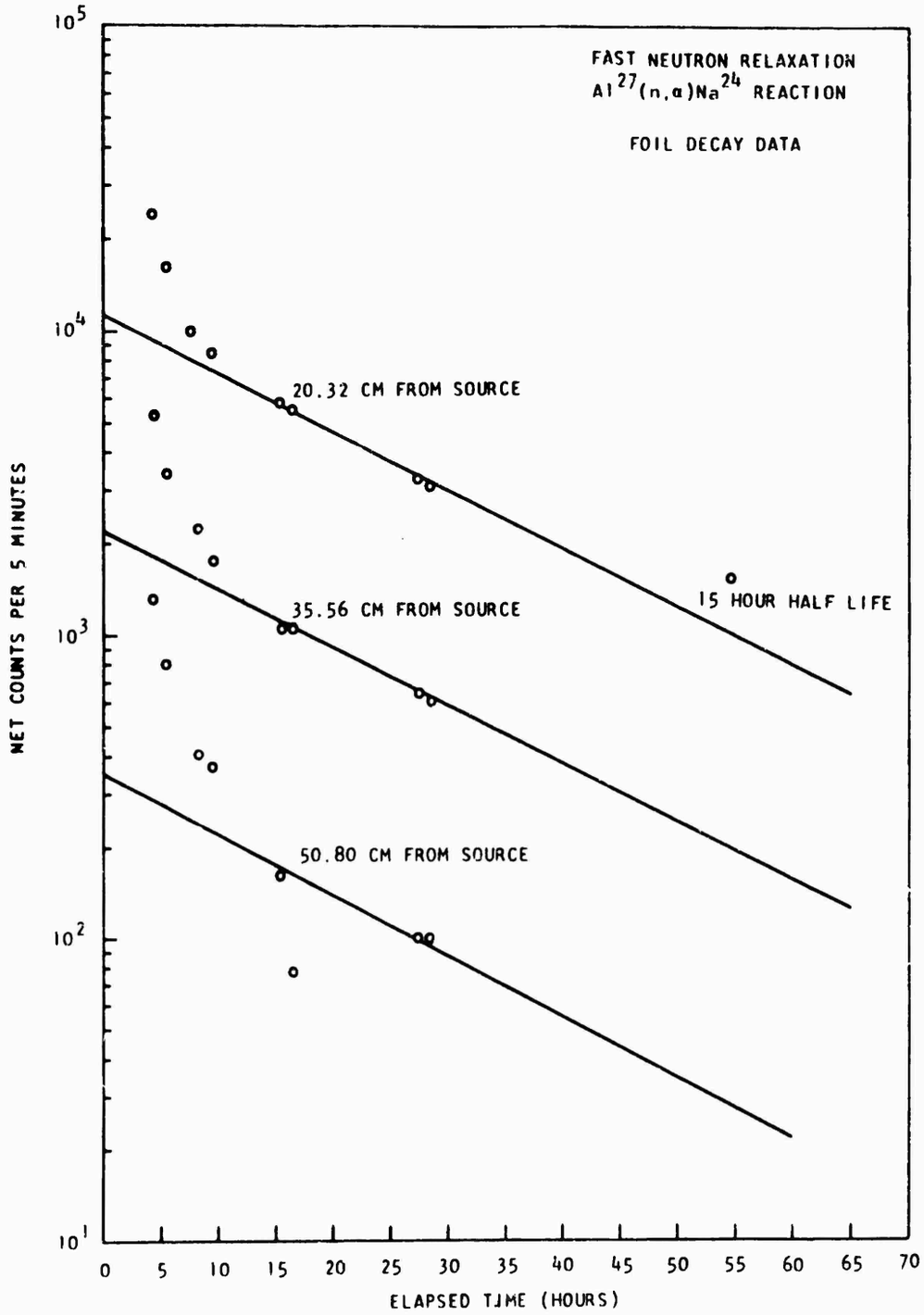

Fig. 4.5--Decay of the aluminum foils

Table 4.6

$^{27}Al(n,\alpha)^{24}Na$ AND $^{32}S(n,p)^{32}P$ ACTIVITIES

(DIS/SEC-ATOM)

Distance From Source (cm)	Al(n, α)	S(n, p)
20.3	0.0948×10^{-18}	2.66×10^{-18}
35.6	0.0182	0.425×10^{-18}
50.8	0.00285	----
66.0	----	0.0254×10^{-18}

Table 4.7

Al(n, α) AND S(n, p) ACTIVITIES $\times 4\pi r^2$

Distance From Source		dis-sec^{-1} atom^{-1} cm^2	
(cm)	$4\pi r^2$	Al(n, α)	S(n, p)
20.3	0.52×10^4	4.93×10^{-16}	1.38×10^{-14}
35.6	1.60	2.91×10^{-16}	0.68×10^{-14}
50.8	3.25	0.925×10^{-16}	
66.0	5.47	----	0.139×10^{-14}

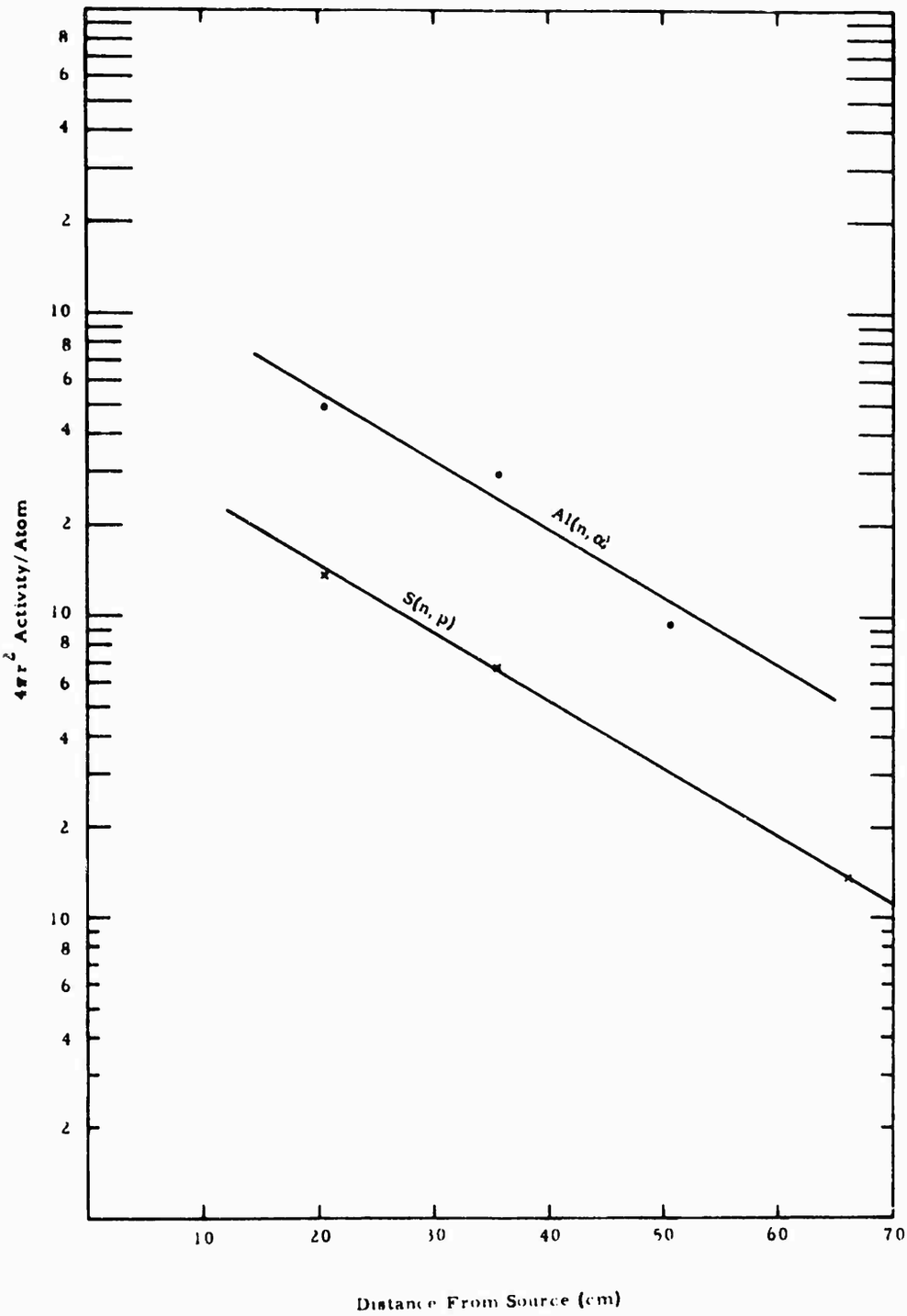

Fig. 4.6--Aluminum and sulfur Z traverse

The sulfur pellets were counted by E. G. and G. and the results reported in disintegrations per minute per gram at the time of removal from the neutron flux. These numbers were divided by a nonsaturation factor, the number of atoms of S-32 per gram, and 60 seconds per minute, to give the saturated activity per atom. These data are tabulated and plotted in Table 4.7 and Fig. 4.6.

The activity of the aluminum foil at 66 cm was too low to count and the sulfur pellet at 35.6 cm had been crushed during removal or insertion in the stack; no activities are available for these two.

Additional data are available on the Al(n, α) and S(n, p) activities from the spectrum measurements which were made at 35.6 cm from the source along an axis 90° from the Z-direction. These numbers are 0.0216×10^{-18} dis/sec-nucleus for the Al(n, α) reaction and 0.4938×10^{-18} dis/sec-nucleus for the S(n, p) reaction, which are in fair agreement with the numbers in Table 4.6.

4.3 THRESHOLD FOIL MEASUREMENTS

Threshold foils are activation foils which have a finite cross section for the reaction of interest above some energy of the incident neutron, called the threshold energy, and zero cross section below this energy. Typical reactions which have this characteristic are (n, p), (n, α), (n, 2n), (n, F) and (n, n'). Thresholds range from a few tenths of a MeV for the (n, F) and (n, n') reaction to 10-20 MeV for (n, α) and (n, 2n) reactions.

If a set of threshold detectors is exposed to a neutron fluence and the resultant activity determined, a set of equations is obtained of the form

$$A_i = \int_{E_{thi}}^{\infty} \sigma_i(E)\Phi(E)\,dE, \qquad (4.3)$$

where the subscript i represents the i^{th} detector and E_{th} is the threshold energy of that detector. From this set of equations the neutron flux spectrum $\Phi(E)$ can be calculated in as many energy intervals as there are detectors.

4.3.1 Selection of Reactions

To be useful for the measurement of fast-neutron spectra the reactions must have the following characteristics.

1. Material: The element must be readily available in a form that can be easily handled. It should be free from impurities that will activate and preferably should be monoisotopic to eliminate interfering reactions.

2. Cross Section: The cross section should have a well-known $\sigma(E)$ curve so the flux can be reconstructed and the cross section should be of convenient magnitude.

3. Half-life: The half-life should be long enough so the product activity can be counted conveniently and it should not be so long that the specific activity will be low.

4. Decay Scheme: The decay scheme should be simple so that the absolute activity can be determined.

With the Linac an additional source of interference is present, i.e., photonuclear reactions produced by the bremsstrahlung. Effectively this eliminates the (n, F) reactions, all of which have sizeable photonuclear cross sections, (n, n') reactions, since the metastable states can also be produced by gamma excitation, and (n, 2n) reactions which are equivalent to (γ, n) reactions. Thus we are left with only (n, p) and (n, α) produced isotopes.

Zijp[14] lists 23 reactions for which the cross sections are known to some extent; 16 of these are either (n, p) or (n, α). Two, $^{23}Na(n, p)^{23}Ne$ and $^{28}Si(n, p)^{28}Al$, can be eliminated because their half-lives, 38 seconds and 23 minutes respectively, are too short. Three more, $^{54}Fe(n, p)^{54}Mn$, $^{63}Cu(n, \alpha)^{60}Co$ and $^{60}Ni(n, p)^{60}Co$ have half-lives that are too long, 314 days and 5.3 years, to be activated to any extent in a reasonable irradiation. $^{31}P(n, p)^{31}Si$ was not used because of the difficulty of obtaining phosphorus in a useful form. The reaction $^{65}Cu(n, p)^{65}Ni$ could not be used because of the difficulty of counting the 2.56 hour ^{65}Ni in the presence of the 12.9 hour ^{64}Cu that would be produced by (n, 2n) and (γ, n) reactions in copper. The two reactions $^{56}Fe(n, p)^{56}Mn$ and $^{59}Co(n, \alpha)^{56}Mn$ were not employed because it is virtually impossible to obtain iron or cobalt without trace impurities of manganese, which will activate by (n, γ) to ^{56}Mn. This would not be a problem in a purely fast-neutron spectrum but in a moderating material with a significant resonance flux, resonance activations in manganese can be significant (manganese has about a 14-barn resonance integral).

This leaves seven reactions $^{24}Mg(n, p)^{24}Na$, $^{27}Al(n, p)^{27}Mg$, $^{27}Al(n, \alpha)^{24}Na$, $^{37}S(n, p)^{32}P$, $^{46}Ti(n, p)^{46}Sc$, $^{58}Ni(n, p)^{58}Co$, and $^{64}Zn(n, p)^{64}Cu$. A titanium foil was obtained from E.G. and G, exposed and returned for counting. The count rate was so low that they were unable to report any activity so this reaction was also discarded. Characteristics of the other six reactions are summarized in Table 4.8.

4.3.2 Reaction Characteristics

Table 4.8

THRESHOLDS AND CROSS SECTIONS

Reaction	E_{th} MeV	σ_{eff} mbarn	$\langle\sigma\rangle$ mbarn	Half-Life
$^{58}Ni(n, p)^{58}Co$	2.8	490	100	71 day
$^{32}S(n, p)^{32}P$	2.7	265	65	14.3 day
$^{64}Zn(n, p)^{64}Cu$	4.4	220	30	12.8 hr
$^{27}Al(n, p)^{27}Mg$	5.4	80	3.5	9.5 min
$^{24}Mg(n, p)^{24}Na$	7.0	124	1.5	15 hr
$^{27}Al(n, \alpha)^{24}Na$	8.1	180	0.65	15 hr

The σ_{eff} and E_{th} values are taken from a table in Ref. (19) and are listed only for comparison. There is no one "good" set of values, but these quantities do not affect the final spectrum. The quantities are defined as

$$\sigma_{eff} \int_{E_{th}}^{\infty} \Phi_o(E)dE = \int_{o}^{\infty} \sigma(E)\, \Phi_o(E)dE \qquad (4.4)$$

and

$$\langle\sigma\rangle = \frac{\int_{o}^{\infty} \sigma(E)\, \Phi_o(E)dE}{\int_{o}^{\infty} \Phi_o(E)dE} \qquad (4.5)$$

where $\Phi_o(E)$ is the spectrum of fission neutrons from ^{235}U fission. Note that σ_{eff} and E_{th} are a dependent pair - one may be chosen arbitrarily which then fixes the other.

We will now discuss decay schemes and possible interfering reactions.

$^{58}Ni(n, p)^{58}Co$

Isotopes	^{58}Ni	^{60}Ni	^{61}Ni	^{62}Ni	^{64}Ni
% Abundance	67.88	26.23	1.19	3.66	1.08

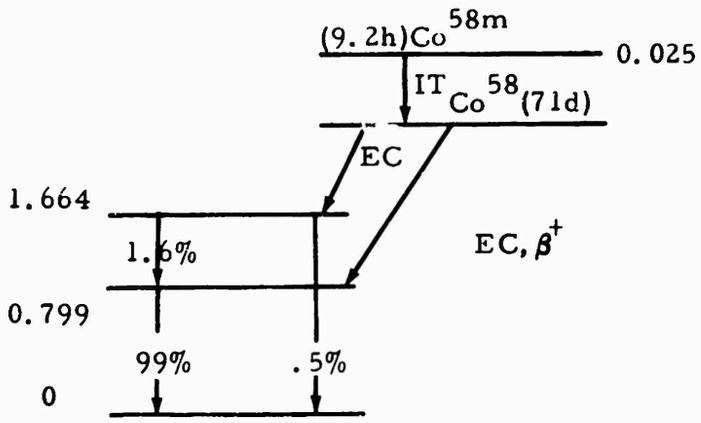

Dominant gamma peaks would be 0.799 MeV (99%) and 0.51 MeV-positron annihilation (15% β+)

Interferences	Half Life	Comment
$^{64}Ni(n, \gamma)^{65}Ni$	2.56 hr	Wait for decay
$^{58}Ni(n, 2n)^{57}Ni$ $^{58}Ni(\gamma, n)^{57}Ni$	36 hr	Wait for decay
$^{58}Ni(\gamma, np)^{56}Co$	77 days	Low cross section
$^{60}Ni(\gamma, np)^{58}Co$	71 days	Low cross section

$^{32}S(n, p)^{32}P$

Isotopes	^{32}S	^{33}S	^{34}S
% Abundance	95	0.76	4.22

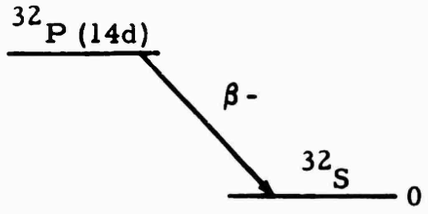

No gammas, must be beta counted.

Interferences	Half-Life	Comment
$^{34}S(n, \gamma)^{35}S$	86.7 day	Low abundance- Long half-life- Low energy
$^{36}S(u, \gamma)^{37}S$	5.1 min	Wait for decay
$^{33}S(n, p)^{33}P$	25 days	Low abundance
$^{33}S(\gamma, p)^{32}P$	15 days	Low abundance
$^{34}S(\gamma, np)^{32}P$	14 days	Low abundance

$^{64}Zn(n, p)^{64}Cu$

Isotopes	^{64}Zn	^{66}Zn	^{67}Zn	^{68}Zn	^{70}Zn
% Abundance	48.8%	27.81	4.11	18.57	0.62

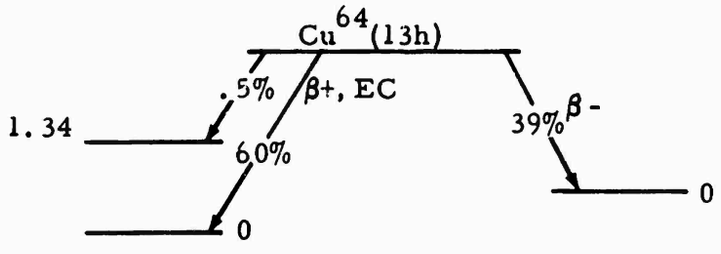

Dominant gamma peaks: 0.51 MeV from positron annihilation (19% β^+)

Interferences:

Reaction	Half-Life	Comment
$^{64}Zn(n, \gamma)^{65}Zn$	245 days	Long half-life can be subtracted
$^{68}Zn(n, \gamma)^{69}Zn$	14 hr	Minimized by cadmium-cover, possible error.
	55 min	No γ, minimized by cadmium cover.
$^{70}Zn(n, \gamma)^{71}Zn$	3.9 hr	Low abundance - short half-life
	2.5 min	Short half-life - wait
$^{66}Zn(n, p)^{66}Cu$	5.1 min	Short half-life-wait
$^{67}Zn(n, p)^{67}Cu$	61 hr	Low abundance - long half-life can be subtracted
$^{66}Zn(n, 2n)Zn^{65}$	245 days	Long half-life
$^{64}Zn(\gamma, np)^{64}Cu$	12.9 hr	Possible error, low production

$^{27}Al(n, p)^{27}Mg$

^{27}Al - 100% abundant

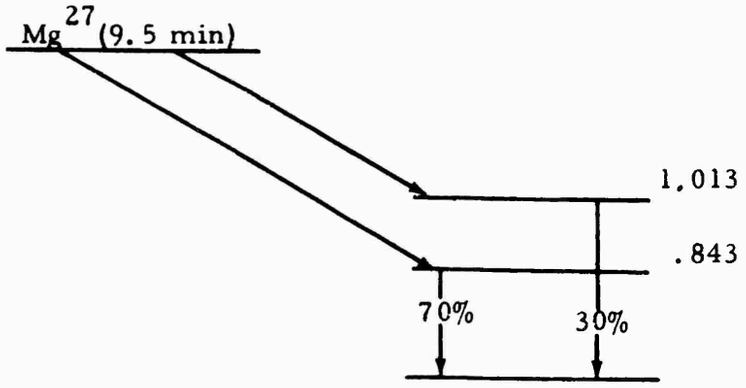

Dominant gammas: 0.843 MeV (70%); 1.013 MeV (30%)

Interferences:

Reaction	Half-Life	Comments
$^{27}Al(n, \gamma)^{28}Al$	2.3 min	Short half-life - wait
$^{27}Al(n,\alpha)^{24}Na$	15 hr	Long half-life can be subtracted

$^{24}Mg(n, p)^{24}Na$

Isotope	^{24}Mg	^{25}Mg	^{26}Mg
% Abundance	78.70	10.13	11.17

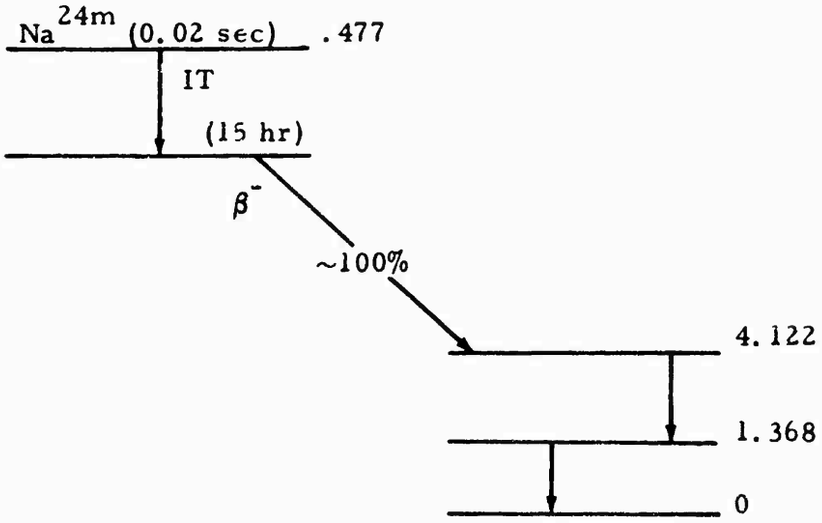

Dominant gammas: 1.37 MeV (100%); 2.76 MeV (100%)

Interferences:

Reaction	Half-Life	Comments
$^{26}Mg(n, \gamma)^{27}Mg$	9.5 min	Short half-life - wait
$^{25}Mg(\gamma, p)^{24}Na$	15 hr	Possible trouble
$^{26}Mg(\gamma, np)^{24}Na$	15 hr	Possible trouble

$^{27}Al(n,\alpha)^{24}Na$

See $^{24}Mg(n, p)^{24}Na$ for decay scheme and $^{27}Al(n, p)^{27}Mg$ for interferences.

4.3.3 Description of Foils

All of the materials were in the form of thin metal foils 2.54 cm in diameter, except for sulfur. The sulfur was a pellet 3.81 cm in diameter by 0.965 cm thick which was obtained from E.G. and G. and returned to them for processing. All metal foils were cut with a die from pure metal sheets (≥ 99.9%) obtained from A. D. MacKay, New York. Table 4.9 is a list of foil weights for each run (runs will be explained later).

Table 4.9

FOIL WEIGHTS (grams)

Material	Run 1	Run 2
Zn	1.0503	----
Mg	----	0.1124
Ni	0.5780	0.5749
Al	0.1793	0.5575

In addition, an aluminum foil weighing approximately 1.2 gm, a magnesium foil weighing 0.78 gm, a nickel foil weighing 2.3 gm and a titanium foil weighing 0.06 gm were exposed during the first run and returned to E.G. and G. for analysis.

4.3.4 Exposures

All foils except for the sulfur were stacked together in a cadmium box with walls 0.0813 cm thick. The sulfur foil was not covered but was placed on top of the can containing the rest of the foils. The entire package fits in an oversized 3.81 cm diameter hole drilled in a graphite stringer such that center of the foil package was 35.56 cm from the center of the neutron source. This position was in a plane normal to the direction of the incident electron beam to minimize the gamma flux which is highest in the forward direction of the electron beam.

Two foil irradiations were made, one on the night of July 24-25 for a total of 7.72 hours and one on the night of July 28-29 for a total of 11.27 hours. Linac conditions and times are listed in Table 4.10. During Run 1 there was a shutdown for over an hour which was accounted for in the calculation of nonsaturation factors for the ^{24}Na and ^{64}Cu activities but not for the longer lived isotopes. During the second run there were some shorter shutdowns that were not accounted for. The reason for the second run was to repeat at higher power some activations which had given low count rates in the first run.

Table 4.10

IRRADIATION CONDITIONS

	Time On	Time Off	Elapsed Time	Pulses per Second	Burst Width μs	Current (mA)
Run 1	2251	2351	1.0 hour	7.5	2	500
	0116	0759	6.72	7.5	4.5	500
Run 2	1829	1929	1.0	15	4.5	400
	1938	0554	10.27	15	4.5	400

4.3.5 Counting Techniques

Except for sulfur, which was analyzed by E.G. and G., the foils were all gamma counted on a 5.08 cm x 5.08 cm NaI crystal with an integral bias set at about 200 kilovolts. The foils were placed in a Lucite plastic dish which was then centered on top of the crystal so the foils could be counted in reproducible geometry. The bottom of the Lucite dish was 0.318 cm thick which was sufficient to stop most of the betas. Each foil was counted many times to insure that the decay had the proper half-life so that shorte ed interferences would not be counted, and that longer lived activities could be subtracted. An attempt was made to set a differential window and count only one gamma peak, e.g., the 1.37 MeV ^{24}Na gamma; however, this was not found to be feasible because of the low count rates involved.

Standard sources of ^{24}Na and ^{64}Cu were made by the General Atomic Chemistry Division (Mr. M. Hiatt) to calibrate the counters. These sources were made by irradiating liquid solutions of NaCl and $CuSO_4$ in the General Atomic Triga reactor. Two 5 ml aliquots of each solution were taken, one to be counted in the chemistry department's standard, calibrated geometry for absolute determination of the activity. The second aliquot was evaporated in a 2.54 cm diameter plastic cup identical to the one made for holding the foils during counting. The cup was then filled with an epoxy resin to seal the source. These calibrated, sealed sources were counted in the same geometry as the foils. Each standard was counted over several half-lives and the data fit by least squares to determine the proper count rate at the time of calibration.

To calibrate the $^{27}Al(n, p)^{27}Mg$ reaction a magnesium foil was exposed for ten minutes in the graphite assembly at a point which had been mapped by the indium (and gold) foils. The magnesium foil was counted for several thirty-second intervals over two half-lives and the data fit by least squares to get the counting rate at time of removal from the irradiating flux.

The ^{58}Co activity produced by the $^{58}Ni(n, p)^{58}Co$ reaction was counted until it was determined that all shorter lived activities had died away and then the foil was taken to the chemistry department where a cobalt carrier was added, the foil dissolved in hot nitric acid and then evaporated to 5 ml for counting in the standard geometry. It was then counted for 800 minutes with a multichannel analyzer and the number of counts in the 800 keV photopeak used to determine the absolute activity. Results are discussed below and summarized in Table 4.11.

Table 4.11

RECOMMENDED VALUES, THRESHOLD FOILS

Reaction	Disintegrations/sec - Nucleus Activated
$^{32}S(n, p)^{32}P$	5.10×10^{-19}
$^{58}Ni(n, p)^{58}Co$	6.88×10^{-19}
$^{64}Zn(n, p)^{64}Cu$	2.64×10^{-18}
$^{27}Al(n, p)^{27}Mg$	7.85×10^{-20}
$^{27}Mg(n, p)^{24}Na$	2.77×10^{-20}
$^{27}Al(n, \alpha)^{24}Na$	2.50×10^{-20}

4.3.6 Calculations and Results

For $^{32}S(n, p)^{32}P$, E.G. and G. counted two foils, 7S57 in Run 1 and 7S66 in Run 2. The activity at the end of exposure was reported as 5.38×10^{3} dis/min-gm in Run 1 and 1.24×10^{4} dis/min-gm in Run 2. The S-32 nuclear density is 1.784×10^{22} S-32 nuclei/gm of sulfur. The activity is divided by the number of S-32 nuclei, 60 sec/min, and the nonsaturation factors (0.0156 for Run 1, 0.0227 for Run 2). The final results are 3.22×10^{-19} dis/sec-nucleus S-32 in Run 1, and 5.10×10^{-19} dis/sec-nucleus in Run 2. All results are normalized to Run 2. Hence the recommended value for this reaction is 5.10×10^{-19} d sec-nucleus S-32 and all Run 1 results of other foils are to be multiplied by the ratio of the sulfur activities, viz. 1.58.

For $^{58}Ni(n, p)^{58}Co$, the Ni foil in Run 1 was counted by E.G. and G and reported as 2.14×10^{2} dis/min-gm, corrected to end of exposure. Dividing by 3.14×10^{-3} (nonsaturation factor), 6.95×10^{21} nuclei N-58/gm Ni, and 60 sec/min, and multiplying by 1.58, we get 2.58×10^{-19} dis/sec-nucleus Ni-58. However, judging from counts made at the Linac for Nickel foil No. 6, irradiated in Run 2, the result obtained by the GA Chemistry Division is more reliable. After a wait of ten days (decay

correction, 0.907), the foil was dissolved and counted by the General Atomic Chemistry Division to obtain 6.86×10^{2} dis/min. The number of Ni-58 nuclei in the 0.5749 gm foil is 3.99×10^{21}. The nonsaturation correction in the exposure is 4.58×10^{-3}. Thus the recommended value, from the Chemistry measurement, is 6.86×10^{-19} dis/sec-nucleus Ni-58.

Run 1 was sufficient for the $^{64}Zn(n, p)^{64}Cu$ reaction. After subtracting a long-lived activity, and neglecting all counts for times shorter than five hours, the resulting counts were fit by least-squares to a half-life of 13.04 hr (vs the accepted value of 12.9 hr). The count rate at the end of exposure was 6200 counts/min. The ^{64}Cu standard of 1.30 μcurie gave a counting rate of 1.118×10^{5} cpm. Thus the Zn(n, p) activity was 2.67×10^{3} d/sec. The nonsaturation factor had to be computed in three steps since the Linac was shut down for 1.42 hr after 1.0 hr of exposure. The correction factor derived was 0.338. The number of Zn-64 nuclei in the 1.0503 gm foil was calculated as 4.73×10^{21}. Then the saturated activity is 1.167×10^{-18} dis/sec-nucleus Zn-64. Normalized to Run 2 by multiplying by 1.58, we get 2.64×10^{-18} dis/sec-nucleus Zn-64.

The $^{27}Al(n, p)^{27}Mg$ irradiation was also carried out only for Run 1(aluminum foil No. 116). First the counter efficiency had to be determined for ^{27}Mg. A magnesium foil was exposed for ten minutes in the graphite assembly, along with the indium foils. The magnesium foil was counted in 30 sec intervals from 4 to 10 minutes after exposure. The counts were fit by least squares to give a half-life of 10.7 min (vs the accepted 9.5 min), and had an activity of 401 counts/30 sec at the end of exposure. The thermal neutron flux at the position of the magnesium foil was 1.813×10^{7} n/cm^{2}sec, obtained from the subcadmium indium foil flux plot, normalized against the standard gold foil. Using an activation cross section of 0.027 barn, 3.11×10^{20} atoms ^{26}Mg in the 0.1124 gm Mg foil, and correcting for nonsaturation in the 10-minute exposure (0.520) and decay in the 30 sec counter interval (0.036), and with the decay constant $\lambda = 1.222 \times 10^{-3}$ sec^{-1}, the efficiency of the counter for ^{27}Mg counting was found to be

$$\epsilon = \frac{\lambda C}{N\sigma\varphi(1-e^{-\lambda t_o})(1-e^{-\lambda \Delta t})}$$

$$= \frac{1.222 \times 10^{-3} \times 4.01 \times 10^{}}{3.11 \times 10^{20} \times 2.7 \times 10^{-2} \times 10^{-24} \times 1.813 \times 10^{7} \times 0.52 \times 0.036}$$

$$= 0.171$$

The aluminum foil activity, with a long-lived background subtracted, was fit by least squares to a half-life of 10.1 min (compared to 9.5 min accepted for ^{27}Mg) and the count rate at the end of exposure was 2045 c/m. The activity was saturated in the 7-hr irradiation. The number of ^{27}Al nuclei in the Al foil was 4.00×10^{21}. Dividing the count rate by the counter efficiency and number of nuclei, we get 4.964×10^{-20} dis/sec-nucleus ^{27}Al. Normalizing to Run 2, we get the recommended value 7.85×10^{-20} dis/sec-nucleus ^{27}Al.

In Run 1 the ^{24}Mg(n, p)^{24}Na activity was low, but E. G. and G. reported $6.76 \pm 0.1 \times 10^{3}$ dis/min-gm Mg at end of exposure. The nonsaturation factor, corrected for the down time during the exposure, was found to be 0.299. The number of nuclei of ^{24}Mg in 1 gm of Mg is 1.95×10^{21}. Thus the saturated activity per gm, normalized to Run 2, is 3.05×10^{-20}. In Run 2 the foil was counted at the Linac for times 3 to 29 hr after exposure. The counting rate at end of exposure was 839 counts/5 min counting interval, with a standard deviation of 10%. The nonsaturation factor was 0.406, and there were 2.19×10^{21} nuclei ^{24}Mg in the 0.1124 gm Mg foil. The 1.73 μc ^{24}Na standard source gave 4.82×10^{5} c/m. The disintegration rate of the foil was then computed as 2.49×10^{-20} dis/sec-nucleus Mg-24. The recommended value is the average of the E. G. and G. and Linac results, 2.77×10^{-20} dis/sec-nucleus Mg-24.

Finally, for $^{27}Al(n,\alpha)^{24}Na$, E. G. and G. obtained (in Run 1), $7.20 \pm 0.1 \times 10^{3}$ dis/min-gm which with 2.24×10^{22} nuclei ^{27}Al/gm and a nonsaturation factor of 0.299, and normalized to Run 2, is 2.83×10^{-20} dis/sec-nucleus Al-27. In Run 2 the foil was counted after 12 hrs to allow a short-lived activity to decay, and continued to 55 hrs after exposure. The counting rate at end of exposure was 4130 counts/5 min with a standard deviation of 6%. This result was divided by the nonsaturation factor of 0.406, the 1.245×10^{21} nuclei of Al-27 in 0.5575 gm Al, and the 4.82×10^{5} c/m per 1.73 μc (6.40×10^{4} dis/sec) of the ^{24}Na standard source, to obtain 2.17×10^{-20} dis/sec-nucleus Al-27. The recommended value is the average of the E.G. and G. (Run 1) and Linac (Run 2) results, or 2.50×10^{-20} dis/sec-nucleus Al-27.

4.3.7 Spectrum Calculations

The quantity which has been measured is the product

$$(\sigma\Phi)_i = \int_{E_{th_i}}^{\infty} \sigma_i(E)\Phi((E)dE = \alpha_i \qquad (4.6)$$

where the subscript i identifies the foil. We have a set of n equations, where n is the total number of foils, which must be solved for the flux spectrum $\Phi(E)$.

In this experiment we were limited to six reactions which means that one must unfold an energy spectrum over the range from about 2 to 14 MeV with only six numbers. Obviously the energy resolution obtainable with threshold foils is very much poorer than the energy resolution obtained in the time-of-flight measurements.

The best review of the various unfolding techniques is in Ref. (19), which lists 14 techniques that have been proposed or used by various

authors, roughly divided into three classifications: (a) mathematical methods: the assumptions on $\Phi(E)$ are of a purely mathematical type; (b) perturbation methods: the assumptions on $\Phi(E)$ are related to a deviation from the fission neutron spectrum $\Phi_o(E)$; and (c) weighting methods: the assumptions on $\Phi(E)$ are of a mathematical type, but include a weighting function which can take into account the rough shape of the spectrum.

(a) An example of the mathematical techniques is the "step curve method" in which the energy range of fast neutrons is divided into successive regions, the number of which is equal to the number of threshold detectors used. The assumption is made that in each interval the flux density is constant. Usually the boundaries are taken equal to the effective thresholds of the detectors. The response of the i^{th} detector can be written as

$$\alpha_i = \frac{\Phi_1}{E_2-E_1}\int_{E_1}^{E_2}\sigma_i(E)dE+\frac{\Phi_2}{E_3-E_2}\int_{E_2}^{E_3}\sigma_i(E)dE+\ \ldots\ +\int_{E_{n-1}}^{E_n}\sigma_i(E)dE$$

$$=\sum_{j=i}^{n}\sigma_{ij}\,\Phi_j\ . \qquad (4.7)$$

As the σ_{ij} values are considered to be known, n linear equations in the n unknown Φ_j are obtained. However, there are certain unsatisfactory facets to this approach. For one the solution depends strongly on the values chosen for E_1, E_2 -- and it is not clear what is the best way of picking these energy limits, other than an iterative process. If they are not properly chosen it is possible to obtain negative values of the flux in certain intervals. Secondly, if the threshold values are not widely spaced, so that the activations strongly overlap in energy, then one will obtain a set of equations that is not truly independent.

Other mathematical techniques involve assuming forms for the flux shape such as a series of polygons, polynomials, orthonormal

polynomials, etc. All of these methods suffer to some extent, as does the step function approach, in that one often gets ill conditioned linear systems.

(b) Perturbation methods: These approaches assume that the spectrum is a deviation from the fission spectrum $\Phi_o(E)$. Probably the best known, and a good example of the approach, is the method of spectral indices. The simplest analytical form of the fission neutron spectrum is

$$\Phi_o(E) = CE^{1/2}e^{-0.775E} \tag{4.8}$$

which suggests the following form of a perturbed fission spectrum

$$\Phi(E) = CE^{1/2}e^{-\beta E} \tag{4.9}$$

where the parameter β takes into account the deformation of the spectrum. The spectral index S_{ij} is defined by the following equation

$$S_{ij} = \frac{\alpha_i}{\alpha_j} = \frac{\int_o^\infty \sigma_i(E)\,\Phi(E)dE}{\int_o^\infty \sigma_j(E)\,\Phi(E)dE} = \frac{\langle\sigma_i\rangle}{\langle\sigma_j\rangle} \tag{4.10}$$

S_{ij} can be calculated for different reactions and for different spectra (i.e., for different β values) when cross section curves are available. Experimental values for S_{ij} are obtained as ratios of measured activities and compared to calculated ones for particular values of β. When they match one assumes that the analytical expression with this β value is the most suitable.

This approach does not attempt to reconstruct the spectrum but only gives some measure of the "hardness" of the spectrum. It is useful for investigating spectral changes, but that seems to be about all.

Note that perturbation techniques would not be expected to be too good if the spectrum deviates appreciably from the assumed fission spectrum.

(c) Weighting methods: The so-called weighting methods are generalizations of the previous approaches and represent attempts to arrive at a general approach.

The analysis used for the graphite measurements is a variation of the iterative approach suggested by Bresesti in Ref. (20) and developed by Mr. G. I. Coulbourn and T. G. Williamson at the University of Virginia.

Assume that the energy range can be divided into n energy intervals, where n is the number of detecting foils. The energies specifying the intervals are arbitrarily selected as values close to the threshold energy for each foil. In each energy interval the flux is assumed to be represented by an exponential of the form.

$$\Phi(E) = Ce^{-KE} \tag{4.11}$$

Thus the activity of the i^{th} detector will be

$$\begin{aligned} \alpha_i &= \sum_n \int_{E_n}^{E_{n+1}} \sigma_{i,n} \Phi_n dE \\ &= \sum_n \int_{E_n}^{E_{n+1}} \sigma_{i,n} C_n e^{-K_n E} dE \end{aligned} \tag{4.12}$$

where the summation is performed over the n energy intervals. The cross sections are calculated from

$$\sigma_{i,n} = \frac{\int_{E_n}^{E_{n+1}} \sigma_i(E)\, \Phi_o(E)\, dE}{\int_{E_n}^{E_{n+1}} \Phi_o(E)\, dE} \tag{4.13}$$

where $\Phi_o(E)$ is an input trial spectrum, usually the fission spectrum.

For the detector of highest response energy, in our case n = 6, choose K_6 as the proper value to match the high energy tail of the fission spectrum so that

$$\alpha_6 = \int_{E_6}^{\infty} \sigma_{6,6}(E)\, C_6 e^{-K_6 E} dE \tag{4.14}$$

With an assumed value of K_6 and α_6 being the measured quantity, the value of C_6 can be calculated. For the next detector

$$\alpha_5 = \int_{E_5}^{E_6} \sigma_{5,5}(E)\, C_5 e^{-K_5 E} dE + \int_{E_6}^{\infty} \sigma_{5,6}(E)\, C_6 e^{-K_6 E} dE \tag{4.15}$$

where $\sigma_{5,5}(E)$ is the cross section of the fifth detector in the fifth energy interval. The boundary condition is

$$C_5 e^{-K_5 E_6} = C_6 e^{-K_6 E_6} \tag{4.16}$$

The values of K_5 and C_5 can now be found. Similarly all values of C_i and K_i can be calculated to give the first trial spectrum $\Phi^1(E)$. From this spectrum new values of the activation integral,

$$\int \sigma_i(E)\, \Phi^1(E)\, dE \tag{4.17}$$

are calculated and compared with the measured values. If they do not agree, new average cross sections,

$$\sigma_{i,n} = \frac{\int_{E_n}^{E_{n+1}} \sigma_i(E)\, \phi^1(E)\, dE}{\int_{E_n}^{E_{n+1}} \phi^1(E)\, dE} \qquad (4.18)$$

are calculated and the process is repeated until the activation values have converged.

The activation values in Table 4.11 were first compared with calculations of activities that would be expected for a fission spectrum. These numbers, normalized to the sulfur data, are listed in Table 4.12.

Table 4.12

COMPARISON OF MEASURED ACTIVITIES WITH THOSE CALCULATED FOR A FISSION SPECTRUM

	Measured	$\int \sigma(E)\, \phi_o(E)\, dE$
S(n, p)	1.0	1.0
Ni(n, p)	1.35	1.5
Zn(n, p)	5.2	0.45
Al(n, p)	0.015	0.06
Mg(n, p)	0.054	0.022
Al(n, α)	0.049	0.009

Since the spectrum in graphite is not a fission spectrum the measured and calculated activities are not expected to be the same. However, the comparison gives some indication of gross errors. It is immediately obvious that the zinc results are a factor of ten higher than might be expected. This is probably due to copper impurities in the zinc. Attempts were made to include the zinc results in the calculations but the program would not work, i.e., the values of the parameters k_i that it attempted to calculate were either too large or too small.

The Mg(n, p) and Al(n,α) numbers are inconsistent. There is no reason for saying which determination is correct since the activities of each were compared with the same standard (Na^{24}) and the count rates for each were about the same. Thus, the errors in each determination should be comparable. Also these two reactions have threshold energies that are very close to each other and responses that overlap. Because of this overlap and the apparent inconsistency in the data the program would not converge when the activities of both foils were included at the same time. Similarly the Ni(n, p) and S(n, p) reactions have thresholds that differ by only a few tenths of an MeV and the reactions have much overlap in their responses. Thus the program was unable to handle both of these foils simultaneously. The best that could be done was to calculate the spectrum three foils at a time in various combinations.

The calculated spectra are tabulated in Table 4.13 and plotted in Fig. 4.7-4.10. Included in the table are the threshold energies, the constants in the flux relation, $\Phi(E) = C e^{-kE}$, the activity as calculated from $A = \int \Phi(E)\,\sigma(E)\,dE$ where $\Phi(E)$ is the final spectrum, the measured activities, and the percent deviation between the two.

It is not evident from the foil results alone which spectrum is the most accurate. However, there was a problem in determining the proper counting efficiency in counting the Ni(n, p) activity, and it has a larger uncertainty than the S(n, p) activity.

The threshold foil results are compared with a calculated spectrum in Section 6.4.

4.3.8 Threshold Reaction Cross Section Data

Nearly all of the cross section data on threshold foils measured up to 1961 is tabulated in:

(a) H. Liskien and A. Poulsen, "Computation of Cross Sections for Some Neutron Induced Threshold reactions," Euratom Central Bureau for Nuclear Measurements, EUR 119.2 (Nov. 1961).

Table 4.13

NEUTRON SPECTRA FROM THRESHOLD FOILS

Reaction	E_n MeV	C	K	$A_{Calc.}$ dis/sec/atm x 10^{-18}	$A_{Meas.}$ dis/sec/atm x 10^{-18}	Deviation (%)
S(n, p)	3.0	2.23×10^{4}	-0.65	0.50	0.51	-2.0
Al(n, p)	5.3	5.24×10^{7}	0.81	0.0816	0.0785	3.9
Mg(n, p)	7.2	3.80×10^{7}	0.766	0.0288	0.0277	4.0
S(n, p)	3.0	1.48×10^{4}	-0.66	0.50	0.51	-2.0
Al(n, p)	5.3	5.13×10^{6}	0.43	0.0803	0.0785	2.3
Al(n, α)	8.0	7.58×10^{6}	0.766	0.0260	0.0250	4.0
Ni(n, p)	2.8	1.34×10^{-3}	-3.67	0.668	0.688	-2.9
Al(n, p)	5.3	5.13×10^{6}	0.43	0.0804	0.0785	2.4
Al(n, α)	8.0	7.58×10^{7}	0.766	0.0260	0.0250	4.0
Ni(n, p)	2.8	6.92×10^{1}	-1.72	0.668	0.688	-2.9
Al(n, p)	5.3	5.24×10^{7}	0.81	0.0816	0.0785	3.9
Mg(n, p)	7.2	3.80×10^{7}	0.766	0.0288	0.0277	4.0

This tabulation has plotted most of the measurements to date and discusses briefly the errors associated with each. Many of the references that follow are taken from this compilation.

Some of the cross sections are also available from

(b) R. J. Howerton, "Tabulated Neutron Cross Sections," UCRL-5226, 1958, however, this reference is incomplete because of its date.

Probably the best reference for the elements of $Z < 20$, which includes Al, Mg and S is

(c) BNL-325, Neutron Cross Sections.

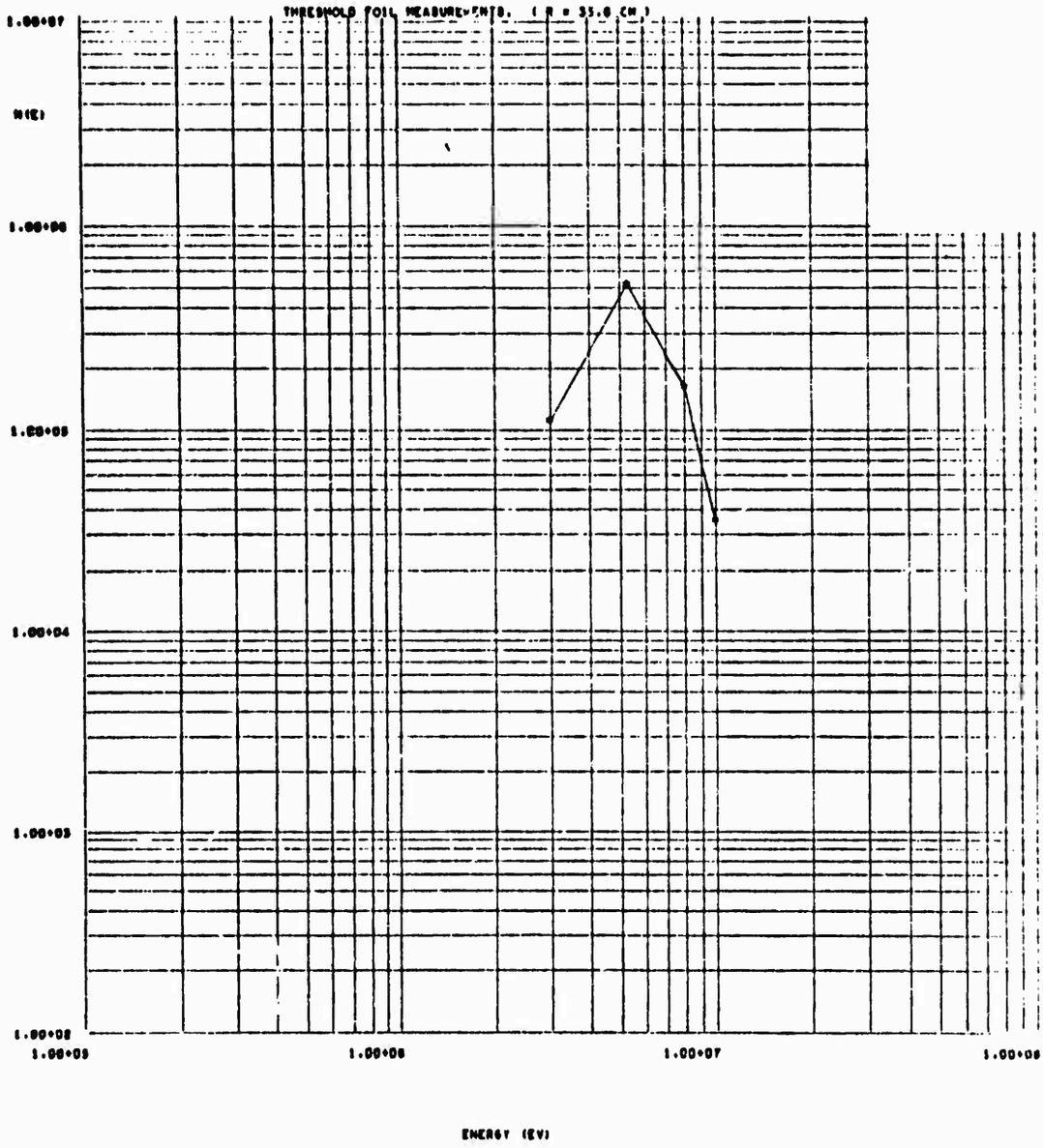

Fig. 4. --Threshold foil spectrum S(n, p), Al(n, p), Al(n,α)

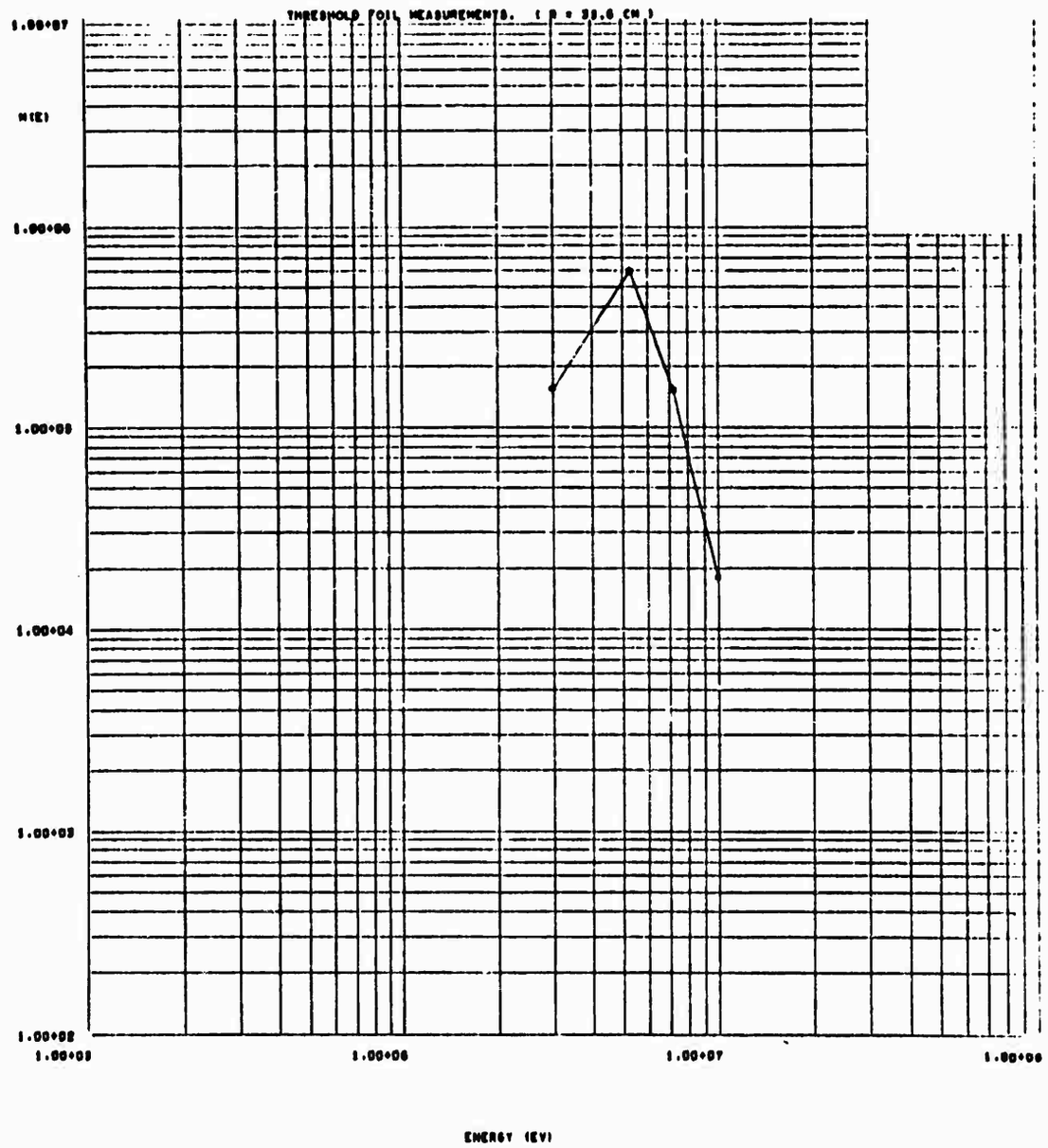

Fig. 4.8--Threshold foil spectrum S(n, p), Al(n, p), Mg(n, p)

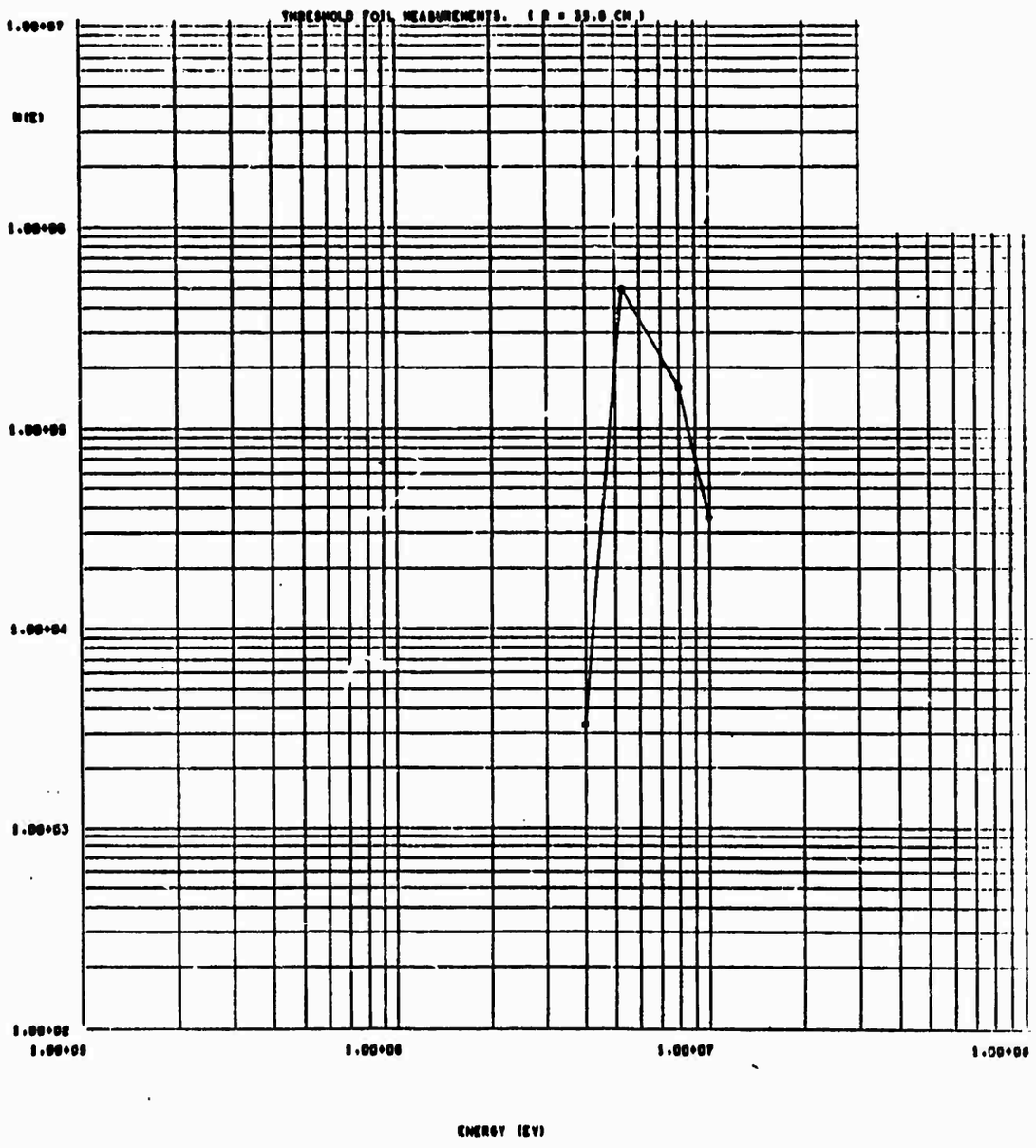

Fig. 4.9--Threshold foil spectrum Ni(n, p), Al(n, p), Al(n, α)

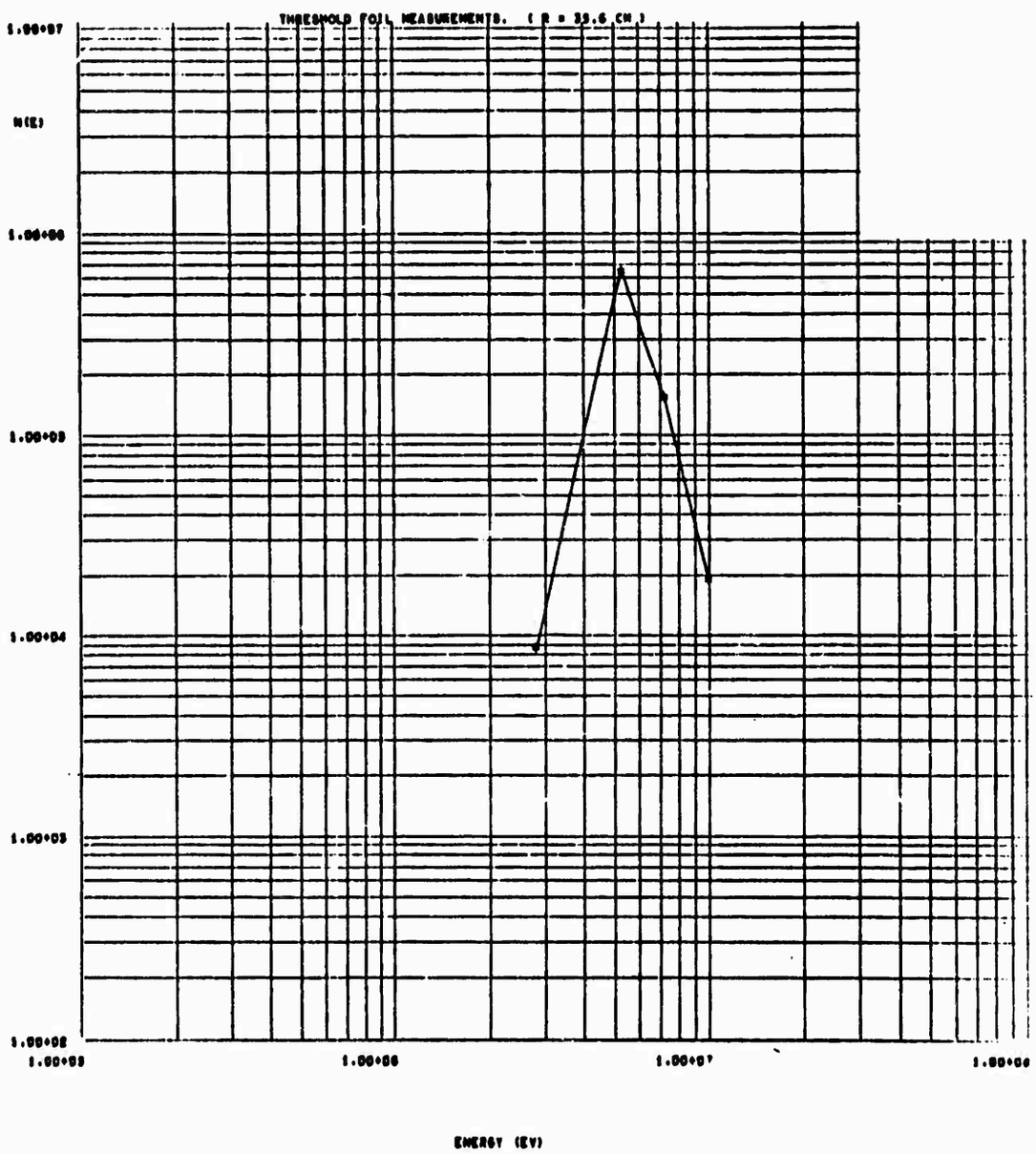

Fig. 4.10--Threshold foil spectrum Ni(n, p), Al(n, p), Mg(n, p)

Specific references follow:

$^{32}S(n, p)P^{32}$

References (a), (b) and (c) above, and Butler & Santry, Canadian Journal of Physics, 41, 372, 1963 (note the data reported in this reference seems to represent a good average of all the other measurements plotted in (a)).

$^{58}Ni(n, p)^{58}Co$

(e) J. F. Barry, "The Cross Section of the $^{58}Ni(n, p)^{58}Co$ Reaction for Neutrons," Journal of Nuclear Energy, A/B 16, 467 (1962).

(f) Nakai, et al., "Excitation Functions of $Ni^{58}(n, p)Co^{58}$ and $Zn^{64}(n, p)Cu^{64}$," Journal of the Physical Society of Japan, 17, 1215, (1962).

(g) T. O. Passell, "The Use of Nickel-58 and Iron-54 as Integrators of Fast-Neutron Flux," Neutron Dosimetry, Vol. 1, International Atomic Energy Agency, Vienna, 501, (1963).

(h) T. O. Passell and R. Heath, Nucl. Sci. Eng., 10, 308 (1961). (For some reason the data here for this reaction does not agree with other data and the later publication (g).)

$Zu^{64}(n, p)Cu^{64}$

References (f) and (h)

$Al^{27}(n, p)Mg^{27}$

Reference (c)

(i) Calvi, et al., "Neutron Reactions in Aluminum from 2.5 to 5 MeV," Nuclear Physics, 39 621 (1962).

(j) Mani, et al., "Neutron Cross Sections in Aluminum," Nuclear Physics, 19, 535 (1960).

(k) Bullock and Moore, "Odd-Even Dependence of Nuclear Level Density," Phys. Rev. 49 721 (1960).

$Mg^{24}(n, p)Na^{24}$

Reference (c) and (d)

$Al^{27}(n, \alpha)Na^{24}$

Reference (c), (d), (j) and (k).

The cross section curves were plotted and smooth curves were fit through the points (smooth curves means the resonance structure was ignored and the points averaged). Cross sections read from these curves are tabulated in Table 4.14, and the product $\sigma\Phi_o$, where Φ_o is the Watt fission spectrum (Reference Goldstein, Fundamental Aspects of Reactor Shielding), is tabulated in Table 4.15.

The products $\sigma(E)\Phi_o(E)$ were numerically integrated (Simpson's Rule) to give the following values:

Foil	$\int\Phi_o(E)\sigma(E)dE$
S(n, p)	67.0×10^{-27}
Ni(n, p)	101
Zn(n, p)	30.6
Al(n, p)	4.06
Mg(n, p)	1.47
Al(n, α)	0.602

Table 4.14

THRESHOLD CROSS SECTIONS-MILLIBARNS

E MeV	S(n, p)	Ni(n, p)	Zn(n, p)	Al(n, p)	Mg(n, p)	Al(n, α)
.5						
1.0						
1.5	2	10				
2.0	25	50	10			
2.5	85	120	26	2		
3.0	145	190	46	4		
3.5	204	262	68	6		
4.0	244	332	93	10		
4.5	275	406	170	14		
5.0	298	478	152	20		
5.5	316	528	188	28	5	
6.0	328	564	222	39	14	2
6.5	334	592	258	50	29	7
7.0	338	614	293	62	46	16
7.5	342	630	328	71	64	28
8.0	345	642	356	79	85	44
8.5	350	645	384	86	105	57
9.0	360	642	410	91	122	70
9.5	374	633	432	96	136	81
10.0	388	620	452	100	149	90
10.5	398	602	466	102	160	100
11.0	400	578	468	103	170	107
11.5	388	552	464	103	179	114
12.0	368	525	452	99	185	119
13.0	306	465	400	90	191	123
14.0	250	395	296	82	187	119
15.0	194	315	270	73	167	109

Table 4.14 (Continued)

E MeV	S(n, p)	Ni(n, p)	Zn(n, p)	Al(n, p)	Mg(n, p)	Al(n, α)
16.0	138	225		64	143	97
17.0	80			56	124	82
18.0	26			47	107	65

Table 4.15

FISSION SPECTRUM ACTIVATION RATES
$\sigma(E)N(E)$

E MeV	$N(E)\sigma(E)$	S(n, p)	Ni(n, p)	Zn(n, p)	Al(n, γ)	Mg(n, p)	Al(n, α)
.5	.347						
1.0	.347						
1.5	.298	.60	2.98				
2.0	.239	5.97	11.98	2.39	.200		
2.5	.184	15.6	22.08	4.78	.368		
3.0	.138	20.0	26.22	6.35	.552		
3.5	.102	20.8	26.72	6.94	.612		
4.0	.0738	18.0	24.50	6.86	.738		
4.5	.0528	14.5	21.43	6.34	.739		
5.0	.0375	11.2	17.92	5.70	.750		
5.5	.0263	8.31	13.89	4.94	.736	.131	
6.0	.0184	6.03	10.38	4.08	.717	.258	.037
6.5	.0127	4.24	7.52	3.28	.635	.368	.089
7.0	8.77×10^{-3}	2.96	5.38	2.57	.544	.403	.140
7.5	6.01	2.05	3.78	1.97	.427	.385	.168
8.0	4.10	1.41	2.63	1.46	.324	.348	.180
8.5	2.79	.976	1.80	1.07	.240	.293	.159
9.0	1.88	.677	1.21	.771	.171	.229	.132
9.5	1.27	.475	.804	.550	.122	.173	.103
10.0	8.56×10^{-4}	.333	.531	.387	.086	.127	.077
10.5	5.74	.227	.345	.267	.058	.092	.057
11.0	3.84	.152	.222	.180	.039	.065	.041
11.5	2.56	.101	.141	.179	.026	.046	.029
12.0	1.70	.063	.089	.077	.017	.031	.020
13.0	7.48×10^{-5}	.021	.035	.030	.007	.014	.009

Table 4.15 (Continued)

E MeV	$N(E)_o(E)$	S(n, p)	Ni(n, p)	Zn(n, p)	Al(n, p)	Mg(n, p)	Al(n, α)
14.0	3.26	.008	.013	.009	.003	.006	.004
15.0	1.41	.003	.004	.004	.001	.002	.001
16.0	6.07×10^{-6}						
17.0	2.59						
18.0	1.10						

5. DISCRETE-ORDINATES CALCULATIONS

Although the research was primarily experimental, a calculation was carried out with the DTF-IV discrete-ordinates transport code.[15] Twenty-five group cross sections were obtained from an infinite medium B_3 ($B = 10^{-10}$ cm^{-1}) calculation with the GAM-II[2] code. The group structure is given in Table 5.1. The source spectrum was the final photoneutron spectrum from Appendix A. The total leakage spectrum from the uranium target might have been a better choice, but since the averaging flux spectrum of the GAM-II calculation cannot match the spatially-dependent spectrum which actually exists in the graphite assembly, the refinement is probably not worthwhile. For the purpose of obtaining multigroup cross sections, it is only necessary that the GAM-II flux have nearly the same shape within each group interval. Macroscopic P_3 cross sections ($N_C = 8.234 \times 10^{-2}$ atoms/barn-cm) were prepared for the transport calculation.

The DTF-IV calculation was performed with a P_{16} angular mesh (Gauss-Legendre ordinates and weights), plus a $\mu = 1$ (0°) angle with zero weight, and the usual $\mu = -1$ angle with zero weight which is used to begin the calculation at the outer boundary. The angular mesh is given in Table 5.2. In order to use the $\mu = 1$ angle it was necessary to modify DTF-IV to eliminate the test for an odd number of angles.

The calculation was made in spherical geometry with the spherical, water-cooled, depleted uranium target (Appendix A) located at the center. The calculation included the uranium, water, and stainless steel jacket. The source spectrum was the adjusted photoneutron spectrum from Appendix A, with isotropic emission in a spherical volume of 2.2 cm^3 imbedded at

the center of the uranium. The inner radius of the graphite was 4.45 cm and the outer radius was 80.0 cm. There were 26 intervals in the target region, one in the air gap, and 48 in the graphite. The total number of spatial intervals was 75, which filled the data storage capacity of the Univac 1108 computer.

The convergence parameter EPS was 10^{-5}. This is a measure of the change from one iteration to the next of the volume-integrated within group scattering source. Convergence took about four minutes.

The calculated angular fluxes times energy, vs energy, are plotted in Figs. 5.1 through 5.3 for forward angles up to 62.7°. (Note, the 30°, 8.3 MeV point in Fig. 5.1 should be plotted one decade higher.) The calculated scalar flux spectrum is plotted in Fig. 5.4.

The storage capacity of the computer was filled at 25 groups, and proper calculation of the flux from 14.92 MeV through 0.002 eV would have required many more low energy groups. However, the GATHER-II[12] calculation carried out in the analysis of the dieaway experiments (Section 3) is of interest. This calculation was made for a buckling corresponding to the asymptotic fundamental mode (geometrical buckling along all three axes) rather than the steady-state spectrum, which is measured in the pulsed source, time-of-flight experiment. The slowing down source was assumed to be 1/E from 1.15 eV to 1.55 eV. The spectrum of the scalar flux is plotted in Fig. 5.5. GATHER-II does not handle a negative buckling directly, and attempts to include the $(i\ 0.04582)^2$ buckling of the T.O.F. spectrum experiment have not been successful thus far. It may be necessary to extend the DTF-IV calculation to lower energies to complete the theory-experiment comparison.

Table 5.1

GROUP STRUCTURE FOR CARBON CALCULATION

Group	E(eV)	Lethargy
1	14.92 + 7 to 10.00 + 7	-0.40 to 0.00
2	6.70 + 6	0.40
3	4.49 + 6	0.80
4	3.01 + 6	1.20
5	2.02 + 6	1.60
6	1.35 + 6	2.00
7	8.21 + 5	2.50
8	4.98 + 5	3.00
9	3.02 + 5	3.50
10	1.83 + 5	4.00
11	1.11 + 5	4.50
12	6.74 + 4	5.00
13	4.09 + 4	5.50
14	2.48 + 4	6.00
15	1.50 + 4	6.50
16	9.12 + 3	7.00
17	5.53 + 3	7.50
18	2.03 + 3	8.50
19	7.49 + 2	9.50
20	2.75 + 2	10.50
21	1.01 + 2	11.50
22	3.73 + 1	12.50
23	1.37 + 1	13.50
24	5.04 + 0	14.50
25	1.86 + 0	15.50

Table 5.2

ANGULAR MESH FOR DTF-IV CALCULATION

μ	Angle	Weight (%)
-1.000000	180.0°	0.00000
-0.989401	171.7°	1.35763
-0.944575	160.8°	3.11268
-0.865631	150.0°	4.75793
-0.755404	139.1°	6.23145
-0.617876	128.2°	7.47980
-0.458017	117.3°	8.45783
-0.281604	106.4°	9.13017
-0.0950125	95.5°	9.47253
0.0950125	84.5°	9.47253
0.281604	73.6°	9.13017
0.458017	62.7°	8.45783
0.617876	51.8°	7.47980
0.755404	40.9°	6.23145
0.865631	30.0°	4.75793
0.944575	19.2°	3.11268
0.989401	8.3°	1.35763
1.000000	0.0°	0.00000

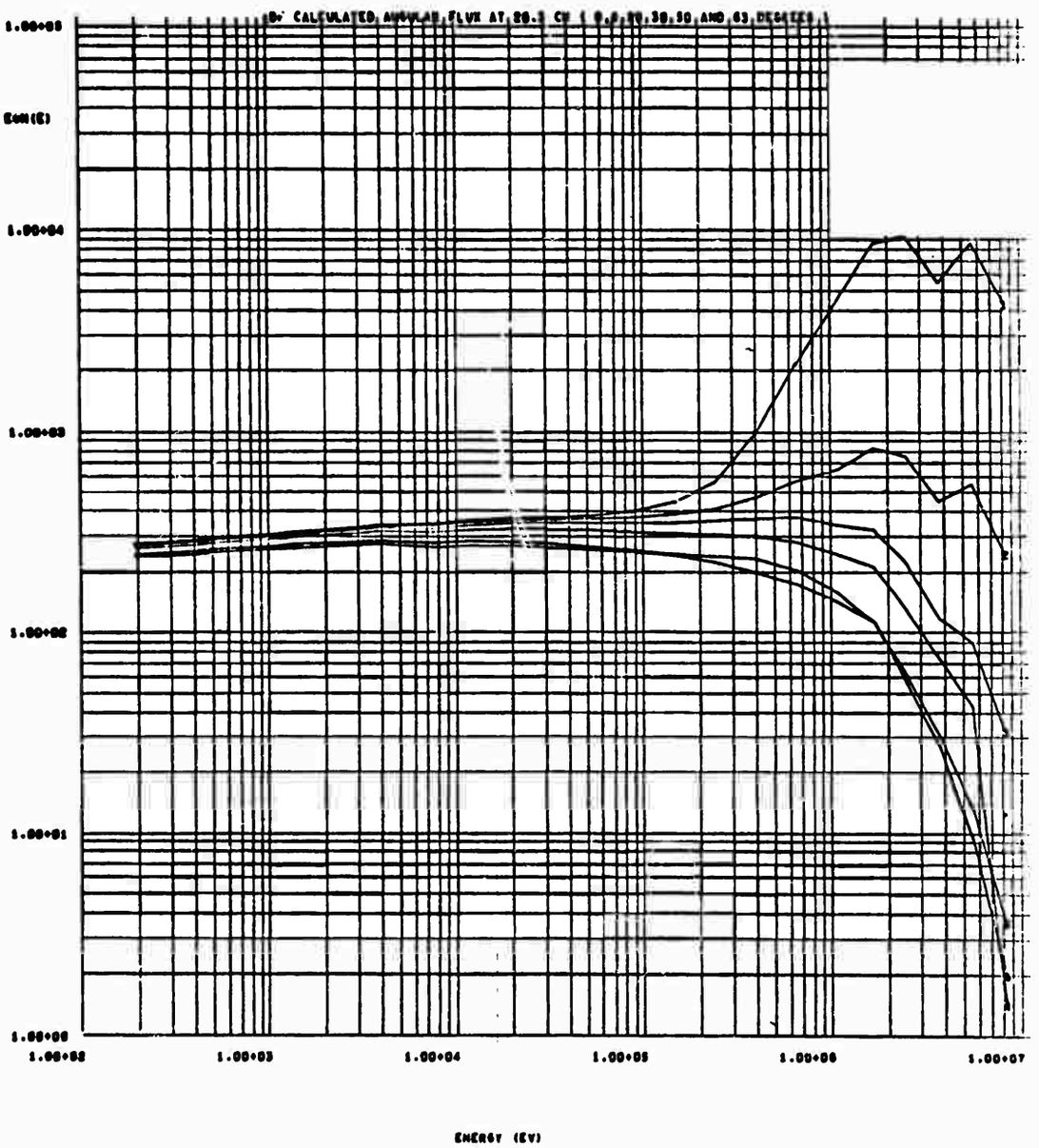

Fig. 5.1--Calculated high energy spectrum at 20.3 cm

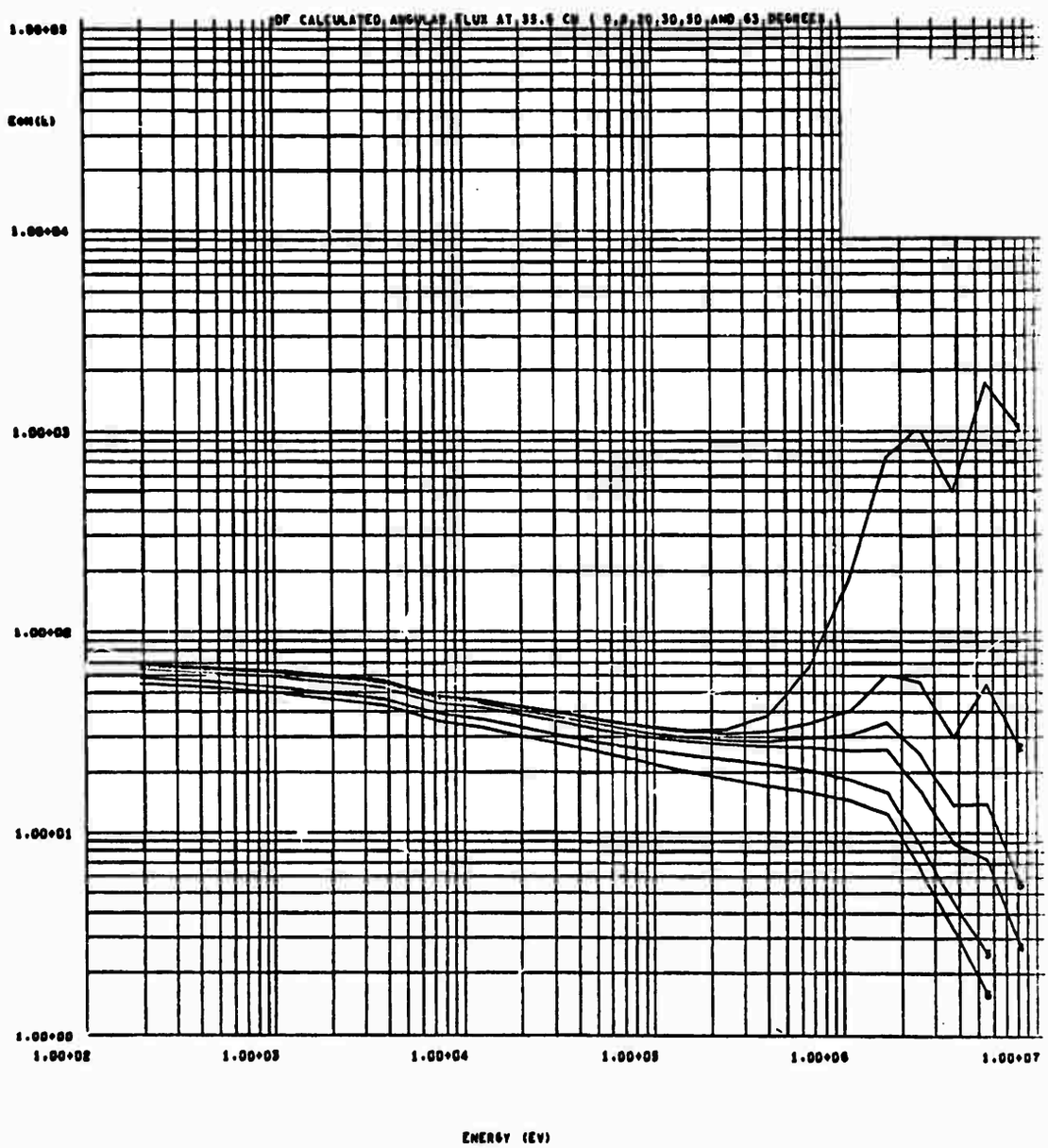

Fig. 5.2--Calculated high energy spectrum at 35.6 cm

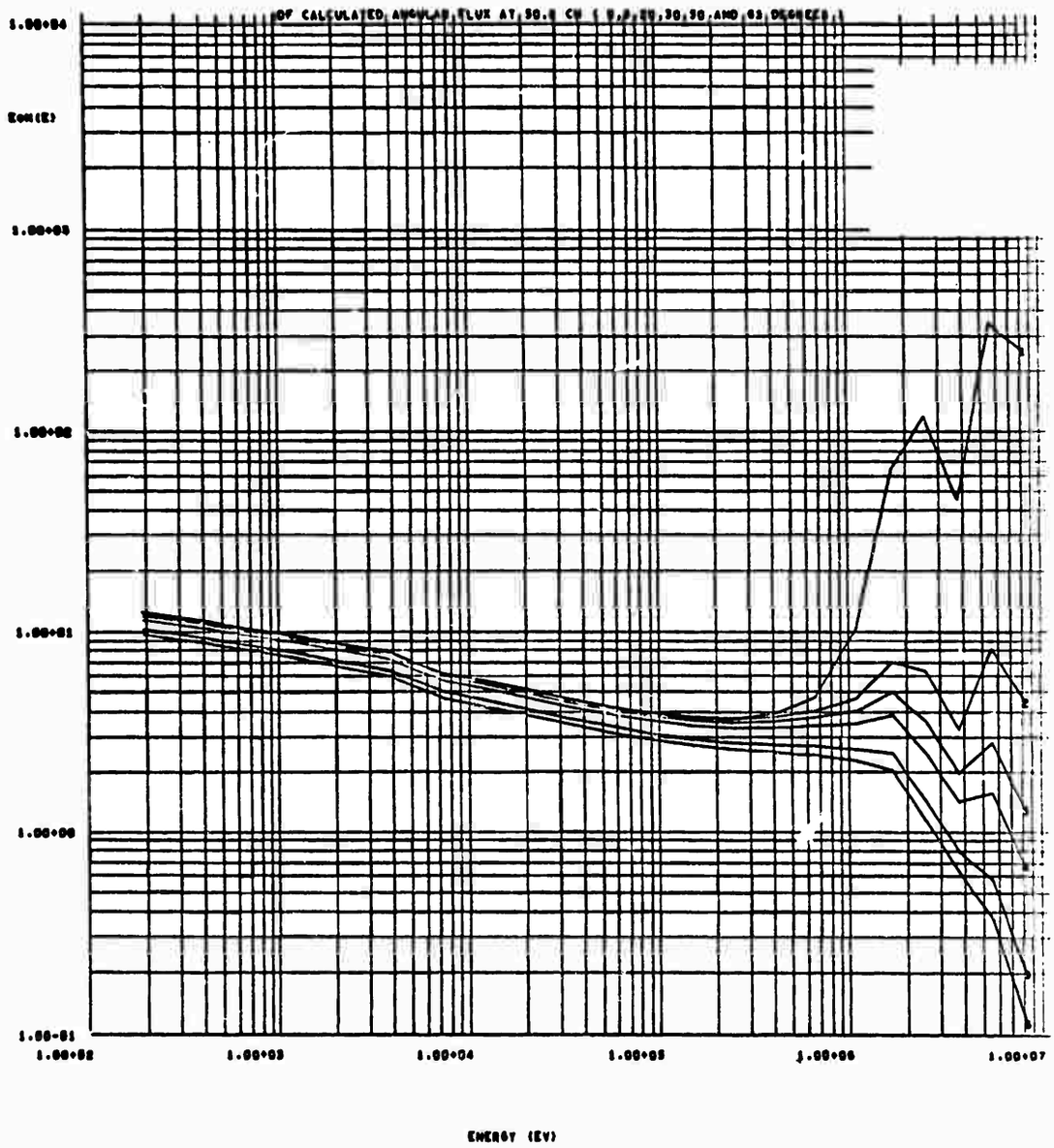

Fig. 5.3--Calculated high energy spectrum at 50.8 cm

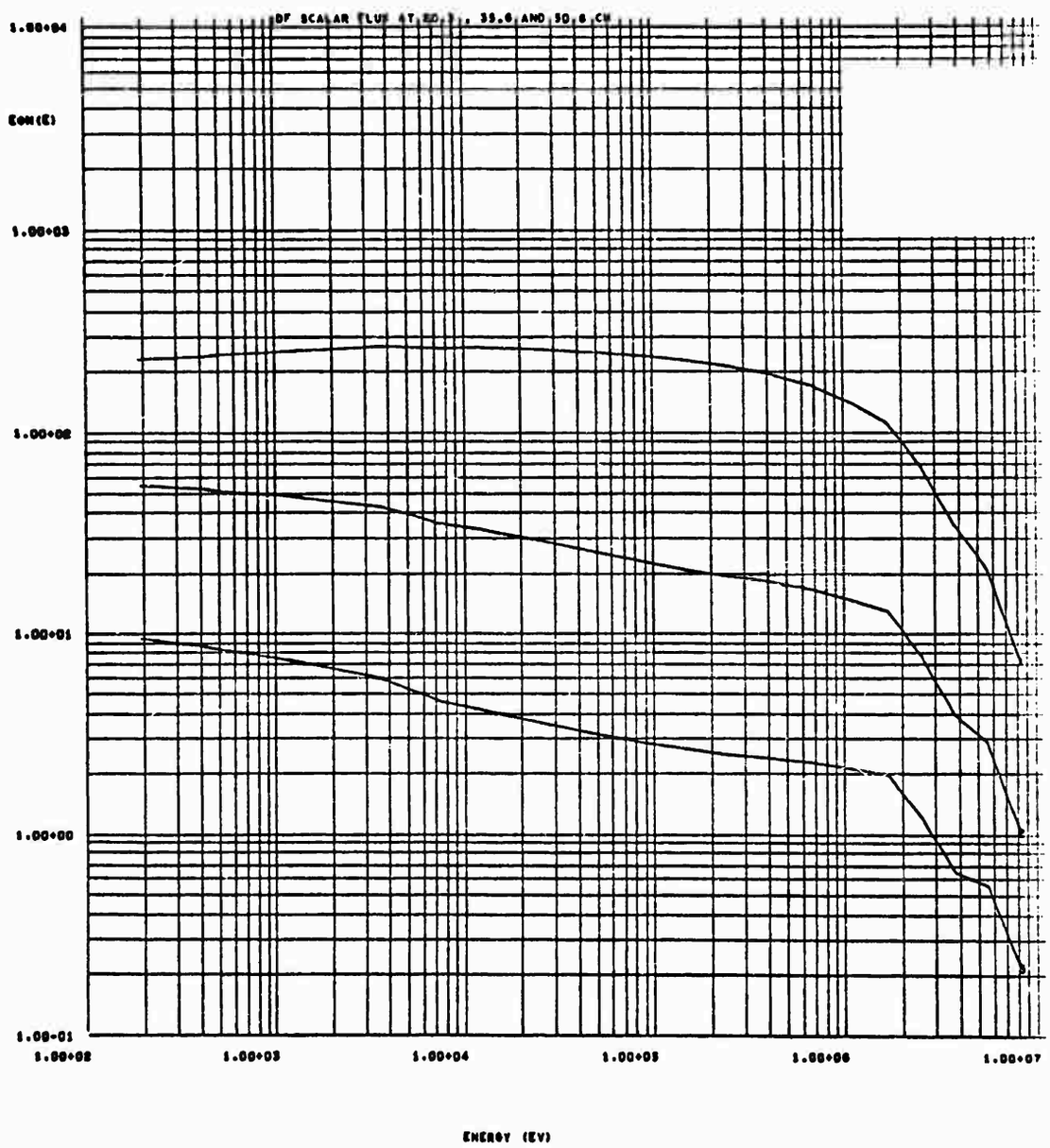

Fig. 5.4--Calculated scalar flux spectrum vs radius

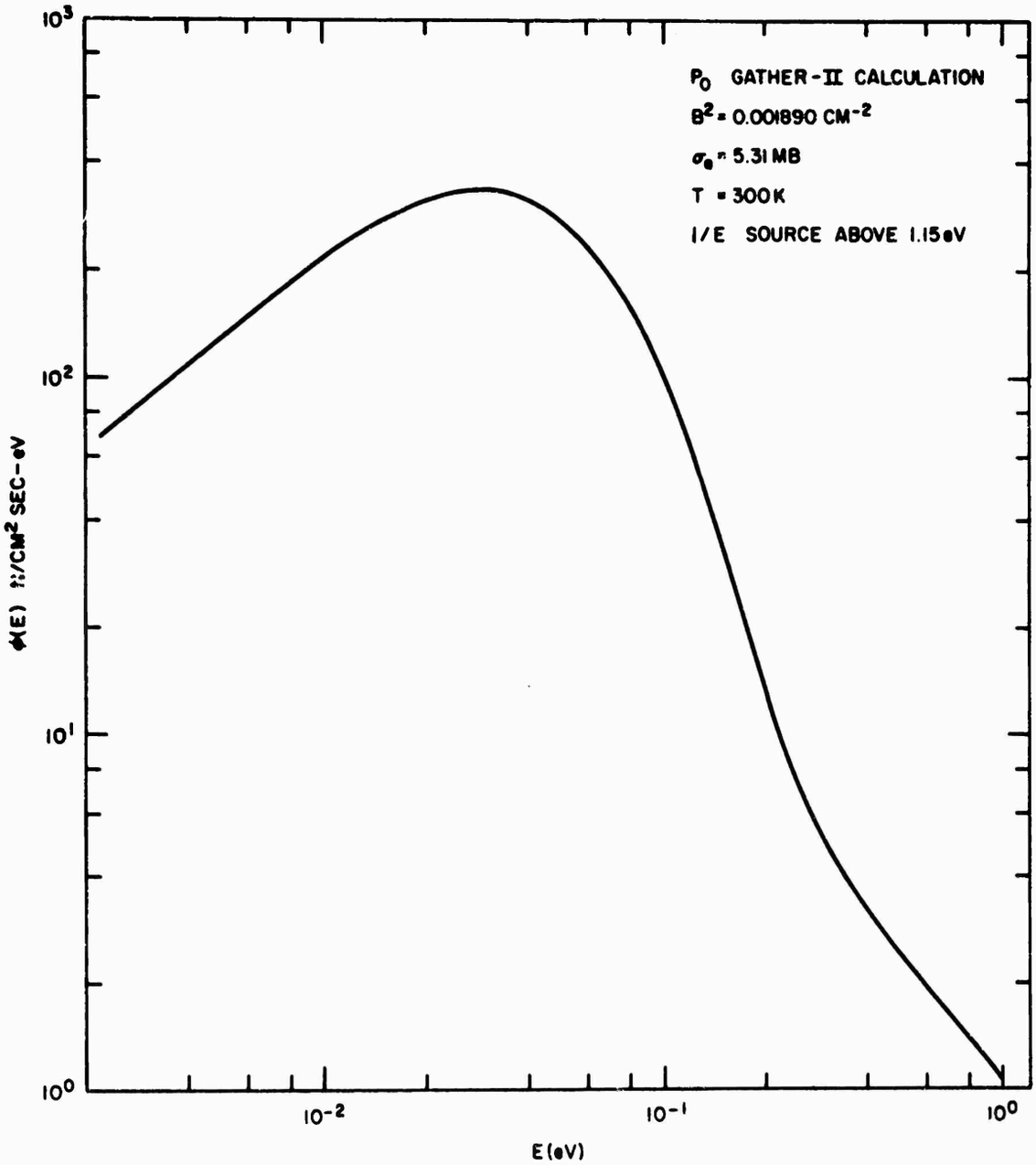

Fig. 5.5--Calculated low energy spectrum

6. DISCUSSION AND RECOMMENDATIONS

6.1 ERROR ANALYSIS

The statistical errors in the time-of-flight measurements, Delta(N)/N, are tabulated with the data in Appendix B. In addition, there are systematic errors, listed in Tables 6.1 and 6.2. The first table is concerned with the energy scale and resolution. The second table is concerned with the relative and absolute magnitude of the angular flux, n/cm^2 sec eV sr, at a standard source intensity.

The neutron burst width in each of the measurements is given in Tables 2.10 and 2.11. If we consider the middle of the neutron burst as the effective time of neutron production, there is no error in the mean energy. However, the contribution of the width Δt_b to the energy resolution $\Delta E/E$ goes as $2 \Delta t_b/t$, where t, the time-of-flight, is proportional to $E^{-1/2}$. The values listed in Table 6.1 are for the maximum Δt_b for each series of runs at the energy cited.

The emission time is discussed in Section 3. The analyzed time interval is corrected for the mean emission time, $< t >$. The residual error after making this correction is small for the fast and intermediate spectrum measurements, but there may be an error of up to 3% near 0.1 eV. The timing uncertainty Δt_e due to the spread in emission time about the mean is generally equated to the standard deviation $\sigma = \sqrt{< t^2 > - < t >^2}$, where $< t^2 >$ is the second time-moment of the distribution. The ratio σ/t is small and fairly constant in the slowing down region, reaches a peak near 0.1 eV, and then decreases again (see Table 3.3 and Fig. 3.1).

The delay in detector response includes the mean time-to-capture in the boron detector (the neutron interaction time in the organic scintillator and BF_3 detector is negligible compared to other uncertainties). The

Table 6.1

ERRORS IN ENERGY

Source of Error	Mean Energy	Energy Resolution
1. Neutron burst width	-	< 10% (10 MeV) < 2% (0.1 MeV) < 2.5% (100 eV)
2. Emission time correction	0.1 to 3% (at 0.1 eV)	0.1% (> 1 eV) 35% (0.1 eV) 12% (0.01 eV)
3. Detector response time	< 1%	2% (10 MeV) 3% (0.1 MeV) 0.5% (100 eV)
4. Zero channel	3% (10 MeV) 0.3% (100 eV)	2% (10 MeV)
5. Channel width	< 0.5%	3% (10 MeV) 1% (0.1 MeV) 3% (100 eV) 0.2% (0.01 eV)
6. Length of flight path	0.1%	-

data are corrected for the average (over incident energy) of the mean time-to-capture: the contribution to the residual error is estimated from the variation in mean-times and the estimated accuracy of the calculations. Delays in cables, etc. are not considered since the flight time is actually measured with respect to the bremsstrahlung channel, and these delays affect neutron and photon signals equally.

The fast neutron detectors have an estimated jitter of 10 nanoseconds, except near the discriminator threshold, where it increases to 30 nanoseconds or more. However, near threshold ($\sim$400 keV) the data cannot be trusted anyway since the efficiency is ill-defined. The boron capture detector has a similar response, but most of the counts occur with pulse heights well above the threshold, and furthermore the timing jitter is small compared to the mean time-to-capture. The jitter of the BF_3 proportional

Table 6.2

ERRORS IN FLUX

Source of Error	Relative Flux	Absolute Flux
1. Intrinsic efficiency	± 5% (NE211, NE213) ± 10% (NE226) ± 5% (BF_3	± 8% (NE211, NE213) ± 16% (NE226) ± 7% (BF_3
2. Geometry factor	1 to 5% (one collimator, detector)	5%
3. Transmission	±3 to ± 12%	± 3 to ± 12%
4. Energy calibration	< 18% (see text)	-
5. Deadtime correction	< 1%	< 1%
6. Monitor normalization	± 2%	± 11%
7. Background	Section 6.2	
8. Perturbations	Section 6.3	

counter is estimated at ± 1 μsec with an additional uncertainty of 0.1 μsec or so in the discriminator triggering.

The zero channel refers to the channel in which the bremsstrahlung signal appears in the scintillation detectors; after subtracting the time-of-flight of the photons, it defines the time of the neutron burst to ± 0.5 channel (the smallest channel width available was 31.2 nsec, hence the zero time under ideal conditions was measured to ± 15.6 nsec). However it has been found that the bremsstrahlung does not always appear in a single channel; the position of the midpoint (or peak) is sensitive to the electron beam current, and there may be errors in the determination of the peak due to deadtime. The zero channel should be measured with a beam current large enough to get the bremsstrahlung signal well above background, including background from accelerator dark current (the very small current observed from gas ionization even when the electron injector is turned off). On the other hand, the beam current should not be so large that deadtime losses or other effects distort the measured time distribution. The discriminator

signal from the BF_3 detector is gated-off for 50 μsec during the bremsstrahlung flash (there is also considerable RF noise pickup during this interval). However, the time-delay between the injector trigger and the opening of the first analysis channel of the modified TMC 212 unit has been measured electronically as 18 μsec, with good precision. Various delays in the electronics, not accounted for in the measurement amount to at most 1 μsec.

The zero-channel should define the zero time. However, the analyzer is started with a signal derived from the injector trigger generator, and there was a jitter of about ±10 nanoseconds in the actual time of the bremsstrahlung burst relative to the analyzer start. This jitter is negligible except at the highest neutron energies.

The channel width of the TMC digital time analyzer is determined by the frequency of an oscillator. The nominal channel widths with the TMC 201 unit are 31.25, 62.5, and 125 nanoseconds. However, a measurement of the oscillator frequency disclosed the channel widths should be 31.166, 62.332, and 124.664 nsec. This correction has been made. Errors in the wider channels of the TMC 211 and TMC 212 units have been found to be negligible. The quoted error in mean energy is based on estimated frequency stability. There remains an uncertainty of ±0.5 channel since the energy is computed for the time at the center of the channel. Channel widths are discussed in Section 2.5. The value quoted at 100 eV is for the 10 μsec channel width, and at 0.01 eV for the 80 μsec channel width.

The uncertainty in the flight path length, including the positioning of the assembly, is estimated at 5 cm, or 0.1%, which is also the percentage error in the flight time.

The error in the mean energy is probably most important in the MeV region, where carbon has several resonances. The zero-degree measurements exhibit dips in the flux at these resonances, and since the energies of the resonances are known, the calibration of the energy scale

can be checked. The 2.08 MeV resonance in carbon appeared at 2.01 MeV (ungrouped channels) in the 0°, 35.6 cm measurement, or 3% low. However, this is hardly outside of the energy resolution and is only off one channel.

We have grouped the channels according to the estimated resolution: 6% at 10 MeV, decreasing as $\sqrt{E}$, for the NE211 and NE213 detectors, 25% at 10 MeV, decreasing as $\sqrt{E}$, for the NE226 detector, and a constant 8% for the BF_3 detector runs. The ungrouped output is on file at General Atomic.

The intrinsic efficiencies of the detectors (Table 6.2) are discussed in Refs. 4, 5, and 6. The error quoted for the relative efficiency due to error in the geometry factor is based on the estimated reproducibility in positioning. The absolute error includes the estimated uncertainty in (ηA_s), A_d, and L^2, when using the average L to calculate the geometry factor. Transmission errors are discussed in Section 2.6.

The uncertainty in the energy scale, and energy resolution, can affect the flux measurement when either the detector efficiency or transmission varies rapidly, as in a resonance. In addition, the energy resolution affects the shape when the actual flux is varying rapidly, as in a resonance or near the transition between the $1/E$ and the thermal spectrum. The efficiency of the BF_3 detector varies smoothly and slowly with energy and there are no resonances in the transmission of the flight path for the BF_3 measurements. The shape of the spectrum in the transition region is identical as measured with the 10 μsec channels and the 80 μsec channels. However, the experimental resolution is mainly determined by the variation in emission time, rather than the channel width. The resolution correction to the time spectrum[22] is given by

$$\varphi(t)_{true} = \varphi(t)_{obs}\left[1 - \frac{1}{2\varphi(t)}\left(\frac{d^2\varphi(t)}{dt^2}\right)\int_{-\infty}^{\infty}\lambda^2 R(\lambda)d\lambda\left\{\frac{\left(\int_{-\infty}^{\infty}\lambda^2 R(\lambda)d\lambda\right)^2}{4}\right.\right.$$

$$\left.\left. - \frac{\int_{-\infty}^{\infty}\lambda^4 R(\lambda)d\lambda}{4!}\right\}\frac{1}{\varphi(t)}\left(\frac{d^4\varphi(t)}{dt^4}\right)\right] \qquad (6.1)$$

The second derivative was evaluated graphically for the time distribution measured in Runs 3 and 4, 7-22-66 (thermal spectrum at 35.6 cm, 0°) with 80 μsec channels. If the resolution function $R(\lambda)$ is taken as a Gaussian with a standard deviation σ obtained from the emission time, the largest correction is 18% and occurs at 0.17 eV. At the same energy, if the resolution function were rectangular with a width of 2σ, the correction would be 6%. Since the resolution correction is fairly small and somewhat uncertain because of the uncertain shape of the resolution function, and since it is significant only in a small energy range, the correction has not been made. Table 6.2 estimates an upper limit of 18% for the resolution correction.

The boron capture(NE226) detector measurements were made with the boron-aluminum filter, which has many resonances. The detector itself has a dip in efficiency due to a boron resonance. It is possible that there may be a small error remaining at the resonances, but the energy calibration and resolution are good, the true flux is smoothly varying, and there is little evidence of spurious oscillations in the grouped flux output. The 0° measurements were made with the depleted uranium filter in the flight path, and there are small residual oscillations at a few keV.

The efficiency of the NE211 and NE213 detectors is slowly varying except near the threshold, where it varies approximately linearly in energy. There are a few resonances in the flight path transmission but they are small. Energy resolution and mean energy calibration are reasonably good. However, in the zero-degree measurements there are large and rapid variations in the true flux due to the carbon resonances. The results quoted are averaged over the instrumental resolution and no attempt has been made to remove the instrumental broadening. Since the resolution is much better in the time-of-flight measurements than in any other experiment, and calculations usually have much poorer resolution, this should be no problem.

The recorded counts vs time are corrected for deadtime in the analyzer. The correction is most important for the TMC 201 unit (which accepts only one count per beam pulse) and the TMC 211 unit (which has a fixed deadtime of 16 μsec). There are two types of correction, one for the "shadowing" of later channels and the other for the coincidence loss within the channel accepting a count. The correction is based on

$$\frac{S(I)}{ROD^*} = \int_0^{WMIC} \exp(-RCI \cdot t)\, RCI \cdot dt = 1 - \exp(-RCI \cdot WMIC) \qquad (6.2)$$

or

$$RCI \cdot WMIC = -\ln(1 - S(I)/ROD^*) \qquad (6.3)$$

where

S(I) = counts recorded in channel I

RCI = the desired quantity, true counting rate per beam pulse

ROD = true number of beam pulses

ROD^* = reduced number of beam pulses

WMIC = channel width, μsec

For the TMC 201 unit,

$$ROD^* = ROD - \sum_{I=1}^{I-1} S(I) \qquad (6.4)$$

and for the TMC 211 unit,

$$ROD^* = ROD - \sum_{A}^{I-1} S(1) \qquad (6.5)$$

where A is the larger of 1 and the integer part of (I - 16/WMIC). In the graphite runs, the largest S(I)/ROD* was 3.14×10^{-3}, and for S(I)/ROD* $<< 1$, Eq. 6.3 is approximately equal to

$$RCI \cdot WMIC = S(I) \cdot ROD^* \tag{6.6}$$

hence the fractional correction is

$$C = 1 - (S(I) \cdot ROD^*) \cdot (S(I) \cdot ROD) = 1 - ROD \cdot ROD^* \tag{6.7}$$

The largest value of Σ S(I) · ROD occurred for Run 1 of 5-27-66, where there was 0.248 counts/beam pulse. For this run the correction was calculated by hand for

1. the highest count in a channel (channel 116); 8.8% correction
2. the largest ratio S(I) · ROD* (channel 121); 10.2% correction
3. the largest ROD · ROD* ratio (channel 512); 33.1% correction

The correction in the last channel looks large, but actually this channel does not contribute to the data except as it is averaged into the "late channel" background. The statistical error of the background averaged in the last 200 channels was ±1.67%, and a 33% correction in all of these channels would result in an error of only 0.55%.

Another possible source of uncertainty is the deadtime correction when the counts/beam pulse ratio is allowed to vary during the run. For example, the accelerator current may drift, and there are often a few minutes at the beginning of the run ir which the current is varied while the counts/beam pulse ratio is being evaluated. Three examples were devised to estimate the importance of this effect:

1. 0.25 counts/beam pulse for 30 minutes and 0.20 counts/beam pulse for 30 minutes. The corrected counts in each separate period were summed and compared .th the counts using the average correction. The difference was 0.083%.
2. 0.25 counts/beam pulse for 10 minutes, and 0.125 counts/beam pulse for 50 minutes. The difference in the separate and the average correction was 0.615%.
3. 0.125 counts/beam pulse for 10 minutes, and 0.25 counts/beam pulse for 50 minutes. The difference in the separate and the average correction was 0.965%.

We concluded that residual error due to inadequate deadtime correction is less than 1%.

The monitor normalization has already been discussed in Section 2.7. The errors quoted by E.G.G., Inc. have been increased slightly to allow for possible nonreproducibility in positioning of the monitor in the graphite stock. Relative error refers to run-to-run normalization, absolute error to the value of the fluence as measured by the sulfur activation.

Background is discussed in Section 6.2 and perturbations in Section 6.3.

6.2 BACKGROUND

The possible sources of background in the graphite time-of-flight experiments are given in Table 6.3. There are three types or classes: background which is constant in time and independent of the accelerator beam current, background which is essentially constant within the interpulse period but which is proportional to the beam current (through the neutron and gamma-ray yield), and time-dependent background which is necessarily also beam-dependent.

Ambient background is included in the counts in the late channels of the fast neutron spectrum analysis (NE211 and NE213 detectors), which are insensitive to neutrons below about 400 keV. Since the background is accumulated during the same run as the data, and is truly constant, no further correction is necessary. As a matter of interest, the ambient counting rates in the lead shield at the 50-meter station are $6.4 \pm 1.6 \times 10^{-5}$ counts/μsec-beam pulse for the 5.08 cm x 5.08 cm NE211 detector, and $1.8 \pm 0.3 \times 10^{-4}$ counts/μsec-beam pulse for the 12.70 cm x 12.70 cm NE213 detector.

Ambient backgrounds for the boron capture detector (NE226 scintillator) and 36 BF_3 bank were measured in separate beam-off runs (Run 015, 5/28/66 for the NE226, and Run 007, 7/22/66 for the BF_3). In the boron detector measurements background is accumulated in a second time analyzer during the same run as the data, with a B^{10} filter in the flight path, as explained

Table 6.3

BACKGROUND

Type	Origin	Detector	Comments	How Measured	How Corrected	Residual Error
1. Time-independent. beam-independent	a. Ambient activity and cosmic rays	Fast Boron BF_3	See text. 6.12×10^{-5} cts/μsec 7.04×10^{-6} cts/μsec all per beam pulse	Not measured separately Beam-off run Beam-off run	Late channels Second analyzer Background run	None ~ ± 10% < 1%
2 Time-independent. beam-dependent	a. Long-lived induced activity	Fast Boron BF_3	Small " "	Not measured separately from ambient	Late channels Second analyzer Background run	Negligible " "
3 Time-dependent. beam-dependent	a. Neutron overlap	Fast Boron BF_3	None None Small	Not measured separately	Not required Not required Not corrected	None None Negligible
	b. Photofission gamma rays	Fast Boron BF_3	Fig. 6.1 and text	Estimated " "	Late channels Second analyzer Background run	Small See text Negligible
	c. Target absorption gamma rays	Fast Boron BF_3	~2000 μsec dieaway " Insensitive	Included in L. C. Estimated Included in B. G. run	Late channels Approx. by 2nd analyzer Background run	Negligible Negligible Negligible
	d. Target delayed neutrons	Fast Boron BF_3	~2000 μsec dieaway " "	Estimated " "	Late channels Second analyzer Not required	Negligible Small Negligible
	e. Graphite inelastic gamma rays	Fast Boron BF_3	Occur before analysis period	Not measured " "	Correction unnecessary " "	None " "
	f. Graphite capture gamma rays	Fast Boron BF_3	~2000 μsec dieaway " Insensitive	Included in L. C. Compare with BF_3 Included in B. G. run	Late channels Second analyzer Background run	Negligible Small Negligible
	g. Afterglow and RF pickup	Fast Boron BF_3	~70 nsec T 1/2 ~100 nsec T 1/2 Before analysis	Fit early channels Fit early channels Not measured	Exponential decay Exponential decay Correction unnecessary	See text Negligible None
	h. Flight path scattered and transmitted neutrons	Fast Boron BF_3	See text	Not measured in this experiment	Not corrected	Small " "

in Section 2.5. The filter is essentially black to neutrons of $\gtrsim 3000$ μsec flight time (~ 1.4 eV), and this procedure should subtract ambient properly, assuming the electronics are reliable. Background is probably known to about ± 10%, plus the statistical error.

The background in the BF_3 detector measurements is subtracted by measuring the spectrum in a separate run with a B^{10} plug located at the bottom of the probe hole in the graphite. The plug should remove essentially all of the neutrons, leaving ambient and any time-dependent gamma-ray background. The HECTO data reduction code normalizes the background run to the data run by the ratio of monitor fluences, rather than beam pulses (or time). However, the background was corrected by hand when the difference in monitor ratio and time ratio was significant. The residual systematic error in the ambient background subtraction is estimated at $< 1\%$.

Long-lived activity is believed to be small in all detectors and in the graphite assembly. In any event, it is correctly subtracted by the late channel and second analyzer procedures, and by the separate run procedure unless the waiting period is too long.

Overlap refers to neutrons which arrive at the detector from previous bursts, due to a long flight time (and emission time) compared to the interpulse period. Fast neutrons are moderated and arrive at the fast neutron detector with no overlap and the fast neutron detector is insensitive to lower-energy neutrons. Intermediate energy neutrons are moderated and arrive at the boron capture detector with no overlap, and the B^{10} filter removes lower-energy neutrons which would otherwise reach the detector and be counted. In the BF_3 detector runs, the repetition rate was 7.5 sec^{-1}, giving an interpulse period of 133,333 μsec. Subtracting a mean emission time of 2090 μsec, the overlap occurs at an energy of 0.00076 eV, while we measure only to 0.002 eV. Any contribution of fast neutrons to the counting rate at 0.002 eV is not seen. The tail of the thermal neutron distribution adds to the faster neutron channels, but this background should

be small with our graphite spectrum, detector sensitivity, and repetition rate. In a typical case, the estimated counts/channel in the tail of the thermal neutron distribution was $\approx$ 350 while the counts/channel at 200 eV was $\approx$ 10,000. This estimate includes the ratio of the sensitivities at $\approx$ 0.001 eV compared to 200 eV.

Photofission gamma rays are delayed gamma rays from fission product isomeric transitions and beta-decay in the depleted uranium target (bremsstrahlung and gamma rays with a half-life of much less than 0.1 μsec arrive before the neutrons). Measurements have been made at the General Atomic Linac[23] of the delayed gamma rays from $^{238}U(\gamma, F)$ in the range of 2 μsec to 1 second after fission. Results are shown in Fig. 6.1, which is the same as Fig. 17 in Ref. 20. The gamma rays were observed with an organic scintillator biased at 510 keV. However, except for one with a few μsec half-life, the same isomers (with different yields) have been observed with a sodium-iodide spectrometer in the neutron-induced fission of ^{235}U and ^{239}Pu, and half-lives from 2.3 μsec to 80 μsec and energies from 110 keV to 1330 keV have been assigned.[24] Absolute intensities are given in terms of photons/second per fission; there are about 2.5 fission neutrons per photofission or 3.0 neutrons per photofission, counting the direct photoneutrons.

Photofission gamma rays (as well as gamma rays from absorption in the target and graphite) are not a problem with the BF_3 detector since it is relatively insensitive to gamma radiation and furthermore the background run should properly remove time-dependent as well as constant background (a possible exception is activity of several minutes half-life whose magnitude would depend on the exact irradiation history; however, no such activity appears to be significant in the BF_3 runs).

In the fast neutron detector measurements, background is measured from 9 μsec to 15 μsec after fission (actually the detector is insensitive to neutrons after 6 μsec). From Fig. 6.1, we see that the rapidly-decaying (isomeric) component falls by a factor of 5 between 1 μsec and 6 μsec, and by

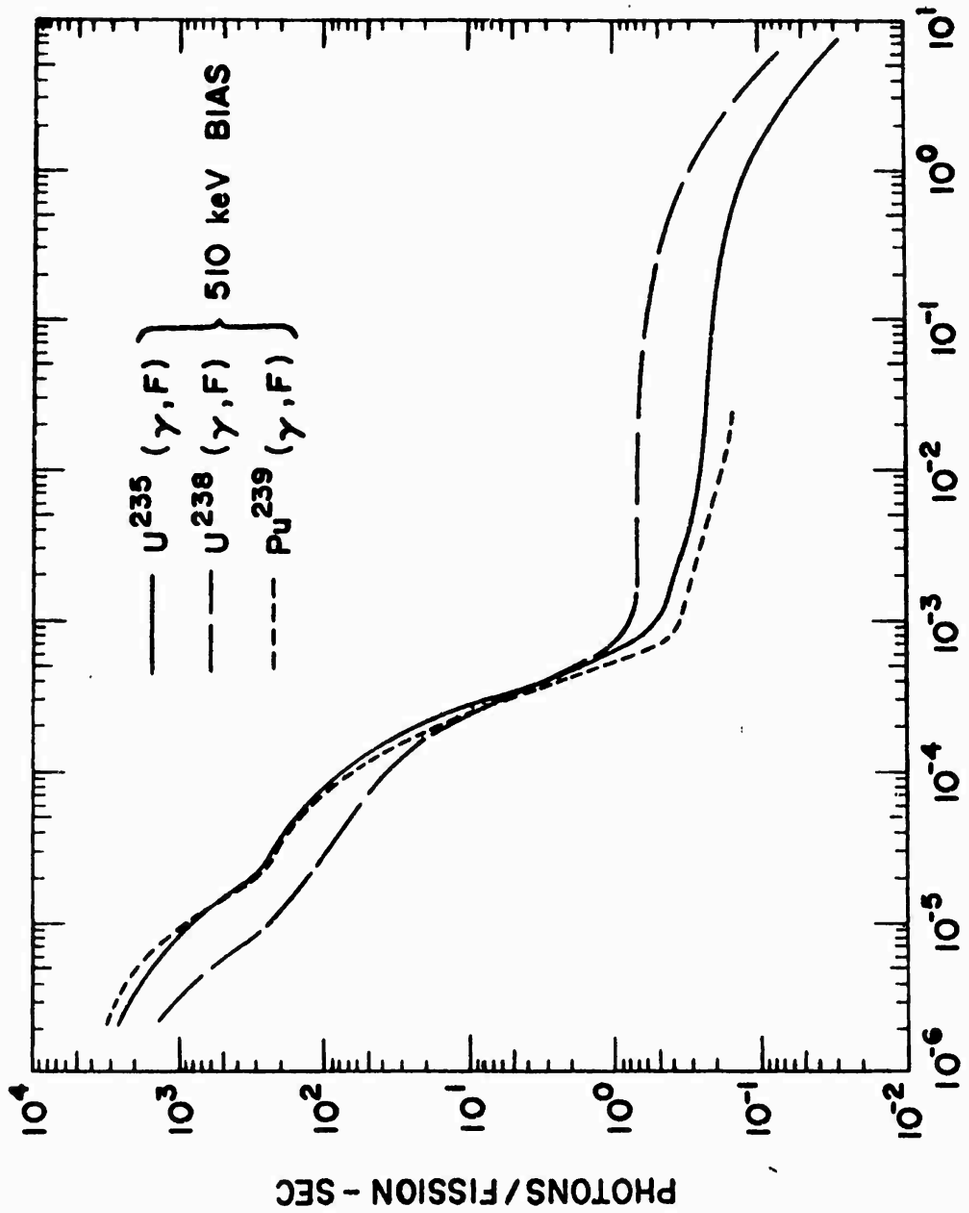

Fig. 6.1--The intensity of photofission gamma rays above 510 keV as a function of time

a factor of 2.5 between 6 μsec and 15 μsec. Thus if the isomeric component is important, we would expect a large decrease in counting rate from 6 to 15 μsec. An examination of the data shows that, on the contrary, the counting rates are nearly constant. The worst situation occurs at 0^{o} and 66 cm, since there the target is viewed directly through graphite, which attenuates neutrons more effectively than gamma rays. In this run the counting rate decreased no more than 20% between 6 and 15 μsec. Extrapolated to 1 μsec the time-dependent background would at most double the background to be subtracted which would result in less than a 1% change in the flux. As a further check, we can estimate the gamma ray/neutron counting rate ratio, assuming equal detection efficiencies and a gamma ray energy of 1330 keV (corresponding to $\mu = 1.17\ cm^{-1}$ in the depleted uranium filter and $\mu = 0.091\ cm^{-1}$ in the graphite). The gamma-ray intensity at, say, 2 μsec is about 1.5×10^{-3} photons/μsec-fission or 0.5 photons/μsec-source neutron. The average neutron intensity, assuming an effective emission time of some 3 μsec at the detector, is about $0.3\ \mu sec^{-1}$ per source neutron. Thus without attenuation the γ/n counting rate ratio is roughly 1.7×10^{-3}. The neutrons are attenuated in the graphite by approximately 10^{4}, and in the flight path (including the uranium filter) by about 3 or 3×10^{4} altogether. The gamma rays are attenuated by 263 in the 61 cm of graphite, and by 40 in the 3.144 cm of uranium, or about 10^{4} altogether. Thus the γ/n counting rate ratio would be $1.7(10^{-3})\ (3) = 5.4 \times 10^{-3}$, which is negligible.

Gamma rays from absorption in the target and graphite should be properly subtracted by the late-channel counts in the fast neutron detectors, since most of these gamma rays will follow the millisecond dieaway of the neutron density, and the change in density between 1 μsec and 15 μsec is negligible.

Photofission and absorption gamma rays are more of a problem in the boron capture detector, since its gamma ray efficiency is on the order of 30 times the neutron detection efficiency (the scintillator area is 0.45 of the neutron-detecting area, but the intrinsic gamma-ray detection

efficiency is probably about 50% compared to a neutron detection efficiency of about 0.7%. The boron capture detector is biased at 150 keV gamma ray energy). Background is measured at ≈ 3000 μsec after fission, in the constant or plateau region corresponding to gamma rays following beta decay. It would be difficult to determine accurately the magnitude of the isomeric component, as detected by the boron-capture detector under our experimental conditions. However, we note that the relative magnitude of the beta-decay component is enhanced by the high repetition rate (180 pps) in these experiments. Without loss of generality we can assume one fission per pulse; the measured intensity of the isomeric component will then be given by the values in Fig. 6.1. The measured intensity of the beta-decay component will be 180 times the total number of beta-decay photons corresponding to irradiation periods on the order of an hour (about 80% of the infinite-irradiation rate). Earlier studies[25, 26] indicate about 4 photons per fission, each with an energy of about 1 MeV. The beta-decay component is then 4(180) = 720 photons/sec and would exceed the isomeric component for all times greater than a few μsec after the pulse. Thus the background at the times corresponding to neutron energies in the 100 eV region, where signal-to-background tends to be poorest, should be correctly subtracted by the counts measured at 3000 μsec. Unfortunately, in some of the runs the counting rate at 255 μsec (≈ 200 eV) was only 20 or 30% above the background so measured (also in these runs the 300 μsec counting rate was typically 1.0 to 1.2 times ambient). A small error in measuring the constant background can lead to a large error in the flux. In this case it is better to adjust background until agreement is achieved with the BF_3 detector in the common energy region. The residual error near 1 MeV can be estimated by comparison with the fast neutron detector results.

Before making such adjustments, we wish to estimate the importance of gamma ray background from thermal neutron capture in the target and in the graphite. These gamma rays will presumably decay with half-lives on the order of milliseconds, and a measurement at 3000 μsec will usually

underestimate them (from Fig. 3.3, graphite captures at large distances from the target may be overestimated, however, the gamma ray flux includes contributions from captures at smaller distances also. The point is, the measurement at 3000 μsec give the 2-255 μsec background only approximately).

From age-diffusion theory for a point source in an infinite medium, we can estimate the order-of-magnitude of the thermal neutron captures in the depleted uranium target, relative to the photofission delayed gamma ray intensity. From page 164 of Ref. 14. the thermal neutron flux per unit fast neutron source intensity is

$$\varphi_{th}(r) = \frac{e^{\tau/L^2}}{8\pi Dr}\left\{e^{-r/L}\left[1+\operatorname{erf}\left(\frac{r}{2\sqrt{\tau}}-\frac{\sqrt{\tau}}{L}\right)\right]-e^{r/L}\left[1-\operatorname{erf}\left(\frac{r}{2\sqrt{\tau}}+\frac{\sqrt{\tau}}{L}\right)\right]\right\} \qquad (6.8)$$

where

τ = age to thermal = 303 cm^2 + 53 cm^2 (Ref. 14, p. 351)

L = diffusion length, 40 cm

D = diffusion coefficient, 0.833 cm.

At r = 0, $\varphi_{th}(r)$ = 1.4 x 10^{-3} n/cm^2 sec per source neutron/second. The capture rate in the target(^{238}U + 0.22% ^{235}U) is

$$R_t = f_t \Sigma_a \dot{V} \varphi_{th} \qquad (6.9)$$

where

f_t = self-shielding factor, ≈ 0.5

Σ_a = 0.048 (2.7 + .0022 (694)) = 0.20 cm^{-1}

V = volume = 232 cm^3

hence R_t = 0.032 absorptions per source neutron. Assuming the dieaway time constant is on the order of 2000 μsec, and taking about 6 photons/absorption, the target thermal neutron absorption gamma ray intensity is

$$I(t) = 0.032 \frac{\text{abs}}{\text{fiss}} \cdot 3 \frac{\text{neut}}{\text{fiss}} \cdot 6 \frac{\gamma}{\text{abs}} \frac{e^{-t/2000\ \mu\text{sec}}}{2000\ \mu\text{sec}}$$

$$= 2.9 \times 10^{-4}\ e^{-t/2000} \frac{\text{photons}}{\mu\text{sec-fission}}$$

$$= 2.9 \times 10^{2}\ e^{-t(\mu\text{sec})/2000} \frac{\text{photons}}{\text{sec-fission}} \qquad (6.10)$$

Repetitive pulsing will enhance this by the factor $(1-e^{-T/\tau})^{-1} = 1.07$ where T = interpulse period = 5555 μsec (180 pps), and τ = 2000 μsec. The calculation is only approximate. However, the estimated intensity is small compared to the photofission gamma ray intensity and is probably negligible.

About 27% of the absorptions in the target result in fission, with release of 2.5 neutrons per fission. Thus there will be a slowly decaying tail on the fast neutron pulse with an integrated intensity of about 0.032 (.27) (2.5) = 2% of the prompt neutron emission (in addition to these delayed neutrons there are the usual delayed neutrons following fission, but their intensity is very low). The target delayed neutron background is small and is included in the late channel counts of the fast neutron detectors. The BF_3 detector is relatively insensitive to fast neutrons, and in any event the mean emission time is hardly affected. The contribution to the background of the boron capture detector is small and approximately corrected by the 3000 μsec measurement.

Graphite inelastic scattering gamma rays are emitted within a few nanoseconds of the neutron burst and should not contribute to the background in any of the detectors.

The thermal neutron absorption cross section in our graphite is 38.8×10^{-5} cm^{-1}, compared to 28.1×10^{-5} cm^{-1} for pure carbon (BNL-325, 2nd Ed., Suppl. 2, Vol. 1). Carbon emits one 4.95 MeV gamma ray in 75% of the captures, and two gamma rays (3.68 MeV and 1.26 MeV)

in cascade in 25% of the captures.[27] The impurities in the graphite are not known precisely, but the largest contributor to the absorption is probably boron, which emits one 0.478 MeV gamma ray. The lower energy gamma rays are attenuated more rapidly than the 3.68 MeV and 4.95 MeV carbon gamma rays, and the latter should be the most important. The attenuation coefficient in graphite at 4.95 MeV is 0.05 cm^{-1}, or a 20 cm attenuation length. The attenuation length of the thermal neutron flux varies between the 22 cm observed in the smaller graphite assembly, and the 40 cm diffusion length. Thus we expect the gamma ray/thermal neutron flux ratio to either remain approximately constant or decrease with distance from the target. On the other hand, the cadmium ratio increases, indicating the ratio of epithermal flux to thermal flux is decreasing. An exact calculation of the time-dependent gamma ray background would be difficult. However, we note that for a 1/E spectrum, $\varphi(E) = \varphi_{epi}/E$, the neutron counting rate is proportional to t^{-1}:

$$N(E)\,dE = \frac{\varphi_{epi}\,dE}{E} = N(t)dt$$

$$E = gL^2/t^2$$

$$N(t) = \frac{\varphi_{epi}}{E}\,\frac{dE}{dt} = \frac{2\,\varphi_{epi}}{t} \qquad (6.11)$$

The gamma-ray intensity varies more slowly than t^{-1}, hence the largest gamma ray to neutron ratio occurs at large t (low energy). The reasonable agreement between the off-zero degree calculations and boron capture detector measurements indicates the graphite capture gamma ray background is probably small.

Figure 6.2 shows the 0° spectra at 20.3 cm, 35.6 cm, and 50.8 cm after attempting to adjust the boron capture detector background to match the

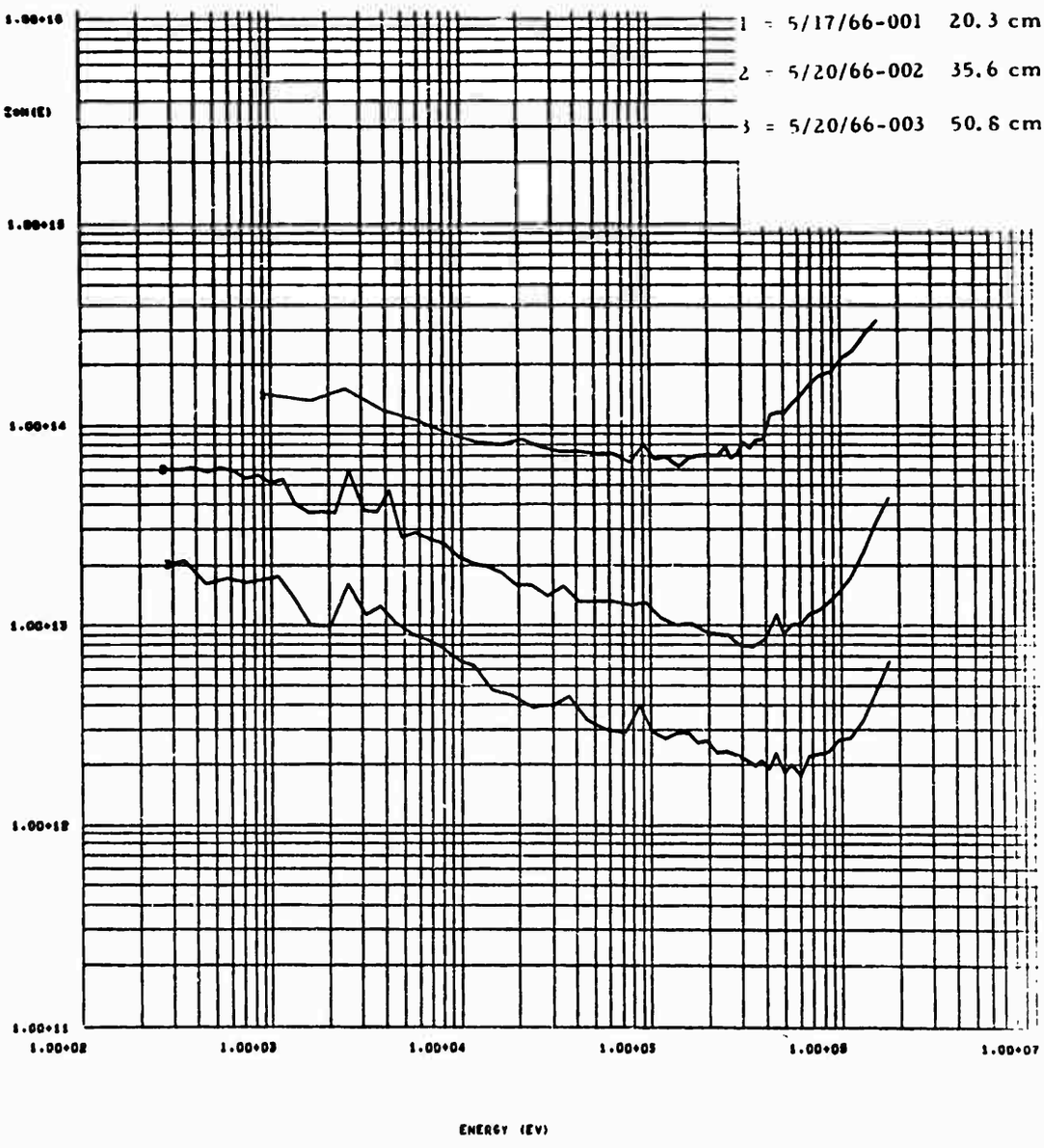

Fig. 6.2--Zero degree intermediate spectra after correction for background

"correct", approximately 1/E, flux as measured by the BF_3 detector. The ratio of the 1/E flux as measured by the BF_3 detector, to the flux near 200 eV as measured by the boron capture detector, was used to correct the net counts of the boron capture detector and thus to find an adjusted, larger, constant background. The final correction still does not bring the boron capture results into agreement with the BF_3 results. However, the counting rate of the boron capture detector in the hundred eV region is only ~20% above the background obtained from the second analyzer. The computed flux is extremely sensitive to the amount of background subtracted, and statistics are very poor so that the lowest grouped point is found in the kilovolt range or higher. Even if this could be overcome, e.g. by the use of smoothed data, the results could not be trusted since the correction depends too sensitively on the accuracy of the flux measurements and the assumed constancy of gamma-ray background. The 0° boron capture detector results may still contain sizeable errors in the few hundred eV range, but should be accurate above about 10 keV since the signal/background ratio is much larger at the higher energies.

Afterglow refers to the rapidly decaying exponential counting rate observed just after the photomultiplier tube is gated on; it arises from the scintillator phosphorescence and possibly electronic recovery effects following the overload from the bremsstrahlung flash. It is often significant above ~8 MeV in zero-degree and near zero-degree measurements, even with the uranium filter in the flight path. An approximate correction for the afterglow in the NE213 detector measurements was made by comparing the NE213 and NE211 measurements at 0°, 35.6 cm. (The NE211 detector, which has a faster fluorescence dieaway and smaller bremsstrahlung energy absorption because of its smaller size, exhibits very little afterglow background.) In the NE213 the afterglow background is quite negligible at 6.67 MeV. A mean-life of 120 nanoseconds for the NE213 afterglow was found, and the ratio of the neutron flux at 6.67 MeV to that at 13.7 MeV was 49. Using the neutron flux ratio, we found the magnitude of the afterglow

at 13.7 MeV and corrected the 6.67 MeV-13.7 MeV NE213 results by subtracting an exponentially decaying background with the proper magnitude at 13.7 MeV and a 120 nsec mean-life. At other positions and angles, we used the same mean-life and assumed the same neutron flux ratio to derive the afterglow correction. The correction was often quite large, $\sim$ 100% at 10 MeV. Since there is no guarantee that the flux ratio is correct, there may still be sizeable errors in our NE213 results above $\approx$ 8 MeV.

Background due to neutrons scattered in the collimators, or transmitted through them is thought to be very small, based on earlier experiments with the same collimation system.

6.3 PERTURBATIONS

Even if the flux were assumed to be measured with perfect accuracy, there might still be a discrepancy between experiment and any calculation which did not take into account the exact geometry and composition, boundary conditions, and radiation sources pertaining to the experiment. In a simplified calculation the deviations from the ideal small, isotropic neutron source in infinite homogeneous graphite may be considered as perturbations.

Possible perturbations are listed in Table 6.4.

Source anisotropy is discussed in Appendix A. Fission, scattering, and absorption interactions of back-scattered neutrons with the target materials may be considered a perturbation if the target is not included explicitly in the calculation, although this is more in the nature of an approximation than a perturbation. We did try a calculation with the target in a 7.62 cm radius cavity and compared it with the calculation in a 4.45 cm radius cavity. At a depth of penetration of 31.2 cm in graphite, corrected for the difference in $1/r^2$ attenuation, the scalar fluxes at an arbitrary "medium" energy of 145 keV were essentially identical. Since there would be considerably less interaction in the larger cavity, this suggests that the interaction effect with the smaller cavity is small. Also, in Section 3

Table 6.4

PERTURBATIONS

1.	Source anisotropy	± 5%
2.	Interactions in source material	< 5%
3.	Spurious sources	Small
4.	Non-infinite geometry	Calculable
5.	Room return	Negligible
6.	Probe-hole perturbation	< 10%
7.	Electron-beam perturbation	Small

we estimated the thermal neutron absorption in the target influenced the dieaway by less than 5%, and in Section 4 the flux plots indicate little if any flux distortion which might be attributed to the target.

No measurements were made of spurious sources of neutrons, such as photoneutrons produced in the electron beam piping or in the graphite. Based on previous experience and comparisons of theory and experiment in similar experiments, we believe spurious sources are small.

The influence of non-infinite geometry in the high energy experiments is discussed in Section 2.2. It should be negligible, especially since in most calculations there will actually be an outer boundary, probably spherical, to maintain a one-dimensional configuration. Low energy spectrum calculations must include the boundary explicitly or account for leakage by a local buckling which can be calculated from the flux plots in Section 4.

Room return, i.e., an external (delayed) source on the outer boundary due to neutrons backscattered from the walls and floors of the room, should have little effect on the high-energy spectrum measurements since they are made a few mean-free-paths from the boundaries. The thermal neutron flux plots indicate the perturbation of even the support table is negligible.

Perturbations by the probe hole for extraction of the neutron beam are more important, since the hole would seldom be included in a calculation and the unperturbed spectrum at the point of measurement is desired.

Various experimental and analytical studies have been made, but few general conclusions have been drawn. The perturbation is smaller with smaller probe hole diameter, and it is reasonable to measure the diameter in terms of mean-free-paths in the surrounding medium. In the thermal experiments, the d/λ ratio was 1.5. In the intermediate neutron energy range, the d/λ ratio varied from 3.0 to about one. In the fast neutron range the ratio varied from one to 0.3. On this basis, the largest perturbation would be expected at the lower energy end of the spectrum measured with the 7.62 cm diameter probe hole and boron-capture detector. Another consideration is the angular distribution. The 0° flux, which is mostly uncollided, has essentially zero perturbation. Removal of the scatterer in the probe hole volume would be expected to make the most difference at large angles, toward the backward direction. To test the probe hole perturbation in graphite we made one boron-capture detector measurement at 60° and 35.6 cm radius with the usual 7.62 cm diameter hole (Run 8, 5-21-66) and one with a 3.81 cm diameter hole for the first 30 cm (Run 1, 5-24-66). Results are plotted in Fig. 6.3. The flux as measured with the smaller probe-hole was equal to or somewhat larger than the spectrum measured with the perturbation of the larger hole. If the fluxes are normalized in the 100 keV - 1 MeV region, where the perturbation should be smallest, the two runs agree to within 10% or so at all energies except perhaps the very lowest. We conclude that the probe hole perturbation is less than 10%. Since the electron beam tube and entrance hole are small and far removed from the measurement position, their perturbation should be even smaller.

6.4 COMPARISON OF RESULTS

The time-of-flight and foil activation measurements contain a great deal of information. It will take some time to exploit them to the fullest extent. Meanwhile we have made some preliminary comparisons of the measurements with each other, and with the available calculations.

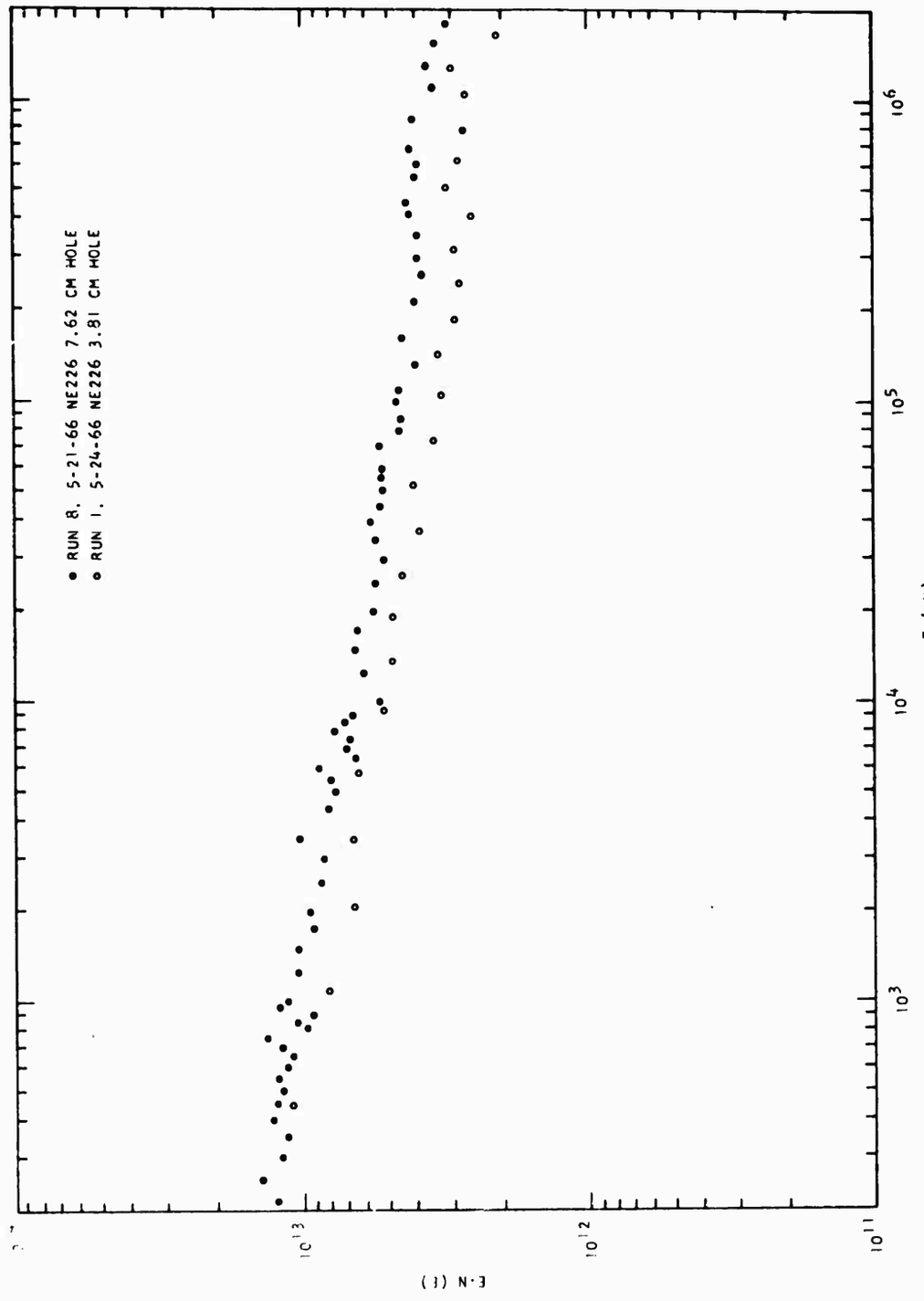

Fig. 6.3--Comparison of 60^{o} spectra vs probe-hole diameter

The spatial distribution of the absolute thermal neutron flux, as measured by indium and gold foils, is discussed in Section 4.1. The values normalized to unit sulfur monitor fluence are plotted in Fig. 6.4. These may be compared with 4π times the angular flux (n/cm^2 sr per unit sulfur monitor fluence) as measured at 90° in the time-of-flight experiment. The flux per unit energy was integrated numerically from 0.002 eV to 0.5 eV, multiplied by 4π steradian, and divided by 7.15×10^{13}. The latter figure arises from a peculiarity (to be corrected) of our data reduction code which multiplies the flux by an arbitrary factor of 7.15×10^6, and from an arbitrary factor of 10^7 between M, the monitor value used, and the actual sulfur monitor fluence. At 35.6 cm, where the gold foil was located, the fluxes agree to within better than 10%. At 20.3 cm and 50.8 cm the results differ by 25-30%, only slightly outside the estimated experimental errors.

The relative spatial distributions of the flux at 1.5 eV are plotted in Fig. 6.5. The cadmium-covered indium activity, which is mostly due to capture in the 1.46 eV resonance, is plotted from the Z-direction traverse (Table 4.4), extrapolated from 25.4 cm to 20.3 cm using the shape of the vertical traverse (Table 4.3). The indium activity is normalized at 20.3 cm to the 90° angular flux measured in the time-of-flight experiment. At 35.6 cm the fluxes agree to within 12%, and to within 30% at 50.8 cm. However, there is some evidence that the 90° flux at 50.8 cm is somewhat too high, judging from the 0° angular flux, which is also plotted. The DTF-IV calculation of the scalar flux, normalized at 20.3 cm, is also shown. The calculation is actually for the lowest energy group, which extends from 1.86 eV to 5.04 eV, but the relative spatial distribution is not expected to be significantly different at 1.5 eV. The slope of the calculated flux is somewhat steeper than either the foil or time-of-flight measurements.

Relative spatial distributions of the S(n, p) and Al(n, α) foil activations are discussed in Section 4.2. These activations should be proportional to

$$\int_{\text{Threshold}}^{\infty} \varphi(E)\, \sigma_{Act}(E)\, dE \qquad (6.12)$$

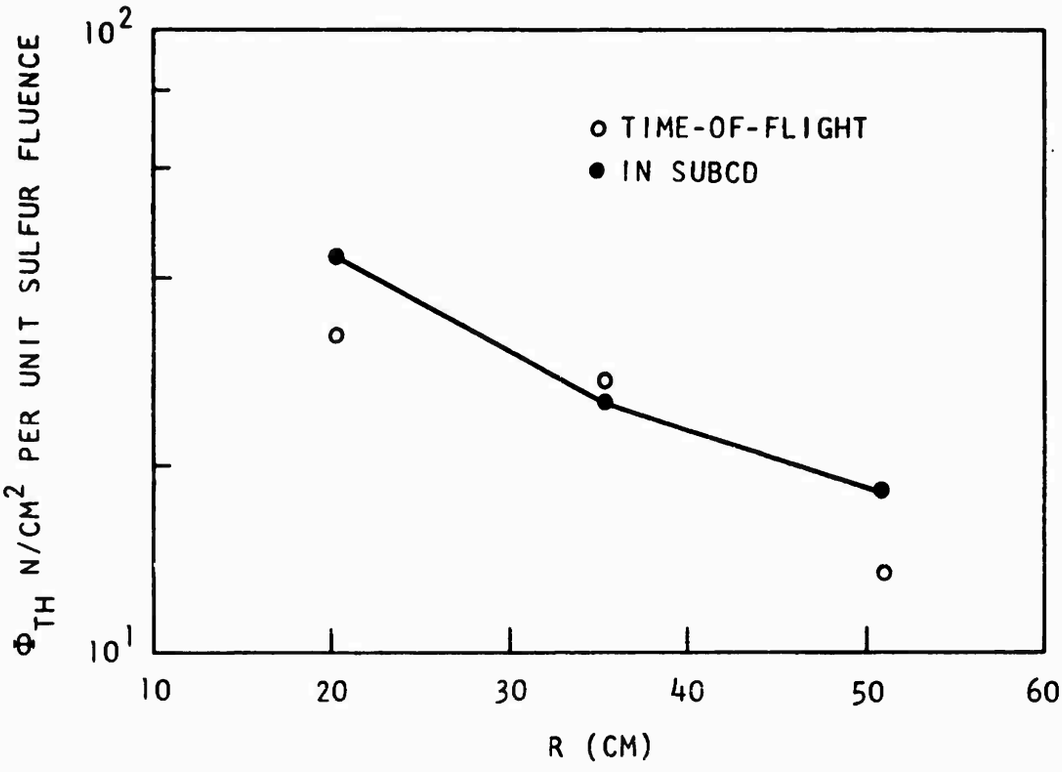

Fig. 6.4--Comparison of absolute thermal neutron flux

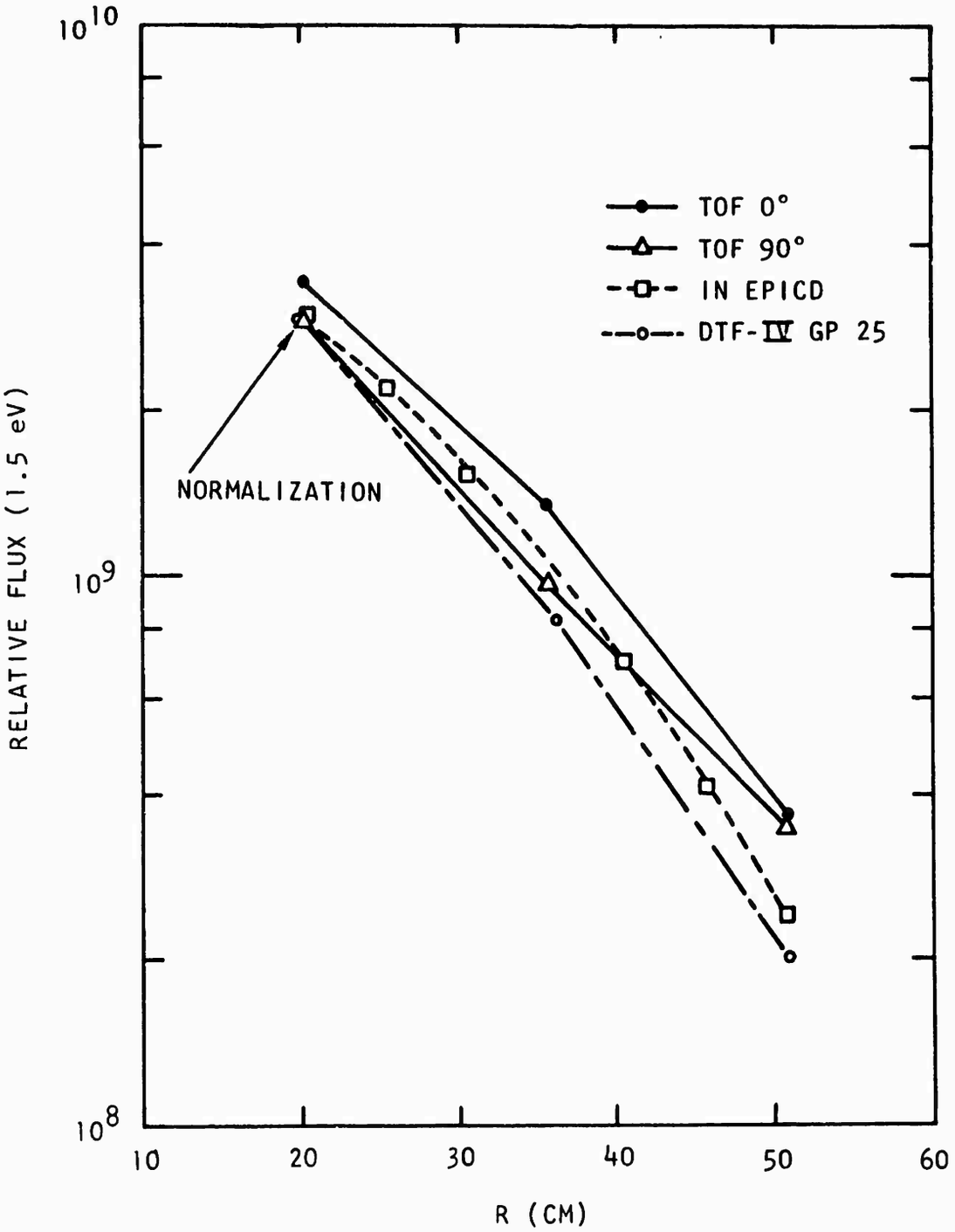

Fig. 6.5--Comparison of relative flux at 1.5 eV

where ϕ is the scalar flux. The time-of-flight experiment does not measure scalar flux, but angular flux, and since the fast neutron flux is very anisotropic it will take more time and effort to derive the scalar flux from the measurements. However, we can compare the foil results with the relative activation calculated from the cross sections given in Table 4.14 and the scalar flux (Table 6.5) in the DTF-IV calculation of Section 5. An approximate numerical integration of the weighted group fluxes gave the S(n, p) and Al(n, α) relative activations given in Table 6.5. The foil activation results from Table 4.7 are replotted in Fig. 6.6. The calculated activities, normalized to experiment at 20.3 cm, are also plotted. The calculated and measured Al(n, α) activities agree very well at 50.8 cm but the foil result appears to be about 40% too high at 35.6 cm. This deviation from a smooth exponential attenuation may also be noted in Fig. 4.6. The S(n, p) activities definitely appear to have different slopes, the calculated attenuation being greater than that measured by the sulfur foils. This requires further investigation but is probably related to the resonance structure in the actual flux spectrum.

Figure 6.7 is a plot of the fast neutron scalar flux spectrum at 35.6 cm as measured by the threshold foils (discussed in Section 4.3), and the DTF-IV calculation arbitrarily normalized in this case to the {S(n, p), Al(n, p), Al(n, α)} set at 10 MeV. There are only a few points, but it can be said that agreement is fair above 5 MeV and widely discrepant below that. The calculation should be repeated with a finer group structure, however it appears that S(n, p) exaggerates the dip at 3.5 MeV.

The fast neutron angular flux spectra at 35.6 cm are compared with the DTF-IV angular flux calculations in Fig. 6.8. Here the 17° measurements have been normalized to the 19° calculations at 2 MeV. Obviously the seven energy groups between 1 and 15 MeV do not reproduce the detail in the time-of-flight spectra, but approximately average the flux. There

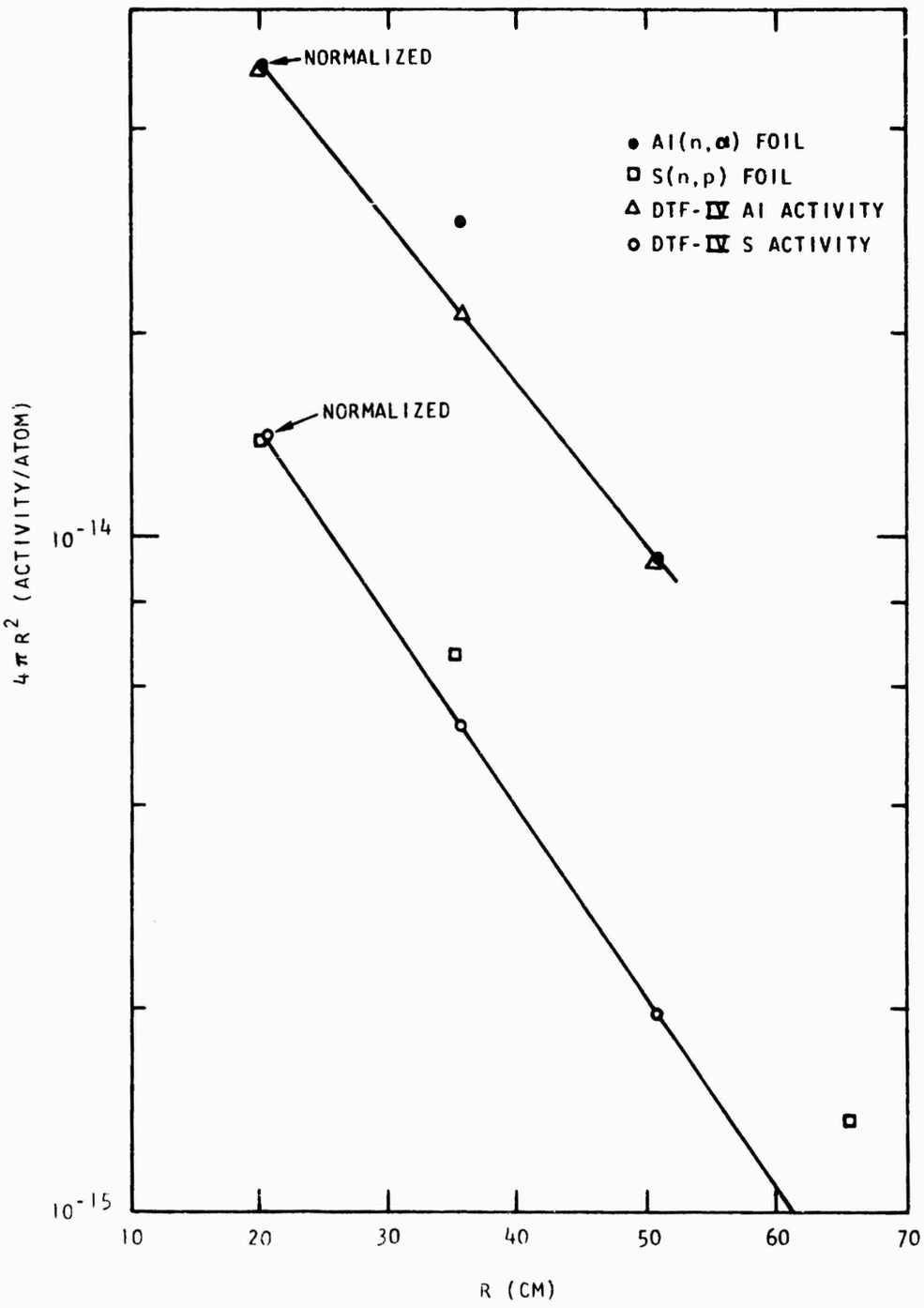

Fig. 6.6--Calculated and measured relative sulfur and aluminum activities

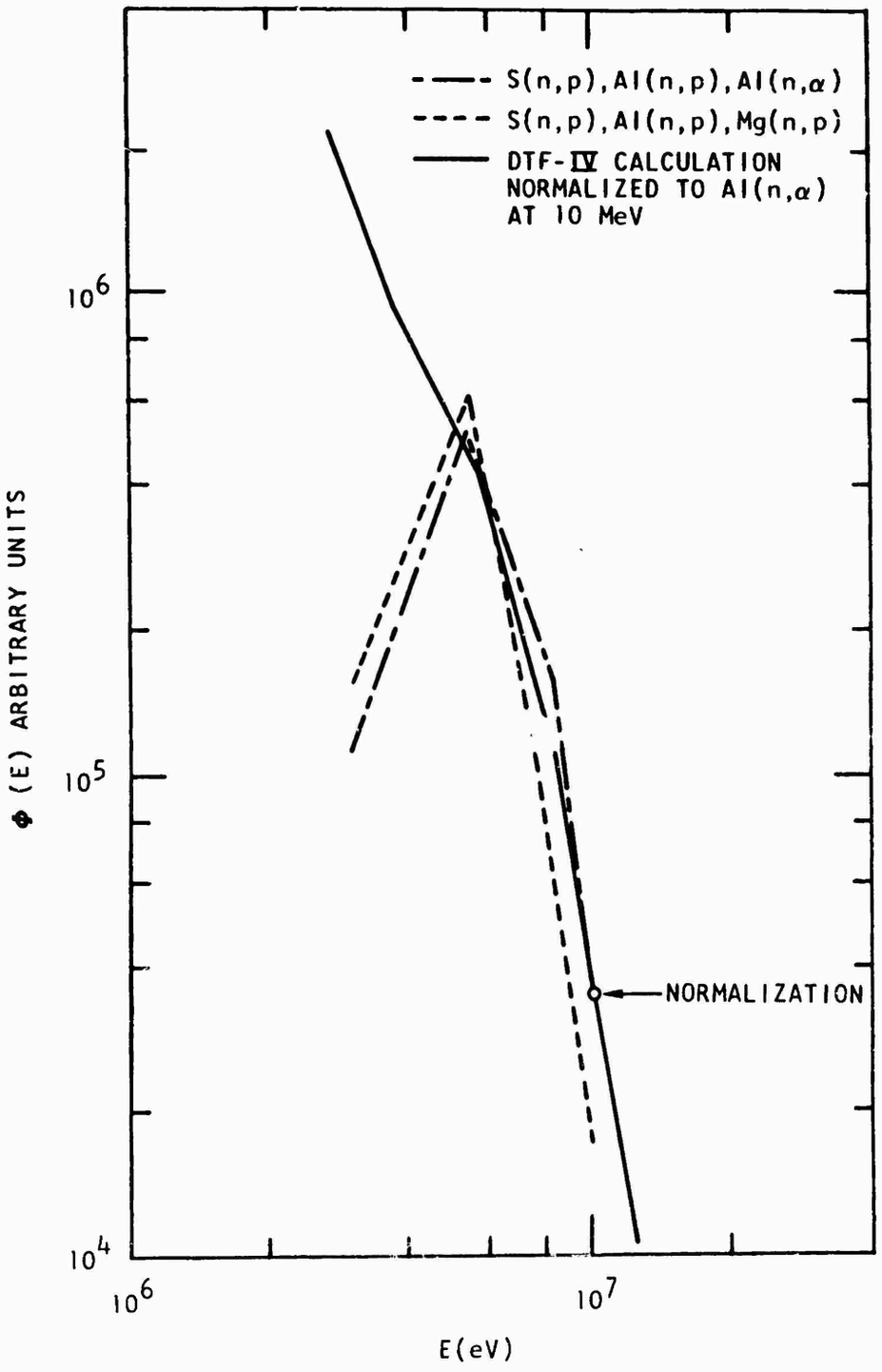

Fig. 6.7--Measured and calculated scalar flux spectrum at 35.6 cm

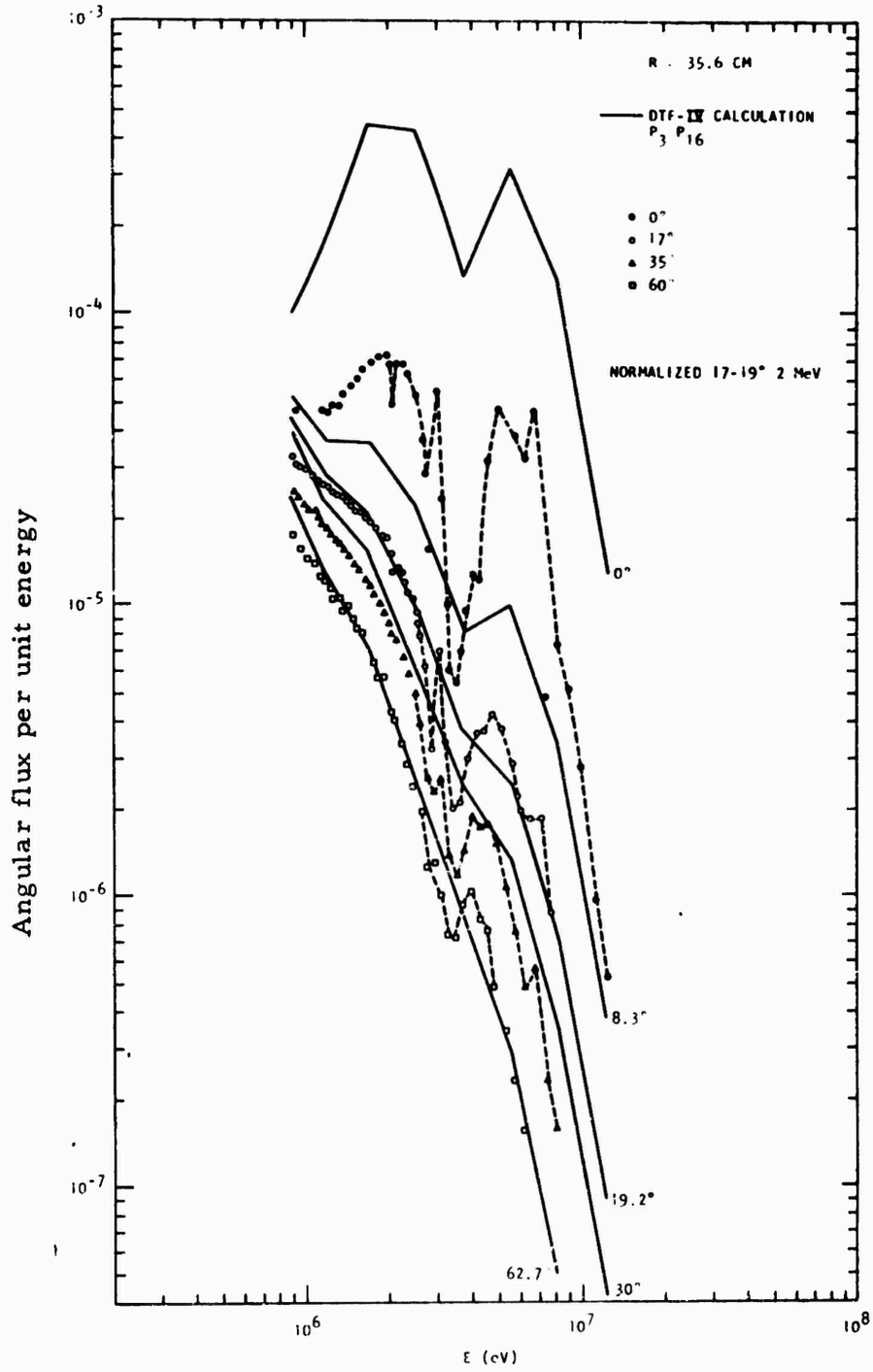

Fig. 6.3--Measured and calculated fast neutron angular flux spectra at 35.6 cm

Table 6.5

DTF-IV SCALAR FLUX

Gp	E_{mid} (eV)	ΔE(eV)	φ(E) 20.3 cm	35.6 cm	50.8 cm
1	1.25 + 7	4.92 + 6	2.77-5	3.10-6	4.87-7
2	8.4 + 6	3.30 + 6	9.40-6	1.05-6	1.74-7
3	5.6 + 6	2.21 + 6	3.79-6	5.14-7	1.00-7
4.	3.75 + 6	1.48 + 6	8.64-7	1.24-7	2.62-8
5	2.5 + 6	9.93 + 5	8.07-8	1.25-8	2.94-9
		$S = \sum_J \varphi_J \sigma(S)_J \Delta E_J$	9.211 + 3	1.131 + 3	2.060 + 2
		$Al = \sum_J \varphi_J \sigma(Al)_J \Delta E_J$	2.135 + 2	3.112 + 1	6.736 + 0
		$4\pi r^2$ S	4.79 + 7	1.81 + 7	0.67 + 7
		$4\pi r^2$ Al	1.11 + 6	0.498 + 6	0.219 + 6

is evidence of a systematic discrepancy at lower energies, the calculations predicting somewhat lower fluxes than were measured. The zero-degree measurement lies between the calculated 0° and 8.3° fluxes (except at the large resonance dip), as it should. The "0°" measurement is actually an average over a finite angular resolution of $\pm 5.1^\circ$. It includes all the uncollided flux from the target, which lies within an angle of about $\pm 1.3^\circ$. However, the DTF-IV code does not properly calculate this sharply peaked angular distribution and thus there is no proper way of averaging the calculations over the experimental resolution.

The 20.3 cm, 30° intermediate-energy ($\approx 10^3$ to 10^5 eV) spectrum measured by time-of-flight agrees quite well (±10-20%) with the DTF-IV calculation, and both are nearly 1/E (there is a slight decrease at lower energies). At 35.6 cm both theory and experiment rise approximately twice as fast as 1/E, with decreasing energy. At 50.8 cm experiment and theory rise

approximately three times as fast as 1/E. Qualitatively, this variation is expected since the spectrum softens with distance in a graphite column.

There are no DTF-IV calculations available yet for energies below a few eV. Th low-energy spectrum in reactor-grade graphite is very sensitive to leakage (as well as to the scattering kernel), and the positive-buckling GATHER-II calculation does not agree at all with the measurements. Attempts to calculate the spectrum with a negative buckling have been unsuccessful so far.

6.5 RECOMMENDATIONS

The experimental research in this program has provided a rather complete description of the penetration of neutrons in graphite, comprising time-of-flight and foil measurements of spectra and energy-integrated fluxes, as well as dieaway measurements. Many more comparisons could be made between experimental results, particularly to explore the reliability of threshold-foil measurements. However, the main purpose of the research was to provide an experimental standard for guiding and testing transport calculations. The choice of input meshes, and other numerical and physical approximations, is always restricted by finite computer storage and computation time. Given accurate, high-resolution measurements of the space-energy-angle distribution, as well as some time-dependent information, it should be possible to track down the sources of discrepancies between theory and experiment with much more insight and confidence than has hitherto been possible.

A start has been made on theory-experiment comparison, as discussed in Section 6.4. However, perhaps the most interesting aspect, viz. the influence of the energy-group structure and cross sections on the calculation of the spectrum and spatial distribution, could not be investigated. Reliable thermal neutron calculations are entirely lacking. Graphite, like some other non-hydrogenous materials, has interesting neutron attenuation properties. The flux is attenuated much more strongly in the resonances

than between or below them, which severely tests the multigroup approximation. In hydrogenous materials the low-energy flux follows the fast neutron attenuation and reaches an asymptotic spectrum, while in graphite the low energy neutrons are attenuated less rapidly than the fast neutrons, and the spectrum continues to soften with distance. Approximations which might be valid for hydrogenous materials may not work for graphite. In Monte Carlo calculations it is necessary to include some form of variance-reduction to obtain decent statistical precision even at moderate penetrations. Comparison of Monte Carlo calculations with the measurements should help evaluate the reliability of different variance-reduction procedures. Additional calculations by Monte Carlo and discrete-ordinates codes are strongly recommended.

The graphite assemblies could not be made truly infinite for low-energy neutrons. With so little absorption, the spectrum is quite sensitive to leakage. There is probably a real difference in the flux at 200 eV in the smaller and larger graphite assemblies, although the monitoring may have been somewhat different and the accuracy of both the BF_3 and the boron-capture detector measurements is poorest here (the signal/background ratio is small and the efficiency of the BF_3 detector is not too well known). This question bears more investigation, however, we note that the thermal spectrum can still be calculated separately, using the spatial distribution of the slowing-down source from the indium foil activations.

In future work we recommend studying the common hydrogenous material, water, the common high-Z material, iron, and then iron/water laminated shields. Neutron angular flux spectrum measurements, and later gamma-ray angular flux spectrum measurements, will test the oxygen and iron cross sections and the theoretical procedures for handling the important problems of inelastic scattering, secondary gamma ray production, and the spatial distribution of the low energy flux near the iron/water interface. The neutron spectrum measurements can be performed as in the graphite, except our new high-efficiency, low-background

intermediate-energy detector would be used and either a larger NE211 detector or the NE213 detector with pulse-shape discrimination. The new on-line computer will permit time-compression of the analysis channels, and more flexibility in accumulating and subtracting background. A concurrent effort in analysis should be carried out if maximum benefit is to be realized.

REFERENCES

1. J. H. Alexander, G. W. Hinman, and J. K. Triplett, "GAPLSN - A Modified DSN Program for the Solution of the One-Dimensional Anisotropic Transport Equation," General Atomic Report GA-4972 (1964).

2. G. D. Joanou and J. S. Dudek, "GAM-II - A B_3 Code for the Calculation of Fast Neutron Spectra and Associated Multigroup Constants," General Atomic Report GA-4265 (September 16, 1963).

3. A. E. Profio, "Verification of Analytical Techniques (GAPLSN - Transport Theory and O5R - Monte Carlo Theory) by Utilization of Measured Fast Neutron Spectra in Infinite Paraffin and Spherical Paraffin Shields," Air Force Weapons Laboratory Report AFWL-TR-65-193, General Atomic Division, General Dynamics Corporation (March, 1966).

4. A. E. Profio, J. C. Young, and P. L. Phelps, "Design and Efficiency Calibration of the 5 cm and 13 cm Fast Neutron Fast Neutron Detectors", General Atomic Report GA-7483 (1966).

5. A. E. Profio, "The Boron Capture Detector for Time-of-Flight Measurements", General Atomic Report GA-7578 (1966).

6. J. M. Neill, D. S. Scipione, and A. E. Profio, "Efficiency of the $^{32}BF_3$ and $^{36}BF_3$ Detector Banks", General Atomic Report GA-7497 (1966).

7. H. C. Honeck, "CAP, A Collimator Analysis Program, "General Atomic Report GA-5418, July 16, 1964.

8. H. M. Antunez et al., "HECTO, A FORTRAN-IV Code for Reduction of Time-of-Flight Data", General Atomic Report GAMD-7527 (1967).

9. J. R. Brown and K. R. Van Howe, "GAPS, A Fortran Code for Analyzing Data from Pulsed Neutron Source Experiments, General Atomic Report GAMD-6781, October 11, 1965.

10. N. Corngold and P. Michael, Nucl. Sci. Eng. 19, 91 (1964).

11. K. H. Beckurts, in Vol 2 of Pulsed Neutron Research, IAEA (1965), p. 16.

12. H. Klose, M. Kuchle and W. Reichardt, USAEC Report BNL 719, Brookhaven National Laboratory (1962) p. 935.

13. E. Starr and G. A. Price, USAEC Report BNL 719, Brookhaven National Laboratory (1962) p. 1034.

14. K. H. Beckurts and K. Wirtz, Neutron Physics, Springer-Verlag, New York, 1964.

15. ANL 5800, 2nd Edition, Reactor Physics Constants (1963).

16. A. E. Profio, J. U. Koppel and A. Adamantiades, Pulsed Neutron Research, Vol. I, IAEA, Vienna, 1965, p. 129.

17. G. D. Joanou, C. V. Smith, and H. A. Vieweg, "GATHER II." General Atomic Report GA-4132, July 1963. Input is described in the GGC-II report, C. V. Smith and H. A. Vieweg, General Atomic Report GA-4436 (1963).

18. J. A. Young, N. F. Wikner and D. E. Parks, Nukleonik, 7, No. 6, (1965) p. 295-300.

19. W. L. Zijp, "Review of Activation Methods for the Determination of Fast Neutron Spectra," Netherlands Report RCN 37, 1965.

20. M. Bresesti et al., "Fast Neutron Measurements by Threshold Detectors in Ispra-1 (CP-5 Type) and Avogadro RS1 (Swimming-Pool) Reactors", Neutron Dosimetry, Vol. 1, IAEA, Vienna, 1963, pp. 27-50.

21. K. D. Lathrop, "DTF-IV, A Fortran-IV Program for Solving the Multigroup Transport Equation with Anisotropic Scattering." USAEC Report LA-3373, Los Alamos Scientific Laboratory (1965).

22. J. R. Beyster et al., "Integral Neutron Thermalization Annual Summary Report, October 1, 1960 through September 30, 1961", USAEC Report GA-2544 General Atomic Division General Dynamics Corporation (1961).

23. R. E. Sund and R. B. Walton, "Gamma Rays from Short-Lived Fission-Fragment Isomers", Phys. Rev. 146, 824-835 (1966).

24. R. B. Walton and R. E. Sund, "Delayed Gamma Rays from Fission", AFWL Report GA-7348 General Atomic Division General Dynamics Corporation (1966).

25. F. C. Maienschein, R. W. Peele, W. Zobel, and T. A. Love, in Second United Nations Conf. Peaceful Uses Atomic Energy, Geneva, 1958, Vol. 15, p. 360.

26. P. C. Fisher and L. B. Engle, Phys. Rev. 134, B796 (1964).

27. L. V. Groshev et al., Atlas of γ-Ray Spectra from Radiative Capture of Thermal Neutrons, Pergamon Press, London, 1959.

28. T. Rockwell, Reactor Shielding Design Manual, Van Nostrand, Princeton, 1956, p. 353.

APPENDIX A

ANGULAR FLUX SPECTRUM AND OTHER CHARACTERISTICS OF THE 7.62 cm URANIUM TARGET

GENERAL ATOMIC

DIVISION OF

GENERAL DYNAMICS

JOHN JAY HOPKINS LABORATORY FOR PURE AND APPLIED SCIENCE

P.O. BOX 608, SAN DIEGO, CALIFORNIA 92112

GA-7409

ANGULAR FLUX SPECTRUM AND OTHER CHARACTERISTICS OF THE 7.62-CM DIAMETER URANIUM TARGET*

Work done by:

H. M. Antunez
J. H. Audas
J. H. Diaz
M. R. Hackney
G. K. Houghton
A. E. Profio
J. L. Russell, Jr.
D. S. Scipione
G. D. Trimble

Report written by:

A. E. Profio
M. R. Hackney
G. D. Trimble
H. M. Antunez
J. L. Russell, Jr.

*Based on work supported by the National Aeronautics and Space Administration, Defense Atomic Support Agency, Air Force Weapons Laboratory, and Atomic Energy Commission.

September 1, 1966

1. INTRODUCTION

Measurements of neutron spectra in shields, moderators, and subcritical reactors are made by the pulsed source, time-of-flight technique at the General Atomic Linear Accelerator Laboratory. The object of this report is to describe the characteristics of the 7.62-cm diameter depleted uranium target developed as the standard neutron source for fast and intermediate spectrum measurements.

In any comparison of calculated and measured spectra it is essential that the source spectrum and angular distribution be known accurately. An advantage of the Linac measurements is that the angular flux spectrum of the source can be measured by the time-of-flight technique, just as in the assembly itself. Since the target is often imbedded in the shield or reactor, it is desirable that the emission be reasonably independent of position on the target surface. The position-independence, or spherical symmetry, is sometimes expressed by saying the target is isotropic (with respect to the axis of the electron beam). This is particularly important when the flux at different angles is measured at supposedly equivalent positions within the experimental assembly, a situation which often arises since it is impossible to rotate the flight path and it is often inconvenient to bend the electron beam. In measurements of the penetration of neutrons to great depths in shields, a very intense pulsed source is required. To accept the full electron beam power from the Linear Accelerator, the target must be water-cooled instead of air-cooled, but the isotropy relative to the electron beam should not be impaired. It is desirable also that there be little degradation of the fast neutron spectrum.

2. TARGET DESIGN

Figure 1 is a photograph of the target showing the water coolant connections in one standard configuration. Figure 2 is a simplified cross section. From time to time, modifications have been made in the design

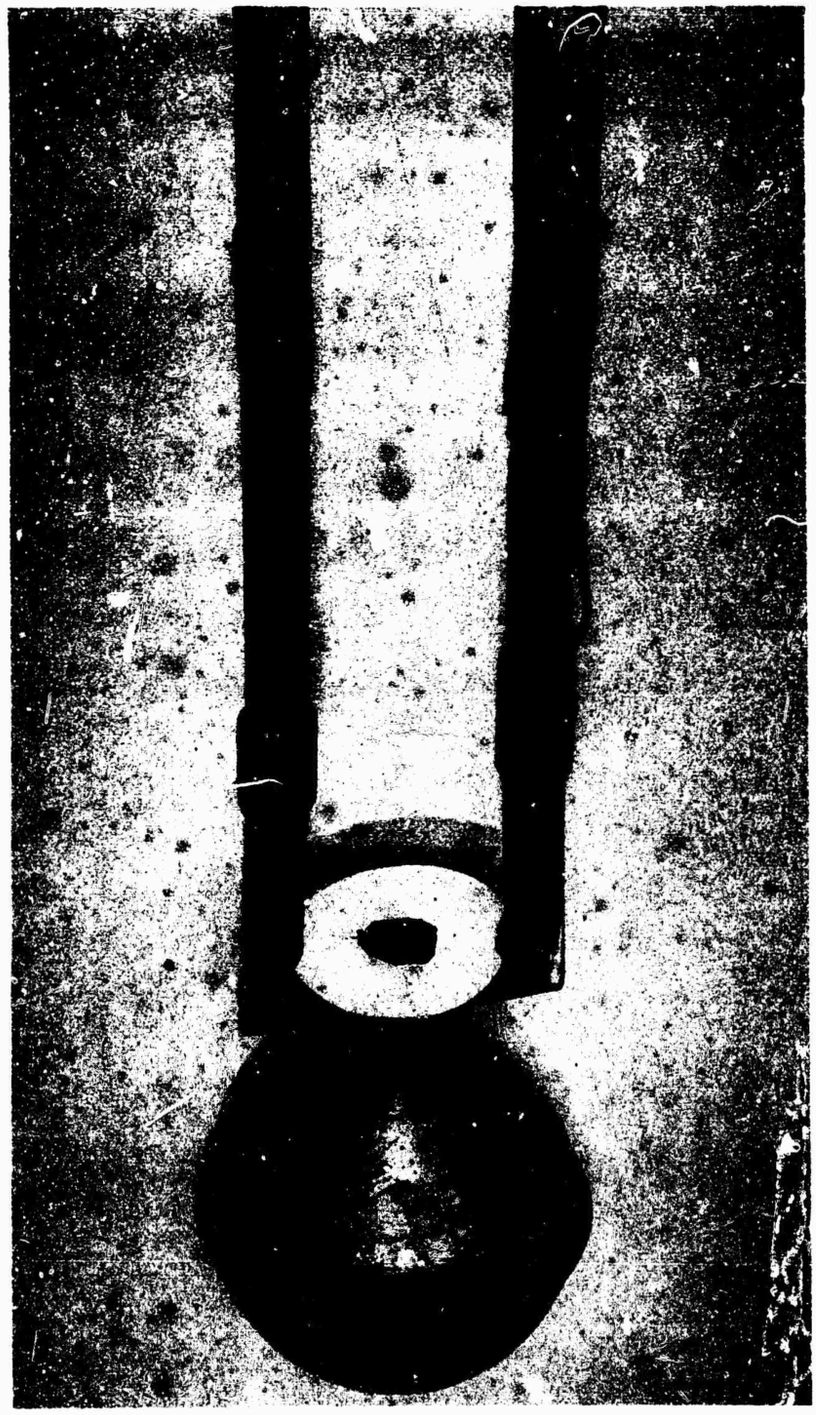

Fig. 1--Photograph of the 7.62 cm water-cooled uranium target

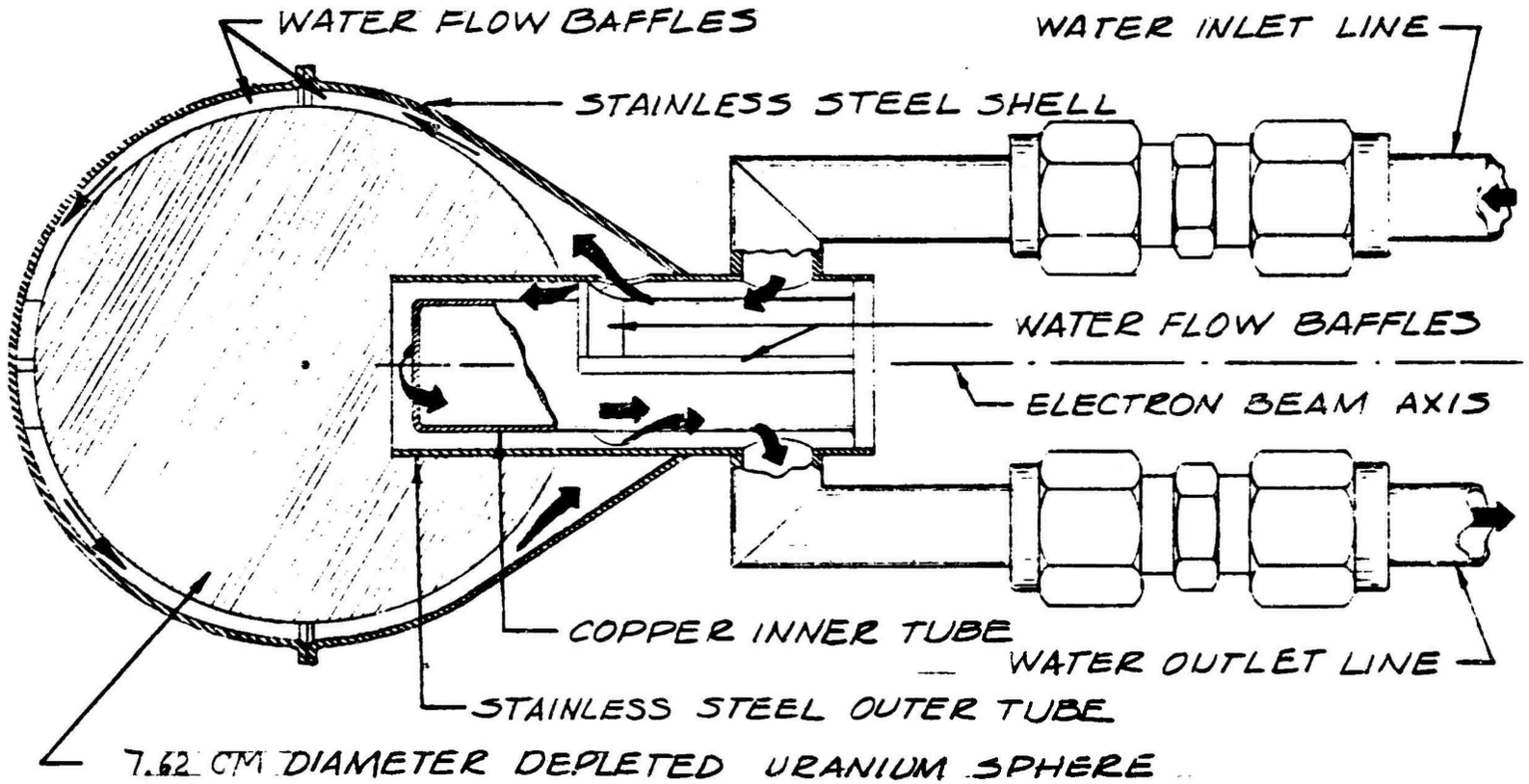

Fig. 2--Cross section of the water-cooled uranium target

of the electron beam inlet snout, water connections, support, and method of assembly, but these should not change the neutron emission characteristics appreciably. The basic component is the depleted uranium sphere (0.22 weight percent ^{235}U), 7.62 cm in diameter, with a 2.54 cm diameter cylindrical reentrant hole extending to within 0.85 cm of the center of the sphere. The electron beam impinges on the bottom of this hole. To avoid fission-product and uranium contamination of the water, the sphere is plated with 0.0254 cm of copper and 0.0127 cm of nickel. (The main difficulty with the target is getting a satisfactory plating of the reentrant hole.) The cooling water flows between the bottom of the reentrant hole and the 0.0813 cm thick copper window admitting the electron beam. A parallel stream flows around the outside of the sphere, directed by thin vanes not shown in the figure. The water is contained by a 0.0762 cm thick jacket of Type 304 stainless steel. Because of variations in fabrication and assembly, the outer water stream may vary from 0.18 cm to 0.23 cm thickness. The stream at the electron impingement surface is 0.32 cm thick.

The depth of the reentrant hole and the diameter of the sphere were carefully chosen as a result of the investigations of G. D. Trimble, et al.,[1] at the Linear Accelerator Laboratory. The depth of the hole was chosen to make the centroid of photoneutron production coincide with the center of the sphere. Three radiation lengths between the electron impingement surface and the center of the sphere was found to be best in experiments with Fansteel (89% W, 7% Ni, 4% Cu) and depleted uranium targets. The neutrons then traverse the same amount of material in every direction, except at the reentrant hole itself. The target diameter was made sufficiently large that scattering smooths out the remaining anisotropy; the larger diameter also helps attenuate the bremsstrahlung incident on the experimental assembly and neutron detector. Fansteel spheres of 2.54, 7.62, and 9.60 cm diameter were investigated, as well as 5.08 and 7.62 cm

diameter spheres of depleted uranium. The emission vs angle to the electron beam was measured by activation of sulfur and aluminum foils placed in a ring around the target, and by time-of-flight measurements. The emission of the 7.62 cm diameter uranium sphere is as uniform as the 9.60 cm diameter Fansteel sphere, presumably because of the isotropy of photofission neutron production. The photoneutron yield of uranium is twice as large as that for Fansteel,[2] and uranium was chosen despite the disadvantage of fission-product contamination in event of cooling or plating failure.

With air cooling, the target can dissipate about 200 watts without excessive temperature rise. To handle higher electron beam power, and to contain any fission products or uranium which may escape, the water cooling jacket was added. Calculated heat removal capacity is 1.5 kW at 250°F maximum uranium temperature, at a flow rate of 6 gal/min and system backpressure of 25-30 lb/in^2. Measurements indicate the design is conservative, and somewhat higher power could be accommodated.

3. MEASURED NEUTRON EMISSION

3.1 ISOTROPY RELATIVE TO THE ELECTRON BEAM

Figure 3 is a polar plot of the relative activation of sulfur foils placed around the air-cooled or water-cooled target at a radius of 15 cm. The reaction is $^{32}S(n,p)^{32}P$, with a 3 MeV threshold. Figure 4 is a plot for the activity from $^{27}Al(n,\alpha)^{24}Na$, which has a 7 MeV threshold. The deviations from uniform emission, as seen by the foils, are 6-10%, except in the backward direction. In shield and reactor spectrum measurements, the neutron beam is generally extracted from the assembly in the 30° to 100° region.

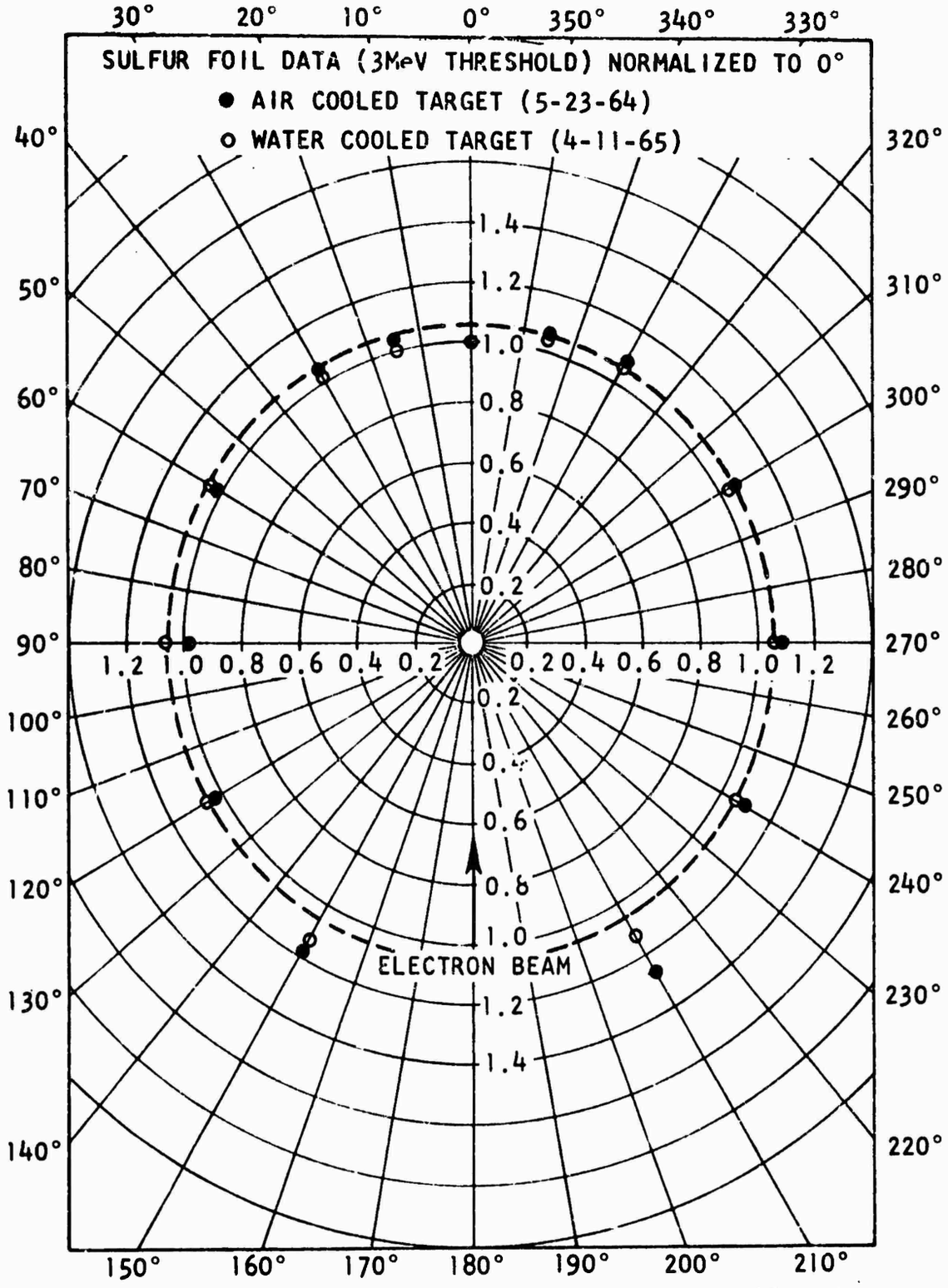

Fig. 3--Sulfur activation, air and water-cooled 7.62 cm target

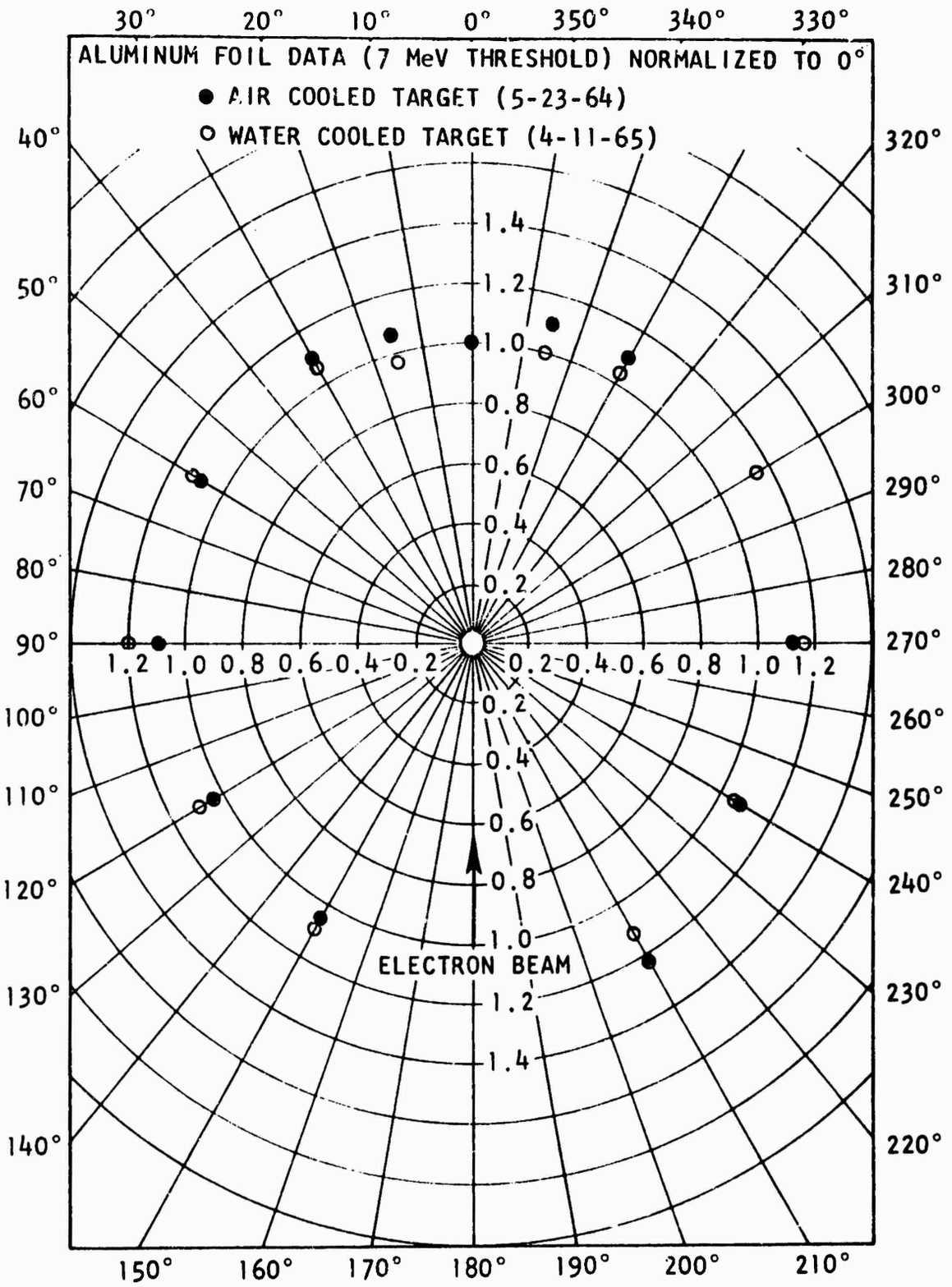

Fig. 4--Aluminum activation, air and water-cooled 7.62 cm target

3.2 MEASUREMENTS OF THE ANGULAR FLUX SPECTRUM

Measurements of the spectrum have been made by the time-of-flight method on at least three separate occasions.[1, 3] These measurements have been made at different angles to the radius vector, different positions on the surface, and with different size collimators. All confirm the rather high degree of position-independence implied by the foil activation experiments at MeV energies, and the uniformity should be even better at lower energies. The latest series of measurements will be discussed here. For these measurements the electron beam was bent by an electromagnet, and the target was translated left-to-right or up-and-down, so that different areas on the target surface and different angles to the radius vector could be observed.

At each position and angle the spectrum was measured with the 5.08 cm by 5.08 cm NE211 liquid scintillation detector biased at 0.054 cobalt units,[3] or about 500 keV neutron energy. For measurements below about 1.5 MeV, our 19 cm diameter boron capture detector was used. This consists of a disk of boron carbide plus paraffin mixture (approximately 75 weight percent B_4C, and 25 weight percent CH_2), 19 cm diameter and 10 cm thick, which slows down and captures neutrons. The 480 keV boron capture gamma ray is detected in a 12.7 cm diameter by 7.6 cm thick NE226 (hexafluorobenzene base) liquid scintillator. The scintillation detector is mounted coaxially and in contact with the borated disk; bias was 145 keV electron energy. The efficiency of the NE211 scintillator was obtained from the Verbinski calculations.[3] The efficiency of the boron capture detector was obtained in two steps. First the probability and spatial distribution of captures for selected neutron energies was calculated with the O5R Monte Carlo code. Secondly the absolute detection efficiency for 480 keV gamma rays was measured with a 1 cm by 1 cm Be^7 source, as a function of position in a duplicate borated disk. The

over-all efficiency is then simply the weighted, volume-integrated capture probability. The O5R code also calculates the first and second moments of the time-to-capture, for corrections to the measured time spectrum.

Run-to-run source output monitoring was accomplished by activation of sulfur foils. The results from the two detectors are expressed as neutrons incident (corrected to a flight path transmission of unity) per eV, per monitor count. To correct for the difference in solid angles of the two detectors, the boron detector results have been multiplied by 11.04, the ratio of the area of the borated disk to the area of the 5.08 cm NE211 detector. In Fig. 5 we see the angular flux at 0° to the radius vector at different positions on the surface, measured with a 1.27 cm diameter collimator. The positions are indicated by the diagram in the figure. In Fig. 6 we have similar measurements, but now at about 30° to the radius vector. The angular flux spectrum from the target is quite symmetric, i.e., independent of position on the surface, in agreement with the activation measurements. The angular distribution is more peaked at 0° than a cosine, as would be expected for a sphere only a mean free path or so in radius. The spectrum is softer at larger angles, indicating the importance of inelastic scattering relative to absorption.

In another series of measurements (with a different sulfur monitor location), the target spectrum was measured with a collimator which viewed the entire hemisphere, (see Fig. 7). The angle between the electron beam and the collimator was 95° in this case. The hemisphere-integrated angular flux

$$\Psi(E) = 2\pi \int_0^{\pi/2} \varphi(E) \sin\theta \, d\theta$$

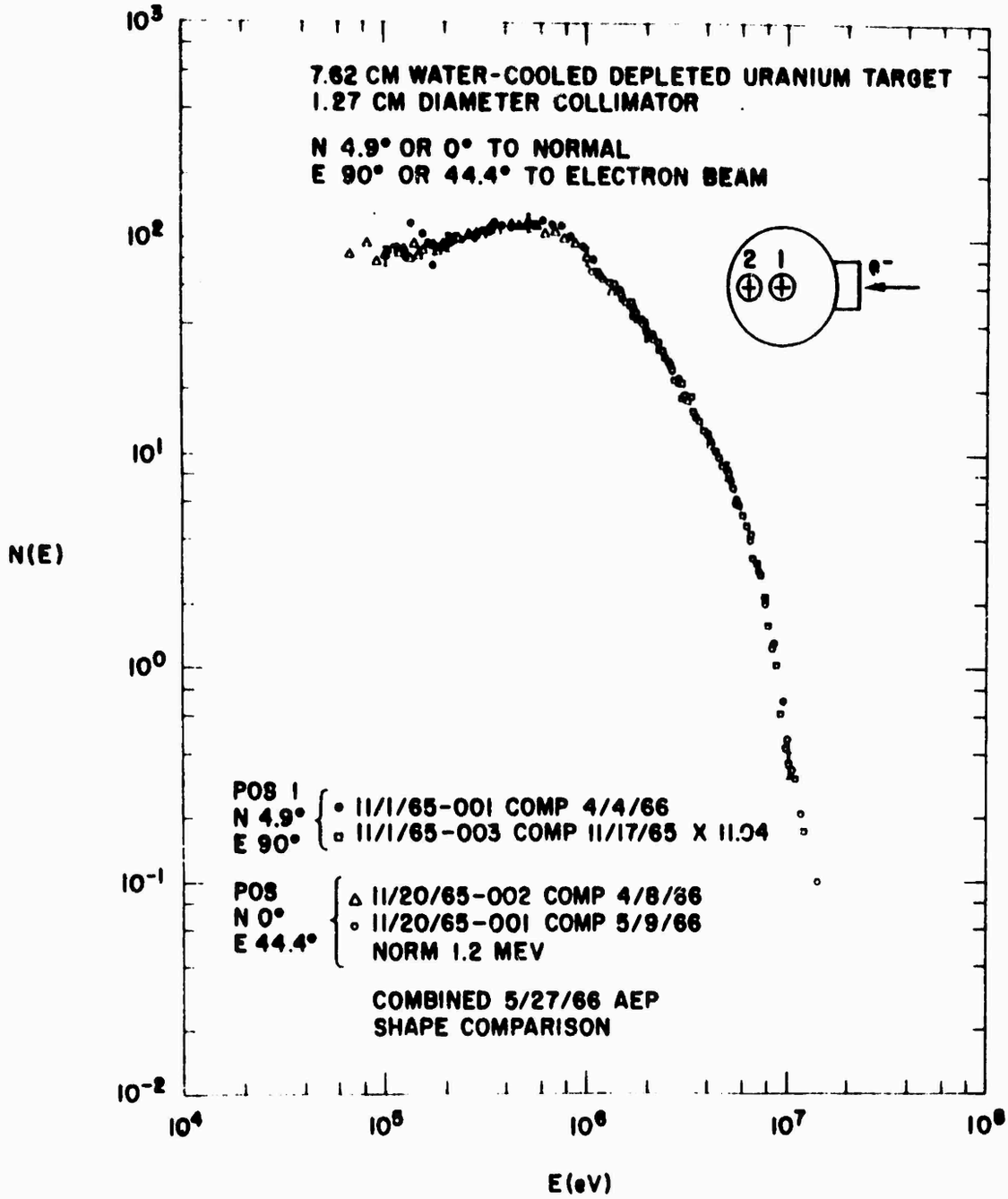

Fig. 5--Angular flux spectrum at 0° to the radius vector

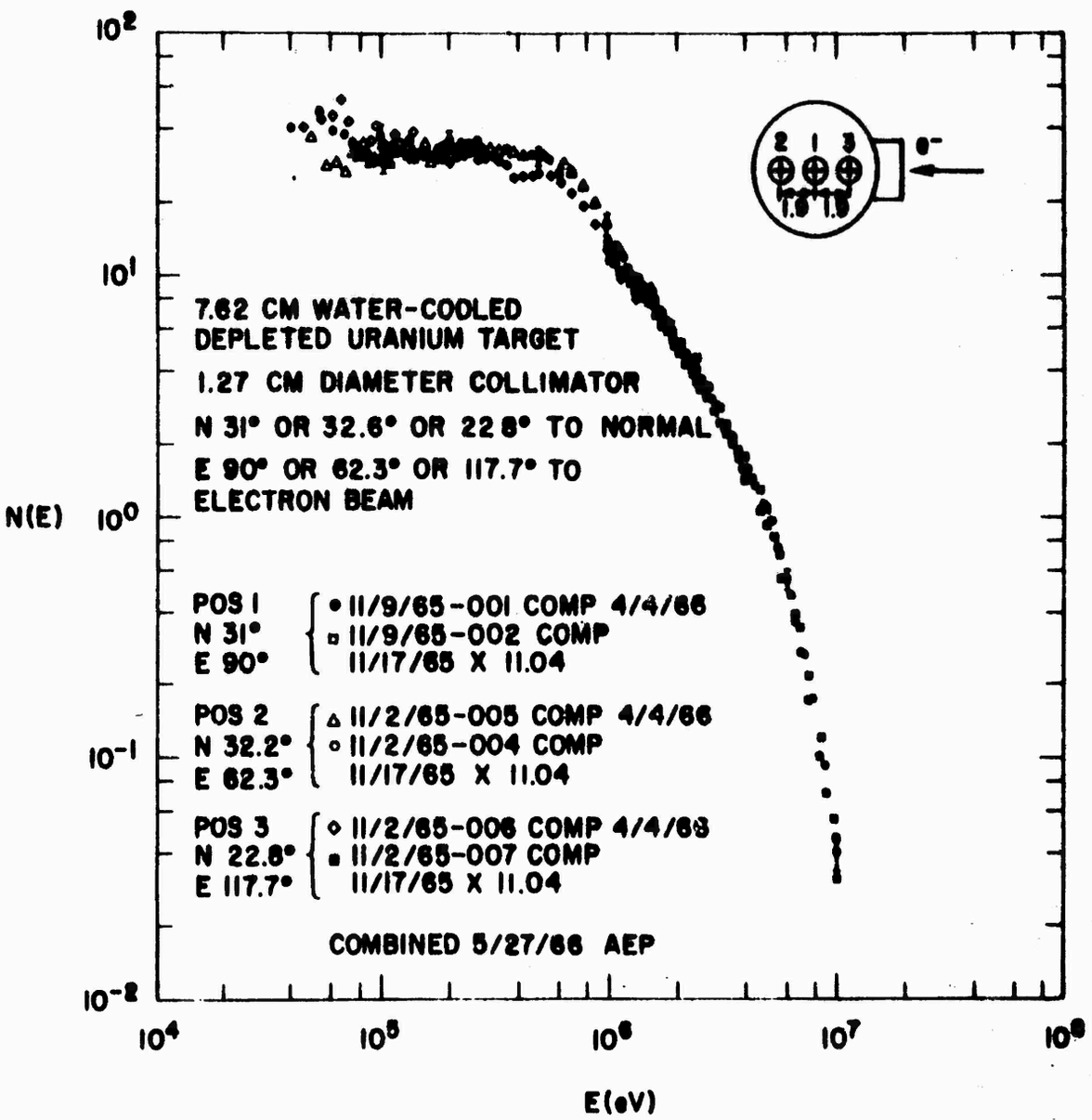

Fig. 6--Angular flux spectrum at approximately 30° to the radius vector

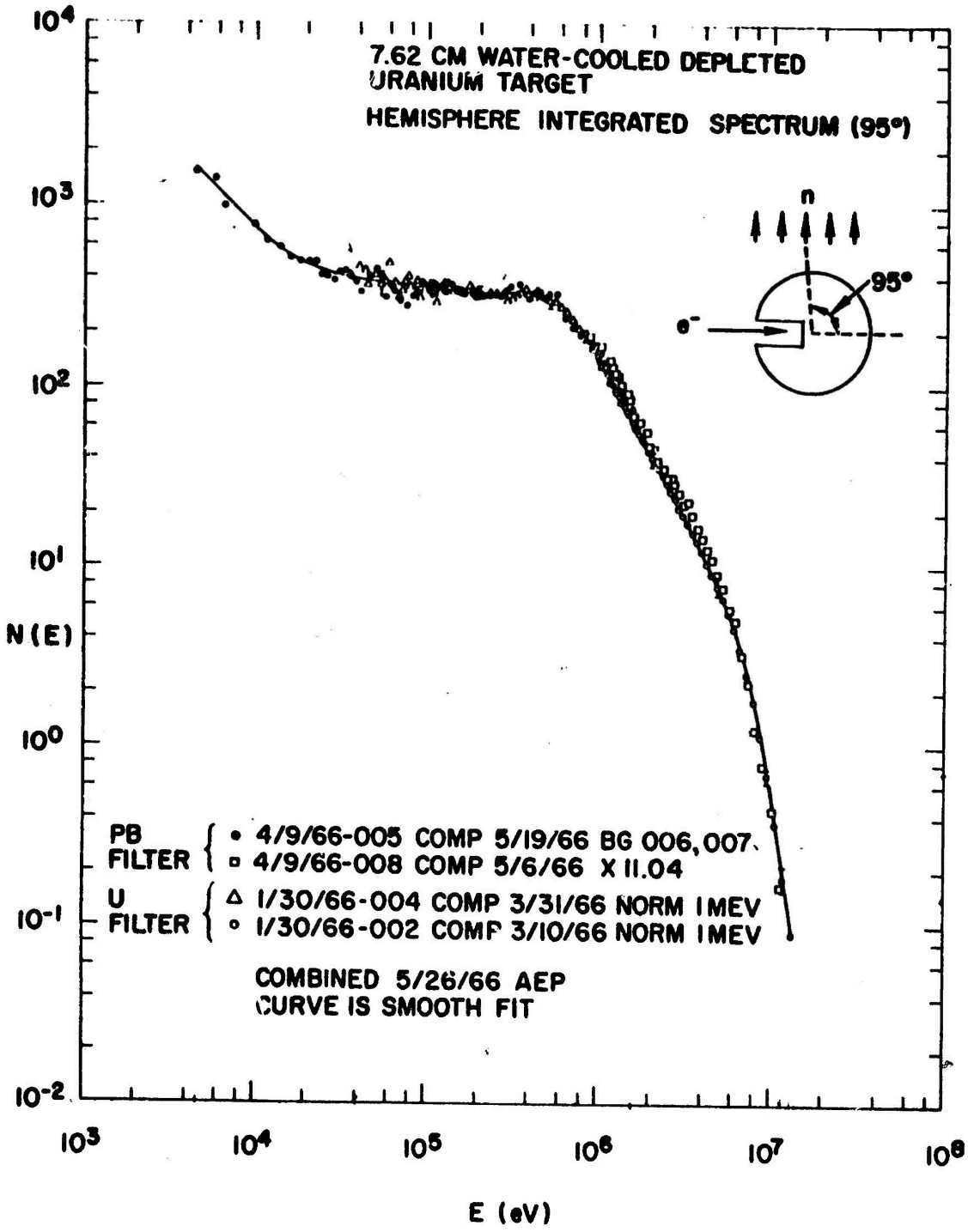

Fig. 7--Hemisphere-integrated flux spectrum

assuming spherical symmetry, where θ is the angle to the radius vector. The result is also equal to the angle-integrated leakage at one point. For some calculations the hemisphere-integrated spectrum (total leakage) may be sufficient; however, for other calculations the angular distribution at the surface has to be included. The measured spectra are listed in Tables I through XIV.

When the target is imbedded in the experimental assembly, interactions of neutrons with the uranium may not be negligible. The uranium is then included in the calculations, and the source is taken as the nascent photoneutron-production. Photoneutron distributions are discussed in the following section.

4. PHOTONEUTRON DISTRIBUTIONS

4.1 MEASURED SPATIAL DISTRIBUTIONS

The spatial distribution of high-energy bremsstrahlung from 28 MeV electrons incident on depleted uranium was measured by activation of 0.318 cm diameter by 0.0076 cm thick copper foils sandwiched between 18 depleted uranium disks each 2.54 cm in diameter, 0.076 cm thick, and plated all over with 0.0127 cm of copper for protection against oxidation. The electron beam (diameter less than 1 cm) was normally incident on axis at one end of the stack, and passed through a 2.54 cm diameter by 0.0076 cm thick copper disk which served for run-to-run beam monitoring. The 10-minute activity from the $^{63}Cu(\gamma, n)^{62}Cu$ reaction was counted on a NaI(Tl) scintillation detector. The (γ, n) cross section peaks at about 18 MeV and has a width in the giant resonance of about 6 MeV (FWHM). For ^{238}U the peak occurs a few MeV lower, but the copper foils should give a reasonable measure of the spatial distribution of photoneutron production. Results are shown in Fig. 8. As a further measure of the spatial distribution, the fission-product activity (gamma rays above 0.511 MeV) from each of the depleted uranium disks was counted 24 hours after

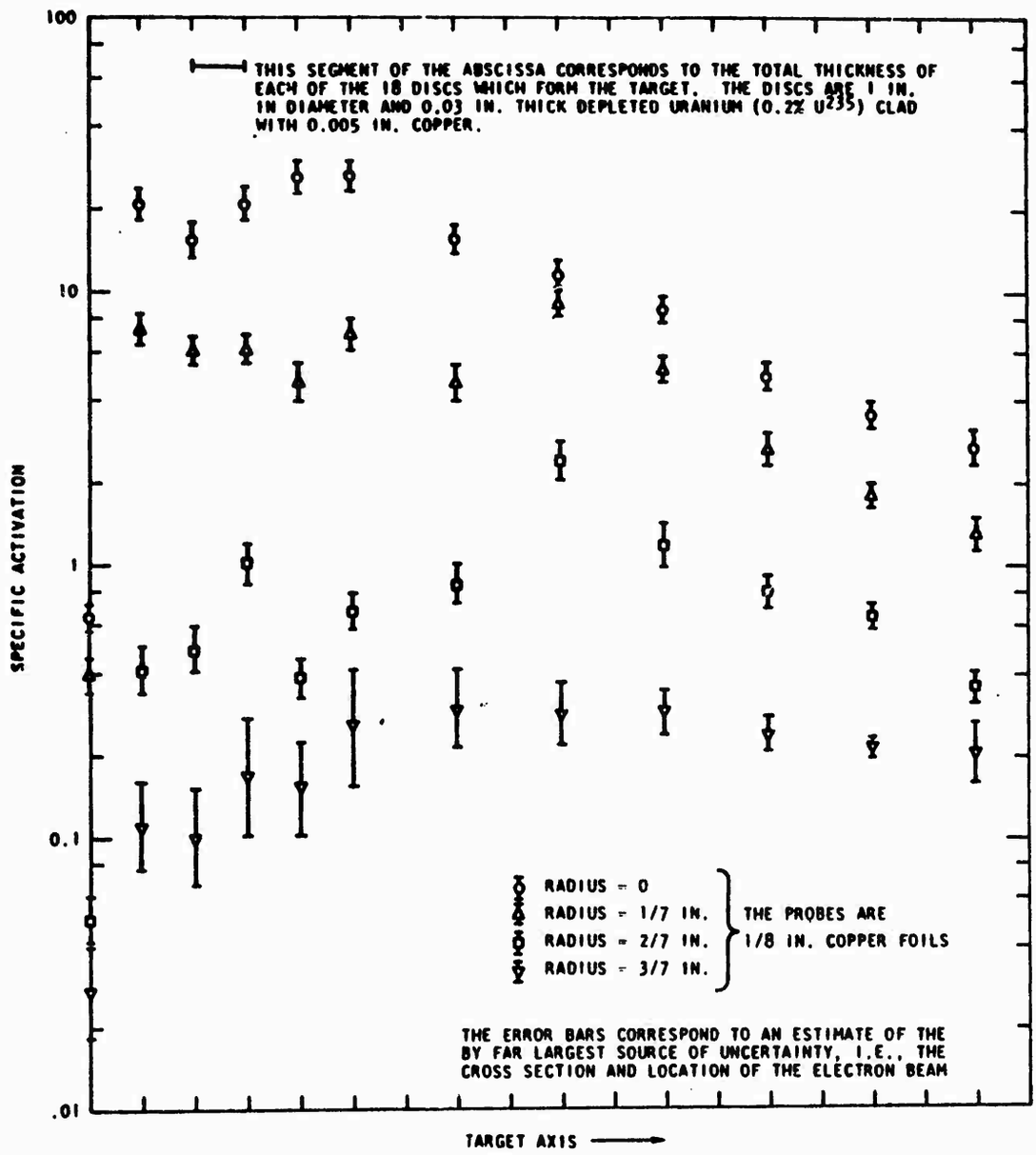

Fig. 8--Spatial distribution of high-energy bremsstrahlung in depleted uranium

irradiation. The relative activation is plotted vs thickness (actually number of disks) in Fig. 9. From these measurements we conclude that the photoneutron-photofission neutron production can be approximately represented as a uniform distribution within a sphere of 0.85 cm radius, located at the center of the target sphere.

4.2 SPECTRUM AND ANGULAR DISTRIBUTION

No measurements have been made of the angular distribution of thin-target photoneutrons. We have made one measurement of the spectrum from a thin (0.46 cm) disk of depleted uranium, plotted in Fig. 10. However, the statistics below 50 keV were poor and there was some question about the performance of both the NE211 and boron detectors. This experiment may be repeated later, but it is difficult to get reliable results with thin targets. There is a very large scattered gamma ray background, and the neutron spectrum from a thin target may not be representative of the spectrum of photoneutrons in a thick target such as the 7.62 cm sphere. Nevertheless, it is a point of departure for calculations, as discussed later.

MacGregor[4] states that the (γ, n) process yields neutrons principally in an evaporation spectrum peaking at about 2 MeV, plus a high energy tail. The (γ, F) process produces a neutron spectrum peaked around 1 MeV. The spectrum is essentially independent of electron bombarding energy (at high energy), presumably because the photonuclear cross section is peaked at about 15 MeV. MacGregor refers to nuclear emulsion data[5] for 70 MeV bremsstrahlung in Pb, Sn, Cu, Fe, Al, and C. The photoneutron spectra were interpreted as a combination of evaporation and direct absorption. The evaporation spectrum is of the form

$$N(E) = \text{const. } E \exp(-E/T)$$

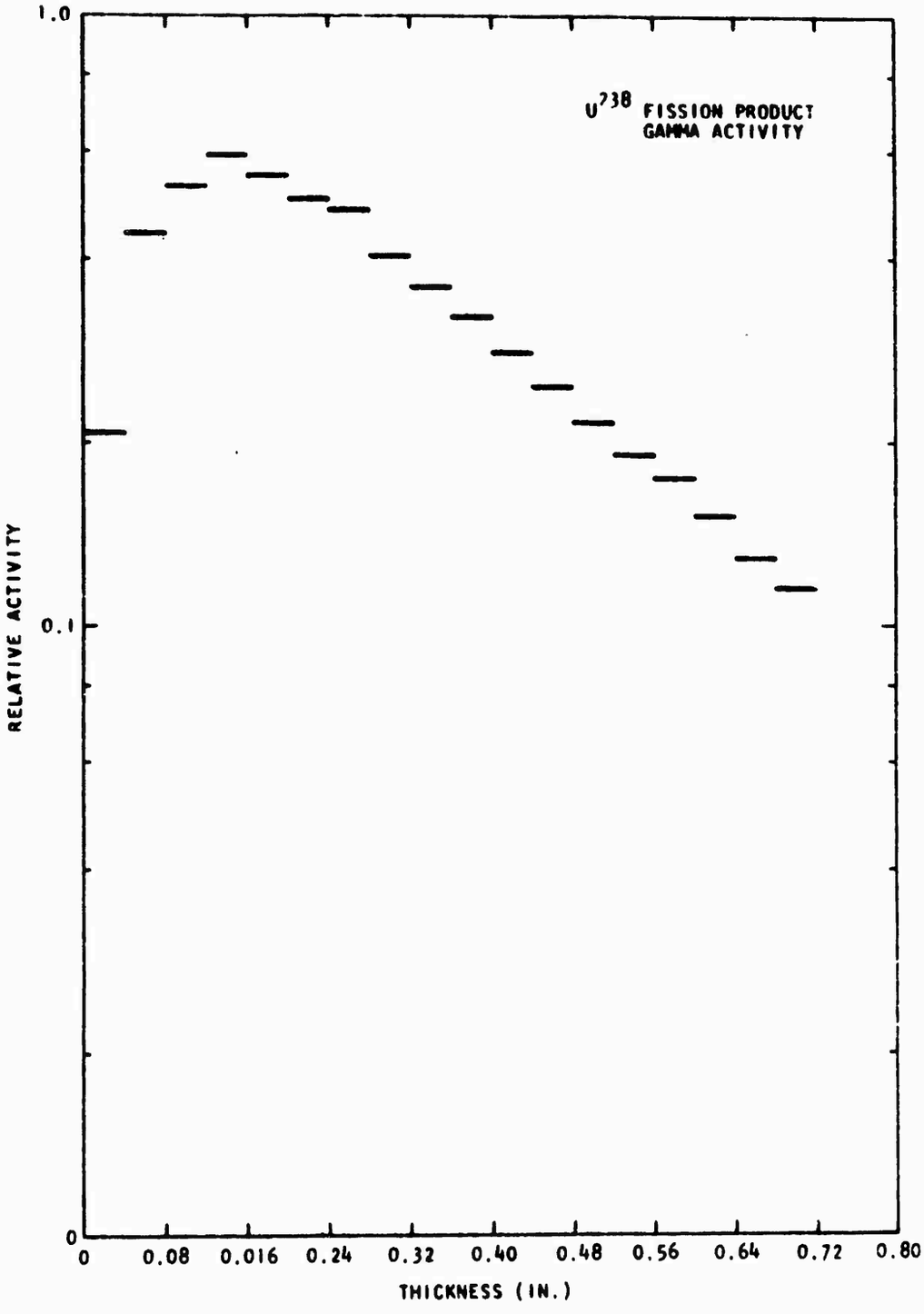

Fig. 9--Spatial distribution of uranium fissions in depleted uranium

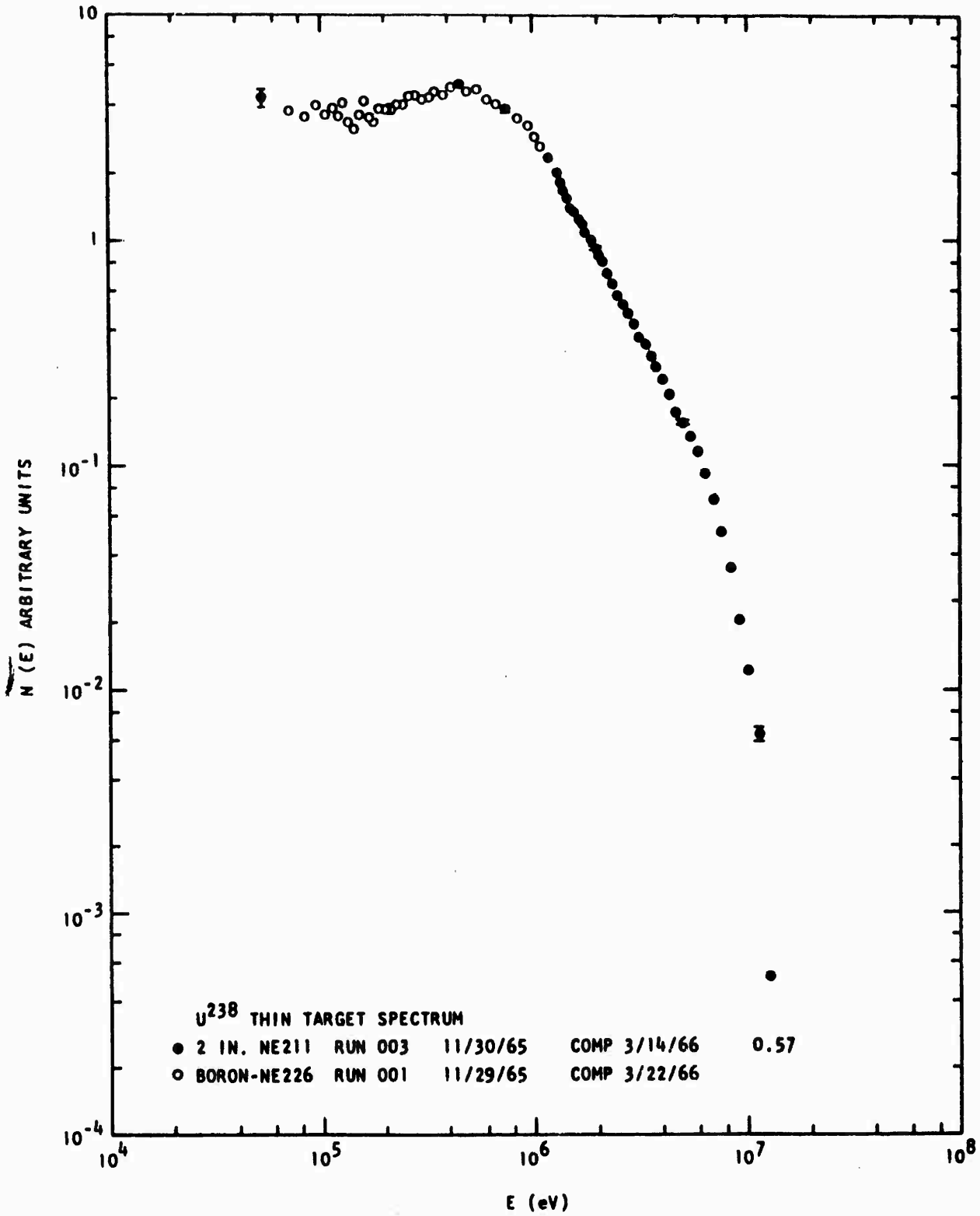

Fig. 10--Thin depleted uranium target spectrum

with a constant nuclear temperature of 1.2 ± 0.1 MeV for Cu and 1.0 ± 0.2 MeV for Pb. The evaporation neutrons are emitted isotropically in the laboratory system. The direct component contributes a spectrum peaking at about 5 MeV and is anisotropic. The work of the MIT Linac group[6] shows angular distributions are fitted by $W(\theta) = a_0 + a_1 P_1 + a_2 P_2$ where P_1 and P_2 are the Legendre polynomials and θ is the angle of neutron emission relative to the electron and bremsstrahlung beam. At 15 MeV maximum bremsstrahlung energy, $a_1 = 0$ and $-a_2/a_0$ varies from 0 to 0.8 depending on the nuclide and the neutron energy (the coefficients are given for evaporation plus direct neutrons, but the anisotropy comes in with the direct component). Thus the angular distribution is symmetric about and peaks at 90°. The fraction of photoneutrons which are direct is 0.2 to 0.3. Photoneutrons from uranium are expected to follow the same general behavior as those from other heavy elements.

The photofission neutron spectrum has the same form as the neutron-induced fission neutron spectrum,

$$N(E) = \text{const.} \sqrt{E} \exp(-E/T_{eff})$$

where T_{eff} is an effective temperature. The spectrum from thermal neutron fission of ^{235}U and the ^{238}U photofission neutron spectrum[7] as measured just above threshold (~5 MeV) are essentially identical, with $T_{eff} = 1.3$ MeV. For higher excitation energy we might expect the photofission spectrum to be somewhat harder. If MacGregor's statement is to be taken literally, $T_{eff} = 2$ MeV since this gives a spectrum peaking at 1 MeV. The angular distribution of photofission neutrons is isotropic in the lab system.

Spectrum measurements are rare, but there are some measurements of photonuclear cross sections.[8, 9] The ratio of the integrated photofission cross section to the integrated total neutron emission cross

section is 0.24 in ^{238}U. Taking an average $\bar{\nu} = 3$ for the neutrons per fission, we find that some 72% of the neutrons should come from photofission and hence be emitted isotropically and follow a $\sqrt{E}$ dependence at low energies.

The discussion above indicates in a broad way what to expect, but the photoneutron distributions should receive more attention. Meanwhile, we rely on the thick target (sphere) angular flux spectrum measurements.

5. TARGET CALCULATIONS

An extensive series of calculations were carried out on the leakage spectrum from the depleted uranium target. The target was calculated as a 3.03 in. (7.69 cm) diameter sphere of depleted uranium (0.20% ^{235}U), surrounded by a spherical shell of water 0.090 in. (0.229 cm) thick, and then a spherical shell of stainless steel 0.034 in. (0.086 cm) thick. Cross sections were generated for 26 energy groups extending from 14.9 MeV to 1.86 eV, using the GAM-II code.[10] The group structure is given in Table V. The source spectrum used in GAM-II was an extrapolated, measured ^{238}U thin target photoneutron spectrum. A resonance calculation was done for ^{238}U, at a temperature of 300°K, and the buckling was 10^{-10} in the B_3 calculation.

The angular flux at the surface and the total leakage vs energy (computed by $2\pi r^2 \sum_i \Psi_i(\bar{\mu}) \bar{\mu} \Delta\mu$) were calculated with GAPLSN.[11] The extrapolated, measured thin-target ^{238}U photoneutron spectrum was used in an isotropic source distributed in a small volume (2.1 cm^3) at the center of the uranium. The group intensity, Q_0, is listed in Table XV for the trial calculations made to determine the effect of different approximations.

5.2 EFFECT OF ANGULAR MESH

The total leakage, with P_3 cross sections, was calculated in the S_4, S_{16}, and S_{32} approximations. The S_{16} and S_{32} angular meshes agree to 1% or better even in the highest energy groups where the flux is most anisotropic. The S_4 predicted flux tends to be low, about 10% in the highest energy groups and less at lower energies. The angular flux at the surface is not predicted at all well by S_4 for energies in the MeV region. The S_{16} and S_{32} results are closer, deviations being about 20% at 2.5 MeV. The S_{16} calculation is probably adequate for most purposes, although S_{32} is desirable for very high energy neutrons.

5.3 EFFECT OF SPATIAL MESH

The number of spatial intervals was increased from 33 to 54 with no significant difference in either the total leakage or the angular flux. This indicates that 33 intervals are sufficient, and a fewer number might have been adequate.

The angular flux at the "surface" is actually the average flux in the last spatial interval, which was about 0.04 cm wide. Thus it is possible to get a small, but non-zero, computed flux for $\mu < 0$. Usually this is of no consequence. A calculation was carried out for a 0.4 cm void outside of the target. As expected, the return flux ($\mu < 0$) was actually zero, the total leakage was not affected, and the angular flux was more forward-peaked (as the distance from the target is increased, the angular distribution approaches that from a point source). In subsequent calculations the average flux in the small outer interval (no void) was accepted.

5.4 EFFECT OF ENERGY GROUPING

An investigation was made of the adequacy of the 25 energy group structure. Results for groups 1-11 of the 25-group structure were

compared with results for 28 groups over the same energy range (14.9-0.11 MeV). This represents the maximum detail available (GAM-II fine group structure, $\Delta\mu = 0.1$) and removes any dependence on the averaging flux spectrum. The total leakage at the higher energies is 6-8% lower with 11 groups than with 28 groups, but only 2-3% lower at lower energies. The angular fluxes at the surface for the first group differ by 8%, but less than 3% below group 3. Thus the coarser energy grouping is probably adequate except perhaps near 14.9 MeV.

5.5 EFFECT OF CONVERGENCE PARAMETER

Most of the calculations were performed with the GAPLSN convergence parameter (change in the volume integrated scalar flux between iterations) equal to 10^{-5}, which should be sufficiently small. To test this, one calculation was done with a convergence parameter of 10^{-6}. No significant differences in the fluxes were found.

5.6 EFFECT OF SOURCE VOLUME

In most of the calculations the isotropic source was assumed to be uniformly distributed in a 2.1 cm^3 spherical volume at the center of the target. This is slightly less than the effective volume derived from the activation measurements in Section 4.1. To investigate the importance of the source volume, the calculation was repeated with a volume of 7.2 cm^3. The total leakage, normalized to the same number of source neutrons, is the same within 2%. The angular flux spectrum at the surface also agrees to within 2%, except for $\mu = 1$. However, the $\mu = 1$ (0^o) flux is calculated by a special version of GAPLSN. It has zero weight and is not used in the angular integration. Previous experience has indicated that the magnitude of the $\mu = 1$ calculation is probably in error. This effect is being investigated in calculations with the DTF-IV code where angles nearer $\mu = 1$ can be included for the same number of angular intervals.

5.7 EFFECT OF WATER AND STAINLESS STEEL JACKET

A possible variation of 0.06 in. (0.152 cm) to 0.09 in. (0.229 cm) in the thickness of the water jacket may arise from fabrication and assembly tolerances. A calculation with 0.152 cm water thickness showed essentially no difference in total leakage at energies above 100 keV (Table XVI). At lower energies, however, the moderation of the additional 0.076 cm of water becomes significant, and at 100 eV the leakage is 50% larger with the thicker layer. The angular flux at the surface essentially unchanged above 1 MeV, is 20% larger at 10 keV, and twice as large with the thicker layer at lower energies. This shows the importance of maintaining a uniform water thickness for low energy work in heavy metal assemblies. However, the variation in water thickness should make little difference in light materials such as graphite or CH_2, because the low energy spectrum is determined mainly by elastic moderation rather than by the source spectrum.

In another calculation the water, and the stainless steel jacket, were removed entirely. Without them, the leakage is 3% higher at 12 MeV, 8% higher at 1 MeV, and more than a factor of 2 lower below 10 keV. Large differences also occur in the angular fluxes. The 0.229 cm water and stainless steel jacket were included in all other calculations.

5.8 COMPARISON OF CALCULATED AND MEASURED SPECTRA

The total leakage spectra as measured (Fig. 7) and as computed in a P_2, S_{16}, 25-group, 2.1-cm^3 source GAPLSN calculation using the trial photoneutron spectrum from Table V are plotted in Fig. 11. The photoneutron spectrum is also plotted. Calculations are normalized to the measurement at 2.5 MeV. The calculated leakage spectrum is in rather good agreement above 2 MeV, but is too high at lower energies.

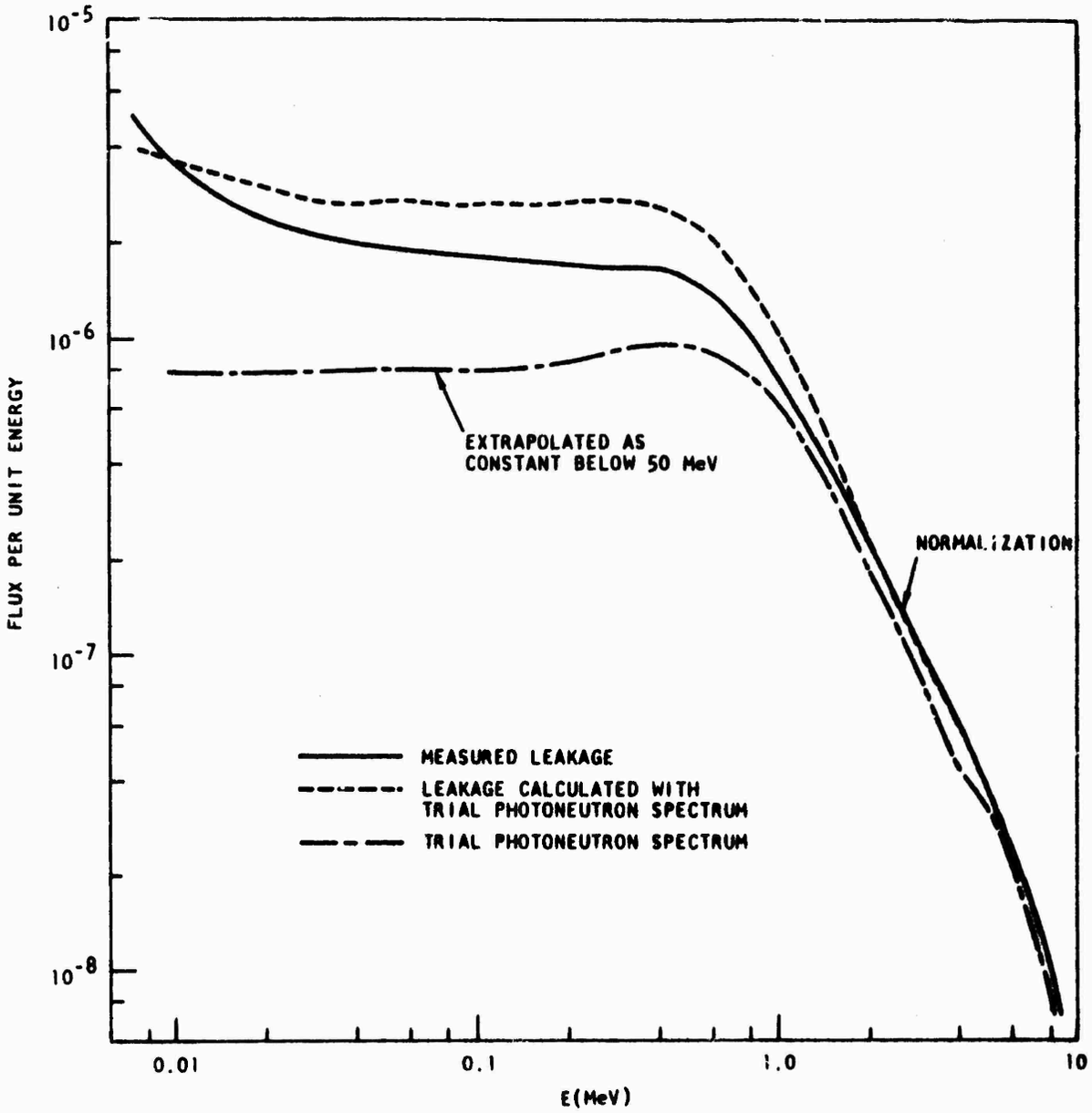

Fig. 11--Total leakage spectra, measured and calculated with trial photoneutron source

Since the photoneutron spectrum has not been measured accurately between 50 keV and 1.5 MeV, and the extrapolation below 50 keV is uncertain, we have elected to adjust the low energy source spectrum downward to force close agreement in the total leakage spectra. Thus when the adjusted source is used in a similar discrete-ordinates calculation, the correct leakage spectrum will be produced. Table XVII lists the group intensity Q_0 and $Q_0/\Delta E$ of the adjusted source spectrum, and the ratio of calculated to measured total leakage with this source. The adjustment has achieved agreement to within a few percent except at the lowest energies. Also compared in Table XVII are the calculated and measured angular flux spectra at 0°, and the flux calculated at an average angle of 20° compared to the flux measured at about 30°. All spectra are normalized at 2.5 MeV for shape comparison. Agreement is within 20% or so except at the highest energies, where the S_{16} calculation may be inadequate.

The agreement in total leakage strictly holds only for a similar discrete-ordinates calculation. For other types of calculations the source may have to be adjusted slightly to match calculated and measured spectra.

The calculated angular fluxes are listed in Table XVIII.

11/1/65-001 COMPUTED 4/4/66 TABLE I

3 INCH WATER COOLED DEPLETED URANIUM SPHERE SPECTRUM
90 DEGREES POSITION 1 .5 INCH PRECOLLIMATOR
1.238 INCH URANIUM FILTER AT 16 METERS.
NE 226 DETECTOR 125. NSECOND CHANNEL WIDTH
RESOLUTION FOR GROUPING = .267 AT 10MEV. LARGEST FRACTIONAL ERROR = .1

ENERGY (E V)	N(E) (ARBITR. UNITS)	DELTA(N)/N	ENERGY (E V)	N(E) (ARBITR. UNITS	DELTA(N)/N
.1453+07	.5981+02	.1477-01	.2992+06	.1126+03	.4136-01
.1245+07	.6653+02	.1509-01	.2786+06	.1027+03	.4653-01
.1079+07	.8262+02	.1504-01	.2600+06	.1079+03	.4879-01
.9439+06	.9457+02	.1528-01	.2432+06	.1013+03	.5428-01
.8327+06	.1062+03	.1595-01	.2280+06	.1054+03	.5693-01
.7400+06	.1192+03	.1697-01	.2142+06	.9944+02	.6300-01
.6620+06	.1215+03	.1887-01	.2015+06	.1074+03	.6454-01
.5957+06	.1247+03	.2049-01	.1900+06	.9361+02	.7481-01
.5389+06	.1212+03	.2304-01	.1795+06	.9534+02	.7980-01
.4899+06	.1189+03	.2572-01	.1697+06	.7673+02	.9660-01
.4472+06	.1186+03	.3013-01	.1608+06	.9611+02	.9026-01
.4099+06	.1172+03	.3266-01	.1526+06	.1076+03	.8955-01
.3771+06	.6625+03	.1385-01	.1431+06	.9118+02	.8620-01
.3481+06	.1214+03	.3502-01	.1345+06	.1204+03	.9617-01
.3223+06	.1105+03	.3909-01	.1252+06	.8292+02	.9333-01

11/1/65-003 COMPUTED 11/17/65 TABLE II

3 INCH WATER COOLED DEPLETED URANIUM SPHERE SPECTRUM
90 DEGREES POSITION 1 .5 INCH PRECOLLIMATOR
1.238 INCH URANIUM FILTER AT 16 METERS. N(E) HAS BEEN MULTIPLIED BY 11.04
NE 211 DETECTOR 31.25 NSECOND CHANNEL WIDTH
RESOLUTION FOR GROUPING = .020 LARGEST FRACTIONAL ERROR = .1

ENERGY (E V)	N(E) (ARBITR. UNITS)	DELTA(N)/N	ENERGY (E V)	N(E) (ARBITR. UNITS	DELTA(N)/N
.1205+08	.1A01-00	.8390-01	.2767+07	.2353+02	.2759-01
.1106+08	.3112-00	.9512-01	.2692+07	.2561+02	.2682-01
.1047+08	.3681-00	.9071-01	.2620+07	.2728+02	.2638-01
.9927+07	.4363-00	.A6A7-01	.2550+07	.2758+02	.2662-01
.9424+07	.6319-00	.7506-01	.2484+07	.2839+02	.2657-01
.8959+07	.1070+01	.5981-01	.2420+07	.2873+02	.2673-01
.8528+07	.1335+01	.5551-01	.2358+07	.3167+02	.2579-01
.8127+07	.1652+01	.5202-01	.2299+07	.3096+02	.2659-01
.7754+07	.2241+01	.4625-01	.2242+07	.3489+02	.2549-01
.7405+07	.2A28+01	.4258-01	.2187+07	.3497+02	.2581-01
.7080+07	.3177+01	.4154-01	.2134+07	.3487+02	.2617-01
.6776+07	.3740+01	.3970-01	.2082+07	.3610+02	.2611-01
.6491+07	.4468+01	.3744-01	.2033+07	.3931+02	.2536-01
.6223+07	.4A72+01	.3702-01	.1986+07	.3847+02	.2599-01
.5972+07	.5422+01	.3617-01	.1940+07	.4319+02	.2486-01
.5736+07	.5A74+01	.3575-01	.1895+07	.4169+02	.2571-01
.5513+07	.5987+01	.3643-01	.1853+07	.4363+02	.2548-01
.5303+07	.7353+01	.3378-01	.1811+07	.4666+02	.2504-01
.5105+07	.8569+01	.3223-01	.1771+07	.4396+02	.2610-01
.4918+07	.8A44+01	.3228-01	.1733+07	.4557+02	.2595-01
.4741+07	.9029+01	.3273-01	.1695+07	.4977+02	.2515-01
.4573+07	.9942+01	.3215-01	.1659+07	.5369+02	.2497-01
.4414+07	.1074+02	.3168-01	.1624+07	.5123+02	.2567-01
.4263+07	.1144+02	.3121-01	.1590+07	.5393+02	.2539-01
.4120+07	.1147+02	.3176-01	.1557+07	.5280+02	.2589-01
.3984+07	.1290+02	.3061-01	.1525+07	.5478+02	.2570-01
.3854+07	.1330+02	.3074-01	.1494+07	.5733+02	.2547-01
.3731+07	.1545+02	.2913-01	.1449+07	.5927+02	.1804-01
.3614+07	.1482+02	.3031-01	.1393+07	.5906+02	.1854-01
.3502+07	.1526+02	.3038-01	.1340+07	.6209+02	.1873-01
.3395+07	.1627+02	.2985-01	.1289+07	.6521+02	.1866-01
.3293+07	.1772+02	.2910-01	.1242+07	.6710+02	.1884-01
.3195+07	.1A35+02	.2902-01	.1197+07	.6690+02	.1944-01
.3102+07	.1965+02	.2840-01	.1154+07	.6997+02	.1973-01
.3013+07	.1904+02	.2932-01	.1114+07	.7401+02	.2008-01
.2927+07	.2251+02	.2736-01	.1076+07	.7163+02	.2101-01
.2846+07	.2188+02	.2817-01	.1039+07	.7183+02	.2185-01

11/20/65-002 COMPUTED 4/8/66 TABLE III

3 INCH WATER COOLED DEPLETED URANIUM SPHERE SPECTRUM
44 DEGREES POSITION 1 .5 INCH PRECOLLIMATOR
1.238 INCH URANIUM FILTER AT 16 METERS.
NE 226 DETECTOR 125. NSECOND CHANNEL WIDTH
RESOLUTION FOR GROUPING = .267 AT 10MEV. LARGEST FRACTIONAL ERROR = .1

ENERGY (E V)	N(E) (ARBITR. UNITS)	DELTA(N)/N	ENERGY (E V)	N(E) (ARBITR. UNITS	DELTA(N)/N
.1313+07	.5745+02	.1159-01	.2304+06	.1011+03	.4270-01
.1132+07	.6975+02	.1158-01	.2163+06	.9739+02	.4686-01
.9859+06	.8318+02	.1179-01	.2033+06	.9678+02	.5061-01
.8663+06	.9639+02	.1187-01	.1916+06	.9528+02	.5492-01
.7673+06	.1012+03	.1285-01	.1808+06	.8750+02	.6197-01
.6843+06	.1090+03	.1379-01	.1708+06	.9384+02	.6365-01
.6140+06	.1089+03	.1498-01	.1617+06	.9543+02	.6716-01
.5541+06	.1171+03	.1648-01	.1533+06	.8906+02	.7443-01
.5025+06	.1215+03	.1818-01	.1456+06	.8277+02	.8288-01
.4578+06	.1148+03	.2143-01	.1384+06	.9481+02	.8132-01
.4188+06	.1167+03	.2423-01	.1317+06	.8001+02	.9719-01
.3846+06	.1163+03	.2453-01	.1240+06	.8986+02	.7995-01
.3545+06	.1110+03	.2712-01	.1157+06	.8594+02	.9005-01
.3277+06	.1105+03	.2895-01	.1081+06	.8821+02	.9680-01
.3038+06	.1047+03	.3161-01	.1002+06	.8429+02	.9645-01
.2825+06	.1043+03	.3384-01	.9041+05	.7706+02	.9907-01
.2634+06	.1039+03	.3644-01	.8036+05	.9512+02	.9943-01
.2461+06	.1018+03	.3966-01	.6719+05	.8588+02	.9765-01

11/20/65-001 COMPUTED 5/9/66 TABLE IV

3 INCH WATER COOLED DEPLETED URANIUM SPHERE SPECTRUM
44 DEGREES POSITION 1 .5 INCH PRECOLLIMATOR
1.238 INCH URANIUM FILTER AT 16 METERS. N(E) HAS BEEN NORMALIZED AT 1.2 MEV
NE 211 DETECTOR 31.25 NSECOND CHANNEL WIDTH
RESOLUTION FOR GROUPING = .059 AT 10MEV. LARGEST FRACTIONAL ERROR = .1

ENERGY (E V)	N(E) (ARBITR. UNITS)	DELTA(N)/N	ENERGY (E V)	N(E) (ARBITR. UNITS	DELTA(N)/N
.1417+08	.9954-01	.7702-01	.2422+07	.2791+02	.1996-01
.1179+08	.2078-00	.8198-01	.2300+07	.3128+02	.1944-01
.1055+08	.3355-00	.6954-01	.2188+07	.3492+02	.1899-01
.9488+07	.7029-00	.5200-01	.2083+07	.3572+02	.1932-01
.8580+07	.1313+01	.4114-01	.1986+07	.3883+02	.1905-01
.7797+07	.2046+01	.3556-01	.1896+07	.4105+02	.1908-01
.7116+07	.2894+01	.3201-01	.1811+07	.4406+02	.1906-01
.6521+07	.4029+01	.2904-01	.1732+07	.4428+02	.1934-01
.5997+07	.5442+01	.2656-01	.1659+07	.4828+02	.1898-01
.5535+07	.6975+01	.2618-01	.1589+07	.5210+02	.1888-01
.5123+07	.7621+01	.2501-01	.1524+07	.5276+02	.1910-01
.4756+07	.8951+01	.2424-01	.1463+07	.5621+02	.1904-01
.4427+07	.1030+02	.2374-01	.1406+07	.5551+02	.1972-01
.4131+07	.1162+02	.2323-01	.1352+07	.6054+02	.1956-01
.3864+07	.1265+02	.2320-01	.1301+07	.6009+02	.2015-01
.3622+07	.1472+02	.2233-01	.1252+07	.6360+02	.2007-01
.3401+07	.1600+02	.2214-01	.1207+07	.6456+02	.2059-01
.3201+07	.1785+02	.2157-01	.1163+07	.6772+02	.2077-01
.3017+07	.1964+02	.2115-01	.1123+07	.6841+02	.2160-01
.2849+07	.2206+02	.2056-01	.1084+07	.7064+02	.2191-01
.2695+07	.2440+02	.2017-01	.1047+07	.7025+02	.2279-01
.2553+07	.2635+02	.2000-01	.1012+07	.6882+02	.2395-01

11/9/65-001 COMPUTED 4/4/66 TABLE V

3 INCH WATER COOLED DEPLETED URANIUM SPHERE SPECTRUM
90 DEGREES POSITION 1 .5 INCH PRECOLLIMATOR
1.238 INCH URANIUM FILTER AT 16 METERS.
NE 226 DETECTOR 125. NSECOND CHANNEL WIDTH
RESOLUTION FOR GROUPING = .267 AT 10MEV. LARGEST FRACTIONAL ERROR = .1

ENERGY (E V)	N(E) (ARBITR. UNITS)	DELTA(N)/N	ENERGY (E V)	N(E) (ARBITR. UNITS	DELTA(N)/N
.1545+07	.8828+01	.1407-01	.1915+06	.3496+02	.4536-01
.1315+07	.9910+01	.1417-01	.1807+06	.3353+02	.4981-01
.1134+07	.1256+02	.1384-01	.1708+06	.3124+02	.5549-01
.9870+06	.1639+02	.1343-01	.1617+06	.3044+02	.6020-01
.8672+06	.1986+02	.1323-01	.1532+06	.3087+02	.6346-01
.7679+06	.2333+02	.1352-01	.1455+06	.3216+02	.6601-01
.6847+06	.2622+02	.1419-01	.1383+06	.3276+02	.6967-01
.6144+06	.2624+02	.1543-01	.1316+06	.3310+02	.7377-01
.5543+06	.2979+02	.1645-01	.1254+06	.3042+02	.8292-01
.5027+06	.3093+02	.1818-01	.1197+06	.3250+02	.8451-01
.4580+06	.3111+02	.2073-01	.1143+06	.3397+02	.8705-01
.4189+06	.3151+02	.2351-01	.1092+06	.3279+02	.9425-01
.3847+06	.3144+02	.2382-01	.1045+06	.3384+02	.9810-01
.3545+06	.3236+02	.2536-01	.1001+06	.3679+02	.9810-01
.3277+06	.3207+02	.2712-01	.9502+05	.3560+02	.8820-01
.3038+06	.3255+02	.2858-01	.8937+05	.3372+02	.9967-01
.2825+06	.3296+02	.3035-01	.8341+05	.3515+02	.9287-01
.2633+06	.3551+02	.3132-01	.7658+05	.3515+02	.9479-01
.2460+06	.3402+02	.3444-01	.6932+05	.3772+02	.9527-01
.2304+06	.3375+02	.3729-01	.6149+05	.3856+02	.9851-01
.2162+06	.3477+02	.3934-01	.5362+05	.4706+02	.9866-01
.2033+06	.3591+02	.4155-01	.4079+05	.4044+02	.9960-01

3 INCH WATER COOLED DEPLETED URANIUM SPHERE SPECTRUM
90 DEGREES POSITION 1 .5 INCH PRECOLLIMATOR
1.238 INCH URANIUM FILTER AT 16 METERS. N(E) HAS BEEN MULTIPLIED BY 11.04
NE 211 DETECTOR 31.25 NSECOND CHANNEL WIDTH
RESOLUTION FOR GROUPING = .020 LARGEST FRACTIONAL ERROR = .1

ENERGY (E V)	N(E) (ARBITR. UNITS)	DELTA(N)/N	ENERGY (E V)	N(E) (ARBITR. UNITS	DELTA(N)/N
.1402+08	.1103-01	.9239-01	.2638+07	.3600+01	.3909-01
.9755+07	.5678-01	.7855-01	.2567+07	.3850+01	.3836-01
.8579+07	.1206+00	.7175-01	.2499+07	.4474+01	.3609-01
.7973+07	.1661-00	.9106-01	.2433+07	.4280+01	.3733-01
.7606+07	.2194-00	.8176-01	.2371+07	.4441+01	.3710-01
.7264+07	.2591-00	.7795-01	.2310+07	.4683+01	.3680-01
.6945+07	.3478-00	.6941-01	.2252+07	.4709+01	.3733-01
.6646+07	.4335-00	.6447-01	.2196+07	.4895+01	.3712-01
.6366+07	.4736-00	.6368-01	.2142+07	.5106+01	.3680-01
.6103+07	.5798-00	.5928-01	.2090+07	.4988+01	.3775-01
.5856+07	.6885-00	.5603-01	.2040+07	.5178+01	.3759-01
.5624+07	.7249-00	.5629-01	.1992+07	.5866+01	.3577-01
.5406+07	.8273-00	.5403-01	.1945+07	.5637+01	.3700-01
.5200+07	.9225-00	.5259-01	.1900+07	.6214+01	.3584-01
.5005+07	.1085+01	.4953-01	.1857+07	.6022+01	.3685-01
.4822+07	.1155+01	.4917-01	.1815+07	.7051+01	.3455-01
.4648+07	.1252+01	.4859-01	.1774+07	.6547+01	.3633-01
.4483+07	.1210+01	.5060-01	.1735+07	.6895+01	.3582-01
.4327+07	.1451+01	.4737-01	.1697+07	.7212+01	.3548-01
.4179+07	.1574+01	.4625-01	.1660+07	.7706+01	.3508-01
.4039+07	.1815+01	.4383-01	.1625+07	.7488+01	.3600-01
.3905+07	.1723+01	.4590-01	.1590+07	.7774+01	.3586-01
.3778+07	.1874+01	.4515-01	.1557+07	.7748+01	.3626-01
.3657+07	.1980+01	.4456-01	.1525+07	.8840+01	.3433-01
.3542+07	.2127+01	.4383-01	.1494+07	.8512+01	.3545-01
.3432+07	.2440+01	.4157-01	.1463+07	.8575+01	.3572-01
.3327+07	.2416+01	.4243-01	.1419+07	.8611+01	.2570-01
.3227+07	.2657+01	.4108-01	.1364+07	.9714+01	.2493-01
.3131+07	.2880+01	.3998-01	.1312+07	.1023+02	.2498-01
.3040+07	.2800+01	.4112-01	.1263+07	.9797+01	.2605-01
.2952+07	.2955+01	.4070-01	.1216+07	.1034+02	.2610-01
.2869+07	.3293+01	.3912-01	.1172+07	.1053+02	.2675-01
.2788+07	.3498+01	.3853-01	.1130+07	.1232+02	.2578-01
.2711+07	.3527+01	.3894-01	.1091+07	.1168+02	.2743-01

11/2/65-005 COMPUTED 4/4/66 TABLE VII

3 INCH WATER COOLED DEPLETED URANIUM SPHERE SPECTRUM
62 DEGREES POSITION 2 .5 INCH PRECOLLIMATOR
1.238 INCH URANIUM FILTER AT 16 METERS.
NE 226 DETECTOR 125. NSECOND CHANNEL WIDTH
RESOLUTION FOR GROUPING = .267 AT 10MEV. LARGEST FRACTIONAL ERROR = .1

ENERGY (E V)	N(E) (ARBITR. UNITS)	DELTA(N)/N	ENERGY (E V)	N(E) (ARBITR. UNITS	DELTA(N)/N
.1578+07	.8597+01	.1188-01	.1746+06	.3173+02	.4343-01
.1344+07	.9534+01	.1195-01	.1653+06	.2817+02	.4937-01
.1158+07	.1025+02	.1156-01	.1567+06	.3448+02	.4674-01
.1008+07	.1611+02	.1127-01	.1487+06	.3043+02	.5285-01
.8860+06	.1943+02	.1110-01	.1414+06	.2961+02	.5690-01
.7846+06	.2289+02	.1126-01	.1346+06	.3022+02	.5941-01
.6997+06	.2621+02	.1176-01	.1282+06	.3187+02	.6101-01
.6278+06	.2856+02	.1260-01	.1223+06	.3022+02	.6626-01
.5665+06	.3008+02	.1371-01	.1168+06	.3115+02	.6863-01
.5138+06	.3086+02	.1495-01	.1117+06	.3062+02	.7327-01
.4680+06	.3161+02	.1671-01	.1069+06	.2821+02	.8115-01
.4282+06	.3034+02	.1961-01	.1024+06	.2946+02	.8353-01
.3932+06	.3166+02	.1982-01	.9816+05	.2885+02	.8895-01
.3623+06	.3027+02	.2084-01	.9419+05	.2956+02	.9243-01
.3349+06	.3182+02	.2241-01	.9046+05	.2845+02	.9933-01
.3106+06	.3280+02	.2340-01	.8694+05	.3110+02	.9888-01
.2887+06	.3270+02	.2491-01	.8363+05	.3424+02	.9758-01
.2692+06	.3232+02	.2678-01	.7975+05	.2985+02	.9277-01
.2515+06	.3403+02	.2791-01	.7477+05	.3142+02	.8494-01
.2355+06	.3306+02	.3028-01	.6901+05	.2571+02	.9809-01
.2210+06	.3386+02	.3186-01	.6284+05	.2882+02	.9471-01
.2078+06	.3261+02	.3464-01	.5612+05	.2778+02	.9917-01
.1957+06	.2904+02	.3937-01	.4966+05	.3646+02	.9545-01
.1847+06	.2908+02	.4249-01	.4197+05	.3136+02	.9960-01

11/2/65-004 COMPUTED 11/17/65 TABLE VIII

3 INCH WATER COOLED DEPLETED URANIUM SPHERE SPECTRUM
62 DEGREES POSITION 2 .5 INCH PRECOLLIMATOR
1.238 INCH URANIUM FILTER AT 16 METERS. N(E) HAS BEEN MULTIPLIED BY 11.04
NE 211 DETECTOR 31.25 NSECOND CHANNEL WIDTH
RESOLUTION FOR GROUPING = .020 LARGEST FRACTIONAL ERROR = .1

ENERGY (E V)	N(E) (ARBITR. UNITS)	DELTA(N)/N	ENERGY (E V)	N(E) (ARBITR. UNITS	DELTA(N)/N
.1428+08	.8087-02	.8064-01	.2693+07	.3393+01	.2957-01
.1020+08	.3919-01	.8244-01	.2621+07	.3491+01	.2958-01
.9427+07	.6424-01	.9577-01	.2551+07	.3705+01	.2912-01
.8962+07	.9091-01	.8333-01	.2485+07	.3864+01	.2849-01
.8531+07	.1057+00	.8006-01	.2420+07	.3909+01	.2906-01
.8130+07	.1705-00	.6551-01	.2359+07	.4143+01	.2858-01
.7756+07	.2008-00	.6250-01	.2299+07	.4433+01	.2816-01
.7408+07	.2571-00	.5708-01	.2242+07	.4599+01	.2814-01
.7082+07	.3071-00	.5227-01	.2187+07	.4637+01	.2840-01
.6778+07	.3498-00	.5242-01	.2134+07	.4716+01	.2850-01
.6493+07	.4354-00	.4840-01	.2083+07	.5047+01	.2796-01
.6225+07	.5227-00	.4560-01	.2034+07	.5375+01	.2745-01
.5974+07	.6213-00	.4307-01	.1986+07	.5703+01	.2702-01
.5738+07	.7121-00	.4138-01	.1941+07	.5741+01	.2729-01
.5515+07	.7035-00	.4284-01	.1896+07	.5765+01	.2767-01
.5305+07	.9274-00	.3832-01	.1853+07	.6079+01	.2731-01
.5107+07	.1032+01	.3743-01	.1812+07	.6441+01	.2695-01
.4920+07	.1059+01	.3756-01	.1772+07	.6596+01	.2695-01
.4742+07	.1064+01	.3841-01	.1733+07	.6683+01	.2709-01
.4575+07	.1257+01	.3639-01	.1696+07	.7293+01	.2626-01
.4416+07	.1301+01	.3664-01	.1659+07	.7590+01	.2649-01
.4265+07	.1483+01	.3488-01	.1624+07	.7576+01	.2666-01
.4122+07	.1547+01	.3480-01	.1590+07	.7676+01	.2689-01
.3985+07	.1504+01	.3606-01	.1557+07	.8339+01	.2602-01
.3856+07	.1650+01	.3509-01	.1525+07	.8032+01	.2680-01
.3733+07	.1813+01	.3420-01	.1495+07	.8328+01	.2668-01
.3615+07	.1904+01	.3400-01	.1450+07	.8622+01	.1888-01
.3503+07	.2068+01	.3317-01	.1393+07	.9298+01	.1864-01
.3396+07	.2282+01	.3203-01	.1340+07	.9691+01	.1891-01
.3294+07	.2199+01	.3321-01	.1290+07	.9753+01	.1923-01
.3196+07	.2594+01	.3101-01	.1242+07	.1022+02	.1925-01
.3103+07	.2749+01	.3050-01	.1197+07	.1151+02	.1868-01
.3014+07	.2710+01	.3121-01	.1155+07	.1197+02	.1901-01
.2928+07	.2911+01	.3056-01	.1114+07	.1259+02	.1938-01
.2847+07	.3019+01	.3044-01	.1076+07	.1236+02	.2014-01
.2768+07	.3117+01	.3043-01	.1040+07	.1299+02	.2046-01

11/2/65-006 COMPUTED 4/4/66 TABLE IX

3 INCH WATER COOLED DEPLETED URANIUM SPHERE SPECTRUM
118 DEGREES POSITION 3 .5 INCH PRECOLLIMATOR
1.238 INCH URANIUM FILTER AT 16 METERS.
NE 226 DETECTOR 125. NSECOND CHANNEL WIDTH
RESOLUTION FOR GROUPING = .267 AT 10MEV. LARGEST FRACTIONAL ERROR = .1

ENERGY (E V)	N(E) (ARBITR. UNITS)	DELTA(N)/N	ENERGY (E V)	N(E) (ARBITR. UNITS	DELTA(N)/N
.1578+07	.6880+01	.1743-01	.1847+06	.3188+02	.5342-01
.1344+07	.7766+01	.1737-01	.1746+06	.3061+02	.5871-01
.1158+07	.9579+01	.1714-01	.1653+06	.3101+02	.6230-01
.1008+07	.1263+02	.1669-01	.1567+06	.3048+02	.6649-01
.8860+06	.1601+02	.1602-01	.1487+06	.3030+02	.7057-01
.7846+06	.1892+02	.1623-01	.1414+06	.2861+02	.7744-01
.6997+06	.2138+02	.1704-01	.1346+06	.3578+02	.7180-01
.6278+06	.2382+02	.1807-01	.1282+06	.3292+02	.7978-01
.5665+06	.2507+02	.1969-01	.1223+06	.3496+02	.8130-01
.5138+06	.2562+02	.2152-01	.1168+06	.3791+02	.8182-01
.4680+06	.2487+02	.2475-01	.1117+06	.3411+02	.9213-01
.4282+06	.2480+02	.2878-01	.1069+06	.3410+02	.9735-01
.3932+06	.2467+02	.2956-01	.1013+06	.3498+02	.8343-01
.3623+06	.2803+02	.2942-01	.9614+05	.4099+02	.9913-01
.3349+06	.2904+02	.3081-01	.9138+05	.3568+02	.9402-01
.3106+06	.3079+02	.3172-01	.8528+05	.3275+02	.9496-01
.2887+06	.2962+02	.3444-01	.7830+05	.3369+02	.9333-01
.2692+06	.2937+02	.3698-01	.7212+05	.4285+02	.9853-01
.2515+06	.3161+02	.3817-01	.6723+05	.5295+02	.9421-01
.2355+06	.3083+02	.4132-01	.6180+05	.4500+02	.9571-01
.2210+06	.3108+02	.4393-01	.5483+05	.4339+02	.9724-01
.2078+06	.2891+02	.4870-01	.4563+05	.4047+02	.9898-01
.1957+06	.3410+02	.4764-01			

11/2/65-007 COMPUTED 11/17/65 TABLE X

3 INCH WATER COOLED DEPLETED URANIUM SPHERE SPECTRUM
118 DEGREES POSITION 3 .5 INCH PRECOLLIMATOR
1.238 INCH URANIUM FILTER AT 16 METERS. N(E) HAS BEEN MULTIPLIED BY 11.04
NE 211 DETECTOR 31.25 NSECOND CHANNEL WIDTH
RESOLUTION FOR GROUPING = .020 LARGEST FRACTIONAL ERROR = .1

ENERGY (E V)	N(E) (ARBITR. UNITS)	DELTA(N)/N	ENERGY (E V)	N(E) (ARBITR. UNITS	DELTA(N)/N
.1744+08	.4429-02	.8722-01	.2621+07	.3252+01	.3044-01
.1020+08	.3164-01	.9030-01	.2551+07	.3502+01	.2975-01
.9195+07	.7252-01	.6434-01	.2485+07	.3682+01	.2940-01
.8531+07	.1013+00	.8078-01	.2420+07	.3744+01	.2950-01
.8130+07	.1308-00	.7407-01	.2359+07	.4137+01	.2843-01
.7756+07	.1715-00	.6693-01	.2299+07	.4236+01	.2864-01
.7408+07	.2119-00	.6223-01	.2242+07	.4544+01	.2814-01
.7082+07	.2735-00	.5659-01	.2187+07	.4499+01	.2866-01
.6778+07	.3352-00	.5298-01	.2134+07	.4573+01	.2878-01
.6493+07	.3940-00	.5036-01	.2083+07	.4680+01	.2888-01
.6225+07	.4129-00	.5082-01	.2034+07	.4547+01	.2969-01
.5974+07	.5494-00	.4535-01	.1986+07	.5025+01	.2864-01
.5738+07	.5972-00	.4476-01	.1941+07	.5343+01	.2815-01
.5515+07	.6508-00	.4410-01	.1896+07	.5354+01	.2858-01
.5305+07	.7874-00	.4120-01	.1853+07	.5739+01	.2797-01
.5107+07	.9250-00	.3916-01	.1812+07	.5728+01	.2845-01
.4920+07	.1050+01	.3737-01	.1772+07	.6024+01	.2808-01
.4742+07	.1024+01	.3877-01	.1733+07	.5846+01	.2884-01
.4575+07	.1239+01	.3632-01	.1696+07	.6334+01	.2807-01
.4416+07	.1313+01	.3613-01	.1659+07	.6634+01	.2823-01
.4265+07	.1395+01	.3564-01	.1624+07	.6963+01	.2771-01
.4122+07	.1369+01	.3666-01	.1590+07	.6826+01	.2842-01
.3985+07	.1564+01	.3505-01	.1557+07	.6801+01	.2872-01
.3856+07	.1713+01	.3413-01	.1525+07	.7496+01	.2766-01
.3733+07	.1768+01	.3434-01	.1495+07	.7322+01	.2837-01
.3615+07	.1987+01	.3300-01	.1450+07	.7940+01	.1962-01
.3503+07	.2021+01	.3327-01	.1393+07	.8421+01	.1955-01
.3396+07	.2156+01	.3268-01	.1340+07	.8384+01	.2028-01
.3294+07	.2297+01	.3222-01	.1290+07	.8821+01	.2019-01
.3196+07	.2368+01	.3220-01	.1242+07	.9609+01	.1981-01
.3103+07	.2577+01	.3126-01	.1197+07	.9661+01	.2036-01
.3014+07	.2636+01	.3140-01	.1155+07	.1011+02	.2066-01
.2928+07	.2889+01	.3044-01	.1114+07	.1082+02	.2089-01
.2847+07	.2986+01	.3038-01	.1076+07	.1086+02	.2148-01
.2768+07	.3136+01	.3012-01	.1040+07	.1129+02	.2193-01
.2693+07	.3252+01	.2998-01			

4/9/66-005 COMPUTED 5/19/66 TABLE XI

3 INCH WATER COOLED DEPLETED URANIUM SPHERE SPECTRUM
95 DEGREES WHOLE SPHERE 3.94 INCH PRECOLLIMATOR
2 INCH LEAD FILTER AT 16 METERS.
NE 226 DETECTOR 250. NSECOND CHANNEL WIDTH
RESOLUTION FOR GROUPING = .28A AT 10MEV. LARGEST FRACTIONAL ERROR = .1

ENERGY (E V)	N(E) (ARBITR. UNITS)	DELTA(N)/N	ENERGY (E V)	N(E) (ARBITR. UNITS	DELTA(N)/N
.1332+07	.7616+02	.1352-01	.9303+05	.3851+03	.6404-01
.1148+07	.9097+02	.1182-01	.8935+05	.3069+03	.7577-01
.9992+06	.1301+03	.1076-01	.8587+05	.3356+03	.7511-01
.8777+06	.1731+03	.1041-01	.8260+05	.3128+03	.8046-01
.7771+06	.1848+03	.1027-01	.7804+05	.2286+03	.7322-01
.6928+06	.2030+03	.1058-01	.7382+05	.3147+03	.8586-01
.6216+06	.2281+03	.1102-01	.7120+05	.3059+03	.9013-01
.5607+06	.2182+03	.1147-01	.6872+05	.2947+03	.9811-01
.5084+06	.2186+03	.1107-01	.6637+05	.4203+03	.8156-01
.4631+06	.3087+03	.1237-01	.6414+05	.3316+03	.9506-01
.4236+06	.3232+03	.1466-01	.6202+05	.3529+03	.9589-01
.3890+06	.3020+03	.1580-01	.6000+05	.3749+03	.9589-01
.3584+06	.4570+03	.1816-01	.5716+05	.3108+03	.8161-01
.3313+06	.2708+03	.1781-01	.5367+05	.4102+03	.7803-01
.3071+06	.3533+03	.1835-01	.5048+05	.4408+03	.8573-01
.2855+06	.3371+03	.2049-01	.4757+05	.5287+03	.8688-01
.2661+06	.3129+03	.2272-01	.4429+05	.2879+03	.9091-01
.2486+06	.3174+03	.2375-01	.4077+05	.3311+03	.8157-01
.2328+06	.3144+03	.2532-01	.3814+05	.3768+03	.9801-01
.2185+06	.3187+03	.2698-01	.3576+05	.4028+03	.8207-01
.2054+06	.3272+03	.2831-01	.3319+05	.4375+03	.8231-01
.1935+06	.3175+03	.3075-01	.3089+05	.4328+03	.8899-01
.1826+06	.3289+03	.3255-01	.2850+05	.3824+03	.9296-01
.1725+06	.3433+03	.3443-01	.2608+05	.3995+03	.9291-01
.1633+06	.3261+03	.3829-01	.2396+05	.4148+03	.9955-01
.1548+06	.3313+03	.4075-01	.2209+05	.4947+03	.9648-01
.1470+06	.3344+03	.4318-01	.2024+05	.4865+03	.9724-01
.1397+06	.3670+03	.4365-01	.1812+05	.4850+03	.9520-01
.1330+06	.3801+03	.4542-01	.1577+05	.5387+03	.9194-01
.1267+06	.3389+03	.5091-01	.1352+05	.5687+03	.9936-01
.1209+06	.3661+03	.5113-01	.1148+05	.6536+03	.9834-01
.1154+06	.3555+03	.5425-01	.9315+04	.7189+03	.9941-01
.1103+06	.3767+03	.5492-01	.7266+04	.1076+04	.9808-01
.1056+06	.3595+03	.5889-01	.5651+04	.1403+04	.9818-01
.1011+06	.3504+03	.6236-01	.4292+04	.1607+04	.9831-01
.9696+05	.3759+03	.6244-01	.3031+04	.2177+04	.9987-01

4/9/66-008 COMPUTED 5/ 9/66 TABLE XII

3 INCH WATER COOLED DEPLETED URANIUM SPHERE SPECTRUM
95 DEGREES WHOLE SPHERE 3.94 INCH PRECOLLIMATOR
2 INCH LEAD FILTER AT 16 METERS. N(E) HAS BEEN MULTIPLIED BY 11.04
NE 211 DETECTOR 31.25 NSECOND CHANNEL WIDTH
RESOLUTION FOR GROUPING = .288 AT 10MEV. LARGEST FRACTIONAL ERROR = .1

ENERGY (E V)	N(E) (ARBITR. UNITS)	DELTA(N)/N	ENERGY (E V)	N(E) (ARBITR. UNITS	DELTA(N)/N
.1137+08	.1581-00	.9258-01	.1861+07	.5168+02	.1789-01
.9922+07	.4190-00	.7572-01	.1780+07	.5605+02	.1766-01
.8959+07	.7391-00	.6026-01	.1703+07	.5833+02	.1769-01
.8130+07	.1161+01	.5127-01	.1632+07	.5674+02	.1850-01
.7411+07	.2112+01	.4071-01	.1565+07	.6366+02	.1797-01
.6783+07	.3059+01	.3584-01	.1501+07	.7873+02	.1662-01
.6232+07	.4681+01	.3168-01	.1442+07	.8628+02	.1649-01
.5745+07	.5468+01	.3124-01	.1386+07	.8755+02	.1709-01
.5313+07	.7023+01	.2959-01	.1334+07	.9601+02	.1711-01
.4928+07	.8508+01	.2860-01	.1284+07	.1043+03	.1685-01
.4584+07	.1022+02	.2794-01	.1237+07	.1089+03	.1717-01
.4274+07	.1149+02	.2743-01	.1192+07	.1204+03	.1697-01
.3995+07	.1324+02	.2664-01	.1150+07	.1263+03	.1679-01
.3742+07	.1528+02	.2563-01	.1110+07	.1238+03	.1678-01
.3513+07	.1814+02	.2454-01	.1072+07	.1214+03	.1722-01
.3304+07	.2143+02	.2415-01	.1036+07	.1568+03	.1683-01
.3113+07	.2052+02	.2454-01	.1002+07	.1459+03	.1737-01
.2938+07	.2422+02	.2310-01	.9696+06	.1450+03	.1765-01
.2777+07	.2671+02	.2273-01	.9387+06	.1597+03	.1780-01
.2630+07	.2892+02	.2213-01	.9091+06	.1506+03	.1784-01
.2494+07	.2910+02	.2183-01	.8810+06	.1769+03	.1713-01
.2368+07	.3294+02	.2062-01	.8541+06	.2384+03	.1694-01
.2251+07	.3560+02	.2014-01	.8285+06	.2482+03	.1771-01
.2143+07	.3632+02	.2013-01	.8040+06	.2017+03	.1909-01
.2042+07	.4152+02	.1910-01	.7805+06	.1829+03	.2072-01
.1949+07	.4342+02	.1909-01	.7581+06	.2771+03	.1875-01

1/30/66-004 COMPUTED 3/31/66 TABLE XIII

3 INCH WATER COOLED DEPLETED URANIUM SPHERE SPECTRUM
95 DEGREES WHOLE SPHERE 3.94 INCH PRECOLLIMATOR
1.238 INCH URANIUM FILTER AT 16 METERS. N(E) HAS BEEN NORMALIZED AT 1.0 MEV
NE 226 DETECTOR 62.5 NSECOND CHANNEL WIDTH
RESOLUTION FOR GROUPING = .28A AT 10MEV. LARGEST FRACTIONAL ERROR = .1

ENERGY (E V)	N(E) (ARBITR. UNITS)	DELTA(N)/N	ENERGY (E V)	N(E) (ARBITR. UNITS	DELTA(N)/N
.1392+07	.6530+02	.1323-01	.1545+06	.2703+03	.5080-01
.1242+07	.7445+02	.1310-01	.1486+06	.2687+03	.5281-01
.1114+07	.9060+02	.1289-01	.1431+06	.2685+03	.5492-01
.1006+07	.1096+03	.1273-01	.1378+06	.2745+03	.5638-01
.9121+06	.1268+03	.1259-01	.1329+06	.2732+03	.5876-01
.8310+06	.1444+03	.1276-01	.1282+06	.2593+03	.6278-01
.7603+06	.1657+03	.1298-01	.1237+06	.2890+03	.6146-01
.6982+06	.1832+03	.1351-01	.1195+06	.2915+03	.6353-01
.6434+06	.2029+03	.1401-01	.1155+06	.2645+03	.6952-01
.5949+06	.2148+03	.1477-01	.1116+06	.2236+03	.7903-01
.5516+06	.2299+03	.1541-01	.1080+06	.2512+03	.7691-01
.5129+06	.2300+03	.1667-01	.1046+06	.2593+03	.7855-01
.4781+06	.2396+03	.1783-01	.1013+06	.2772+03	.7855-01
.4467+06	.2491+03	.1971-01	.9812+05	.2810+03	.8081-01
.4184+06	.2495+03	.2130-01	.9513+05	.2695+03	.8567-01
.3926+06	.2374+03	.2184-01	.9227+05	.2857+03	.8567-01
.3692+06	.2633+03	.2184-01	.8953+05	.2376+03	.9826-01
.3478+06	.2547+03	.2322-01	.8692+05	.2990+03	.8897-01
.3282+06	.2448+03	.2481-01	.8442+05	.2715+03	.9689-01
.3102+06	.2357+03	.2643-01	.8202+05	.2850+03	.9734-01
.2937+06	.2313+03	.2794-01	.7936+05	.2790+03	.8845-01
.2784+06	.2459+03	.2851-01	.7647+05	.3100+03	.8679-01
.2643+06	.2423+03	.3030-01	.7373+05	.2932+03	.9324-01
.2512+06	.2527+03	.3131-01	.7082+05	.2687+03	.9217-01
.2391+06	.2408+03	.3378-01	.6750+05	.2424+03	.9501-01
.2279+06	.2558+03	.3440-01	.6440+05	.2925+03	.9759-01
.2174+06	.2426+03	.3705-01	.6152+05	.2687+03	.9899-01
.2076+06	.2420+03	.3886-01	.5881+05	.3735+03	.9335-01
.1985+06	.2520+03	.3996-01	.5607+05	.2892+03	.9802-01
.1900+06	.2560+03	.4180-01	.5271+05	.2820+03	.9525-01
.1820+06	.2577+03	.4396-01	.4944+05	.3235+03	.9976-01
.1745+06	.2752+03	.4461-01	.4631+05	.3127+03	.9896-01
.1674+06	.2642+03	.4754-01	.4288+05	.3357+03	.9476-01
.1608+06	.2633+03	.4960-01	.3941+05	.3520+03	.9780-01

1/30/66-002 COMPUTED 3/10/66 TABLE XIV

3 INCH WATER COOLED DEPLETED URANIUM SPHERE SPECTRUM
95 DEGREES WHOLE SPHERE 3.94 INCH PRECOLLIMATOR
1.238 INCH URANIUM FILTER AT 16 METERS. N(E) HAS BEEN NORMALIZED AT 1.0 MEV
NE 211 DETECTOR 31.25 NSECOND CHANNEL WIDTH
RESOLUTION FOR GROUPING = .28A AT 10MEV. LARGEST FRACTIONAL ERROR = .1

ENERGY (E V)	N(E) (ARBITR. UNITS)	DELTA(N)/N	ENERGY (E V)	N(E) (ARBITR. UNITS	DELTA(N)/N
.1552+08	.2A47-01	.A372-01	.2012+07	.3327+02	.1115-01
.1325+08	.7579-01	.6696-01	.1921+07	.3557+02	.1114-01
.1179+08	.1555-00	.4975-01	.1836+07	.3948+02	.1091-01
.1055+08	.3107-00	.3780-01	.1756+07	.4244+02	.1083-01
.9504+07	.5781-00	.2995-01	.1682+07	.4477+02	.1082-01
.8604+07	.9378-00	.2548-01	.1612+07	.4934+02	.1069-01
.7826+07	.1498+01	.2171-01	.1546+07	.5247+02	.1062-01
.7149+07	.2114+01	.1949-01	.1484+07	.5630+02	.1059-01
.6556+07	.2A84+01	.1787-01	.1426+07	.6035+02	.1058-01
.6033+07	.3A54+01	.1653-01	.1372+07	.6319+02	.1070-01
.5571+07	.4665+01	.1589-01	.1320+07	.665A+02	.1083-01
.5160+07	.5561+01	.1534-01	.1271+07	.7153+02	.1064-01
.4793+07	.6576+01	.1481-01	.1225+07	.7773+02	.1061-01
.4464+07	.7615+01	.1454-01	.1181+07	.8289+02	.1066-01
.4167+07	.8817+01	.1406-01	.1140+07	.8866+02	.1075-01
.3899+07	.1027+02	.1360-01	.1101+07	.9366+02	.1100-01
.3657+07	.1136+02	.1346-01	.1063+07	.9886+02	.1105-01
.3436+07	.1292+02	.1306-01	.1028+07	.1056+03	.1122-01
.3234+07	.1437+02	.1278-01	.9944+06	.1090+03	.1143-01
.3050+07	.1632+02	.1234-01	.9624+06	.1192+03	.1118-01
.2881+07	.1744+02	.1234-01	.9319+06	.1271+03	.1123-01
.2726+07	.2039+02	.1179-01	.9028+06	.1387+03	.1122-01
.2583+07	.2165+02	.1182-01	.8751+06	.1446+03	.1146-01
.2451+07	.2400+02	.1157-01	.8486+06	.1127+03	.1351-01
.2329+07	.2647+02	.1136-01	.8233+06	.1639+03	.1173-01
.2215+07	.2A84+02	.1127-01	.7992+06	.1715+03	.1200-01
.2110+07	.3074+02	.1127-01	.7760+06	.1881+03	.1220-01

Table XV

GROUP STRUCTURE AND TRIAL SOURCE

Group	Energy Interval (eV)	Lethargy Interval	Trial Q_0	Trial $Q_0/\Delta E$
1	1.492 + 7 - 1.000 + 7	-0.4 - 0.0	2.300-3	4.67-10
2	6.703 + 6	0.4	1.748-2	5.30-9
3	4.493 + 6	0.8	4.016-2	1.82-8
4	3.012 + 6	1.2	6.041-2	4.08-8
5	2.019 + 6	1.6	8.425-2	8.48-8
6	1.353 + 6	2.0	1.636-1	1.75-7
7	8.209 + 5	2.5	2.0241-1	3.80-7
8	4.979 + 5	3.0	1.8416-1	5.70-7
9	3.020 + 5	3.5	1.2813-1	6.54-7
10	1.832 + 5	4.0	6.887-2	5.80-7
11	1.111 + 5	4.5	3.883-2	5.39-7
12	6.738 + 4	5.0	2.305-2	5.27-7
13	4.087 + 4	5.5	1.396-2	5.3-7
14	2.479 + 4	6.0	8.470-3	5.3-7
15	1.503 + 4	6.5	5.140-3	5.3-7
16	9.119 + 3	7.0	3.120-3	5.3-7
17	5.531 + 3	7.5	1.890-3	5.3-7
18	2.035 + 3	8.5	1.840-3	5.3-7
19	7.485 + 2	9.5	6.800-4	5.3-7
20	2.754 + 2	10.5	2.500-4	5.3-7
21	1.013 + 2	11.5	9.2-5	5.3-7
22	3.727 + 1	12.5	3.4-5	5.3-7
23	1.371 + 1	13.5	1.2-5	5.3-7
24	5.043 + 0	14.5	4.6-6	5.3-7
25	1.855 + 0	15.5	1.7-6	5.3-7

Table XVI

COMPARISON OF TOTAL LEAKAGE FOR WATER THICKNESS OF 0.229 cm AND 0.152 cm

Group	0.229 cm Water	0.152 cm Water
1	5.49-10	5.47-10
2	5.82-9	5.82-9
3	1.96-8	1.95-8
4	4.34-8	4.34-8
5	9.53-8	9.56-8
6	2.25-7	2.27-7
7	6.27-7	6.41-7
8	1.28-6	1.30-6
9	1.70-6	1.73-6
10	1.80-6	1.81-6
11	1.74-6	1.70-6
12	1.72-6	1.67-6
13	1.82-6	1.71-6
14	1.75-6	1.56-6
15	1.99-6	1.72-6
16	2.30-6	1.92-6
17	2.60-6	2.07-6
18	3.47-6	2.66-6
19	5.16-6	3.66-6
20	7.67-6	5.01-6
21	1.18-5	7.16-6
22	1.83-5	1.05-5
23	2.57-5	1.37-5
24	4.44-5	2.21-5
25	7.19-5	3.32-5

Table XVII

ADJUSTED SOURCE AND TARGET FLUX SPECTRA

Group	E(eV)	Adjusted Q_0	$Q_0/\Delta E$	Total Leakage Calculated/ Measured	Flux at 0° Calculated/ Measured	Flux at 20° Calculated/ Measured
1	1.25+7	3.00-3	6.10-10	0.99	1.14	----
2	8.35+6	2.08-2	6.31-9	1.00	1.43	1.56
3	5.60+6	5.36-2	2.42-8	1.01	1.00	1.07
4	3.76+6	8.19-2	5.53-8	1.01	0.99	1.01
5	2.52+6	1.089-1	1.10-7	1.00	1.00	1.00
6	1.69+6	1.252-1	1.88-7	1.00	1.09	0.98
7	1.09+6	1.765-1	3.32-7	1.00	1.25	1.14
8	6.59+5	1.605-1	4.97-7	1.01	1.16	0.99
9	4.00+5	1.075-1	5.49-7	1.00	1.10	1.02
10	2.43+5	5.28-2	4.44-7	1.02	0.97	0.79
11	1.47+5	3.65-2	5.06-7	0.94	0.98	0.81
12	8.92+4	2.42-2	5.54-7	0.97		
13	5.41+4	1.44-2	5.43-7	0.99		
14	3.28+4	9.20-3	5.72-7	0.97		
15	1.99+4	6.10-3	6.25-7	0.95		
16	1.21+4	5.10-3	8.64-7	0.89		
17	7.23+3	5.40-3	1.50-6	0.80		
18	3.78+3	5.20-3	1.5-6			
19	1.39+3	1.90-3	1.5-6			
20	5.12+2	7.00-4	1.5-6			
21	1.88+2	2.60-4	1.5-6			
22	5.2+1	9.40-5	1.5-6			
23	2.5+1	3.50-5	1.5-6			
24	1.0+1	1.30-5	1.5-6			
25	3.4+0	4.80-6	1.5-6			

Table XVIII

S_{16} GAPLSN CALCULATED ANGULAR FLUX PER UNIT ENERGY

Group	0°	20.1°	35.5°	46.5°	55.7°	64.0°	71.8°	79.2°	86.4°
1	4.168-10	5.506-11	3.796-12	1.026-12	6.002-14				
2	3.815-9	5.318-10	4.888-11	1.705-11	5.212-12	1.071-12			
3	1.319-8	2.004-9	2.525-10	1.040-10	4.519-11	1.802-11	6.730-12	1.610-12	
4	2.848-8	4.534-9	6.900-10	3.259-10	1.735-10	8.816-11	4.630-11	3.365-11	1.866-11
5	5.869-8	9.344-9	1.506-9	7.656-10	4.445-10	2.238-10	1.119-10	1.052-10	6.705-11
6	1.088-7	1.764-8	3.147-9	1.732-9	1.082-9	5.916-10	3.216-10	2.878-10	1.777-10
7	2.002-7	3.634-8	8.684-9	5.258-9	3.479-9	1.909-9	9.684-10	7.334-10	4.183-10
8	2.837-7	6.348-8	2.139-8	1.400-8	9.724-9	5.514-9	2.849-9	2.059-9	1.142-9
9	2.719-7	7.309-8	3.082-8	2.145-8	1.561-8	1.011-8	6.256-9	4.137-9	2.063-9
10	2.068-7	6.662-8	3.322-8	2.441-8	1.858-8	1.339-8	9.012-9	5.040-9	2.044-9
11	1.928-7	6.397-8	3.396-8	2.612-8	2.081-8	1.712-8	1.304-8	7.040-9	2.577-9
12	1.799-7	6.233-8	3.506-8	2.810-8	2.334-8	2.125-8	1.769-8	9.258-9	3.014-9
13	1.604-7	5.993-8	3.641-8	3.062-8	2.667-8	2.662-8	2.381-8	1.218-8	3.554-9
14	1.429-7	5.666-8	3.714-8	3.288-8	3.009-8	3.172-8	2.941-8	1.917-8	9.375-9
15	1.427-7	5.955-8	4.122-8	3.810-8	3.616-8	4.112-8	4.058-8	1.945-8	4.043-9
16	1.833-7	7.509-8	5.182-8	4.815-8	4.605-8	5.236-8	5.208-8	2.764-8	8.092-9
17	2.859-7	1.128-7	7.436-8	6.687-8	6.230-8	6.739-8	6.552-8	3.896-8	1.540-8
18	3.143-7	1.370-7	9.810-8	9.176-8	8.809-8	9.953-8	9.939-8	5.470-8	1.756-8
19	2.680-7	1.664-7	1.411-7	1.393-7	1.375-7	1.621-7	1.663-7	8.554-8	2.221-8
20	4.000-7	2.334-7	2.021-7	2.052-7	2.082-7	2.493-7	2.543-7	1.416-7	4.937-8
21	3.571-7	3.094-7	3.018-7	3.155-7	3.202-7	3.927-7	4.131-7	2.179-7	6.203-8
22	7.028-7	4.934-7	4.640-7	4.847-7	5.017-7	6.148-7	6.402-7	3.315-7	8.977-8
23	6.926-7	6.554-7	6.550-7	6.868-7	6.958-7	8.511-7	8.991-7	4.629-7	1.208-7
24	1.455-6	1.103-6	1.092-6	1.168-6	1.238-6	1.526-6	1.578-6	8.221-7	2.299-7
25	2.134-6	1.744-6	1.765-6	1.896-6	2.020-6	2.477-6	2.549-6	1.331-6	3.755-7

REFERENCES

1. G. D. Trimble, G. K. Houghton, and J. H. Audas, "Measurement of Neutron Spectra in Liquid Hydrogen," NASA Report NASA CR-54230, General Atomic Division, General Dynamics Corporation, September 30, 1964.

2. R. H. Stahl, J. L. Russell, Jr., and G. R. Hopkins, "Pulsed Neutron Sources," General Atomic Report GA-5533 (August 7, 1964).

3. A. E. Profio, "Verification of Analytical Techniques (GAPLSN - Transport Theory and O5R - Monte Carlo Theory) by Utilization of Measured Fast Neutron Spectra in Infinite Paraffin and Spherical Paraffin Shields," Air Force Weapons Laboratory Report AFWL-TR-65-193, General Atomic Division, General Dynamics Corporation, March 1966.

4. M. H. Macgregor, "Neutron Production by Electron Bombarding of Uranium," GAMD-6805 (November 23, 1965).

5. W. R. Dixon, "Energy and Angular Distribution of Photoneutrons Produced by 70 MeV X-Rays," Canadian Journal of Physics, 33, 785 (1955).

6. W. Bertozzi, S. Kowalski, G. S. Mutchler, C. P. Sargent, and W. Turchinetz, "The Energy and Angular Distributions of Photoneutrons from Heavy Elements," Paper presented at 1965 Gordon Photonuclear Conference.

7. June Matthews, "Energy Spectra and Angular Distributions of Neutrons Limited in Photofission of Even-Mass Nuclei," S. M. Thesis, MIT Dept. of Physics, June, 1962.

8. Earl K. Hyde, The Nuclear Properties of the Heavy Elements, Fission Phenomena (Prentice-Hall, Englewood Cliffs, N. J., 1964) Vol. III, p. 494.

9. B. I. Gavrilor and L. E. Lazareva, "Yields of Photoneutrons for Intermediate and Heavy Nuclei," Soviet Physics JETP, 3, 871 (1957).

10. G. D. Joanou and J. S. Dudek, "GAM-II - A B_3 Code for the Calculation of Fast Neutron Spectra and Associated Multigroup Constants," General Atomic Report GA-4265 (1963).

11. J. H. Alexander, G. W. Hinman, and J. R. Triplett, "GAPLSN - A Modified DSN Program for the Solution of the One-Dimensional Anisotropic Scattering Transport Equation," General Atomic Report GA-4972 (1964).

APPENDIX B

TABULATED TIME-OF-FLIGHT DATA

INFINITE MEDIUM GRAPHITE SPECTRUM

7/22/66 005(10) R=20.3 0 DEGREES BF3

(COMPUTED 1/10/67)

ENERGY (EV)	N(E)	E*N(E)	DELTA(N)/N	ENERGY (EV)	N(E)	E*N(E)	DELTA(N)/N
9.4088+02	2.2960+10	2.1602+13	1.4389-02	1.7483+00	9.9132+12	1.5543+13	1.6516-02
8.9454+02	3.1063+10	2.1991+13	1.4259-02	1.5990+00	9.7430+12	1.5579+13	1.5575-02
5.3364+02	4.1735+10	2.2271+13	1.4859-02	1.4582+00	1.0743+13	1.5665+13	1.5740-02
4.2279+02	4.9300+10	2.0843+13	1.5115-02	1.3351+00	1.1528+13	1.5392+13	1.5208-02
3.4322+02	6.2577+10	2.1478+13	1.5436-02	1.2200+00	1.2915+13	1.5756+13	1.5196-02
2.8416+02	6.9552+10	1.9765+13	1.5972-02	1.1128+00	1.3946+13	1.5519+13	1.5519-02
2.3916+02	8.3232+10	1.9898+13	1.6324-02	1.0189+00	1.3423+13	1.5714+13	1.5669-02
2.0403+02	9.0652+10	1.8537+13	1.7347-02	9.3172-01	1.6459+13	1.5336+13	1.5075-02
1.7611+02	1.0735+11	1.8905+13	1.7423-02	8.5098-01	1.7913+13	1.5244+13	1.5273-02
1.5356+02	1.2026+11	1.9389+13	1.7480-02	7.8033-01	1.9326+13	1.5781+13	1.5452-02
1.3363+02	1.3090+11	1.9033+13	1.7919-02	7.1498-01	2.1539+13	1.5400+13	1.4636-02
1.1974+02	1.5091+11	1.9028+13	1.8388-02	6.5463-01	2.2900+13	1.4991+13	1.5042-02
1.0688+02	1.7522+11	1.8727+13	1.8705-02	5.9920-01	2.6148+13	1.5668+13	1.4209-02
9.5980+01	1.9522+11	1.8737+13	1.8984-02	5.4832-01	2.9898+13	1.5845+13	1.4372-02
8.6870+01	2.1367+11	1.8519+13	1.9561-02	5.0182-01	3.1924+13	1.6020+13	1.3999-02
7.8650+01	2.4295+11	1.9037+13	1.9510-02	4.5936-01	3.5787+13	1.6439+13	1.3892-02
7.1693+01	2.4577+11	1.7691+13	2.0534-02	4.2073-01	4.0192+13	1.6910+13	1.3348-02
6.5621+01	2.7744+11	1.8206+13	2.0644-02	3.8563-01	4.3885+13	1.6924+13	1.3628-02
5.7936+01	3.1190+11	1.8070+13	1.4440-02	3.5403-01	4.9370+13	1.7479+13	1.3138-02
4.9542+01	3.6462+11	1.8064+13	1.5171-02	3.2481-01	5.5650+13	1.8076+13	1.2731-02
4.2651+01	4.2790+11	1.8336+13	1.5450-02	2.9832-01	6.2965+13	1.8754+13	1.2320-02
3.7425+01	4.7202+11	1.7667+13	1.6141-02	2.7406-01	7.2765+13	1.9942+13	1.1321-02
3.2573+01	5.3656+11	1.7692+13	1.6457-02	2.5169-01	8.3480+13	2.1011+13	1.0540-02
2.9269+01	5.9743+11	1.7486+13	1.6918-02	2.3126-01	9.6542+13	2.2326+13	9.9180-03
2.6155+01	6.6445+11	1.7379+13	1.7297-02	2.1252-01	1.1065+14	2.4790+13	8.9659-03
2.3514+01	7.3451+11	1.7271+13	1.7654-02	1.9505-01	1.4114+14	2.7529+13	8.2193-03
2.1254+01	8.0641+11	1.7182+13	1.8011-02	1.7908-01	1.7136+14	3.0687+13	7.8527-03
1.9305+01	8.8833+11	1.7149+13	1.8357-02	1.6452-01	2.1690+14	3.5634+13	7.2008-03
1.7611+01	9.6854+11	1.7022+13	1.8715-02	1.5107-01	2.7051+14	4.0891+13	6.7834-03
1.6131+01	1.0342+12	1.6682+13	1.9072-02	1.3881-01	3.4790+14	4.8292+13	6.3661-03
1.4536+01	1.1013+12	1.7174+13	1.5642-02	1.2760-01	4.4870+14	5.7254+13	5.9885-03
1.2911+01	1.2733+12	1.6446+13	1.6312-02	1.1718-01	5.7100+14	6.6909+13	5.5929-03
1.1542+01	1.4051+12	1.6217+13	1.6746-02	1.0758-01	7.1263+14	7.6664+13	5.3819-03
1.0360+01	1.5619+12	1.6212+13	1.7020-02	9.9068-02	8.8032+14	8.7261+13	5.2783-03
9.3852+00	1.7556+12	1.6477+13	1.7105-02	9.0771-02	1.0154+15	9.2166+13	5.6204-03
8.5267+00	1.8861+12	1.6083+13	1.7684-02	8.4341-02	1.0603+15	9.3670+13	1.9153-02
7.7109+00	2.0942+12	1.6295+13	1.7804-02	9.6081-02	9.5922+14	9.2163+13	2.7140-02
7.1291+00	2.2519+12	1.6054+13	1.8235-02	8.2481-02	1.2194+15	1.0058+14	2.6223-02
6.4896+00	2.4950+12	1.6140+13	1.6050-02	8.7666-02	1.0820+15	9.4857+13	1.0211-02
5.8189+00	2.7620+12	1.6188+13	1.6310-02	7.8856-02	1.2539+15	9.8869+13	2.6743-02
5.2621+00	3.0130+12	1.5855+13	1.6750-02	9.0875-02	1.0391+15	9.4432+13	2.5781-02
4.7215+00	3.3555+12	1.6045+13	1.6790-02	7.8177-02	1.3057+15	1.0207+14	1.8636-02
4.3039+00	3.5473+12	1.5480+13	1.7423-02	8.7501-02	1.1314+15	9.8996+13	5.7687-03
3.9987+00	4.0169+12	1.6062+13	1.7340-02	6.0949-02	1.2936+15	1.0472+14	4.4448-03
3.6410+00	4.2280+12	1.5431+13	1.6086-02	7.4336-02	1.4826+15	1.1021+14	5.4965-03
3.2962+00	4.8085+12	1.5362+13	1.6415-02	6.8563-02	1.6740+15	1.1477+14	4.5627-03
2.9982+00	5.0995+12	1.5289+13	1.6670-02	6.3050-02	1.8852+15	1.1886+14	4.4772-03
2.7560+00	5.4253+12	1.4959+13	1.7232-02	5.7927-02	2.0576+15	1.1919+14	4.3983-03
2.5116+00	6.3179+12	1.5869+13	1.6373-02	5.3187-02	2.2235+15	1.1826+14	4.4064-03
2.2935+00	6.9708+12	1.5986+13	1.6122-02	4.8879-02	2.4573+15	1.2011+14	4.4066-03
2.0868+00	7.8136+12	1.5986+13	1.5931-02	4.4919-02	2.6279+15	1.1804+14	4.3998-03
1.9055+00	8.1772+12	1.5584+13	1.6332-02				

BLANK PAGE

INFINITE MEDIUM GRAPHITE SPECTRUM

7/22/66 005(80) R=20.3 0 DEGREES BF3

(COMPUTED 1/10/67)

ENERGY (EV)	N(E)	E*N(E)	DELTA(N)/N	ENERGY (EV)	N(E)	E*N(E)	DELTA(N)/N
8.0548+01	1.8531+11	1.4926+13	7.6872-03	1.2880-01	3.5941+14	4.6292+13	4.9789-03
5.4491+01	2.7081+11	1.4757+13	8.2063-03	1.1764-01	4.6302+14	5.4469+13	4.3794-03
3.9300+01	3.6761+11	1.4447+13	8.7911-03	1.0686-01	5.9465+14	6.3544+13	4.1892-03
2.9678+01	4.8536+11	1.4404+13	9.2278-03	9.8544-02	7.3545+14	7.2474+13	4.7670-03
2.3201+01	6.0776+11	1.4101+13	9.7429-03	8.3926-02	9.8417+14	8.2597+13	2.4922-03
1.8635+01	7.5199+11	1.4013+13	1.0174-02	7.5435-02	1.1935+15	9.0034+13	4.4854-03
1.5294+01	9.1968+11	1.4066+13	1.0473-02	6.8840-02	1.3763+15	9.4748+13	3.5450-03
1.2778+01	1.0550+12	1.3480+13	1.1019-02	6.2736-02	1.5593+15	9.7824+13	3.5446-03
1.0835+01	1.2175+12	1.3191+13	1.1447-02	5.7364-02	1.7148+15	9.8365+13	3.5789-03
9.3039+00	1.4468+12	1.3461+13	1.1586-02	5.2626-02	1.8625+15	9.8018+13	3.6364-03
8.0755+00	1.6322+12	1.3181+13	1.2053-02	4.8197-02	2.0475+15	9.8682+13	3.4928-03
7.0756+00	1.8550+12	1.3125+13	1.2360-02	4.4074-02	2.2023+15	9.7063+13	3.5877-03
6.2503+00	2.1181+12	1.3239+13	1.2590-02	4.0440-02	2.3301+15	9.4229+13	3.7180-03
5.5616+00	2.3215+12	1.2911+13	1.2983-02	3.7067-02	2.4277+15	8.9989+13	3.6696-03
4.9806+00	2.6087+12	1.2993+13	1.3152-02	3.3943-02	2.5153+15	8.5376+13	3.8032-03
4.4862+00	2.8837+12	1.2937+13	1.3394-02	3.1067-02	2.5750+15	7.9999+13	3.8216-03
4.0618+00	3.1698+12	1.2875+13	1.3648-02	2.8419-02	2.6474+15	7.5236+13	4.0222-03
3.6950+00	3.4805+12	1.2861+13	1.3896-02	2.6091-02	2.7003+15	7.0453+13	4.2555-03
3.3757+00	3.7505+12	1.2660+13	1.4222-02	2.3948-02	2.7056+15	6.4793+13	4.3249-03
2.9729+00	4.2162+12	1.2534+13	1.0331-02	2.1976-02	2.6752+15	5.8791+13	4.5958-03
2.5349+00	4.9887+12	1.2646+13	1.0561-02	2.0169-02	2.5869+15	5.2176+13	4.7656-03
2.1869+00	5.8946+12	1.2891+13	1.0745-02	1.8512-02	2.5588+15	4.7369+13	5.0719-03
1.9064+00	6.8343+12	1.3029+13	1.0964-02	1.6997-02	2.5131+15	4.2715+13	5.2367-03
1.6773+00	7.5536+12	1.2670+13	1.1351-02	1.5566-02	2.4585+15	3.8269+13	5.4480-03
1.4870+00	8.7346+12	1.2988+13	1.1409-02	1.4263-02	2.3148+15	3.3016+13	5.9420-03
1.3271+00	9.6163+12	1.2762+13	1.1760-02	1.3082-02	2.2440+15	2.9356+13	6.1833-03
1.1918+00	1.0914+13	1.3008+13	1.1846-02	1.1981-02	2.1763+15	2.6074+13	6.5125-03
1.0761+00	1.1906+13	1.2812+13	1.2156-02	1.0986-02	2.1056+15	2.3132+13	7.0880-03
9.7635-01	1.3310+13	1.2995+13	1.2236-02	1.0087-02	2.0657+15	2.0837+13	7.4466-03
8.8985-01	1.4179+13	1.2617+13	1.2502-02	9.2490-03	1.8539+15	1.7147+13	8.0045-03
8.1441-01	1.5241+13	1.2412+13	1.2705-02	8.4909-03	1.7318+15	1.4704+13	8.6548-03
7.3329-01	1.7237+13	1.2640+13	1.0409-02	7.8053-03	1.6162+15	1.2615+13	9.2983-03
6.5061-01	1.9392+13	1.2617+13	1.0610-02	7.1699-03	1.5647+15	1.1219+13	9.8707-03
5.8118-01	2.2296+13	1.2958+13	1.0637-02	6.5838-03	1.4841+15	9.7708+12	1.0592-02
5.2234-01	2.5054+13	1.3087+13	1.0785-02	6.0445-03	1.4170+15	8.5652+12	1.1362-02
4.7206-01	2.8607+13	1.3504+13	1.0781-02	5.5476-03	1.3384+15	7.4252+12	1.2353-02
4.2879-01	3.2083+13	1.3757+13	1.0897-02	5.0911-03	1.3281+15	6.7616+12	1.3124-02
3.9136-01	3.5863+13	1.4035+13	1.1002-02	4.6732-03	1.2975+15	6.0636+12	1.3794-02
3.5413-01	4.0756+13	1.4433+13	9.5657-03	4.2910-03	1.2491+15	5.3597+12	1.5016-02
3.1848-01	4.7265+13	1.5053+13	9.5877-03	3.9419-03	1.2187+15	4.8041+12	1.6131-02
2.8925-01	5.4807+13	1.5853+13	9.5009-03	3.6236-03	1.1974+15	4.3388+12	1.6937-02
2.6268-01	6.3842+13	1.6770+13	8.3035-03	3.3286-03	1.1639+15	3.8742+12	1.8140-02
2.3885-01	7.4832+13	1.7874+13	8.1042-03	3.0559-03	1.1238+15	3.4341+12	1.9631-02
2.1754-01	9.1821+13	1.9975+13	7.0478-03	2.8081-03	1.0861+15	3.0497+12	2.1411-02
1.9801-01	1.1239+14	2.2255+13	6.7132-03	2.5799-03	1.1068+15	2.8554+12	2.2368-02
1.8114-01	1.3689+14	2.4797+13	6.4258-03	2.3699-03	1.0647+15	2.5232+12	2.4479-02
1.6609-01	1.7453+14	2.8988+13	5.9903-03	2.1793-03	9.8437+14	2.1452+12	2.8069-02
1.5250-01	2.1685+14	3.3070+13	5.6481-03	2.0047-03	9.2358+14	1.8515+12	3.2187-02
1.4012-01	2.8083+14	3.9350+13	5.2707-03	1.8408-03	9.6707+14	1.7802+12	3.2685-02

INFINITE MEDIUM GRAPHITE SPECTRUM

7/23/66 002(10) R=20.3 90 DEGREES $B^2$3

(COMPUTED 1/10/67)

ENERGY (EV)	N(E)	E*N(E)	DELTA(N)/N	ENERGY (EV)	N(E)	E*N(E)	DELTA(N)/N
9.0021+02	1.7545+10	1.6671+13	2.025d-02	1.9246+00	6.9924+12	1.3458+13	2.4048-02
7.3142+02	2.4090+10	1.6397+13	2.0867-02	1.7655+00	7.5164+12	1.3270+13	2.4697-02
5.3394+02	3.1269+10	1.6863+13	2.1806-02	1.6148+00	7.9996+12	1.2915+13	2.3710-02
4.2699+02	3.9035+10	1.6664+13	2.1746-02	1.4727+00	8.3798+12	1.3077+13	2.3974-02
3.4062+02	4.8019+10	1.6922+13	2.2549-02	1.3383+00	9.8399+12	1.3267+13	2.3926-02
2.8700+02	5.4134+10	1.5526+13	2.3880-02	1.2321+00	1.1233+13	1.3340+13	2.2149-02
2.4153+02	6.7915+10	1.6404+13	2.3777-02	1.1238+00	1.2130+13	1.3632+13	2.2741-02
2.0303+02	7.5407+10	1.5330+13	2.5135-02	1.0290+00	1.3087+13	1.3467+13	2.3264-02
1.7706+02	8.5344+10	1.5179+13	2.5877-02	9.4095-01	1.3956+13	1.3132+13	2.2503-02
1.5303+02	9.8779+10	1.5119+13	2.6398-02	8.5940-01	1.5143+13	1.3019+13	2.2739-02
1.3342+02	1.1032+11	1.5132+13	2.6879-02	7.8806-01	1.6373+13	1.2903+13	2.2968-02
1.2393+02	1.3372+11	1.6171+13	2.6570-02	7.2205-01	1.9131+13	1.3792+13	2.1916-02
1.0794+02	1.4405+11	1.5549+13	2.7682-02	6.6111-01	2.0478+13	1.3538+13	2.1788-02
9.6331+01	1.6146+11	1.5551+13	2.8024-02	6.0512-01	2.1929+13	1.3270+13	2.1257-02
8.7529+01	1.7031+11	1.4907+13	2.9390-02	5.5374-01	2.5102+13	1.3900+13	2.1032-02
7.9430+01	1.9502+11	1.5393+13	2.9307-02	5.0678-01	2.7008+13	1.3687+13	2.0937-02
7.2404+01	2.0407+11	1.4775+13	3.0499-02	4.6389-01	3.0509+13	1.4153+13	2.0999-02
6.6271+01	2.3510+11	1.5579+13	2.9540-02	4.2486-01	3.4299+13	1.4572+13	1.9911-02
6.0631+01	2.5032+11	1.5027+13	2.1950-02	3.8939-01	3.7915+13	1.4764+13	2.0020-02
5.5334+01	2.7530+11	1.5175+13	2.2462-02	3.5742-01	4.4667+13	1.5965+13	1.9971-02
4.5275+01	3.3343+11	1.4429+13	2.3515-02	3.2784-01	4.9525+13	1.6236+13	1.9886-02
3.7799+01	3.8615+11	1.4672+13	2.4075-02	3.0099-01	5.6692+13	1.7061+13	1.7743-02
3.1501+01	4.3711+11	1.4556+13	2.4719-02	2.7637-01	6.2238+13	1.7201+13	1.6937-02
2.6259+01	4.9031+11	1.4444+13	2.5137-02	2.5367-01	7.2636+13	1.8426+13	1.5497-02
2.2415+01	5.3634+11	1.4225+13	2.6075-02	2.3298-01	8.4942+13	1.9790+13	1.4354-02
2.1747+01	5.9717+11	1.4419+13	2.6295-02	2.1403-01	1.0079+14	2.1572+13	1.3197-02
2.1405+01	5.5788+11	1.4121+13	2.6933-02	1.9641-01	1.2738+14	2.5019+13	1.1853-02
1.9496+01	7.6259+11	1.4864+13	2.6691-02	1.8036-01	1.5236+14	2.7480+13	1.1398-02
1.7780+01	7.4792+11	1.3302+13	2.8737-02	1.6571-01	1.9311+14	3.2000+13	1.0410-02
1.6291+01	9.0338+11	1.4717+13	2.7790-02	1.5220-01	2.4823+14	3.7791+13	9.6676-03
1.4882+01	9.7314+11	1.4483+13	2.8415-02	1.3989-01	3.1564+14	4.4155+13	9.0990-03
1.3539+01	1.0495+12	1.3684+13	2.4341-02	1.2863-01	4.0030+14	5.1490+13	8.6174-03
1.2356+01	1.2140+12	1.4150+13	2.4423-02	1.1815-01	5.1286+14	6.0594+13	7.9884-03
1.0483+01	1.3057+12	1.4526+13	2.4472-02	1.0850-01	6.5309+14	7.0861+13	7.6125-03
9.4783+00	1.4312+12	1.4039+13	2.5524-02	9.9643-02	8.1226+14	8.0936+13	7.1931-03
8.0113+00	1.5612+12	1.3616+13	2.6094-02	9.3646-02	9.0050+14	8.4328+13	1.5752-02
7.0301+00	1.8300+12	1.4380+13	2.5941-02	8.6724-02	1.0160+15	8.8116+13	1.5568-02
7.1398+00	1.9499+12	1.4039+13	2.6499-02	9.1505-02	9.6135+14	8.7968+13	3.7814-02
6.5331+00	2.1207+12	1.3894+13	2.3552-02	8.4732-02	1.0722+15	9.0953+13	1.2567-02
5.8766+00	2.2552+12	1.3429+13	2.4543-02	7.4802-02	1.3264+15	9.9219+13	2.5842-02
5.3143+00	2.5180+12	1.3381+13	2.5044-02	9.1601-02	1.0025+15	9.1831+13	3.6851-02
4.8269+00	2.7213+12	1.3141+13	2.5706-02	8.0944-02	1.1161+15	9.0340+13	3.9155-02
4.4372+00	3.1218+12	1.3750+13	2.5333-02	8.6868-02	1.1024+15	9.5763+13	7.0347-03
4.0384+00	3.4158+12	1.3794+13	2.5673-02	7.9707-02	1.2543+15	9.9980+13	6.1053-03
3.6771+00	3.6194+12	1.3309+13	2.3740-02	7.2207-02	1.3039+15	1.0959+14	7.0832-03
3.3269+00	4.0141+12	1.3363+13	2.4079-02	6.6813-02	1.4604+15	1.1094+14	6.2123-03
3.0279+00	4.2366+12	1.2979+13	2.5000-02	6.1361-02	1.4801+15	1.1301+14	6.1263-03
2.7300+00	4.8350+12	1.3376+13	2.4793-02	5.6381-02	1.9486+15	1.1212+14	6.1498-03
2.5307+00	5.1519+12	1.3145+13	2.5507-02	5.1840-02	2.1401+15	1.1302+14	6.1354-03
2.3163+00	5.8110+12	1.3923+13	2.2950-02	4.7654-02	2.3973+15	1.1424+14	6.2600-03
2.1367+00	6.2954+12	1.3263+13	2.3972-02	4.3804-02	2.5715+15	1.1264+14	6.1189-03

INFINITE MEDIUM GRAPHITE SPECTRUM

7/20/66 002(80) R=20.3 90 DEGREES BF3

(COMPUTED 1/10/67)

ENERGY (EV)	N(E)	E*N(E)	DELTA(N)/N	ENERGY (EV)	N(E)	E*N(E)	DELTA(N)/N
3.1346+01	1.3478+11	1.2916+13	1.1386-02	1.2984-01	3.4302+14	4.4537+13	7.0516-03
3.5032+01	2.3165+11	1.2803+13	1.2240-02	1.1861-01	4.4599+14	5.2999+13	6.1309-03
3.9498+01	3.1450+11	1.2641+13	1.2993-02	1.0778-01	5.8395+14	6.2938+13	5.4247-03
2.9472+01	4.2527+11	1.2086+13	1.3680-02	9.8775-02	7.2707+14	7.1816+13	5.6017-03
2.3431+01	5.3907+11	1.2645+13	1.4270-02	8.7656-02	9.3673+14	8.2110+13	4.0923-03
1.8826+01	6.5505+11	1.2343+13	1.5032-02	7.8373-02	1.1307+15	8.8619+13	5.2198-03
1.5445+01	8.0937+11	1.2502+13	1.5478-02	7.0306-02	1.3670+15	9.6111+13	4.8160-03
1.2903+01	9.4427+11	1.2186+13	1.6091-02	6.4051-02	1.5463+15	9.9041+13	4.9331-03
1.0942+01	1.1017+12	1.2055+13	1.6704-02	5.8546-02	1.7045+15	9.9794+13	4.8744-03
9.3461+00	1.2950+12	1.2174+13	1.7012-02	5.3692-02	1.8360+15	9.8580+13	4.9709-03
8.1865+00	1.4946+12	1.2222+13	1.7374-02	4.9153-02	2.0393+15	1.0024+14	4.7479-03
7.1456+00	1.7811+12	1.2156+13	1.7851-02	4.4932-02	2.2175+15	9.9638+13	4.8407-03
6.2123+00	1.8696+12	1.1770+13	1.8651-02	4.1214-02	2.3670+15	9.7554+13	4.9998-03
5.3167+00	2.0723+12	1.1640+13	1.9151-02	3.7762-02	2.4830+15	9.3763+13	4.9263-03
5.0000+00	2.2982+12	1.1560+13	1.9599-02	3.4568-02	2.5654+15	8.8681+13	5.1137-03
4.3167+00	2.6305+12	1.1945+13	1.9465-02	3.1628-02	2.6656+15	8.4308+13	5.0935-03
4.1921+00	2.9449+12	1.2080+13	1.9742-02	2.8923-02	2.7036+15	7.8195+13	5.4074-03
3.7165+00	3.3679+12	1.1523+13	2.0600-02	2.6546-02	2.8106+15	7.4610+13	5.6545-03
3.4032+00	3.7437+12	1.1036+13	2.0599-02	2.4356-02	2.8255+15	6.8834+13	5.7696-03
3.0824+00	3.9650+12	1.1726+13	1.4901-02	2.2347-02	2.7807+15	6.2141+13	6.1487-03
2.8380+00	4.3659+12	1.1791+13	1.5513-02	2.0504-02	2.7129+15	5.5626+13	6.3380-03
2.6033+00	5.3609+12	1.1906+13	1.5569-02	1.8815-02	2.6466+15	4.9796+13	6.7982-03
1.9253+00	6.1914+12	1.1921+13	1.5938-02	1.7271-02	2.6259+15	4.5352+13	7.0122-03
1.6965+00	6.9122+12	1.1703+13	1.6561-02	1.5859-02	2.5294+15	4.0113+13	7.5811-03
1.5017+00	7.5738+12	1.1374+13	1.7206-02	1.4570-02	2.3918+15	3.4849+13	7.9979-03
1.3362+00	8.0897+12	1.1407+13	1.7035-02	1.3356-02	2.3019+15	3.0744+13	8.3166-03
1.2435+00	1.0072+13	1.2122+13	1.7195-02	1.2257-02	2.2131+15	2.7126+13	9.0707-03
1.0967+00	1.0913+13	1.1659+13	1.7716-02	1.1262-02	2.1747+15	2.4491+13	9.5397-03
9.6594-01	1.2403+13	1.1835+13	1.7942-02	1.0334-02	2.0963+15	2.1564+13	1.0169-02
8.9367-01	1.2737+13	1.1446+13	1.8543-02	9.4701-03	1.9203+15	1.8196+13	1.1047-02
8.2243-01	1.3678+13	1.1250+13	1.8835-02	8.6891-03	1.7859+15	1.5518+13	1.1865-02
7.4754-01	1.5815+13	1.1493+13	1.5300-02	7.9834-03	1.7154+15	1.3695+13	1.2517-02
6.8704-01	1.7975+13	1.1610+13	1.5323-02	7.3297-03	1.5932+15	1.1678+13	1.3645-02
5.8992-01	2.0263+13	1.1987+13	1.5632-02	6.7268-03	1.5059+15	1.0130+13	1.4399-02
5.4750-01	2.3215+13	1.2246+13	1.5594-02	6.1729-03	1.4076+15	8.6839+12	1.6216-02
4.7371-01	2.5968+13	1.2370+13	1.5803-02	5.6632-03	1.3034+15	7.3812+12	1.8089-02
4.3566-01	2.9725+13	1.2871+13	1.5722-02	5.1950-03	1.3222+15	6.8690+12	1.8927-02
3.9818-01	3.3627+13	1.3051+13	1.5993-02	4.7664-03	1.2431+15	5.9249+12	2.0794-02
3.3753-01	3.8378+13	1.3721+13	1.3736-02	4.3749-03	1.1785+15	5.1558+12	2.2800-02
3.2143-01	4.3837+13	1.4091+13	1.3913-02	4.0173-03	1.1841+15	4.7569+12	2.4416-02
2.9179-01	5.1307+13	1.4988+13	1.3719-02	3.6915-03	1.1403+15	4.2093+12	2.6455-02
2.6902-01	5.8972+13	1.5617+13	1.2036-02	3.3943-03	1.1660+15	3.9578+12	2.7825-02
2.4867-01	6.9287+13	1.6675+13	1.1815-02	3.1192-03	1.0852+15	3.3849+12	3.0481-02
2.2911-01	8.3328+13	1.8389+13	1.0291-02	2.8651-03	1.0480+15	3.0026+12	3.4041-02
1.9948-01	1.0025+14	2.1187+13	9.6404-03	2.6343-03	1.0189+15	2.6840+12	3.9496-02
1.8242-01	1.1533+14	2.3300+13	9.1292-03	2.4217-03	9.3795+14	2.2714+12	4.2992-02
1.6729-01	1.3459+14	2.7367+13	8.5883-03	2.2260-03	9.1422+14	2.0350+12	4.7965-02
1.5394-01	1.5109+14	3.2739+13	7.8978-03	2.0476-03	7.1020+14	1.4542+12	5.6085-02
1.4120-01	2.0613+14	3.7860+13	7.4401-03	1.8826-03	8.6023+14	1.6195+12	6.2814-02

INFINITE MEDIUM GRAPHITE SPECTRUM

7/22/66 003(10) R=35.6 0 DEGREES BF3

(COMPUTED 1/10/67)

ENERGY (EV)	N(E)	E*N(E)	DELTA(N)/N	ENERGY (EV)	N(E)	E*N(E)	DELTA(N)/N
9.3544+02	4.5116+09	4.3139+12	2.1509-02	2.4972+00	2.2537+12	5.6280+12	2.0162-02
6.9052+02	6.2353+09	4.3401+12	2.1894-02	2.2803+00	2.5487+12	5.8117+12	1.8426-02
5.3056+02	9.1556+09	4.8788+12	2.1562-02	2.0739+00	2.8177+12	5.8437+12	1.8742-02
4.2035+02	1.0704+10	4.4995+12	2.2538-02	1.8948+00	3.2394+12	6.1380+12	1.8546-02
3.4123+02	1.4439+10	4.9269+12	2.2380-02	1.7382+00	3.5823+12	6.2267+12	1.8678-02
2.8254+02	1.6626+10	4.6976+12	2.2719-02	1.5898+00	3.7984+12	6.0387+12	1.7840-02
2.3777+02	2.0679+10	4.9169+12	2.2621-02	1.4498+00	4.2401+12	6.1474+12	1.7926-02
2.0285+02	2.3693+10	4.8467+12	2.3334-02	1.3274+00	4.7504+12	6.3057+12	1.8051-02
1.7509+02	2.7321+10	4.7837+12	2.4084-02	1.2130+00	5.2243+12	6.3371+12	1.7054-02
1.5267+02	3.2673+10	4.8973+12	2.4331-02	1.1063+00	5.5664+12	6.1561+12	1.7606-02
1.3430+02	3.6932+10	4.9600+12	2.4541-02	1.0130+00	6.2773+12	6.3589+12	1.7524-02
1.1903+02	4.2868+10	5.1035+12	2.4758-02	9.2634-01	6.7584+12	6.2606+12	1.6895-02
1.0626+02	4.8184+10	5.1201+12	2.5346-02	8.4606-01	7.5385+12	6.3781+12	1.6825-02
9.5424+01	5.4683+10	5.1609+12	2.5583-02	7.7583-01	8.3392+12	6.4698+12	1.6834-02
8.6169+01	6.1668+10	5.3139+12	2.5523-02	7.1085-01	8.9630+12	6.3713+12	1.6294-02
7.8195+01	6.2712+10	4.9038+12	2.7133-02	6.5086-01	1.0006+13	6.5126+12	1.6253-02
7.1277+01	7.0819+10	5.0754+12	2.6038-02	5.9574-01	1.0916+13	6.5031+12	1.5759-02
6.5241+01	7.8207+10	5.1023+12	2.7364-02	5.4516-01	1.2535+13	6.8338+12	1.5586-02
5.7501+01	8.8097+10	5.1321+12	1.9670-02	4.9898-01	1.3725+13	6.8486+12	1.5046-02
4.9256+01	1.0675+11	5.2578+12	1.9932-02	4.5687-01	1.5374+13	7.0240+12	1.5197-02
4.2503+01	1.2656+11	5.3918+12	2.0103-02	4.1854-01	1.7416+13	7.2891+12	1.4592-02
3.7211+01	1.4280+11	5.5371+12	2.0327-02	3.8376-01	1.9308+13	7.4098+12	1.4772-02
3.2782+01	1.6428+11	5.3853+12	2.1147-02	3.5249-01	2.1816+13	7.6999+12	1.4189-02
2.9100+01	1.8689+11	5.3221+12	2.1609-02	3.2368-01	2.4853+13	8.0445+12	1.3584-02
2.6004+01	2.0674+11	5.3239+12	2.2045-02	2.9695-01	2.9186+13	8.6669+12	1.2510-02
2.3378+01	2.3263+11	5.4383+12	2.2286-02	2.7216-01	3.3152+13	9.0227+12	1.1676-02
2.1151+01	2.5934+11	5.3956+12	2.2832-02	2.4973-01	3.8190+13	9.5371+12	1.0916-02
1.9193+01	2.8913+11	5.5492+12	2.2765-02	2.2955-01	4.5632+13	1.0475+13	9.9743-03
1.7509+01	3.1543+11	5.5229+12	2.3229-02	2.1118-01	5.7896+13	1.2226+13	8.2865-03
1.6038+01	3.4909+11	5.5987+12	2.3431-02	1.9410-01	7.2060+13	1.3987+13	8.0589-03
1.4454+01	3.9640+11	5.7296+12	1.9206-02	1.7817-01	9.4082+13	1.6763+13	7.2684-03
1.2656+01	4.4465+11	5.3840+12	2.0264-02	1.6359-01	1.2300+14	2.0121+13	6.6851-03
1.1475+01	4.7271+11	5.4243+12	2.0556-02	1.5034-01	1.6182+14	2.4328+13	6.1328-03
1.0520+01	5.3978+11	5.5705+12	2.0536-02	1.3821-01	2.1131+14	2.9205+13	5.7130-03
9.5309+00	5.8905+11	5.4963+12	2.1019-02	1.2704-01	2.8122+14	3.5726+13	5.2871-03
8.4773+00	6.6922+11	5.6731+12	2.1143-02	1.1678-01	3.6500+14	4.2625+13	4.9699-03
7.7359+00	7.1369+11	5.5211+12	2.1722-02	1.0729-01	4.6553+14	4.9947+13	4.6399-03
7.0678+00	7.7885+11	5.5204+12	2.2074-02	9.8551-02	5.9384+14	5.8524+13	4.4034-03
6.4315+00	8.9768+11	5.7734+12	1.9043-02	9.0534-02	7.0975+14	6.4257+13	4.2094-03
5.7652+00	9.8512+11	5.6991+12	1.9465-02	8.3112-02	8.3196+14	6.9146+13	4.0379-03
5.2316+00	1.0785+12	5.6424+12	2.0006-02	7.6341-02	9.5475+14	7.2887+13	3.9815-03
4.7536+00	1.1939+12	5.6757+12	2.0193-02	7.0206-02	1.1245+15	7.8947+13	3.8540-03
4.3387+00	1.3274+12	5.7590+12	2.0409-02	6.4570-02	1.2728+15	8.2134+13	3.7822-03
3.9756+00	1.4681+12	5.5982+12	2.1007-02	5.9387-02	1.4106+15	8.3771+13	3.7304-03
3.6199+00	1.5766+12	5.7070+12	1.8765-02	5.4576-02	1.5413+15	8.4117+13	3.6583-03
3.2771+00	1.7519+12	5.7412+12	1.9072-02	5.0130-02	1.6977+15	8.5106+13	3.6619-03
2.9808+00	1.9775+12	5.8945+12	1.9065-02	4.6046-02	1.8386+15	8.4661+13	3.6394-03
2.7230+00	2.1463+12	5.8442+12	1.9569-02				

INFINITE MEDIUM GRAPHITE SPECTRUM

7/22/66 003(80) RE35.6 0 DEGREES BF3

(COMPUTED 1/10/67)

ENERGY (EV)	N(E)	E*N(E)	DELTA(N)/N	ENERGY (EV)	N(E)	E*N(E)	DELTA(N)/N
6.0082+01	5.2642+10	4.1677+12	1.0224-02	1.2657-01	2.3372+14	2.9582+13	4.1114-03
5.4176+01	7.8041+10	4.2279+12	1.0842-02	1.1514-01	3.1267+14	3.6001+13	3.9403-03
3.9073+01	1.1156+11	4.3589+12	1.1305-02	1.0487-01	4.1274+14	4.3285+13	3.6162-03
2.9506+01	1.4956+11	4.4071+12	1.1817-02	9.5669-02	5.2130+14	4.9872+13	3.4550-03
2.0067+01	1.9122+11	4.4109+12	1.2324-02	8.7459-02	6.2278+14	5.4468+13	3.3446-03
1.0527+01	2.4417+11	4.5238+12	1.2689-02	8.0127-02	7.2594+14	5.8160+13	3.2946-03
1.3266+01	3.0260+11	4.6621+12	1.2936-02	7.3573-02	8.4238+14	6.1977+13	3.2919-03
1.2704+01	3.6223+11	4.4747+12	1.3586-02	6.7357-02	9.8545+14	6.6377+13	2.3959-03
1.0772+01	4.1.49+11	4.5080+12	1.3887-02	6.1483-02	1.1060+15	6.7998+13	3.3048-03
9.2501+00	4.9668+11	4.5381+12	1.4183-02	5.6297-02	1.2264+15	6.9043+13	3.3128-03
8.0828+00	5.5975+11	4.4942+12	1.4651-02	5.1447-02	1.3535+15	6.9533+13	2.3804-03
7.0347+00	6.3524+11	4.6164+12	1.4797-02	4.6943-02	1.4910+15	6.9994+13	2.3321-03
6.2142+00	7.0166+11	4.7269+12	1.4943-02	4.2991-02	1.6018+15	6.8861+13	3.0130-03
5.5294+00	8.4356+11	4.6644+12	1.5325-02	3.9320-02	1.7119+15	6.7313+13	2.9526-03
4.9518+00	9.3492+11	4.6543+12	1.5654-02	3.5933-02	1.7849+15	6.4136+13	3.0390-03
4.4632+00	1.0355+12	4.7077+12	1.5857-02	3.2957-02	1.8412+15	6.0681+13	3.1859-03
4.0383+00	1.1456+12	4.6264+12	1.6282-02	3.0206-02	1.8919+15	5.7145+13	3.1398-03
3.6736+00	1.2710+12	4.6693+12	1.6394-02	2.7570-02	1.9331+15	5.3406+13	3.2723-03
3.3061+00	1.3672+12	4.5804+12	1.6773-02	2.5341-02	1.9763+15	5.0081+13	3.4162-03
2.9557+00	1.6415+12	4.8514+12	1.1796-02	2.3205-02	1.9660+15	4.5622+13	3.6341-03
2.6202+00	1.9054+12	4.8020+12	1.2223-02	2.1252-02	1.9168+15	4.0735+13	3.7412-03
2.1743+00	2.2129+12	4.8115+12	1.2527-02	1.9466-02	1.8879+15	3.6751+13	3.8965-03
1.9954+00	2.6275+12	4.9991+12	1.2567-02	1.7839-02	1.8439+15	3.2893+13	4.1388-03
1.8670+00	3.0213+12	5.0383+12	1.2800-02	1.6353-02	1.8226+15	2.9805+13	4.4271-03
1.4784+00	3.4472+12	5.0964+12	1.2969-02	1.4999-02	1.8026+15	2.7037+13	4.5563-03
1.3194+00	3.8727+12	5.1096+12	1.3270-02	1.3765-02	1.7299+15	2.3812+13	4.9202-03
1.1849+00	4.2543+12	5.0765+12	1.3517-02	1.2643-02	1.6792+15	2.1230+13	5.1262-03
1.0699+00	4.7379+12	5.0691+12	1.3796-02	1.1597-02	1.6025+15	1.8585+13	5.4444-03
9.7073-01	5.3122+12	5.2247+12	1.3770-02	1.0624-02	1.5860+15	1.6850+13	5.7078-03
8.8472-01	5.7725+12	5.1070+12	1.4057-02	9.7440-03	1.4845+15	1.4465+13	6.2751-03
8.0971-01	6.4 09+12	5.2476+12	1.4003-02	8.9465-03	1.3347+15	1.1941+13	6.7053-03
7.4965-01	7.2210+12	5.2545+12	1.1521-02	8.2062-03	1.2443+15	1.0211+13	7.1257-03
6.9685-01	8.3056+12	5.3725+12	1.1572-02	7.5220-03	1.1402+15	8.5777+12	7.6340-03
6.7783-01	9.3636+12	5.4105+12	1.1732-02	6.9054-03	1.1420+15	7.8460+12	8.1173-03
5.1934-01	1.0762+13	5.6412+12	1.1710-02	6.3509-03	1.0697+15	6.7936+12	8.9379-03
4.6947-01	1.2241+13	5.7466+12	1.1790-02	5.8387-03	1.0217+15	5.9665+12	9.5741-03
4.2654-01	1.3548+13	5.9067+12	1.1894-02	5.3653-03	9.7569+14	5.2349+12	1.0300-02
3.8943-01	1.5707+13	6.1169+12	1.1874-02	4.9298-03	9.9050+14	4.8829+12	1.0756-02
3.5260-01	1.8033+13	6.3564+12	1.0320-02	4.5305-03	9.7293+14	4.4079+12	1.1330-02
3.1747-01	2.1022+13	6.7690+12	1.0179-02	4.1646-03	9.2762+14	3.8632+12	1.2419-02
2.8485-01	2.4732+13	7.1724+12	1.0040-02	3.8246-03	9.0413+14	3.4579+12	1.2921-02
2.6295-01	2.6729+13	7.5544+12	8.8323-03	3.5096-03	8.8791+14	3.1162+12	1.3740-02
2.3484-01	3.4402+13	8.2654+12	8.4966-03	3.2232-03	8.2845+14	2.6703+12	1.5088-02
2.1925-01	4.2654+13	9.3081+12	7.3419-03	2.9627-03	8.2145+14	2.4337+12	1.5100-02
2.0038-01	5.4143+13	1.0849+13	6.8415-03	2.7223-03	7.9666+14	2.1715+12	1.7344-02
1.8404-01	6.9710+13	1.2829+13	6.3383-03	2.5008-03	7.7574+14	1.9409+12	1.8601-02
1.6826-01	9.2910+13	1.5567+13	5.3551-03	2.2972-03	7.1294+14	1.6379+12	2.0961-02
1.5496-01	1.2582+14	1.9247+13	4.8610-03	2.1097-03	7.2391+14	1.5272+12	2.2189-02
1.3916-01	1.7019+14	2.3679+13	4.4767-03	1.9376-03	6.9608+14	1.3374+12	2.5155-02

INFINITE MEDIUM GRAPHITE SPECTRUM

7/26/66 004(10) R=35.6 90 DEGREES BF3

(COMPUTED 1/10/67)

ENERGY (EV)	N(E)	E*N(E)	DELTA(N)/N	ENERGY (EV)	N(E)	E*N(E)	DELTA(N)/N
9.5521+02	3.0155+09	2.8654+12	2.5280-02	2.5367+00	1.8398+12	4.6669+12	2.0969-02
7.3442+02	4.2213+09	2.9309+12	2.5626-02	2.3163+00	1.9243+12	4.4572+12	2.0045-02
5.6494+02	5.2819+09	3.0588+12	2.4604-02	2.1067+00	2.2429+12	4.7252+12	1.9657-02
4.2659+02	7.3171+09	3.2524+12	2.5359-02	1.9246+00	2.4491+12	4.7135+12	2.0153-02
3.4362+02	1.0134+10	3.5126+12	2.4910-02	1.7655+00	2.7590+12	4.8692+12	2.0010-02
2.8770+02	1.1488+10	3.4405+12	2.5489-02	1.6146+00	2.8946+12	4.6742+12	1.9213-02
2.4153+02	1.4240+10	3.4394+12	2.6130-02	1.4727+00	3.2263+12	4.7513+12	1.9325-02
2.0665+02	1.6903+10	3.4930+12	2.6270-02	1.3483+00	3.5716+12	4.8156+12	1.9503-02
1.7766+02	2.0662+10	3.6785+12	2.6082-02	1.2321+00	4.0586+12	5.0006+12	1.8367-02
1.5304+02	2.5006+10	3.8577+12	2.6696-02	1.1238+00	4.4027+12	4.9479+12	1.8600-02
1.3342+02	2.8719+10	3.8451+12	2.7353-02	1.0290+00	4.6339+12	4.7683+12	1.9308-02
1.2093+02	3.3486+10	3.8523+12	2.7726-02	9.4095-01	5.2576+12	4.9471+12	1.9033-02
1.0794+02	3.9165+10	3.8900+12	2.7994-02	8.5940-01	5.8273+12	5.0080+12	1.9064-02
9.6831+01	4.5925+10	3.9669+12	2.7321-02	7.8806-01	6.2208+12	4.9023+12	1.8429-02
8.7329+01	5.3905+10	3.7642+12	2.8193-02	7.2205-01	6.9431+12	5.0133+12	1.7402-02
7.9430+01	6.3736+10	3.8713+12	2.8827-02	6.6111-01	7.7446+12	5.1200+12	1.7421-02
7.2404+01	7.3852+10	3.8662+12	3.0076-02	6.0512-01	8.3034+12	5.0271+12	1.6475-02
6.5271+01	8.6573+10	3.7359+12	3.0299-02	5.5374-01	9.8761+12	5.4648+12	1.6488-02
5.9611+01	9.8938+10	3.8907+12	3.1347-02	5.0681-01	1.0974+13	5.5617+12	1.5885-02
5.4034+01	7.5442+10	3.7747+12	2.2195-02	4.6403-01	1.1972+13	5.5553+12	1.6245-02
4.9275+01	9.2952+10	4.0021+12	2.2187-02	4.2507-01	1.3496+13	5.7367+12	1.5554-02
4.5079+01	1.0242+11	3.8715+12	2.3033-02	3.8969-01	1.5368+13	5.9886+12	1.5409-02
4.1300+01	1.2235+11	4.0744+12	2.2996-02	3.5784-01	1.7115+13	6.1244+12	1.5084-02
3.7859+01	1.3791+11	4.0764+12	2.3503-02	3.2944-01	1.9546+13	6.4199+12	1.4423-02
3.4715+01	1.6599+11	4.1206+12	2.3751-02	3.0109-01	2.2665+13	6.8242+12	1.3426-02
3.1747+01	1.7668+11	4.0531+12	2.4395-02	2.7569-01	2.6067+13	7.1863+12	1.2476-02
2.9105+01	1.9625+11	4.1910+12	2.4410-02	2.5272-01	3.0590+13	7.7308+12	1.1439-02
2.6696+01	2.0302+11	3.9697+12	2.5616-02	2.3212-01	3.6343+13	8.4360+12	1.0565-02
2.4486+01	2.3449+11	4.1705+12	2.5491-02	2.1345-01	4.5386+13	9.6876+12	9.4924-03
2.2491+01	2.6548+11	4.3413+12	2.5074-02	1.9614-01	5.7843+13	1.1345+13	8.4904-03
2.0702+01	2.9573+11	4.3126+12	2.0995-02	1.8008-01	7.6737+13	1.3819+13	7.5980-03
1.9039+01	3.2437+11	4.2034+12	2.1627-02	1.6539-01	9.9806+13	1.6507+13	7.0078-03
1.7556+01	3.6865+11	4.1572+12	2.2263-02	1.5205-01	1.2977+14	1.9732+13	6.4531-03
1.6183+01	4.1247+11	4.3239+12	2.2044-02	1.3985-01	1.7448+14	2.4401+13	5.8051-03
1.4763+01	4.5976+11	4.3579+12	2.2506-02	1.2862-01	2.3070+14	2.9672+13	5.4746-03
1.3613+01	5.1551+11	4.4392+12	2.2679-02	1.1810-01	3.0266+14	3.5745+13	5.0383-03
1.2581+01	5.4370+11	4.2724+12	2.3501-02	1.0839-01	3.9101+14	4.2382+13	4.7567-03
1.1598+01	6.0596+11	4.3623+12	2.3512-02	9.9605-02	4.9348+14	4.9153+13	4.5527-03
1.0631+01	6.8291+11	4.3309+12	2.0878-02	9.1530-02	6.0227+14	5.5125+13	4.3000-03
9.8766+00	7.6616+11	4.5024+12	2.0763-02	8.4055-02	7.1156+14	5.9810+13	4.1049-03
9.1243+00	8.4601+11	4.4959+12	2.1092-02	7.7232-02	8.3052+14	6.4143+13	4.0146-03
8.4289+00	9.0202+11	4.3554+12	2.1681-02	7.1040-02	9.6962+14	6.8842+13	3.8909-03
7.7872+00	1.0105+12	4.4536+12	2.2004-02	6.5353-02	1.1060+15	7.2281+13	3.8072-03
7.1964+00	1.1130+12	4.5150+12	2.2230-02	6.0048-02	1.2322+15	7.3993+13	3.7045-03
6.6771+00	1.2023+12	4.4210+12	2.0329-02	5.5130-02	1.3463+15	7.4221+13	3.6841-03
6.1889+00	1.3624+12	4.5354+12	2.0373-02	5.0652-02	1.4938+15	7.5662+13	3.6681-03
5.7279+00	1.5435+12	4.6341+12	2.0479-02	4.6534-02	1.6212+15	7.5443+13	3.6399-03
2.7560+00	1.0892+12	4.6723+12	2.0759-02				

INFINITE MEDIUM GRAPHITE SPECTRUM

7/22/66 003(80) R=35.6 0 DEGREES BF3

(COMPUTED 1/10/67)

ENERGY (EV)	N(E)	E*N(E)	DELTA(N)/N	ENERGY (EV)	N(E)	E*N(E)	DELTA(N)/N
6.0082+01	5.2[illegible]+10	3.1677+12	1.0234-02	1.2657-01	2.3372+14	2.9582+13	4.1114-03
5.4476+01	7.6[illegible]+10	4.2279+12	1.0842-02	1.1514-01	3.1267+14	3.6001+13	3.4403-03
3.9073+01	1.1150+11	4.3589+12	1.1305-02	1.0487-01	4.1274+14	4.3245+13	3.4162-03
2.9566+01	1.4[illegible]+11	4.4071+12	1.1817-02	9.5669-02	5.2130+14	4.9872+13	3.4450-03
2.0867+01	1.9122+11	4.4109+12	1.2324-02	8.7459-02	6.2278+14	5.4468+13	3.3446-03
1.0527+01	2.4[illegible]+11	4.5236+12	1.2839-02	8.0127-02	7.2594+14	5.8160+13	3.2846-03
1.5206+01	3.0[illegible]+11	4.6621+12	1.2936-02	7.3573-02	8.4238+14	6.1977+13	3.2419-03
1.2704+01	3.5223+11	4.4747+12	1.3596-02	6.7357-02	9.8545+14	6.6377+13	2.3959-03
1.0772+01	4.1[illegible]+11	4.5060+12	1.3647-02	6.1483-02	1.1060+15	6.7998+13	3.2042-03
9.2501+00	4.9[illegible]+11	4.5361+12	1.4143-02	5.6297-02	1.2254+15	6.9043+13	3.2128-03
8.0208+00	5.5[illegible]+11	4.4942+12	1.4651-02	5.1447-02	1.3535+15	6.9633+13	2.3804-03
7.0347+00	6.3[illegible]+11	4.6164+12	1.4737-02	4.6943-02	1.4910+15	6.9994+13	2.3321-03
6.2142+00	7.[illegible]+11	4.7269+12	1.4943-02	4.2991-02	1.6018+15	6.8861+13	3.0130-03
5.5294+00	8.[illegible]+11	4.6644+12	1.5325-02	3.9320-02	1.7119+15	6.7313+13	2.9526-03
4.9518+00	9.3[illegible]+11	4.6543+12	1.5654-02	3.5933-02	1.7949+15	6.4136+13	3.0590-03
4.4002+00	1.0[illegible]+12	4.7077+12	1.5857-02	3.2957-02	1.8412+15	6.0681+13	3.1459-03
4.0383+00	1.1[illegible]+12	4.6284+12	1.6232-02	3.0206-02	1.8919+15	5.7146+13	3.1498-03
3.6736+00	1.2710+12	4.6693+12	1.6334-02	2.7570-02	1.9301+15	5.3206+13	3.1723-03
3.3561+00	1.3[illegible]+12	4.5884+12	1.6773-02	2.5341-02	1.9763+15	5.0081+13	3.4162-03
3.0957+00	1.4[illegible]+12	4.4516+12	1.7196-02	2.3205-02	1.9660+15	4.5622+13	3.6341-03
2.8262+00	1.5[illegible]+12	4.4020+12	1.2225-02	2.1252-02	1.9168+15	4.0735+13	3.7412-03
2.1743+00	2.2129+12	4.8115+12	1.2527-02	1.9466-02	1.8879+15	3.6761+13	3.9966-03
1.8354+00	2.6[illegible]+12	4.9991+12	1.2567-02	1.7839-02	1.8439+15	3.2893+13	4.1348-03
1.6676+00	3.0[illegible]+12	5.0383+12	1.2803-02	1.6353-02	1.8226+15	2.9805+13	4.4271-03
1.4784+00	3.4[illegible]+12	5.0964+12	1.2369-02	1.4999-02	1.8026+15	2.7037+13	4.6563-03
1.3194+00	3.8727+12	5.1096+12	1.3270-02	1.3765-02	1.7299+15	2.3812+13	4.9302-03
1.1849+00	4.2[illegible]+12	5.0765+12	1.3517-02	1.2643-02	1.6792+15	2.1230+13	5.1262-03
1.0699+00	4.7[illegible]+12	5.0691+12	1.3796-02	1.1597-02	1.6025+15	1.8585+13	5.3444-03
9.7873-01	5.3[illegible]+12	5.2247+12	1.3770-02	1.0624-02	1.5866+15	1.6850+13	5.7078-03
8.8472-01	5.7725+12	5.1070+12	1.4057-02	9.7440-03	1.4845+15	1.4465+13	6.2751-03
8.0971-01	6.4[illegible]+12	5.2476+12	1.4003-02	8.9465-03	1.3347+15	1.1941+13	6.7053-03
7.2905-01	7.2[illegible]+12	5.2645+12	1.1521-02	8.2062-03	1.2443+15	1.0211+13	7.1257-03
6.4685-01	8.3[illegible]+12	5.3725+12	1.1572-02	7.5220-03	1.1802+15	8.8777+12	7.6340-03
5.7783-01	9.3[illegible]+12	5.4105+12	1.1732-02	6.9054-03	1.1420+15	7.8860+12	8.3173-03
5.1934-01	1.0[illegible]+13	5.6412+12	1.1710-02	6.3509-03	1.0697+15	6.7936+12	8.9379-03
4.6947-01	1.2241+13	5.7456+12	1.1790-02	5.8387-03	1.0217+15	5.9655+12	9.6741-03
4.2854-01	1.3[illegible]+13	5.9067+12	1.1894-02	5.3653-03	9.7569+14	5.2349+12	1.0300-02
3.8943-01	1.5707+13	6.1109+12	1.1874-02	4.9298-03	9.9050+14	4.8828+12	1.0756-02
3.5260-01	1.8[illegible]+13	6.3584+12	1.0320-02	4.5305-03	9.7293+14	4.4078+12	1.1330-02
3.1747-01	2.1[illegible]+13	6.7690+12	1.0173-02	4.1646-03	9.2762+14	3.8633+12	1.2419-02
2.8365-01	2.4[illegible]+13	7.1724+12	1.0040-02	3.8246-03	9.0413+14	3.4579+12	1.3321-02
2.5295-01	2.8729+13	7.5544+12	8.8323-03	3.5096-03	8.9791+14	3.1162+12	1.3740-02
2.2484-01	3.4[illegible]+13	8.2654+12	9.4966-03	3.2232-03	8.2845+14	2.6703+12	1.5098-02
2.1925-01	4.2[illegible]+13	9.3081+12	7.3419-03	2.9627-03	8.2145+14	2.4337+12	1.5100-02
2.0036-01	5.4[illegible]+13	1.0849+13	6.8415-03	2.7223-03	7.8656+14	2.1415+12	1.7344-02
1.8404-01	6.9710+13	1.2829+13	6.3383-03	2.5008-03	7.7574+14	1.9400+12	1.8601-02
1.6820-01	9.2[illegible]+13	1.5567+13	5.3551-03	2.2972-03	7.1294+14	1.6374+12	2.0941-02
1.5298-01	1.2[illegible]+14	1.9247+13	4.8610-03	2.1097-03	7.2391+14	1.5272+12	2.2189-02
1.3916-01	1.7[illegible]+14	2.3879+13	4.4767-03	1.937[illegible]-03	4.[illegible]+14	1.3274+12	2.5155-02

INFINITE MEDIUM GRAPHITE SPECTRUM

7/26/66 004(10) R=35.6 90 DEGREES BF3

(COMPUTED 1/10/67)

ENERGY (EV)	N(E)	E*N(E)	DELTA(N)/N	ENERGY (EV)	N(E)	E*N(E)	DELTA(N)/N
9.5321+02	3.0155+09	2.8654+12	2.5290-02	2.5367+00	1.8398+12	4.6669+12	2.0969-02
7.0142+02	4.2213+09	2.9609+12	2.5626-02	2.3163+00	1.9243+12	4.4572+12	2.0045-02
5.[illegible]94+02	6.2319+09	3.3586+12	2.4604-02	2.1067+00	2.2429+12	4.7252+12	1.9657-02
4.2099+02	7.3171+09	3.2524+12	2.5359-02	1.9246+00	2.4491+12	4.7135+12	2.0153-02
3.4362+02	1.0134+10	3.5126+12	2.4910-02	1.7655+00	2.7540+12	4.8692+12	2.0010-02
2.8700+02	1.1988+10	3.4405+12	2.5480-02	1.6148+00	2.8946+12	4.6742+12	1.9213-02
2.4153+02	1.4240+10	3.4394+12	2.6130-02	1.4727+00	3.2263+12	4.7513+12	1.9325-02
2.0065+02	1.6993+10	3.4830+12	2.6270-02	1.3483+00	3.5716+12	4.8156+12	1.9503-02
1.7760+02	2.0062+10	3.5785+12	2.6082-02	1.2321+00	4.0586+12	5.0006+12	1.8367-02
1.5508+02	2.3886+10	3.6577+12	2.6696-02	1.1238+00	4.4027+12	4.9479+12	1.8600-02
1.3342+02	2.8719+10	3.8451+12	2.7353-02	1.0290+00	4.6339+12	4.7683+12	1.9308-02
1.2093+02	3.4206+10	3.6523+12	2.7726-02	9.4095-01	5.2576+12	4.9471+12	1.8933-02
1.0794+02	3.4185+10	3.6900+12	2.7990-02	8.5940-01	5.8273+12	5.0080+12	1.8064-02
9.6931+01	4.0925+10	3.9669+12	2.7021-02	7.8806-01	6.2208+12	4.9023+12	1.8429-02
8.7529+01	4.3005+10	3.7642+12	2.8893-02	7.2205-01	6.9431+12	5.0133+12	1.7402-02
7.9430+01	4.8736+10	3.8713+12	2.8827-02	6.6111-01	7.7446+12	5.1200+12	1.7421-02
7.2400+01	5.0962+10	3.6602+12	3.0076-02	6.0512-01	8.9034+12	5.3271+12	1.6475-02
6.5271+01	5.6173+10	3.7359+12	3.0299-02	5.5374-01	9.8761+12	5.4698+12	1.6488-02
5.9511+01	6.0696+10	3.8907+12	2.1387-02	5.0681-01	1.0974+13	5.5617+12	1.5885-02
5.4034+01	7.5442+10	3.7747+12	2.2195-02	4.6403-01	1.1972+13	5.5553+12	1.6245-02
4.9275+01	9.2462+10	4.0021+12	2.2187-02	4.2507-01	1.3496+13	5.7367+12	1.5554-02
4.7799+01	1.0242+11	3.8715+12	2.3033-02	3.8969-01	1.5368+13	5.9886+12	1.5469-02
3.9500+01	1.2235+11	4.0744+12	2.2946-02	3.5784-01	1.7115+13	6.1244+12	1.5084-02
2.9359+01	1.3791+11	4.0764+12	2.3503-02	3.2944-01	1.9546+13	6.4194+12	1.4423-02
2.6615+01	1.5599+11	4.1206+12	2.3751-02	3.0109-01	2.2665+13	6.8242+12	1.3426-02
2.3747+01	1.7068+11	4.0531+12	2.4398-02	2.7569-01	2.6067+13	7.1863+12	1.2476-02
2.1+05+01	1.9525+11	4.1910+12	2.4410-02	2.5272-01	3.0590+13	7.7308+12	1.1439-02
1.9196+01	2.1032+11	3.9697+12	2.5616-02	2.3212-01	3.6343+13	8.4363+12	1.0565-02
1.7760+01	2.3449+11	4.1706+12	2.5471-02	2.1345-01	4.5386+13	9.6876+12	9.4924-03
1.6291+01	2.6648+11	4.3413+12	2.5074-02	1.9614-01	5.7843+13	1.1345+13	8.4904-03
1.4+82+01	2.9373+11	4.3126+12	2.0995-02	1.8008-01	7.6737+13	1.3819+13	7.5980-03
1.3039+01	3.2237+11	4.2034+12	2.1627-02	1.6539-01	9.9806+13	1.6507+13	7.0078-03
1.1956+01	3.5065+11	4.1572+12	2.2263-02	1.5205-01	1.2977+14	1.9732+13	6.4531-03
1.0+63+01	4.1247+11	4.3239+12	2.2044-02	1.3985-01	1.7448+14	2.4401+13	5.9051-03
9.4763+00	4.5976+11	4.3579+12	2.2506-02	1.2862-01	2.3070+14	2.9672+13	5.4746-03
8.6113+00	5.1651+11	4.4392+12	2.2679-02	1.1810-01	3.0266+14	3.5745+13	5.0383-03
7.8581+00	5.4370+11	4.2724+12	2.3501-02	1.0839-01	3.9101+14	4.2382+13	4.7567-03
7.1398+00	6.0596+11	4.3623+12	2.3512-02	9.9605-02	4.9348+14	4.9153+13	4.5527-03
6.5331+00	6.6291+11	4.3309+12	2.0878-02	9.1530-02	6.0227+14	5.5125+13	4.3000-03
5.8766+00	7.3616+11	4.5024+12	2.0763-02	8.4055-02	7.1156+14	5.9810+13	4.1049-03
5.3143+00	8.4601+11	4.4959+12	2.1092-02	7.7232-02	8.3052+14	6.4143+13	4.0146-03
4.8289+00	9.0202+11	4.3558+12	2.1881-02	7.1040-02	9.6962+14	6.8882+13	3.8909-03
4.4372+00	1.0105+12	4.4536+12	2.2004-02	6.5353-02	1.1060+15	7.2281+13	3.8072-03
4.0364+00	1.1180+12	4.5150+12	2.2230-02	6.0048-02	1.2322+15	7.3993+13	3.7045-03
3.6771+00	1.2023+12	4.4210+12	2.0329-02	5.5130-02	1.3463+15	7.4221+13	3.6841-03
3.3289+00	1.3624+12	4.5354+12	2.0373-02	5.0652-02	1.4938+15	7.5662+13	3.6681-03
3.0279+00	1.5405+12	4.6341+12	2.0479-02	4.6534-02	1.6212+15	7.5443+13	3.6399-03
2.7560+00	1.6892+12	4.6723+12	2.0759-02				

INFINITE MEDIUM GRAPHITE SPECTRUM

7/20/66 004:80) R=35.0 90 DEGREES BF3

(COMPUTED 1/10/67)

ENERGY (EV)	N(E)	E*N(E)	DELTA(N)/N	ENERGY (EV)	N(E)	E*N(E)	DELTA(N)/N
6.1346+01	3.7416+10	3.0437+12	1.1349-02	1.2815-01	1.9027+14	2.4383+13	4.2772-03
5.0032+01	5.6118+10	3.0883+12	1.2015-02	1.1663-01	2.5626+14	2.9888+13	3.9772-03
3.9690+01	7.9[illegible]+10	3.1572+12	1.2595-02	1.0627-01	3.3695+14	3.5807+13	3.7514-03
2.9972+01	1.0943+11	3.2798+12	1.2987-02	9.6983-02	4.2544+14	4.1261+13	3.5941-03
2.0431+01	1.5[illegible]2+11	3.2667+12	1.3614-02	8.8681-02	5.2199+14	4.6291+13	3.4507-03
1.8820+01	1.7765+11	3.3320+12	1.4055-02	8.1270-02	6.1368+14	4.9874+13	3.3549-03
1.5446+01	2.2[illegible]78+11	3.4566+12	1.4201-02	7.4638-02	7.1867+14	5.3640+13	3.2997-03
1.2905+01	2.6613+11	3.4344+12	1.4656-02	6.8340-02	8.3991+14	5.7399+13	3.0401-03
1.0942+01	3.0[illegible]9+11	3.3654+12	1.5161-02	6.2393-02	9.5553+14	5.9618+13	3.0330-03
9.3901+00	3.6705+11	3.4409+12	1.5473-02	5.7136-02	1.0531+15	6.0172+13	3.0516-03
8.1655+00	4.2911+11	3.4996+12	1.5812-02	5.2219-02	1.1658+15	6.0879+13	2.9060-03
7.1458+00	4.8725+11	3.4818+12	1.6146-02	4.7649-02	1.2883+15	6.1387+13	2.9540-03
6.3123+00	5.5[illegible]79+11	3.5335+12	1.6382-02	4.3641-02	1.3878+15	6.0564+13	3.0284-03
5.5167+00	6.3[illegible]80+11	3.5767+12	1.6606-02	3.9917-02	1.4894+15	5.9452+13	2.9635-03
5.0000+00	7.0[illegible]67+11	3.5495+12	1.6984-02	3.6480-02	1.5575+15	5.6816+13	3.0748-03
4.5307+00	8.0148+11	3.6313+12	1.7089-02	3.3461-02	1.6056+15	5.3726+13	3.1931-03
4.1321+00	8.9127+11	3.6561+12	1.7322-02	3.0669-02	1.6615+15	5.0955+13	3.1867-03
3.7315+00	9.7134+11	3.6247+12	1.7642-02	2.8095-02	1.7108+15	4.8065+13	3.3539-03
3.4092+00	1.0[illegible]15+12	3.5846+12	1.8036-02	2.5732-02	1.7495+15	4.5019+13	3.3987-03
3.0024+00	1.2499+12	3.7527+12	1.2761-02	2.3563-02	1.7552+15	4.1357+13	3.6037-03
2.5000+00	1.4558+12	3.7217+12	1.3122-02	2.1581-02	1.7291+15	3.7316+13	3.6938-03
2.2689+00	1.7126+12	3.7824+12	1.3403-02	1.9768-02	1.6889+15	3.3387+13	3.9622-03
1.9253+00	1.9[illegible]49+12	3.7830+12	1.3775-02	1.8116-02	1.6717+15	3.0285+13	4.0718-03
1.6538+00	2.2[illegible]74+12	3.8405+12	1.3911-02	1.6608-02	1.6219+15	2.6936+13	4.3975-03
1.4017+00	2.5[illegible]08+12	3.7554+12	1.4361-02	1.5234-02	1.5767+15	2.4020+13	4.5811-03
1.1402+00	2.9171+12	3.9095+12	1.4372-02	1.3980-02	1.4973+15	2.0933+13	4.9711-03
1.0235+00	3.3510+12	4.0329+12	1.4379-02	1.2841-02	1.4403+15	1.8494+13	5.1944-03
1.0367+00	3.8523+12	4.0124+12	1.4738-02	1.1778-02	1.3916+15	1.6390+13	5.4769-03
9.5598-01	3.9[illegible]85+12	3.9109+12	1.5136-02	1.0790-02	1.3594+15	1.4668+13	5.7937-03
8.9[illegible]67-01	4.5598+12	4.0976+12	1.4876-02	9.8962-03	1.2978+15	1.2843+13	6.3343-03
8.2248-01	4.9[illegible]06+12	4.0471+12	1.5133-02	9.0866-03	1.1879+15	1.0794+13	6.7050-03
7.[illegible]54-01	5.4091+12	4.0057+12	1.2554-02	8.3349-03	1.1018+15	9.1833+12	7.1484-03
6.8704-01	6.2[illegible]81+12	4.1184+12	1.2562-02	7.6401-03	1.0410+15	7.9535+12	7.6635-03
5.[illegible]092-01	7.3[illegible]26+12	4.2978+12	1.2499-02	7.0138-03	9.9487+14	6.9778+12	8.4098-03
5.2750-01	8.3151+12	4.3862+12	1.2576-02	6.4503-03	9.2681+14	5.9782+12	9.1133-03
4.7682-01	9.4323+12	4.4975+12	1.2678-02	5.9304-03	8.7315+14	5.4154+12	9.5776-03
4.[illegible]320-01	1.0[illegible]05+13	4.5941+12	1.2758-02	5.4499-03	8.5132+14	4.6396+12	1.0509-02
3.[illegible]946-01	1.2243+13	4.8435+12	1.2650-02	5.0076-03	8.4677+14	4.2403+12	1.1106-02
3.[illegible]795-01	1.3[illegible]29+13	4.9359+12	1.1035-02	4.6020-03	8.0722+14	3.7148+12	1.1981-02
3.[illegible]208-01	1.[illegible]528+13	5.2589+12	1.0974-02	4.2304-03	7.7861+14	3.2938+12	1.2916-02
2.[illegible]277-01	1.9160+13	5.6153+12	1.0802-02	3.8905-03	7.6894+14	2.9916+12	1.3729-02
2.[illegible]020-01	2.[illegible]582+13	6.0124+12	9.3925-03	3.5751-03	7.3165+14	2.6157+12	1.4656-02
2.[illegible]463-01	2.[illegible]06+13	6.5185+12	9.0699-03	3.2830-03	7.0716+14	2.3216+12	1.5945-02
2.2164-01	3.[illegible]11+13	7.4053+12	7.8125-03	3.0173-03	6.8249+14	2.0593+12	1.7264-02
2.[illegible]250-01	4.[illegible]243+13	8.6352+12	7.2805-03	2.7722-03	6.6612+14	1.8466+12	1.8581-02
1.[illegible]500-01	5.[illegible]704+13	1.0376+13	6.6754-03	2.5463-03	6.3814+14	1.6249+12	2.0391-02
1.7089-01	7.[illegible]212+13	1.2623+13	5.6456-03	2.3389-03	5.9513+14	1.3920+12	2.2993-02
1.[illegible]70-01	1.[illegible]504+14	1.547[illegible]+13	5.1423-03	2.1481-03	5.6963+14	1.2236+12	2.5377-02
1.4[illegible]86-01	1.[illegible]50+14	1.9500+13	4.6626-03	1.9742-03	5.6346+14	1.1124+12	2.7196-02

INFINITE MEDIUM GRAPHITE SPECTRUM

7/22/66 001(10) R=50.8 0 DEGREES BF3

(COMPUTED 1/10/67)

ENERGY (EV)	N(E)	E*N(E)	DELTA(N)/N	ENERGY (EV)	N(E)	E*N(E)	DELTA(N)/N
9.2987+02	7.1338+03	6.6335+11	3.9933-02	2.7068+00	5.9189+11	1.6021+12	2.6188-02
8.6940+02	1.0482+09	7.1947+11	3.8335-02	2.4824+00	6.2736+11	1.5574+12	2.7262-02
5.2740+02	1.4455+09	7.6236+11	3.9379-02	2.2667+00	6.9643+11	1.5786+12	2.5189-02
4.1784+02	1.9018+09	7.9466+11	3.7159-02	2.0616+00	7.7471+11	1.5971+12	2.5483-02
3.3420+02	2.5104+09	8.5152+11	3.7798-02	1.8835+00	8.6412+11	1.6276+12	2.5484-02
2.6085+02	3.0259+09	8.4982+11	3.7509-02	1.7279+00	9.1234+11	1.5764+12	2.6341-02
2.3636+02	3.5579+09	8.4095+11	3.9209-02	1.5804+00	1.0456+12	1.6525+12	2.4126-02
2.0164+02	4.4503+09	8.9735+11	3.8419-02	1.4412+00	1.1710+12	1.6876+12	2.4185-02
1.7405+02	5.0990+09	8.8747+11	3.9682-02	1.3195+00	1.3025+12	1.7187+12	2.4375-02
1.5176+02	6.3755+09	9.2202+11	3.9807-02	1.2058+00	1.4425+12	1.7394+12	2.3147-02
1.3350+02	7.1956+09	9.6061+11	3.9185-02	1.0998+00	1.6425+12	1.8064+12	2.2940-02
1.1834+02	8.0319+09	1.0215+12	3.8667-02	1.0070+00	1.7639+12	1.7762+12	2.3587-02
1.0563+02	9.1353+09	9.6507+11	4.1127-02	9.2083-01	1.9950+12	1.8370+12	2.1901-02
9.4356+01	1.0499+10	9.9587+11	4.0827-02	8.4103-01	2.2229+12	1.8696+12	2.1965-02
8.5655+01	1.2330+10	1.0561+12	4.0775-02	7.7121-01	2.4398+12	1.8816+12	2.1985-02
7.7729+01	1.2834+10	9.9757+11	4.2427-02	7.0663-01	2.7382+12	1.9349+12	2.0888-02
7.0853+01	1.4008+10	9.9248+11	4.3351-02	6.4699-01	3.1010+12	2.0063+12	2.0716-02
6.4853+01	1.5434+10	1.0009+12	4.3589-02	5.9220-01	3.3424+12	1.9794+12	2.0089-02
5.9258+01	1.9011+10	1.0885+12	3.0145-02	5.4192-01	3.6675+12	1.9875+12	2.0403-02
4.8962+01	2.1590+10	1.0571+12	3.1405-02	4.9613-01	4.1148+12	2.0815+12	1.9688-02
4.2349+01	2.7137+10	1.1492+12	3.0795-02	4.5439-01	4.6995+12	2.1354+12	1.9496-02
3.8389+01	3.0537+10	1.1295+12	3.1763-02	4.1640-01	5.4122+12	2.2536+12	1.8507-02
3.2587+01	3.7530+10	1.2165+12	3.1238-02	3.8196-01	6.0963+12	2.3285+12	1.8528-02
2.8926+01	4.0710+10	1.1776+12	3.2349-02	3.5110-01	6.8502+12	2.4051+12	1.7879-02
2.5349+01	4.6539+10	1.2030+12	3.2758-02	3.2191-01	8.0229+12	2.5826+12	1.6372-02
2.3239+01	5.3165+10	1.2355+12	3.3054-02	2.9519-01	9.4569+12	2.7916+12	1.5552-02
2.1405+01	6.0416+10	1.2690+12	3.2790-02	2.7084-01	1.1098+13	3.0057+12	1.3928-02
1.9879+01	6.5390+10	1.2476+12	3.4077-02	2.4857-01	1.2863+13	3.1973+12	1.2972-02
1.7405+01	7.0959+10	1.2350+12	3.4714-02	2.2844-01	1.6442+13	3.7559+12	1.1286-02
1.5342+01	7.9106+10	1.2611+12	3.5122-02	2.1005-01	2.1561+13	4.5289+12	9.9272-03
1.4367+01	8.6974+10	1.2496+12	2.9041-02	1.9309-01	2.9216+13	5.6414+12	8.6254-03
1.2759+01	1.0431+11	1.3309+12	2.8557-02	1.7743-01	4.0528+13	7.1909+12	7.6919-03
1.1406+01	1.1838+11	1.3503+12	2.8923-02	1.6306-01	5.6391+13	9.1951+12	6.7280-03
1.0258+01	1.2763+11	1.3092+12	3.0132-02	1.4972-01	7.8906+13	1.1814+13	6.0019-03
9.2753+00	1.5353+11	1.4240+12	2.9047-02	1.3744-01	1.0868+14	1.4937+13	5.4412-03
8.4268+00	1.5629+11	1.3170+12	3.0937-02	1.2626-01	1.5028+14	1.8974+13	5.0302-03
7.6899+00	1.6034+11	1.4253+12	3.0369-02	1.1596-01	2.0213+14	2.3439+13	4.5758-03
7.0456+00	2.0430+11	1.4394+12	3.0737-02	1.0640-01	2.6621+14	2.8324+13	4.2858-03
6.3932+00	2.1789+11	1.3930+12	2.7274-02	9.7703-02	3.3730+14	3.2955+13	4.0828-03
5.7507+00	2.5439+11	1.4629+12	2.7315-02	8.9719-02	4.1419+14	3.7160+13	3.8487-03
5.2004+00	2.7473+11	1.4287+12	2.7987-02	8.2416-02	4.8670+14	4.0112+13	3.7406-03
4.7255+00	3.1200+11	1.4744+12	2.7923-02	7.5743-02	5.7001+14	4.3174+13	3.5991-03
4.3128+00	3.3323+11	1.4371+12	2.8864-02	6.9593-02	6.5795+14	4.6484+13	3.4943-03
3.9519+00	3.9096+11	1.5450+12	2.8270-02	6.3934-02	7.6864+14	4.9142+13	3.4055-03
3.5384+00	4.2142+11	1.5164+12	2.5956-02	5.8731-02	8.4937+14	4.9884+13	3.3682-03
3.2576+00	4.6037+11	1.5649+12	2.5714-02	5.3974-02	9.4232+14	5.0861+13	3.3257-03
2.9631+00	5.2194+11	1.5466+12	2.6558-02	4.9584-02	1.0468+15	5.1906+13	3.2693-03

INFINITE MEDIUM GRAPHITE SPECTRUM

7/22/66 001(80) R=50.8 0 DEGREES BF3

(COMPUTED 1/10/67)

ENERGY (EV)	.(E)	E*N(E)	DELTA(N)/N	ENERGY (EV)	N(E)	E*N(E)	DELTA(N)/N
7.9605+01	1.0276+10	8.1803+11	1.6366-02	1.2691-01	1.2180+14	1.5458+13	4.0020-03
5.3653+01	1.6490+10	8.8804+11	1.6693-02	1.1588-01	1.6636+14	1.9278+13	3.6914-03
3.4850+01	2.4494+10	9.5133+11	1.7056-02	1.0587-01	2.2186+14	2.3488+13	3.4477-03
2.9330+01	3.3106+10	9.7105+11	1.7785-02	9.6813-02	2.8336+14	2.7433+13	3.2803-03
2.2929+01	4.3538+10	1.0063+12	1.9211-02	8.8674-02	3.4825+14	3.0881+13	3.1451-03
1.8417+01	5.5810+10	1.0131+12	1.8955-02	8.1363-02	4.0948+14	3.3317+13	3.0542-03
1.5115+01	6.8492+10	1.0353+12	1.9339-02	7.4365-02	4.8672+14	3.6195+13	2.7894-03
1.2629+01	8.3961+10	1.0603+12	1.9634-02	6.7754-02	5.7575+14	3.9010+13	2.7533-03
1.0708+01	1.0110+11	1.0825+12	2.0085-02	6.1904-02	6.5752+14	4.0703+13	2.7364-03
9.1349+00	1.2298+11	1.1400+12	1.9994-02	5.6719-02	7.2816+14	4.1300+13	2.7442-03
7.9009+00	1.4216+11	1.1348+12	2.0594-02	5.1864-02	8.1491+14	4.2265+13	2.6019-03
6.9928+00	1.6342+11	1.1537+12	2.0864-02	4.7347-02	9.0091+14	4.2655+13	2.6436-03
6.1771+00	1.8685+11	1.1419+12	2.1410-02	4.3374-02	9.7390+14	4.2242+13	2.7056-03
5.4965+00	2.1074+11	1.1309+12	2.2126-02	3.9683-02	1.0512+15	4.1714+13	2.6388-03
4.9225+00	2.4233+11	1.1929+12	2.1821-02	3.6272-02	1.0957+15	3.9743+13	2.7349-03
4.4337+00	2.6734+11	1.1849+12	2.2362-02	3.3271-02	1.1359+15	3.7791+13	2.9396-03
4.0143+00	3.0917+11	1.2411+12	2.2268-02	3.0497-02	1.1734+15	3.5786+13	2.8335-03
3.6617+00	3.3927+11	1.2389+12	2.2539-02	2.7936-02	1.1934+15	3.3340+13	2.9975-03
3.3361+00	3.7596+11	1.2542+12	2.2725-02	2.5583-02	1.2203+15	3.1220+13	3.0379-03
2.9361+00	4.3053+11	1.2649+12	1.6372-02	2.3424-02	1.2225+15	2.8636+13	3.2245-03
2.6052+00	5.1458+11	1.2641+12	1.6695-02	2.1451-02	1.2045+15	2.5838+13	3.2984-03
2.1313+00	6.0576+11	1.3092+12	1.7016-02	1.9646-02	1.1692+15	2.2971+13	3.5543-03
1.8942+00	7.1157+11	1.3539+12	1.7122-02	1.8000-02	1.1509+15	2.0716+13	3.6620-03
1.6578+00	8.1545+11	1.3485+12	1.7504-02	1.6497-02	1.1514+15	1.8995+13	3.8859-03
1.4956+00	9.1423+11	1.3671+12	1.7737-02	1.5127-02	1.1548+15	1.7468+13	3.9792-03
1.3216+00	1.0734+12	1.4039+12	1.7946-02	1.3878-02	1.1282+15	1.5657+13	4.2515-03
1.1779+00	1.2294+12	1.4599+12	1.7842-02	1.2743-02	1.0767+15	1.3721+13	4.4569-03
1.0535+00	1.4041+12	1.4933+12	1.7496-02	1.1686-02	1.0349+15	1.2094+13	4.7192-03
9.6948-01	1.5684+12	1.4942+12	1.8176-02	1.0729-02	1.0236+15	1.0982+13	5.0761-03
8.7746-01	1.7204+12	1.5130+12	1.8241-02	9.8617-03	9.5626+14	9.4304+12	5.4425-03
8.0490-01	1.8773+12	1.5114+12	1.8432-02	9.0508-03	8.7713+14	7.9387+12	5.7438-03
7.2672-01	2.1424+12	1.5383+12	1.4796-02	8.2982-03	8.0500+14	6.6800+12	6.1419-03
6.4301-01	2.5112+12	1.6147+12	1.4948-02	7.6183-03	7.5455+14	5.7464+12	6.7651-03
5.7440-01	2.8425+12	1.6327+12	1.5076-02	7.0043-03	7.1670+14	5.0200+12	7.2474-03
5.1630-01	3.1293+12	1.6209+12	1.5465-02	6.4378-03	6.8472+14	4.4041+12	7.7441-03
4.6886-01	3.7204+12	1.7370+12	1.5227-02	5.9154-03	6.5616+14	3.8814+12	8.2436-03
4.2432-01	4.2431+12	1.8004+12	1.5240-02	5.4326-03	6.4252+14	3.4905+12	8.7169-03
3.8757-01	4.9623+12	1.9233+12	1.4961-02	4.9886-03	6.3804+14	3.1829+12	9.2058-03
3.5120-01	5.7428+12	2.0169+12	1.2903-02	4.5818-03	6.2865+14	2.8804+12	9.7026-03
3.1669-01	6.7131+12	2.1263+12	1.2834-02	4.2094-03	6.2025+14	2.6109+12	1.0255-02
2.8677-01	8.0397+12	2.3303+12	1.2423-02	3.8691-03	5.9933+14	2.3189+12	1.1055-02
2.5972-01	9.4652+12	2.4962+12	1.0821-02	3.5536-03	5.6611+14	2.0117+12	1.1671-02
2.3905-01	1.1653+13	2.7930+12	9.4323-03	3.2617-03	5.3866+14	1.7570+12	1.2697-02
2.1450-01	1.3548+13	3.3973+12	8.5712-03	2.9963-03	5.2766+14	1.5810+12	1.3453-02
1.9965-01	2.0900+13	4.1723+12	7.1963-03	2.7549-03	5.0233+14	1.3939+12	1.4747-02
1.8199-01	3.0132+13	5.4838+12	6.3222-03	2.5324-03	4.8665+14	1.2324+12	1.5770-02
1.6525-01	4.2927+13	7.1357+12	5.5340-03	2.3274-03	4.7007+14	1.0941+12	1.7092-02
1.5149-01	6.1378+13	9.3282+12	4.9280-03	2.1409-03	4.4680+14	9.5655+11	1.8873-02
1.3992-01	8.5083+13	1.1896+13	4.4432-03	1.9697-03	4.1677+14	8.2091+11	2.1379-02

INFINITE MEDIUM GRAPHITE SPECTRUM

7/25/66 001(10) R=50.8 90 DEGREES BF3

(COMPUTED 1/10/67)

ENERGY (EV)	N(E)	E*N(E)	DELTA(N)/N	ENERGY (EV)	N(E)	E*N(E)	DELTA(N)/N
9.5021+02	5.6201+08	5.3403+11	4.9406-02	2.7660+00	5.5349+11	1.5309+12	3.0823-02
7.0142+02	9.2233+08	6.4975+11	4.5234-02	2.5367+00	5.6690+11	1.4380+12	3.2598-02
5.2694+02	1.3115+09	7.0681+11	4.5456-02	2.3163+00	6.4239+11	1.4880+12	2.9825-02
4.2299+02	1.5448+09	6.5962+11	4.7247-02	2.1067+00	7.2940+11	1.5366+12	2.9878-02
3.4662+02	2.2136+09	7.6726+11	4.5086-02	1.9246+00	8.3009+11	1.5976+12	2.9662-02
2.8700+02	2.5679+09	7.3700+11	4.6096-02	1.7655+00	9.4205+11	1.6632+12	2.9386-02
2.4153+02	3.1948+09	7.7160+11	4.7587-02	1.6148+00	9.5204+11	1.5374+12	2.3957-02
2.0005+02	3.8598+09	7.9531+11	4.7143-02	1.4727+00	1.1434+12	1.6839+12	2.7957-02
1.7766+02	4.4751+09	7.9593+11	4.7463-02	1.3483+00	1.2724+12	1.7155+12	2.9074-02
1.5506+02	5.5736+09	8.6439+11	4.7401-02	1.2321+00	1.4152+12	1.7436+12	2.6372-02
1.3646+02	6.2220+09	8.4855+11	4.8672-02	1.1238+00	1.5280+12	1.7172+12	2.7099-02
1.2063+02	7.1870+09	8.6670+11	4.6501-02	1.0290+00	1.7138+12	1.7635+12	2.7222-02
1.0794+02	8.3609+09	9.0247+11	4.9311-02	9.4095-01	1.9087+12	1.7960+12	2.5761-02
9.6931+01	8.9764+09	8.7010+11	5.0625-02	8.5940-01	2.0411+12	1.7541+12	2.6164-02
8.7529+01	1.1758+10	1.0293+12	4.6613-02	7.8806-01	2.3073+12	1.8183+12	2.5784-02
7.9428+01	1.1745+10	9.3291+11	5.0164-02	7.2205-01	2.5814+12	1.8639+12	2.4513-02
7.2404+01	1.2402+10	8.9794+11	5.2159-02	6.6111-01	2.8870+12	1.9086+12	2.4338-02
6.6271+01	1.4719+10	9.7581+11	5.0141-02	6.0512-01	3.2103+12	1.9426+12	2.3576-02
6.0611+01	1.7116+10	1.0015+12	3.6371-02	5.5374-01	3.5349+12	1.9574+12	2.3700-02
5.5034+01	2.0560+10	1.0457+12	3.6196-02	5.0687-01	4.0391+12	2.0473+12	2.2524-02
4.9475+01	2.3705+10	1.0258+12	3.7729-02	4.6421-01	4.2901+12	1.9915+12	2.3194-02
4.4799+01	2.7304+10	1.0321+12	3.8696-02	4.2537-01	5.0544+12	2.1500+12	2.1778-02
4.0300+01	2.9725+10	4.8984+11	4.0151-02	3.9009-01	5.5503+12	2.1651+12	2.2203-02
3.6559+01	3.8686+10	1.1494+12	3.7581-02	3.5840-01	6.5881+12	2.3612+12	2.0729-02
3.2815+01	4.2469+10	1.1223+12	3.9186-02	3.2924-01	7.4210+12	2.4433+12	2.0118-02
2.9747+01	5.1430+10	1.2213+12	3.8147-02	3.0226-01	8.8838+12	2.6852+12	1.9301-02
2.7465+01	5.3831+10	1.1555+12	4.0247-02	2.7734-01	1.0215+13	2.8329+12	1.7025-02
1.9496+01	5.5038+10	1.0730+12	4.2607-02	2.5447-01	1.2460+13	3.1707+12	1.4996-02
1.7766+01	5.8265+10	1.0361+12	4.6984-02	2.3336-01	1.5326+13	3.5764+12	1.3373-02
1.6291+01	6.8829+10	1.1063+12	4.4483-02	2.1427-01	2.0069+13	4.3002+12	1.1787-02
1.4882+01	7.9240+10	1.1634+12	3.5257-02	1.9685-01	2.7425+13	5.3987+12	1.0213-02
1.3039+01	9.9895+10	1.2999+12	3.3313-02	1.8091-01	3.7818+13	6.8417+12	9.1173-03
1.1656+01	1.0459+11	1.2773+12	3.4317-02	1.6632-01	5.4494+13	9.0634+12	7.8478-03
1.0463+01	1.1126+11	1.2167+12	3.5917-02	1.5281-01	7.6915+13	1.1753+13	6.9569-03
9.4763+00	1.1418+11	1.2718+12	3.5425-02	1.4036-01	1.0652+14	1.4953+13	6.2657-03
8.6113+00	1.1261+11	1.2260+12	3.6706-02	1.2890-01	1.4584+14	1.8799+13	5.7399-03
7.8561+00	1.0842+11	1.2606+12	3.7201-02	1.1828-01	1.9916+14	2.3557+13	5.2596-03
7.1494+00	1.0794+11	1.2091+12	3.8396-02	1.0860-01	2.6449+14	2.8723+13	4.9047-03
6.5331+00	2.0734+11	1.3546+12	3.1946-02	9.9775-02	3.4388+14	3.4310+13	4.6149-03
5.9766+00	2.3325+11	1.3707+12	3.2461-02	9.1650-02	4.2327+14	3.8793+13	4.3553-03
5.5143+00	2.5667+11	1.3746+12	3.3210-02	8.4224-02	5.0866+14	4.2841+13	4.1986-03
5.1289+00	2.6612+11	1.3527+12	3.3859-02	7.7426-02	5.9217+14	4.5849+13	4.0413-03
4.8072+00	3.2288+11	1.4230+12	3.3164-02	7.1150-02	6.9717+14	4.9693+13	3.9126-03
4.5384+00	3.3469+11	1.3516+12	3.4577-02	6.5379-02	8.0295+14	5.2496+13	3.8150-03
4.0774+00	3.6416+11	1.4127+12	3.0703-02	6.0069-02	9.1090+14	5.4717+13	3.7322-03
3.7229+00	4.2284+11	1.4076+12	3.1460-02	5.5209-02	9.9512+14	5.4937+13	3.7103-03
3.4279+00	4.9259+11	1.4915+12	3.0974-02	5.0717-02	1.1020+15	5.5891+13	3.6478-03

INFINITE MEDIUM GRAPHITE SPECTRUM

7/25/66 001(60) R=5).d 90 DEGREES BF3

(COMPUTED 1/10/67)

ENERGY (EV)	N(E)	E*N(E)	DELTA(N)/N	ENERGY (EV)	N(E)	E*N(E)	DELTA(N)/N
8.1346+01	9.0997+09	7.4022+11	1.9675-02	1.2899-01	1.1901+14	1.5351+13	4.6452-03
5.6032+01	1.4782+10	8.1350+11	2.0124-02	1.1786-01	1.6384+14	1.9311+13	4.2562-03
3.9690+01	2.0624+10	8.1356+11	2.1361-02	1.0775-01	2.2021+14	2.3727+13	3.9570-03
2.9372+01	2.9472+10	8.6333+11	2.1441-02	9.8594-02	2.8799+14	2.8394+13	3.7232-03
2.3431+01	3.6795+10	9.0991+11	2.2151-02	9.0338-02	3.5663+14	3.2217+13	3.5609-03
1.9320+01	4.6542+10	8.6953+11	2.4670-02	8.2928-02	4.2426+14	3.5183+13	3.4473-03
1.5446+01	5.8757+10	9.0756+11	2.4316-02	7.5821-02	5.0210+14	3.8070+13	3.1480-03
1.2905+01	7.0473+10	1.0127+12	2.3229-02	6.9099-02	5.9885+14	4.1380+13	3.0345-03
1.0342+01	9.3196+10	1.0274+12	2.3662-02	6.3153-02	6.9059+14	4.3613+13	3.0648-03
8.3361+00	1.1079+11	1.0411+12	2.3965-02	5.7875-02	7.7236+14	4.4700+13	3.0619-03
6.8355+00	1.2994+11	1.0194+12	2.5143-02	5.2926-02	8.4983+14	4.4983+13	2.9199-03
7.4756+00	1.4496+11	1.0294+12	2.5446-02	4.8322-02	9.4589+14	4.5707+13	2.9600-03
6.5123+00	1.5579+11	1.0654+12	2.5683-02	4.4274-02	1.0277+15	4.5500+13	3.0239-03
5.8167+00	2.0437+11	1.1473+12	2.5384-02	4.0510-02	1.1115+15	4.5026+13	2.9467-03
5.0360+00	2.2490+11	1.1267+12	2.6002-02	3.7029-02	1.1675+15	4.3230+13	3.0558-03
4.3507+00	2.4693+11	1.0904+12	2.6820-02	3.3969-02	1.2067+15	4.0990+13	3.1734-03
4.1021+00	2.6795+11	1.0992+12	2.7172-02	3.1139-02	1.2471+15	3.8833+13	3.1645-03
3.7316+00	3.0793+11	1.1491+12	2.6913-02	2.8526-02	1.2855+15	3.6670+13	3.1260-03
3.4092+00	3.2738+11	1.1161+12	2.7902-02	2.6125-02	1.3165+15	3.4394+13	3.1661-03
3.0824+00	3.9430+11	1.1633+12	1.9473-02	2.3922-02	1.3366+15	3.1975+13	3.1600-03
2.6500+00	4.7602+11	1.2033+12	1.9877-02	2.1908-02	1.3185+15	2.8895+13	3.6438-03
2.2398+00	5.5622+11	1.2329+12	2.0284-02	2.0066-02	1.3002+15	2.6090+13	3.8868-03
1.9253+00	6.0966+11	1.2881+12	2.0177-02	1.8385-02	1.2717+15	2.3381+13	4.0262-03
1.6838+00	7.0355+11	1.2933+12	2.0609-02	1.6851-02	1.2394+15	2.0885+13	4.3404-03
1.5017+00	8.0361+11	1.3570+12	2.0480-02	1.5453-02	1.1988+15	1.8525+13	4.5333-03
1.3502+00	1.0339+12	1.3956+12	2.0657-02	1.4178-02	1.1548+15	1.6372+13	4.3870-03
1.2035+00	1.1008+12	1.3971+12	2.0884-02	1.3018-02	1.0997+15	1.4316+13	5.1285-03
1.0837+00	1.2965+12	1.4089+12	2.1395-02	1.1937-02	1.0686+15	1.2756+13	5.3940-03
9.6598-01	1.4343+12	1.4142+12	2.1709-02	1.0960-02	1.0404+15	1.1 03+13	5.8533-03
8.9567-01	1.5922+12	1.4309+12	2.1610-02	1.0074-02	1.0097+15	1.0171+13	5.1695-03
8.2245-01	1.7643+12	1.4511+12	2.1615-02	9.2464-03	9.2927+14	8.5924+12	5.5402-03
7.4854-01	2.0677+12	1.4868+12	1.7639-02	8.4773-03	8.4811+14	7.1902+12	7.0008-03
6.9704-01	2.3245+12	1.5273+12	1.7669-02	7.7835-03	8.0105+14	6.2350+12	7.6479-03
6.6092-01	2.6421+12	1.5507+12	1.8025-02	7.1563-03	7.5672+14	5.4153+12	8.2325-03
6.2751-01	3.0130+12	1.5920+12	1.7920-02	6.5771-03	7.1346+14	4.6925+12	9.8491-03
4.7696-01	3.4737+12	1.6569+12	1.7869-02	6.0437-03	6.9509+14	4.2000+12	9.3607-03
4.6347-01	3.9445+12	1.7098+12	1.7822-02	5.5510-03	6.6185+14	3.6739+12	9.9954-03
3.9584-01	4.4439+12	1.7591+12	1.8 1 -02	5.0975-03	6.5441+14	3.3359+12	1.0636-02
3.5.51-01	5.3446+12	1.9161+12	1.8233-02	4.6818-03	6.2256+14	2.9147+12	1.1364-02
3.2295-01	6.3278+12	2.0436+12	1.5134-02	4.3014-03	6.0895+14	2.6193+12	1.2197-02
2.9908-01	7.5276+12	2.2108+12	1.4730-02	3.9535-03	5.8332+14	2.3061+12	1.3171-02
2.8614-01	9.0133+12	2.4141+12	1.2735-02	3.6311-03	5.7494+14	2.0877+12	1.3649-02
2.4319-01	1.1155+13	2.7129+12	1.1041-02	3.3327-03	5.5769+14	1.8586+12	1.4610-02
2.2156-01	1.4668+13	3.2525+12	1.0129-02	3.0616-03	5.3503+14	1.6399+12	1.5080-02
2.0235-01	1.9934+13	4.0336+12	8.4816-03	2.8150-03	5.1706+14	1.4555+12	1.7991-02
1.8449-01	2.6761+13	5.0099+12	7.4452-03	2.5876-03	5.2652+14	1.3427+12	1.7590-02
1.6858-01	4.1851+13	7.0553+12	6.5056-03	2.3782-03	4.7825+14	1.1374+12	2.0002-02
1.5422-01	5.9991+13	9.2519+12	5.7245-03	2.1856-03	4.8065+14	1.0505+12	2.1018-02
1.4106-01	8.5891+13	1.2005+13	5.1102-03	2.0082-03	4.5801+14	9.1977+11	2.3420-02

INFINITE MEDIUM GRAPHITE SPECTRUM

7/25/66 001(60) R=50.0 90 DEGREES BF3

(COMPUTED 1/10/67)

ENERGY (EV)	.(E)	E*N(E)	DELTA(N)/N	ENERGY (EV)	N(E)	E*N(E)	DELTA(N)/N
6.1346+01	9.0897+09	7.4022+11	1.9675-02	1.2899-01	1.1901+14	1.5351+13	4.6452-03
5.0032+01	1.4782+10	8.1350+11	2.0124-02	1.1766-01	1.6384+14	1.9311+13	4.2562-03
3.9390+01	2.0624+10	8.1356+11	2.1361-02	1.0775-01	2.2021+14	2.3727+13	3.9570-03
2.9372+01	2.9472+10	8.6333+11	2.1441-02	9.8594-02	2.8799+14	2.8394+13	3.7232-03
2.0431+01	3.8795+10	9.0901+11	2.2151-02	9.0336-02	3.5663+14	3.2217+13	3.5609-03
1.5320+01	4.5542+10	8.6963+11	2.4670-02	8.2928-02	4.2426+14	3.5193+13	3.4473-03
1.0440+01	5.3757+10	9.0756+11	2.4516-02	7.5821-02	5.0210+14	3.8070+13	3.1490-03
1.2905+01	7.0473+10	1.0127+12	2.3229-02	6.9099-02	5.9885+14	4.1380+13	3.1945-03
1.0442+01	9.3790+10	1.0274+12	2.3662-02	6.3153-02	6.9059+14	4.3613+13	3.1648-03
9.0901+00	1.1179+11	1.0413+12	2.3965-02	5.7875-02	7.7236+14	4.4700+13	3.0619-03
8.1655+00	1.2504+11	1.0196+12	2.5143-02	5.2926-02	8.4983+14	4.4910+13	2.9199-03
7.1936+00	1.4006+11	1.0294+12	2.5446-02	4.8322-02	9.4589+14	4.5707+13	2.8600-03
6.3123+00	1.5579+11	1.0054+12	2.5665-02	4.427--02	1.0277+15	4.5510+13	3.0038-03
5.6107+00	2.0437+11	1.1479+12	2.5384-02	4.0510-02	1.1115+15	4.5726+13	2.9467-03
5.0360+00	2.2490+11	1.1267+12	2.6002-02	3.7029-02	1.1675+15	4.3230+13	3.1559-03
4.5507+00	2.4883+11	1.0904+12	2.6820-02	3.3969-02	1.2067+15	4.0990+13	3.1734-03
4.1021+00	2.6795+11	1.0992+12	2.7172-02	3.1139-02	1.2471+15	3.8433+13	3.1645-03
3.7316+00	3.0793+11	1.1491+12	2.6913-02	2.8526-02	1.3855+15	3.6677+13	3.1260-03
3.4092+00	3.2738+11	1.1161+12	2.7902-02	2.6125-02	1.3165+15	3.4304+13	3.1661-03
3.0824+00	3.9439+11	1.1838+12	1.9473-02	2.3922-02	1.3366+15	3.1975+13	3.1600-03
2.8100+00	4.7002+11	1.2033+12	1.9377-02	2.1908-02	1.3185+15	2.8845+13	3.1439-03
2.5209+00	5.5522+11	1.2329+12	2.0284-02	2.0066-02	1.3002+15	2.6100+13	3.1864-03
1.9253+00	6.0906+11	1.2981+12	2.0177-02	1.8385-02	1.2717+15	2.3381+13	3.0262-03
1.6233+00	7.0355+11	1.2933+12	2.0609-02	1.6851-02	1.2394+15	2.0833+13	3.1404-03
1.5117+00	9.0561+11	1.3570+12	2.0480-02	1.5443-02	1.1988+15	1.8525+13	3.1333-03
1.3902+00	1.0735+12	1.3355+12	2.0657-02	1.4174-02	1.1548+15	1.6372+13	3.2470-03
1.2835+00	1.1668+12	1.3974+12	2.0884-02	1.3018-02	1.0997+15	1.4316+13	3.1235-03
1.1736+00	1.2965+12	1.4039+12	2.1395-02	1.1937-02	1.0686+15	1.2756+13	3.3940-03
9.8698-01	1.4343+12	1.4142+12	2.1709-02	1.0960-02	1.0404+15	1.1402+13	3.3531-03
8.9967-01	1.5922+12	1.4309+12	2.1610-02	1.0074-02	1.0097+15	1.0171+13	3.1495-03
8.2243-01	1.7543+12	1.4511+12	2.1815-02	9.2464-03	9.2927+14	8.5924+12	3.3402-03
7.4954-01	2.0077+12	1.4868+12	1.7639-02	8.4779-03	8.4811+14	7.1902+12	7.0008-03
6.8704-01	2.3245+12	1.5274+12	1.7669-02	7.7835-03	8.0105+14	6.2350+12	7.5479-03
5.8892-01	2.6021+12	1.5507+12	1.8025-02	7.1563-03	7.5672+14	5.4193+12	8.2325-03
5.2751-01	3.0186+12	1.5920+12	1.7920-02	6.5771-03	7.1346+14	4.6925+12	8.8491-03
4.7098-01	3.4737+12	1.6564+12	1.7869-02	6.0437-03	6.9509+14	4.2009+12	9.7607-03
4.2047-01	3.9445+12	1.7098+12	1.7922-02	5.5510-03	6.6185+14	3.6739+12	9.9954-03
3.9364-01	4.4439+12	1.7591+12	1.3110-02	5.0975-03	6.5441+14	3.3359+12	1.0636-02
3.6151-01	5.0446+12	1.8161+12	1.5233-02	4.6818-03	6.2256+14	2.9147+12	1.1364-02
3.2245-01	6.0276+12	2.0436+12	1.5134-02	4.3014-03	6.0895+14	2.6193+12	1.2197-02
2.9400-01	7.0576+12	2.2106+12	1.4730-02	3.9535-03	5.8332+14	2.3061+12	1.3171-02
2.6814-01	8.0835+12	2.4141+12	1.2735-02	3.6311-03	5.7494+14	2.0877+12	1.3649-02
2.4319-01	1.1155+13	2.7129+12	1.1041-02	3.3327-03	5.5769+14	1.8586+12	1.4610-02
2.2456-01	1.4680+13	3.2525+12	1.0129-02	3.0616-03	5.3563+14	1.6399+12	1.5090-02
2.0635-01	1.9934+13	4.0336+12	8.4816-03	2.8150-03	5.1706+14	1.4555+12	1.7091-02
1.8949-01	2.6784+13	5.0799+12	7.4452-03	2.5876-03	5.2662+14	1.3627+12	1.7590-02
1.7458-01	4.1851+13	7.6553+12	6.5056-03	2.3782-03	4.7825+14	1.1374+12	2.0002-02
1.6422-01	5.9991+13	9.8519+12	5.7245-03	2.1856-03	4.8065+14	1.0505+12	2.1018-02
1.4106-01	8.5091+13	1.2005+13	5.1102-03	2.0082-03	4.5801+14	9.1977+11	2.3420-02

INFINITE MEDIUM GRAPHITE SPECTRUM

5/17/66 001 R=20.3 0 DEGREES NE226

(COMPUTED 2/15/67)

ENERGY (EV)	N(E)	E*N(E)	DELTA(N)/N	ENERGY (EV)	N(E)	E*N(E)	DELTA(N)/N
1.5703+06	2.1318+08	3.3476+14	1.4333-02	1.7713+05	3.9971+08	7.0801+13	5.1716-02
1.3359+06	2.1286+08	2.8436+14	1.5461-02	1.5867+05	4.3128+08	6.8431+13	5.7680-02
1.1504+06	2.0512+08	2.3597+14	1.7051-02	1.3950+05	4.4619+08	6.2243+13	5.4015-02
1.0009+06	2.1514+08	2.1533+14	1.8766-02	1.2065+05	5.7333+08	6.9172+13	5.4701-02
8.7881+05	2.1076+08	1.8522+14	2.0718-02	1.0537+05	6.4470+08	6.7932+13	5.9807-02
7.7776+05	2.2899+08	1.7810+14	2.2050-02	9.1014+04	8.7877+08	7.9981+13	5.4426-02
6.9319+05	2.3456+08	1.6259+14	2.3809-02	7.6486+04	8.5020+08	6.5028+13	5.8743-02
6.2170+05	2.2843+08	1.4202+14	2.6388-02	6.3000+04	1.1430+09	7.2009+13	5.5139-02
5.6072+05	2.3033+08	1.2915+14	2.8791-02	5.1196+04	1.4120+09	7.2289+13	5.7605-02
5.0830+05	2.2754+08	1.1566+14	3.2362-02	4.1272+04	1.7994+09	7.4265+13	5.8460-02
4.6289+05	2.5007+08	1.1576+14	3.5645-02	3.2399+04	2.2835+09	7.3984+13	5.7385-02
4.2331+05	2.6800+08	1.1345+14	3.9211-02	2.5483+04	3.0692+09	7.8212+13	5.9903-02
3.8860+05	2.1874+08	8.5001+13	4.4141-02	2.0591+04	4.1020+09	8.4465+13	5.9666-02
3.5799+05	2.3435+08	8.3894+13	4.5171-02	1.6157+04	4.9270+09	7.9605+13	5.9297-02
3.3086+05	2.3219+08	7.6823+13	4.9055-02	1.2073+04	6.7302+09	8.1254+13	5.8995-02
3.0669+05	2.6543+08	8.1405+13	4.9693-02	8.6805+03	1.0357+10	8.9904+13	5.9787-02
2.8509+05	2.5440+08	7.2527+13	5.5356-02	5.9829+03	1.7454+10	1.0442+14	5.9046-02
2.6569+05	2.5797+08	6.8540+13	5.8153-02	3.8874+03	3.0596+10	1.1894+14	5.9133-02
2.4820+05	3.1258+08	7.7581+13	5.6713-02	2.4544+03	6.1961+10	1.5208+14	5.9921-02
2.2521+05	3.1235+08	7.0344+13	4.4777-02	1.5973+03	8.3583+10	1.3351+14	5.9761-02
1.9901+05	3.5991+08	7.1625+13	4.7762-02	9.0246+02	1.5796+11	1.4255+14	5.9534-02

INFINITE MEDIUM GRAPHITE SPECTRUM

5/27/66 002 R=20.3 30 DEGREES NE226

(COMPUTED 2/15/67)

ENERGY (EV)	N(E)	E*N(E)	DELTA(N)/N	ENERGY (EV)	N(E)	E*N(E)	DELTA(N)/N
1.6078+06	2.7435+07	4.959d+13	2.9201-02	2.9272+04	1.6401+09	4.800R+13	5.3256-02
1.5209+06	3.3843+07	5.1472+13	2.8704-02	2.7354+04	1.7136+09	4.6873+13	5.4973-02
1.4972+06	3.5924+07	4.6470+13	3.0791-02	2.5619+04	1.9069+09	4.8852+13	5.4730-02
1.1195+06	4.2987+07	4.8124+13	3.1072-02	2.4044+04	1.9899+09	4.7844+13	5.6418-02
9.7591+05	5.0240+07	4.9030+13	3.1315-02	2.2387+04	1.9557+09	4.3783+13	5.2491-02
8.5830+05	5.7983+07	4.9767+13	3.1786-02	2.0690+04	2.1730+09	4.4960+13	5.3067-02
7.6073+05	6.4252+07	4.8879+13	3.2948-02	1.9180+04	2.3372+09	4.4828+13	5.4591-02
6.7691+05	7.5557+07	5.1296+13	3.2760-02	1.7829+04	2.5509+09	4.5480+13	5.5570-02
6.0960+05	8.2751+07	5.0445+13	3.3619-02	1.6616+04	2.9209+09	4.8534+13	5.4912-02
5.5039+05	8.3917+07	4.6187+13	3.6616-02	1.5523+04	2.9679+09	4.6071+13	5.7786-02
4.9941+05	9.6506+07	4.6196+13	3.7639-02	1.4534+04	3.1955+09	4.5862+13	5.9145-02
4.5520+05	1.2029+08	5.4754+13	3.8810-02	1.3532+04	3.6276+09	4.9089+13	5.2058-02
4.1061+05	1.1252+08	4.6878+13	4.3994-02	1.2534+04	3.6440+09	4.5674+13	5.5440-02
3.6272+05	1.1966+08	4.5798+13	4.2183-02	1.1726+04	4.3507+09	5.1017+13	5.9347-02
3.2261+05	1.4218+08	5.0161+13	4.0998-02	1.0996+04	4.1714+09	4.5868+13	5.7802-02
2.8027+05	1.5153+08	4.9441+13	4.2410-02	1.0261+04	4.5502+09	4.6689+13	5.8657-02
2.4262+05	1.5407+08	4.6806+13	4.4945-02	9.5970+03	4.9111+09	4.7132+13	5.9753-02
2.0145+05	1.6033+08	5.0755+13	4.4323-02	8.9396+03	5.2911+09	4.7300+13	5.5752-02
2.0242+05	1.7888+08	4.6943+13	4.6420-02	8.2956+03	5.6645+09	4.6990+13	5.7394-02
2.4526+05	1.9486+08	4.7742+13	4.7240-02	7.6743+03	5.8787+09	4.5115+13	5.6017-02
2.2973+05	2.1368+08	4.9089+13	4.7776-02	7.0794+03	6.3324+09	4.4830+13	5.7575-02
2.1363+05	2.1109+08	4.5516+13	5.0368-02	6.5861+03	7.9150+09	5.2129+13	5.8317-02
2.0279+05	2.3069+08	4.6781+13	5.1556-02	6.1438+03	8.2745+09	5.0837+13	5.8590-02
1.9107+05	2.4758+08	4.7495+13	5.1353-02	5.6586+03	8.2066+09	4.6438+13	5.6677-02
1.8033+05	2.4980+08	4.5046+13	5.4052-02	5.2018+03	9.4455+09	4.9133+13	5.6918-02
1.7047+05	2.7636+08	4.7111+13	5.4131-02	4.7990+03	9.5448+09	4.5805+13	5.7715-02
1.6140+05	3.0409+08	4.9080+13	5.5189-02	4.4211+03	1.0822+10	4.7844+13	5.7626-02
1.5303+05	3.1444+08	4.8119+13	5.6582-02	4.0521+03	1.0730+10	4.3477+13	5.7202-02
1.4572+05	3.5122+08	4.9775+13	4.0398-02	3.7111+03	1.2397+10	4.6005+13	5.9905-02
1.2841+05	3.5402+08	4.5460+13	4.2528-02	3.4120+03	1.3940+10	4.7564+13	5.7892-02
1.1957+05	4.3492+08	5.2482+13	5.9714-02	3.1241+03	1.5038+10	4.6981+13	5.8244-02
1.1170+05	4.0701+08	4.5463+13	4.4672-02	2.8607+03	1.7259+10	4.9372+13	5.8510-02
1.0231+05	4.3360+08	4.4382+13	4.7020-02	2.6292+03	1.9569+10	5.1450+13	5.8470-02
9.4059+04	5.5160+08	5.1901+13	4.6115-02	2.3860+03	1.8302+10	4.3670+13	5.7757-02
8.8766+04	5.5740+08	4.8363+13	5.0855-02	2.1536+03	2.2680+10	4.8844+13	5.9150-02
8.2289+04	5.4328+08	4.3020+13	5.2144-02	1.9542+03	2.4034+10	4.6967+13	5.9556-02
7.4511+04	5.9052+08	4.3263+13	5.2863-02	1.7661+03	2.7904+10	4.9282+13	5.8474-02
6.9335+04	6.9316+08	4.8060+13	5.1053-02	1.5870+03	3.0067+10	4.7716+13	5.8049-02
6.4660+04	7.0722+08	4.5743+13	5.3766-02	1.4227+03	3.4703+10	4.9372+13	5.9547-02
6.0479+04	7.4714+08	4.5186+13	5.5127-02	1.2736+03	3.7849+10	4.8205+13	5.9729-02
5.6674+04	7.7778+08	4.4080+13	5.7235-02	1.1314+03	4.2958+10	4.8603+13	5.9484-02
5.3218+04	9.9589+08	5.2999+13	5.2937-02	9.9474+02	4.8059+10	4.7806+13	5.8695-02
5.0068+04	9.8893+08	4.9513+13	5.6686-02	8.6745+02	5.5072+10	4.7772+13	5.9307-02
4.7190+04	9.7793+08	4.6148+13	5.9394-02	7.4671+02	5.9344+10	4.4313+13	5.9388-02
4.4553+04	1.0503+09	4.6794+13	5.9919-02	6.4032+02	7.5164+10	4.8129+13	5.9832-02
4.2131+04	1.2440+09	5.2411+13	5.7422-02	5.5017+02	8.5577+10	4.7082+13	5.9877-02
3.9380+04	1.2253+09	4.8253+13	5.0824-02	4.6813+02	1.0100+11	4.7282+13	5.9975-02
3.6411+04	1.4420+09	5.2505+13	5.3331-02	3.8435+02	1.0608+11	4.0773+13	5.9540-02
3.3766+04	1.4404+09	4.8637+13	5.6418-02	3.0422+02	1.3811+11	4.2017+13	5.9724-02
3.1399+04	1.3748+09	4.3166+13	5.6068-02	2.4007+02	1.8455+11	4.4306+13	5.9895-02

INFINITE MEDIUM GRAPHITE SPECTRUM

5/20/66 002 R=35.6 0 DEGREES NE226

(COMPUTED 2/15/67)

ENERGY (EV)	N(E)	E*N(E)	DELTA(N)/N	ENERGY (EV)	N(E)	E*N(E)	DELTA(N)/N
1.7952+06	2.4507+07	4.3994+13	1.8451-02	2.2946+04	6.9031+08	1.5840+13	5.7775-02
1.5102+06	2.1162+07	3.1959+13	2.1338-02	1.9074+04	8.3829+08	1.5990+13	5.9393-02
1.2381+06	1.7725+07	2.2831+13	2.5146-02	1.5962+04	1.1606+09	1.8525+13	5.8856-02
1.1116+06	1.5632+07	1.7377+13	2.9994-02	1.3452+04	1.4716+09	1.9796+13	5.7742-02
9.6902+05	1.5168+07	1.4698+13	3.3357-02	1.1327+04	1.8109+09	2.0512+13	5.8292-02
8.5222+05	1.5564+07	1.3264+13	3.6616-02	9.5413+03	2.3037+09	2.1981+13	5.8724-02
7.5533+05	1.5807+07	1.1940+13	4.0000-02	8.0486+03	3.1758+09	2.5561+13	5.9040-02
6.7407+05	1.7009+07	1.1465+13	4.2329-02	6.8042+03	3.9687+09	2.7004+13	5.9157-02
6.0525+05	1.6690+07	1.0102+13	4.6508-02	5.7399+03	5.0223+09	2.8828+13	5.9480-02
5.4646+05	1.8593+07	1.0161+13	4.8944-02	4.8157+03	5.6948+09	2.7425+13	5.9794-02
4.9564+05	1.8382+07	9.1146+12	5.5234-02	4.1122+03	1.1420+10	4.6959+13	5.8999-02
4.5193+05	2.5047+07	1.1319+13	5.5150-02	3.5694+03	1.0254+10	3.6602+13	5.9772-02
3.9679+05	2.1744+07	8.6277+12	4.6188-02	3.0478+03	1.2186+10	3.7141+13	5.9958-02
3.5710+05	2.3202+07	7.8214+12	5.0603-02	2.5523+03	2.3038+10	5.8800+13	5.9908-02
2.8993+05	2.7696+07	8.0299+12	5.4219-02	2.1404+03	1.6983+10	3.6350+13	5.9009-02
2.5201+05	3.5376+07	8.9151+12	5.4616-02	1.8258+03	2.0182+10	3.6847+13	5.9384-02
2.2107+05	4.1207+07	9.1097+12	5.8136-02	1.5640+03	2.3147+10	3.6202+13	5.9603-02
1.9001+05	4.9097+07	9.3288+12	5.1391-02	1.3314+03	3.0163+10	4.0159+13	5.9385-02
1.6046+05	6.4136+07	1.0291+13	5.5470-02	1.1439+03	4.6817+10	5.3554+13	5.9272-02
1.3408+05	7.5129+07	1.0073+13	5.3741-02	9.8370+02	5.2586+10	5.1728+13	5.9504-02
1.1106+05	9.8127+07	1.0898+13	5.6639-02	8.4438+02	6.6749+10	5.6361+13	5.9870-02
9.3493+04	1.3882+08	1.2979+13	5.9333-02	7.2388+02	7.4325+10	5.3802+13	5.9910-02
7.6969+04	1.6612+08	1.2786+13	5.3093-02	6.1973+02	9.5658+10	5.9282+13	5.9897-02
6.2210+04	2.1116+08	1.3136+13	5.7492-02	5.3500+02	1.1458+11	6.1302+13	5.9792-02
5.0587+04	2.6243+08	1.3276+13	5.7445-02	4.5673+02	1.2821+11	5.8558+13	5.9528-02
4.1339+04	3.1864+08	1.3172+13	5.9822-02	3.8598+02	1.5860+11	6.1218+13	5.9675-02
3.4008+04	4.6356+08	1.5765+13	5.7681-02	3.2385+02	1.8400+11	5.9587+13	5.9755-02
2.7830+04	5.0396+08	1.4025+13	5.7946-02	2.6860+02	2.2647+11	6.0829+13	5.9791-02

INFINITE MEDIUM GRAPHITE SPECTRUM

5/27/66 005 R=35.6 17 DEGREES NE226

(COMPUTED 2/15/67)

ENERGY (EV)	N(E)	E*N(E)	DELTA(N)/N	ENERGY (EV)	N(E)	E*N(E)	DELTA(N)/N
1.5371+06	6.8993+06	1.0605+13	2.5785-02	8.7810+03	1.2376+09	1.0867+13	5.9593-02
1.3093+06	7.5347+06	9.8651+12	2.7347-02	8.3034+03	1.2760+09	1.0595+13	5.5249-02
1.1287+06	8.3914+06	9.4713+12	2.8328-02	7.8624+03	1.5012+09	1.1803+13	5.8819-02
9.8299+05	9.4393+06	9.2787+12	2.9409-02	7.4999+03	1.5844+09	1.1883+13	5.9593-02
8.6379+05	1.0608+07	9.1629+12	3.0147-02	7.1217+03	1.6020+09	1.1409+13	5.5723-02
7.6503+05	1.1311+07	8.6534+12	3.1840-02	6.7335+03	1.6656+09	1.1215+13	5.7564-02
6.8229+05	1.2500+07	8.5289+12	3.2748-02	6.3763+03	1.9078+09	1.2165+13	5.5803-02
6.1228+05	1.2796+07	7.8348+12	3.4824-02	6.0467+03	2.3195+09	1.4025+13	5.6790-02
5.5251+05	1.2830+07	7.0885+12	3.8157-02	5.7133+03	2.0971+09	1.1981+13	5.5295-02
5.0109+05	1.5764+07	7.8991+12	3.7910-02	5.3796+03	2.2249+09	1.1969+13	5.4765-02
4.5653+05	1.7337+07	7.9148+12	4.1664-02	5.0385+03	2.5558+09	1.3031+13	5.7828-02
4.1765+05	1.6792+07	7.0547+12	4.6601-02	4.8618+03	2.6846+09	1.3052+13	5.8735-02
3.8354+05	1.7403+07	6.6749+12	4.5437-02	4.6413+03	2.9996+09	1.3922+13	5.7217-02
3.5345+05	1.8510+07	6.5424+12	4.6753-02	4.4159+03	2.6672+09	1.1778+13	5.9456-02
3.2676+05	2.2249+07	7.2700+12	4.5390-02	4.1880+03	3.0694+09	1.2855+13	5.7061-02
3.0298+05	2.2857+07	6.9254+12	4.8024-02	3.9772+03	3.2244+09	1.2824+13	5.8358-02
2.8171+05	2.4695+07	7.0131+12	4.9107-02	3.7666+03	3.3729+09	1.2704+13	5.5562-02
2.6260+05	2.7107+07	7.1183+12	4.8990-02	3.5719+03	3.7828+09	1.3512+13	5.8809-02
2.4537+05	3.0600+07	7.5574+12	4.8757-02	3.4054+03	4.0711+09	1.3864+13	5.9084-02
2.2979+05	3.0123+07	6.9219+12	5.2489-02	3.2258+03	3.8695+09	1.2482+13	5.6292-02
2.1564+05	3.0183+07	6.5086+12	5.5032-02	3.0483+03	4.5807+09	1.3963+13	5.7235-02
2.0276+05	3.6488+07	7.3982+12	5.3372-02	2.8956+03	4.8348+09	1.4000+13	5.8430-02
1.9100+05	3.5764+07	6.8309+12	5.5965-02	2.7445+03	4.9097+09	1.3475+13	5.7412-02
1.8024+05	3.8039+07	7.0003+12	5.6584-02	2.6047+03	5.8459+09	1.5227+13	5.7739-02
1.7036+05	3.9204+07	6.6787+12	5.9591-02	2.4755+03	5.4948+09	1.3602+13	5.9572-02
1.6127+05	4.6714+07	7.5336+12	5.8273-02	2.3555+03	6.4994+09	1.5309+13	5.9883-02
1.4901+05	4.7515+07	7.0802+12	6.3993-02	2.2442+03	6.6217+09	1.4860+13	5.8422-02
1.3464+05	5.4457+07	7.3321+12	6.3375-02	2.1405+03	7.6834+09	1.6446+13	5.9418-02
1.2226+05	6.3044+07	7.7078+12	6.4377-02	2.0439+03	7.6021+09	1.5538+13	5.8945-02
1.1151+05	6.4109+07	7.1488+12	6.6656-02	1.9422+03	7.6343+09	1.4827+13	5.8604-02
1.0211+05	7.7994+07	7.9639+12	6.5827-02	1.8424+03	8.3647+09	1.5411+13	5.8349-02
9.3859+04	7.4052+07	6.9504+12	6.3067-02	1.7453+03	8.7235+09	1.5225+13	5.7099-02
8.6566+04	8.0483+07	6.9671+12	6.6344-02	1.6466+03	8.7112+09	1.4344+13	5.8299-02
8.0092+04	9.1935+07	7.3633+12	6.2776-02	1.5560+03	1.0436+10	1.6239+13	5.7414-02
7.4317+04	1.0368+08	7.7052+12	6.1863-02	1.4727+03	1.0641+10	1.5671+13	5.7578-02
6.9146+04	1.1980+08	8.2834+12	6.1126-02	1.3959+03	1.1769+10	1.6429+13	5.9849-02
6.4496+04	1.2390+08	7.9911+12	6.3362-02	1.3282+03	1.3321+10	1.7694+13	5.8060-02
6.0300+04	1.3823+08	8.3351+12	6.3140-02	1.2623+03	1.4080+10	1.7773+13	5.6577-02
5.6500+04	1.4859+08	8.3956+12	6.4278-02	1.1957+03	1.3963+10	1.6695+13	5.8170-02
5.3049+04	1.5540+08	8.2437+12	6.6171-02	1.1315+03	1.5377+10	1.7399+13	5.7853-02
4.9904+04	1.6369+08	8.1689+12	6.7422-02	1.0748+03	1.7519+10	1.8829+13	5.8462-02
4.6364+04	1.7064+08	7.9117+12	6.8916-02	1.0201+03	1.7137+10	1.7481+13	5.8244-02
4.3166+04	1.9194+08	8.2854+12	6.9461-02	9.6533+02	1.8363+10	1.7727+13	5.8964-02
4.0306+04	2.0997+08	8.4632+12	6.9553-02	9.1304+02	1.9282+10	1.7605+13	5.8283-02
3.7225+04	2.2876+08	8.5157+12	5.3220-02	8.6484+02	2.1284+10	1.8407+13	5.9792-02
3.4484+04	2.4359+08	8.3999+12	5.9040-02	8.2041+02	2.2566+10	1.8514+13	5.8518-02
3.2035+04	2.7331+08	8.7556+12	5.1555-02	7.7927+02	2.5632+10	1.9974+13	5.8641-02
2.9837+04	2.8355+08	8.4604+12	5.2578-02	7.3718+02	2.3097+10	1.7027+13	5.8913-02
2.7859+04	3.2118+08	8.9477+12	5.2025-02	6.9583+02	2.7668+10	1.9253+13	5.8369-02
2.6071+04	3.0777+08	8.0239+12	5.6639-02	6.5570+02	2.5374+10	1.6638+13	5.9275-02
2.4449+04	3.3863+08	8.2793+12	5.6813-02	6.1678+02	2.9910+10	1.8448+13	5.9456-02
2.2975+04	3.9611+08	9.1007+12	5.4655-02	5.8502+02	3.4725+10	2.0315+13	5.9962-02
2.1630+04	3.9545+08	8.5536+12	5.7896-02	5.5657+02	3.7484+10	2.0862+13	5.8198-02
2.0399+04	4.3300+08	8.8329+12	5.8082-02	5.2851+02	3.7751+10	1.9952+13	5.9456-02
1.9271+04	4.6002+08	8.8651+12	5.9237-02	5.0100+02	4.0493+10	2.0287+13	5.8317-02
1.8072+04	5.0380+08	9.1047+12	5.1713-02	4.7214+02	3.7779+10	1.7837+13	5.9471-02
1.6976+04	5.6013+08	9.5088+12	5.9436-02	4.4501+02	4.5508+10	2.0252+13	5.9427-02
1.6117+04	6.2662+08	1.0099+13	5.8460-02	4.2193+02	4.9085+10	2.0711+13	5.9735-02
1.5195+04	6.5684+08	1.0011+13	5.1911-02	3.9794+02	4.6105+10	1.8347+13	5.9712-02
1.4234+04	6.6820+08	9.5123+12	5.4630-02	3.7539+02	5.6320+10	2.1142+13	5.9995-02
1.3465+04	8.4959+08	1.1440+13	5.7347-02	3.5565+02	5.9398+10	2.1125+13	5.8387-02
1.2855+04	8.9403+08	1.1493+13	5.8082-02	3.3576+02	5.9743+10	2.0059+13	5.9712-02
1.2196+04	8.2263+08	1.0033+13	5.5577-02	3.1597+02	6.2459+10	1.9735+13	5.9464-02
1.1501+04	9.3839+08	1.0792+13	5.4249-02	2.9752+02	6.9576+10	2.0700+13	5.9737-02
1.0864+04	8.7853+08	9.5443+12	5.9891-02	2.8096+02	7.6225+10	2.1416+13	5.9521-02
1.0279+04	1.0594+09	1.0889+13	5.6235-02	2.6404+02	7.3934+10	1.9522+13	5.8978-02
9.7396+03	1.0725+09	1.0446+13	5.8819-02	2.4751+02	8.4295+10	2.0864+13	5.9304-02
9.2417+03	1.2125+09	1.1206+13	5.7441-02	2.3250+02	8.9053+10	2.0705+13	5.9244-02

INFINITE MEDIUM GRAPHITE SPECTRUM

5/26/66 010 R=35.6 35 DEGREES ME226

(COMPUTED 2/15/67)

ENERGY (EV)	N(E)	E*N(E)	DELTA(N)/N	ENERGY (EV)	N(E)	E*N(E)	DELTA(N)/N
1.[illegible]+06	[illegible]+06	5.7107+12	2.1539-02	4.5417+03	2.1506+09	9.7681+12	5.2603-02
1.0165+06	4.2741+06	5.6298+12	2.2208-02	4.4209+03	2.1939+09	9.6992+12	5.3311-02
1.[illegible]+06	4.[illegible]+06	5.5297+12	2.2619-02	4.3048+03	2.2259+09	9.5822+12	5.4197-02
9.[illegible]+05	[illegible]+06	5.9873+12	2.2436-02	4.1932+03	2.4499+09	1.0273+13	5.2396-02
8.[illegible]+05	[illegible]+06	5.9717+12	2.2816-02	4.0859+03	2.3457+09	9.5844+12	5.5126-02
7.[illegible]+05	7.2941+06	5.6110+12	2.4199-02	3.9827+03	2.4715+09	9.8431+12	5.4656-02
[illegible]+05	7.9596+06	5.4608+12	2.5025-02	3.8833+03	2.6296+09	1.0211+13	5.1971-02
[illegible]+05	8.7580+06	5.3920+12	2.5651-02	3.7876+03	2.8459+09	1.0779+13	5.2742-02
[illegible]+05	9.4137+06	5.2301+12	2.7038-02	3.6954+03	3.1406+09	1.1606+13	5.0883-02
[illegible]+05	1.0[illegible]+07	5.4561+12	2.7799-02	3.6065+03	3.0214+09	1.0897+13	5.3383-02
[illegible]+05	1.3345+07	6.1263+12	2.8676-02	3.5208+03	3.0034+09	1.0574+13	5.4968-02
[illegible]+05	1.3719+07	5.7618+12	3.1475-02	3.4381+03	3.2956+09	1.1329+13	5.3167-02
[illegible]+05	1.[illegible]+07	4.9400+12	3.2420-02	3.3583+03	3.0858+09	1.0363+13	5.6696-02
[illegible]+05	1.4579+07	5.1819+12	3.1970-02	3.2813+03	3.5198+09	1.1550+13	5.3601-02
[illegible]+05	1.[illegible]+07	5.2169+12	3.2643-02	3.2068+03	3.5583+09	1.1411+13	5.4425-02
[illegible]+05	1.6729+07	5.0969+12	3.4029-02	3.1349+03	3.7553+09	1.1772+13	5.3897-02
[illegible]+05	1.9225+07	5.4462+12	3.3892-02	3.0653+03	3.9778+09	1.2187+13	5.3232-02
[illegible]+05	1.9706+07	5.2039+12	3.4865-02	2.9981+03	3.8569+09	1.1563+13	5.5527-02
[illegible]+05	1.9288+07	4.7592+12	3.7531-02	2.9330+03	3.5586+09	1.0437+13	5.9654-02
[illegible]+05	2.3960+07	5.5367+12	3.5584-02	2.8701+03	4.1299+09	1.1853+13	5.5608-02
[illegible]+05	2.2403+07	4.8584+12	3.8718-02	2.8091+03	3.8431+09	1.0796+13	5.9456-02
[illegible]+05	2.3421+07	4.8571+12	4.0218-02	2.7501+03	3.9964+09	1.0991+13	5.9260-02
1.9208+05	2.6717+07	5.1317+12	3.9159-02	2.6929+03	4.1684+09	1.1225+13	5.8970-02
1.8125+05	3.1216+07	5.6560+12	3.8097-02	2.6374+03	4.2789+09	1.1285+13	5.9260-02
1.7152+05	3.1512+07	5.3987+12	4.0057-02	2.5750+03	4.2224+09	1.0873+13	5.9024-02
1.6218+05	3.5035+07	5.6819+12	4.0414-02	2.5062+03	4.4739+09	1.1212+13	5.2544-02
1.5375+05	3.6008+07	5.5362+12	4.1833-02	2.4482+03	5.0395+09	1.2338+13	5.7465-02
1.4596+05	3.4825+07	5.0831+12	4.5230-02	2.3923+03	4.3814+09	1.0482+13	5.5866-02
1.3875+05	3.6344+07	5.0427+12	4.5184-02	2.3306+03	4.7733+09	1.1125+13	5.4818-02
1.3203+05	4.0360+07	5.3167+12	4.3659-02	2.2713+03	5.1776+09	1.1760+13	5.2955-02
1.2585+05	4.6510+07	5.8553+12	4.2240-02	2.2212+03	5.8367+09	1.2965+13	5.8029-02
1.2006+05	4.4523+07	5.3455+12	4.7242-02	2.1729+03	4.9341+09	1.0721+13	5.7112-02
1.1466+05	5.2146+07	5.9791+12	4.3170-02	2.1195+03	5.4159+09	1.1479+13	5.5232-02
1.0962+03	5.2384+07	5.7424+12	4.4866-02	2.0680+03	5.6516+09	1.1687+13	5.5077-02
1.0490+05	5.7130+07	5.9929+12	4.4687-02	2.0184+03	5.5689+09	1.1240+13	5.7027-02
1.0046+05	6.0742+07	6.1033+12	4.5322-02	1.9706+03	5.6912+09	1.1215+13	5.7633-02
9.6338+04	6.3654+07	6.1333+12	4.5626-02	1.9244+03	6.0113+09	1.1568+13	5.7027-02
9.2445+04	6.1721+07	5.7056+12	5.0287-02	1.8798+03	6.1922+09	1.1640+13	5.7285-02
8.8782+04	6.5183+07	5.7871+12	5.2152-02	1.8368+03	6.5508+09	1.2032+13	5.6605-02
8.5333+04	6.7948+07	5.7962+12	5.2364-02	1.7952+03	6.8631+09	1.2321+13	5.6273-02

8.2082+04	7.0938+07	5.8269+12	5.0735-02	1.7550+03	7.0190+09	1.2318+13	5.6773-02
7.9012+04	7.3367+07	5.1919+12	4.8836-02	1.7162+03	7.0764+09	1.2145+13	5.7810-02
7.8112+04	7.8714+07	5.9911+12	4.9975-02	1.6786+03	7.5289+09	1.2638+13	5.6857-02
7.3368+04	7.5048+07	5.7262+12	5.1735-02	1.6423+03	7.8731+09	1.2930+13	5.6521-02
7.0770+04	8.0437+07	5.0925+12	5.2507-02	1.6071+03	7.8958+09	1.2689+13	5.7721-02
6.8308+04	8.7204+07	5.9567+12	5.1873-02	1.5731+03	9.5157+09	1.3396+13	5.6273-02
6.5972+04	9.8737+07	6.5138+12	5.0037-02	1.5360+03	7.8588+09	1.2071+13	5.4359-02
6.3754+04	9.1160+07	5.8113+12	5.3770-02	1.5003+03	8.8246+09	1.3240+13	5.7810-02
6.1646+04	1.0162+08	6.2642+12	5.2092-02	1.4695+03	9.5828+09	1.4092+13	5.6028-02
5.9641+04	1.1239+08	6.7329+12	5.0606-02	1.4361+03	8.3403+09	1.1977+13	5.6192-02
5.7732+04	1.1000+08	6.3503+12	5.2969-02	1.4037+03	9.3850+09	1.3174+13	5.9566-02
5.5913+04	1.0703+08	5.9341+12	5.5294-02	1.3725+03	9.0580+09	1.2432+13	5.5953-02
5.4179+04	1.1996+08	6.4993+12	5.3464-02	1.3390+03	9.7103+09	1.3002+13	5.4876-02
5.2524+04	1.1436+08	6.0068+12	5.6503-02	1.3093+03	1.0558+10	1.3929+13	5.9470-02
5.0944+04	1.2677+08	6.4583+12	5.4880-02	1.2847+03	1.1812+10	1.5175+13	5.6438-02
4.9434+04	1.3397+08	6.6223+12	5.4718-02	1.2574+03	1.0286+10	1.2934+13	5.6514-02
4.7990+04	1.3211+08	6.3402+12	5.6592-02	1.2280+03	1.0614+10	1.3034+13	5.6760-02
4.6609+04	1.4492+08	6.7546+12	5.5127-02	1.1996+03	1.1604+10	1.3920+13	5.4951-02
4.5286+04	1.3647+08	6.1803+12	5.8374-02	1.1721+03	1.1219+10	1.3149+13	5.7585-02
4.4019+04	1.7155+08	7.5515+12	5.2651-02	1.1457+03	1.1234+10	1.2570+13	5.9108-02
4.2805+04	1.5750+08	6.7419+12	5.6592-02	1.1201+03	1.2242+10	1.3712+13	5.7259-02
4.1640+04	1.6795+08	6.9938+12	5.6062-02	1.0953+03	1.2770+10	1.3987+13	5.7091-02
3.9963+04	1.5310+08	6.1215+12	4.3610-02	1.0714+03	1.2554+10	1.3430+13	5.9108-02
3.8416+04	1.6509+08	7.1437+12	5.7983-02	1.0482+03	1.3803+10	1.4459+13	5.6842-02
3.7425+04	1.5990+08	7.1069+12	5.9583-02	1.0236+03	1.3451+10	1.3758+13	5.4141-02
3.6012+04	2.0619+08	7.4252+12	4.4624-02	9.9769+02	1.4211+10	1.4178+13	5.3721-02
3.4244+04	2.0182+08	6.9110+12	4.7550-02	9.7278+02	1.4081+10	1.3698+13	5.5379-02
3.2603+04	2.0734+08	6.7598+12	4.3774-02	9.4878+02	1.5222+10	1.4442+13	5.4000-02
3.1074+04	2.1456+08	6.6712+12	4.3407-02	9.2566+02	1.4990+10	1.3876+13	5.5912-02
3.0000+04	2.4336+08	7.3007+12	5.8571-02	9.0519+02	1.6374+10	1.4922+13	5.9016-02
2.8983+04	2.2962+08	6.6551+12	4.4024-02	8.8718+02	1.7298+10	1.5347+13	5.8119-02
2.7701+04	2.4139+08	6.8868+12	4.4450-02	8.6799+02	1.6865+10	1.4639+13	5.5155-02
2.6503+04	2.5240+08	6.6895+12	4.5022-02	8.4774+02	1.7096+10	1.4493+13	5.5999-02
2.5381+04	2.9953+08	7.6024+12	4.2471-02	8.2820+02	1.7670+10	1.4634+13	5.6067-02
2.4329+04	2.8284+08	6.8619+12	4.5570-02	8.0932+02	1.7206+10	1.3925+13	5.8453-02
2.3341+04	3.2345+08	7.5496+12	4.3651-02	7.9257+02	1.9634+10	1.5562+13	5.9956-02
2.2412+04	3.0522+08	6.8405+12	4.6728-02	7.7635+02	1.7739+10	1.3771+13	5.9801-02
2.1537+04	3.4532+08	7.4372+12	4.5112-02	7.5921+02	1.8941+10	1.4381+13	5.8453-02
2.0712+04	3.4090+08	7.0603+12	4.7082-02	7.4263+02	2.0858+10	1.5490+13	5.6067-02
1.9934+04	3.6657+08	7.3072+12	4.6776-02	7.2658+02	2.0525+10	1.4913+13	5.7937-02
1.9199+04	3.3671+08	6.4645+12	5.0928-02	7.1105+02	2.2498+10	1.6282+13	5.5081-02
1.8504+04	4.2725+08	7.9061+12	4.5947-02	6.9479+02	1.9865+10	1.3502+13	5.7493-02
1.7846+04	4.1764+08	7.4533+12	4.8140-02	6.7789+02	2.1578+10	1.4627+13	5.5698-02
1.7223+04	4.9111+08	8.4584+12	4.5340-02	6.6160+02	2.1139+10	1.3985+13	5.7987-02
1.6631+04	4.5442+08	8.0565+12	4.7134-02	6.4589+02	2.1829+10	1.4009+13	5.8155-02
1.6070+04	4.9212+08	7.9083+12	4.8195-02	6.3179+02	2.4667+10	1.5594+13	5.9072-02
1.5536+04	5.0108+08	7.7347+12	4.9154-02	6.1815+02	2.4205+10	1.4962+13	5.6694-02
1.5029+04	5.2938+08	7.9561+12	4.9038-02	6.0495+02	2.7054+10	1.6366+13	5.8022-02
1.4540+04	5.0745+08	8.2542+12	4.8527-02	5.9217+02	2.4142+10	1.4296+13	5.9364-02
1.4080+04	5.7440+08	8.0910+12	4.9506-02	5.7792+02	2.5294+10	1.4618+13	5.5200-02
1.3647+04	6.3165+08	8.2107+12	4.9606-02	5.6417+02	2.5971+10	1.4452+13	5.9364-02
1.3229+04	5.8709+08	7.7666+12	5.1651-02	5.5178+02	2.7137+10	1.4974+13	5.9012-02
1.2830+04	6.4721+08	8.3037+12	5.0110-02	5.3980+02	2.9287+10	1.5809+13	5.7250-02
1.2448+04	6.5241+08	8.1212+12	5.1253-02	5.2739+02	2.6463+10	1.3956+13	5.8948-02

1.2063+04	8.1035+08	7.3748+12	5.4718-02	5.1539+02	2.9732+10	1.5324+13	5.9453-02
1.1734+04	7.8142+08	8.5824+12	5.0545-02	5.0381+02	3.0473+10	1.5352+13	5.6002-02
1.1400+04	7.4537+08	8.4972+12	5.1385-02	4.9188+02	2.8650+10	1.4093+13	5.9995-02
1.1060+04	7.8826+08	8.7339+12	5.1057-02	4.8106+02	3.2925+10	1.5839+13	5.9542-02
1.0773+04	8.1904+08	8.8300+12	5.1253-02	4.7061+02	3.2049+10	1.5083+13	5.8111-02
1.0479+04	8.4097+08	8.8126+12	5.1786-02	4.6049+02	3.4802+10	1.6026+13	5.9994-02
1.0197+04	8.2759+08	8.4390+12	5.3638-02	4.5006+02	3.0550+10	1.3749+13	5.9485-02
9.9256+03	8.8636+08	8.7977+12	5.2631-02	4.3997+02	3.8055+10	1.6743+13	5.9187-02
9.6053+03	8.5994+08	8.4082+12	5.4716-02	4.3082+02	3.7507+10	1.6159+13	5.7148-02
9.4150+03	9.0454+08	9.0812+12	5.2759-02	4.2137+02	3.7716+10	1.5893+13	5.8276-02
9.1743+03	9.9093+08	9.6910+12	5.3193-02	4.1167+02	3.4989+10	1.4404+13	5.9399-02
8.9428+03	9.2671+08	8.3053+12	5.6552-02	4.0122+02	3.5032+10	1.4056+13	5.7901-02
8.7159+03	1.0474+09	9.1330+12	5.3940-02	3.9116+02	3.9600+10	1.5490+13	5.7443-02
8.5052+03	9.7213+08	8.2766+12	5.7631-02	3.8197+02	3.8819+10	1.4828+13	5.9830-02
8.2984+03	1.0663+09	8.8485+12	5.5865-02	3.7311+02	4.1340+10	1.5424+13	5.8645-02
8.0950+03	1.1659+09	9.4423+12	5.4170-02	3.6455+02	4.3122+10	1.5720+13	5.8318-02
7.9067+03	1.1902+09	9.4106+12	5.4718-02	3.5673+02	4.7509+10	1.6948+13	5.9119-02
7.7216+03	1.2016+09	9.2780+12	5.5615-02	3.4916+02	4.4719+10	1.5614+13	5.9571-02
7.4980+03	1.1003+09	8.2506+12	4.9201-02	3.4098+02	4.4549+10	1.5190+13	5.8137-02
7.2850+03	1.2414+09	9.0437+12	5.7535-02	3.3268+02	4.4598+10	1.4837+13	5.9690-02
7.1206+03	1.2942+09	9.2159+12	5.7756-02	3.2429+02	4.3430+10	1.4084+13	5.9666-02
6.9621+03	1.3943+09	9.7071+12	5.6034-02	3.1583+02	4.8112+10	1.5195+13	5.7008-02
6.8026+03	1.3679+09	9.3134+12	5.7910-02	3.0770+02	4.6734+10	1.4380+13	5.9916-02
6.6562+03	1.3658+09	9.0963+12	5.9167-02	3.0023+02	5.2875+10	1.5875+13	5.9023-02
6.5166+03	1.4326+09	9.3357+12	5.8674-02	2.9302+02	5.0949+10	1.4929+13	5.9336-02
6.3775+03	1.5448+09	9.8521+12	5.7265-02	2.8608+02	5.7635+10	1.6488+13	5.8455-02
6.2429+03	1.4486+09	9.2933+12	5.9774-02	2.8000+02	6.3997+10	1.7919+13	5.8481-02
6.1125+03	1.5962+09	9.7688+12	5.8577-02	2.7321+02	5.2321+10	1.4295+13	5.7944-02
5.9861+03	2.1037+09	1.2593+13	5.6465-02	2.6636+02	6.2662+10	1.6691+13	5.9438-02
5.8538+03	1.6985+09	1.1075+13	5.0325-02	2.6034+02	6.1069+10	1.5899+13	5.9255-02
5.7263+03	1.7247+09	9.7588+12	4.9030-02	2.5397+02	6.1933+10	1.5729+13	5.7723-02
5.5179+03	1.9092+09	1.0535+13	5.7817-02	2.4783+02	6.6154+10	1.6395+13	5.9012-02
5.3530+03	1.7432+09	9.3837+12	5.1010-02	2.4192+02	6.4870+10	1.5693+13	5.8874-02
5.2273+03	1.7804+09	9.3065+12	5.1725-02	2.3621+02	7.1749+10	1.6948+13	5.8612-02
5.0783+03	1.8374+09	9.3306+12	5.2191-02	2.3070+02	6.8135+10	1.5719+13	5.9838-02
4.9356+03	2.1171+09	1.0449+13	4.9201-02	2.2493+02	6.9765+10	1.5692+13	5.8168-02
4.7986+03	1.9899+09	9.5494+12	5.2396-02	2.1915+02	7.2987+10	1.5995+13	5.7870-02
4.6676+03	1.9632+09	9.2801+12	5.3748-02				

INFINITE MEDIUM GRAPHITE SPECTRUM

5/21/66 008 R=35.6 60 DEGREES NE226

(COMPUTED 2/15/67)

ENERGY (EV)	N(E)	E*N(E)	DELTA(N)/N	ENERGY (EV)	N(E)	E*N(E)	DELTA(N)/N
1.5457+06	2.1932+06	3.3900+12	2.6933-02	8.0498+03	9.0195+08	7.2605+12	5.1784-02
1.3166+06	2.7517+06	3.6229+12	2.6617-02	7.7665+03	9.2745+08	7.2030+12	5.2702-02
1.1350+06	3.0424+06	3.4531+12	2.7528-02	7.4979+03	9.8059+08	7.3524+12	5.2702-02
9.8848+05	3.9370+06	3.8916+12	2.6721-02	7.2430+03	9.0678+08	6.5678+12	5.7479-02
8.6862+05	4.6263+06	4.0185+12	2.6665-02	7.0008+03	1.1036+09	7.7262+12	5.2369-02
7.6931+05	5.1583+06	3.9684+12	2.7569-02	6.7706+03	1.1444+09	7.7479+12	5.2905-02
6.8610+05	6.0595+06	4.1574+12	2.7435-02	6.5165+03	1.0094+09	6.5777+12	5.1824-02
6.1570+05	6.3464+06	3.9087+12	2.8844-02	6.2428+03	1.1194+09	6.9882+12	5.0679-02
5.5561+05	7.2071+06	4.0043+12	2.9565-02	6.0169+03	1.4428+09	8.6813+12	5.5834-02
5.0390+05	8.1637+06	4.1137+12	3.0653-02	5.8037+03	1.3479+09	7.8228+12	5.3579-02
4.5908+05	9.4241+06	4.3264+12	3.2760-02	5.6010+03	1.3712+09	7.6799+12	5.7224-02
4.2000+05	9.8646+06	4.1515+12	3.5659-02	5.4359+03	1.5430+09	8.3874+12	5.4609-02
3.8569+05	9.3511+06	3.6066+12	3.6475-02	5.2525+03	1.4012+09	7.3599+12	5.2200-02
3.5543+05	1.0963+07	3.8968+12	3.5369-02	5.0778+03	1.6429+09	8.3422+12	5.6073-02
3.2859+05	1.1826+07	3.8859+12	3.6308-02	4.9120+03	1.4544+09	7.1443+12	5.4556-02
3.0468+05	1.2876+07	3.9231+12	3.7221-02	4.7539+03	1.6881+09	8.0252+12	5.8896-02
2.8329+05	1.4749+07	4.1782+12	3.7119-02	4.6037+03	1.6799+09	7.7338+12	5.2976-02
2.6408+05	1.4409+07	3.8051+12	3.9215-02	4.4404+03	1.7930+09	7.9615+12	5.2649-02
2.4675+05	1.6566+07	4.0877+12	3.8773-02	4.2856+03	1.6486+09	7.0653+12	5.7806-02
2.3108+05	1.7275+07	3.9918+12	4.0339-02	4.1565+03	2.0667+09	8.5901+12	5.9079-02
2.1665+05	1.8480+07	4.0073+12	4.0904-02	4.0335+03	1.7491+09	7.0549+12	5.9189-02
2.0390+05	2.0684+07	4.2174+12	4.1352-02	3.9156+03	2.2319+09	8.7391+12	5.9736-02
1.9207+05	2.2836+07	4.3860+12	4.0568-02	3.8030+03	2.0710+09	7.8761+12	5.6272-02
1.8125+05	2.2023+07	3.9916+12	4.3793-02	3.6801+03	2.2067+09	8.1207+12	5.5963-02
1.7131+05	2.5771+07	4.4148+12	4.2521-02	3.5630+03	2.3712+09	8.4486+12	5.5210-02
1.6217+05	2.7416+07	4.4460+12	4.3960-02	3.4514+03	2.4482+09	8.4498+12	5.5963-02
1.5374+05	2.5157+07	3.8677+12	4.8528-02	3.3450+03	2.4733+09	8.2732+12	5.7556-02
1.4596+05	2.7670+07	4.0387+12	4.8985-02	3.2435+03	2.7055+09	8.7752+12	5.6117-02
1.3875+05	2.9899+07	4.1484+12	4.7975-02	3.1464+03	2.7089+09	8.5233+12	5.7974-02
1.3206+05	3.0051+07	3.9685+12	4.8870-02	3.0537+03	2.8865+09	8.8145+12	5.7473-02
1.2584+05	3.2009+07	4.0280+12	4.9395-02	2.9650+03	2.8733+09	8.5193+12	5.9640-02
1.2005+05	4.1104+07	4.9345+12	4.7075-02	2.8699+03	3.0335+09	8.7058+12	5.3369-02
1.1465+05	3.6795+07	4.2185+12	4.9816-02	2.7791+03	3.2434+09	9.0136+12	5.9011-02
1.0961+05	4.1645+07	4.5866+12	4.8360-02	2.6927+03	3.2350+09	8.7110+12	5.4858-02
1.0490+05	4.1001+07	4.3010+12	5.1144-02	2.6013+03	3.1320+09	8.1472+12	5.8370-02
1.0048+05	4.7070+07	4.7296+12	4.9694-02	2.5144+03	3.6453+09	9.1658+12	5.4510-02
9.6333+04	5.1420+07	4.9534+12	4.9999-02	2.4318+03	3.6826+09	8.9554+12	5.6239-02
9.2440+04	5.3151+07	4.9133+12	5.2159-02	2.3532+03	3.8388+09	9.0335+12	5.6694-02
8.8777+04	5.0673+07	4.4986+12	5.7451-02	2.2712+03	3.7716+09	8.5661+12	5.4653-02
8.5329+04	5.0975+07	4.3496+12	5.8890-02	2.1932+03	4.0320+09	8.8431+12	5.9302-02

8.2077+04	5.5259+07	4.5437+12	5.5684-02	2.1259+03	4.3605+09	9.2699+12	5.8122-02
7.9006+04	5.6972+07	4.5013+12	5.5684-02	2.0615+03	4.5580+09	9.3963+12	5.8287-02
7.6107+04	5.8577+07	4.4581+12	5.6284-02	1.9941+03	4.5798+09	9.1326+12	5.8200-02
7.3364+04	6.7336+07	4.9401+12	5.3609-02	1.9299+03	4.8752+09	9.4087+12	5.9916-02
7.0766+04	7.5249+07	5.3675+12	5.1745-02	1.8688+03	4.6174+09	8.6291+12	5.9060-02
6.8304+04	6.7382+07	4.6025+12	5.7267-02	1.8054+03	5.0621+09	9.1392+12	5.7618-02
6.5968+04	7.2599+07	4.7392+12	5.6725-02	1.7451+03	5.1796+09	9.0389+12	5.8895-02
6.3750+04	7.8071+07	5.0153+12	5.5769-02	1.6878+03	5.4908+09	9.2674+12	5.8731-02
6.1642+04	8.2507+07	5.0859+12	5.5854-02	1.6333+03	5.7164+09	9.3367+12	5.9393-02
5.9637+04	8.5100+07	5.2540+12	5.5433-02	1.5814+03	6.0753+09	9.6075+12	5.8977-02
5.7726+04	9.0758+07	5.2393+12	5.6198-02	1.5319+03	6.5086+09	9.9705+12	5.8247-02
5.5909+04	9.4487+07	5.3106+12	5.6459-02	1.4847+03	6.8852+09	1.0223+13	5.8088-02
5.4175+04	9.2590+07	5.0100+12	5.9090-02	1.4360+03	6.8597+09	9.8505+12	5.6166-02
5.2520+04	1.0235+08	5.3755+12	5.7451-02	1.3827+03	6.6179+09	9.1506+12	5.6596-02
5.0940+04	1.0262+08	5.2274+12	5.9090-02	1.3356+03	8.2955+09	1.1079+13	5.7618-02
4.9430+04	1.0541+08	5.2102+12	5.9910-02	1.2940+03	7.9578+09	1.0297+13	5.7101-02
4.7986+04	1.1092+08	5.2459+12	6.2872-02	1.2543+03	8.7482+09	1.0973+13	5.9647-02
4.6609+04	1.1849+08	5.2907+12	6.3498-02	1.2164+03	8.9455+09	1.0991+13	5.6521-02
4.5219+04	1.2301+08	5.2187+12	6.4833-02	1.1748+03	8.7919+09	1.0329+13	5.6044-02
3.9962+04	1.3307+08	5.3606+12	6.5546-02	1.1301+03	8.6644+09	9.7916+12	5.6116-02
3.7918+04	1.3851+08	5.2522+12	6.8115-02	1.0904+03	9.9446+09	1.0844+13	5.9916-02
3.6009+04	1.0285+08	5.6642+12	6.9509-02	1.0550+03	1.0085+10	1.0639+13	5.7742-02
3.4242+04	1.5790+08	5.4070+12	5.3830-02	1.0213+03	1.1096+10	1.1333+13	5.9750-02
3.2601+04	1.5406+08	5.0226+12	5.0711-02	9.8920+02	1.1173+10	1.1052+13	5.7815-02
3.1075+04	1.7427+08	5.4154+12	4.7692-02	9.5463+02	1.1154+10	1.0648+13	5.6928-02
2.9654+04	1.7903+08	5.3090+12	4.8659-02	9.2368+02	1.2926+10	1.1939+13	5.9833-02
2.8329+04	1.8168+08	5.1526+12	5.0220-02	8.9249+02	1.1694+10	1.0436+13	5.6445-02
2.7090+04	2.0495+08	5.5522+12	4.8714-02	8.5773+02	1.1870+10	1.0181+13	5.8367-02
2.5931+04	2.0612+08	5.3448+12	5.0587-02	8.2496+02	1.2261+10	1.0115+13	5.9467-02
2.4845+04	2.2114+08	5.4943+12	5.0464-02	7.9552+02	1.4228+10	1.1319+13	5.8425-02
2.3825+04	2.3642+08	6.1092+12	4.7955-02	7.6766+02	1.5142+10	1.1624+13	5.5166-02
2.2867+04	2.5999+08	5.9453+12	4.9393-02	7.3987+02	1.4478+10	1.0712+13	5.9467-02
2.1966+04	2.5817+08	5.2317+12	5.4128-02	7.1230+02	1.5182+10	1.0814+13	5.7365-02
2.1117+04	2.3389+08	5.9907+12	5.0525-02	6.8502+02	1.5873+10	1.0874+13	5.7976-02
2.0316+04	2.7777+08	5.6432+12	5.3176-02	6.5928+02	1.6869+10	1.1121+13	5.7839-02
1.9560+04	2.9795+08	5.6279+12	5.2893-02	6.3496+02	1.7936+10	1.1388+13	5.7635-02
1.8845+04	3.1193+08	5.6784+12	5.3464-02	6.1197+02	1.8138+10	1.1100+13	5.9612-02
1.8169+04	3.4346+08	6.2403+12	5.2272-02	5.9020+02	1.9434+10	1.1470+13	5.9030-02
1.7529+04	3.5064+08	6.1463+12	5.3464-02	5.6957+02	2.0436+10	1.1640+13	5.9246-02
1.6921+04	3.5753+08	6.0497+12	5.4460-02	5.4915+02	2.0124+10	1.1051+13	5.9989-02
1.6345+04	3.6470+08	5.9611+12	5.5854-02	5.2737+02	2.0035+10	1.0566+13	5.8717-02
1.5798+04	3.6442+08	5.7570+12	5.7336-02	5.0607+02	2.2120+10	1.1194+13	5.9040-02
1.5278+04	4.2589+08	6.5220+12	5.4128-02	4.8605+02	2.2723+10	1.1045+13	5.8585-02
1.4783+04	4.1839+08	6.1851+12	5.6522-02	4.6785+02	2.6045+10	1.2185+13	5.9269-02
1.4312+04	4.5881+08	6.5666+12	5.5050-02	4.5004+02	2.4243+10	1.0910+13	5.9029-02
1.3863+04	4.1997+08	5.8220+12	5.9936-02	4.3141+02	2.6473+10	1.1421+13	5.7873-02
1.3434+04	4.4035+08	5.9157+12	5.9936-02	4.1447+02	2.8329+10	1.1742+13	5.9526-02
1.3026+04	5.3205+08	6.9305+12	5.4815-02	3.9799+02	2.8125+10	1.1194+13	5.9042-02
1.2635+04	4.9611+08	6.2663+12	5.8956-02	3.8096+02	2.9370+10	1.1189+13	5.9465-02
1.2172+04	4.9663+08	6.0449+12	4.9359-02	3.6500+02	3.1974+10	1.1671+13	5.9171-02
1.1827+04	6.5312+08	6.6142+12	5.0547-02	3.4967+02	3.3763+10	1.1558+13	5.9979-02
9.7289+03	6.9323+08	6.7444+12	5.0667-02	2.7811+02	4.3811+10	1.2184+13	5.8934-02
9.3535+03	6.9421+08	6.4933+12	5.2702-02	2.6549+02	4.1529+10	1.1026+13	5.9647-02
8.9994+03	7.2763+08	6.5482+12	5.3110-02	2.5315+02	4.7822+10	1.2106+13	5.8830-02
8.6650+03	8.1739+08	7.0870+12	5.1217-02	2.4166+02	4.8382+10	1.1692+13	5.9183-02
8.3489+03	8.3141+08	6.9414+12	5.2635-02	2.3046+02	5.2381+10	1.2072+13	5.9898-02

INFINITE MEDIUM GRAPHITE SPECTRUM

5/21/66 009 R=35.6 60 DEGREES NE226

(COMPUTED 2/15/67)

ENERGY (EV)	N(E)	E*N(E)	DELTA(N)/N	ENERGY (EV)	N(E)	E*N(E)	DELTA(N)/N
1.3457+06	2.1551+06	3.3311+12	8.8538-02	4.0284+05	9.6681+06	3.8947+12	9.3616-02
1.3165+06	2.5200+06	3.3178+12	8.8538-02	3.4201+05	1.0765+07	3.6819+12	9.8626-02
1.1350+06	2.8991+06	3.2905+12	8.9934-02	2.8402+05	1.4376+07	4.0831+12	8.4789-02
9.0843+05	3.6301+06	3.5883+12	8.9579-02	2.2464+05	1.5808+07	3.5512+12	9.3770-02
8.3862+05	4.2913+06	3.7275+12	9.0293-02	1.6361+05	2.2636+07	3.7035+12	9.0432-02
7.3931+05	5.6174+06	4.3215+12	8.6559-02	1.1071+05	4.0194+07	4.4499+12	9.3841-02
6.3610+05	6.4267+06	4.4094+12	8.8538-02	7.4099+04	7.4431+07	5.5152+12	9.7453-02
5.3565+05	8.3151+06	3.6984+12	7.3683-02	4.4453+04	1.3335+08	5.9278+12	9.8778-02
4.3149+05	8.6466+06	4.1632+12	7.9298-02	2.1257+04	3.6080+08	7.6695+12	9.8618-02

INFINITE MEDIUM GRAPHITE SPECTRUM

5/24/66 001 R=35.6 60 DEGREES NE226

(COMPUTED 2/15/67)

ENERGY (EV)	N(E)	E*N(E)	DELTA(N)/N	ENERGY (EV)	N(E)	E*N(E)	DELTA(N)/N
1.3977+06	1.8299+06	2.5576+12	7.9224-02	1.5668+05	2.0055+07	3.1422+12	9.3499-02
1.0390+06	2.4968+06	2.5942+12	8.2471-02	1.0027+05	2.7458+07	3.0003+12	9.7021-02
8.0270+05	3.2994+06	2.6485+12	8.5563-02	7.0853+04	4.4614+07	3.1611+12	9.6596-02
6.3575+05	4.3027+06	2.7484+12	8.8393-02	4.7741+04	8.5198+07	4.0675+12	9.9916-02
5.2036+05	5.8379+06	3.0378+12	9.0849-02	3.0616+04	1.2433+08	3.8066+12	9.8498-02
3.9831+05	6.6042+06	2.6305+12	8.5750-02	1.8082+04	2.4182+08	4.3726+12	9.9735-02
2.9056+05	9.5112+06	2.7638+12	9.0922-02	7.6185+03	6.1039+08	4.6503+12	9.9654-02
2.1495+05	1.2361+07	2.6569+12	9.6694-02				

INFINITE MEDIUM GRAPHITE SPECTRUM

5/20/66 003 R=50.8 0 DEGREES NE226

(COMPUTED 2/15/67)

ENERGY (EV)	N(E)	E*N(E)	DELTA(N)/N	ENERGY (EV)	N(E)	E*N(E)	DELTA(N)/N
1.7800+06	3.7236+06	6.6279+12	3.0298-02	5.6862+04	5.2313+07	2.9746+12	9.8945-02
1.4975+06	3.0959+06	4.6361+12	3.6021-02	4.5271+04	7.3593+07	3.3316+12	9.7931-02
1.2772+06	2.5827+06	3.2986+12	4.3026-02	3.6392+04	1.2069+08	4.3922+12	9.8493-02
1.1022+06	2.4424+06	2.6920+12	4.9946-02	2.9562+04	1.3434+08	3.9714+12	9.8931-02
9.6086+05	2.7609+06	2.6528+12	5.1553-02	2.3283+04	1.6572+08	3.8584+12	9.5678-02
8.4506+05	2.7644+06	2.3361+12	5.8230-02	1.8091+04	2.4715+08	4.4712+12	9.7991-02
7.4899+05	3.0130+06	2.2567+12	6.1575-02	1.4241+04	3.3310+08	4.7437+12	9.8109-02
6.6842+05	3.3152+06	2.2159+12	6.4879-02	1.1563+04	5.4000+08	6.2440+12	9.7659-02
6.0016+05	2.9269+06	1.7567+12	7.7031-02	9.6551+03	6.8879+08	6.6504+12	9.8445-02
5.4189+05	3.7132+06	2.0121+12	7.5556-02	8.0327+03	9.4732+08	7.6096+12	9.9728-02
4.9169+05	3.7181+06	1.8231+12	8.6478-02	6.6768+03	1.2557+09	8.3841+12	9.7707-02
4.4815+05	5.1105+06	2.2903+12	8.6178-02	5.4980+03	1.6272+09	8.9463+12	9.7559-02
4.1016+05	4.6129+06	1.8920+12	9.9256-02	4.4433+03	2.3246+09	1.0329+13	9.8859-02
3.7680+05	5.5764+06	2.1012+12	9.1010-02	3.7015+03	3.3730+09	1.2485+13	9.9913-02
3.4735+05	5.6728+06	1.9705+12	9.8380-02	3.1169+03	3.6412+09	1.1349+13	9.8813-02
3.2122+05	6.4882+06	2.0841+12	9.9702-02	2.5167+03	6.4251+09	1.6170+13	9.9523-02
2.8751+05	7.6684+06	2.2048+12	7.3175-02	1.9941+03	4.9551+09	9.8809+12	9.9101-02
2.4991+05	9.3256+06	2.3306+12	7.6547-02	1.5787+03	6.3420+09	1.0012+13	9.8254-02
2.1923+05	1.0462+07	2.2935+12	8.4532-02	1.2801+03	1.0924+10	1.3984+13	9.9101-02
1.9388+05	1.3542+07	2.6255+12	8.4272-02	1.0706+03	1.6522+10	1.7688+13	9.7893-02
1.7268+05	1.4699+07	2.5727+12	9.3511-02	8.9343+02	1.9005+10	1.6979+13	9.7693-02
1.5478+05	1.8658+07	2.8879+12	9.8668-02	7.2291+02	2.2477+10	1.6249+13	9.9851-02
1.3617+05	2.1194+07	2.8860+12	8.4827-02	5.7558+02	2.9701+10	1.7095+13	9.9737-02
1.1784+05	2.2972+07	2.7070+12	9.7194-02	4.4539+02	3.6033+10	1.6049+13	9.9509-02
1.0086+05	2.8981+07	2.9231+12	9.1359-02	3.4910+02	5.9647+10	2.0823+13	9.8772-02
8.5518+04	4.6598+07	3.9849+12	8.5414-02	2.7984+02	7.2198+10	2.0204+13	9.8644-02
7.0920+04	4.0468+07	2.8700+12	9.5561-02				

INFINITE MEDIUM GRAPHITE SPECTRUM

5/27/66 009 R=50.8 12 DEGREES NE226

(COMPUTED 2/15/67)

ENERGY (EV)	N(E)	E*N(E)	DELTA(N)/N	ENERGY (EV)	N(E)	E*N(E)	DELTA(N)/N
1.3282+06	1.2627+06	1.9296+12	3.4775-02	4.7659+03	6.9507+08	3.3126+12	5.9814-02
1.3017+06	1.3604+06	1.7708+12	3.7107-02	4.3905+03	7.0344+08	3.0885+12	5.7921-02
1.1221+06	1.3697+06	1.5370+12	4.0931-02	4.0223+03	8.3833+08	3.3720+12	5.6329-02
9.7726+05	1.5535+06	1.5182+12	4.2068-02	3.7134+03	9.8879+08	3.6718+12	5.7781-02
8.3874+05	1.7244+06	1.4468+12	4.3630-02	3.4663+03	1.1624+09	4.0292+12	5.9081-02
7.0055+05	1.7667+06	1.3437+12	4.7144-02	3.2435+03	1.2063+09	3.9125+12	5.8794-02
6.7828+05	2.2270+06	1.5105+12	4.5240-02	3.0300+03	1.3248+09	4.0142+12	5.9689-02
6.3867+05	2.2416+06	1.3644+12	4.8725-02	2.8170+03	1.3640+09	3.8424+12	5.7631-02
5.4925+05	2.2802+06	1.2524+12	5.3374-02	2.6161+03	1.6262+09	4.2543+12	5.8224-02
4.9813+05	2.5442+06	1.2674+12	5.5947-02	2.4443+03	1.7583+09	4.2979+12	5.9474-02
4.5363+05	3.2570+06	1.4781+12	5.7010-02	2.2816+03	1.8719+09	4.2709+12	5.9900-02
3.9622+05	3.0432+06	1.2119+12	4.5779-02	2.1213+03	2.0510+09	4.3507+12	5.7375-02
3.3808+05	3.5589+06	1.2032+12	4.6351-02	1.9714+03	2.3369+09	4.6070+12	5.6888-02
2.9061+05	4.2574+06	1.2373+12	4.8542-02	1.8368+03	2.4453+09	4.4916+12	5.9747-02
2.5247+05	5.3404+06	1.3483+12	4.7985-02	1.7155+03	2.7378+09	4.6968+12	5.9747-02
2.2138+05	5.5212+06	1.2223+12	5.3566-02	1.5973+03	2.9422+09	4.6995+12	5.7245-02
1.9370+05	6.5080+06	1.2736+12	5.4975-02	1.4907+03	3.5247+09	5.2543+12	5.8754-02
1.7425+05	8.0944+06	1.4104+12	5.4118-02	1.3981+03	3.773[illegible]+09	5.2791+12	5.9134-02
1.5613+05	9.0300+06	1.4099+12	5.8363-02	1.3138+03	4.3369+09	5.6978+12	5.8829-02
1.3731+05	9.0994+06	1.3318+12	5.0787-02	1.2369+03	4.6224+09	5.7174+12	5.7993-02
1.1679+05	1.2358+07	1.4680+12	5.0178-02	1.1613+03	4.9123+09	5.5885+12	5.8709-02
1.0378+05	1.3994+07	1.4523+12	5.3163-02	1.0923+03	5.7589+09	6.2904+12	5.7501-02
9.1446+04	1.7582+07	1.6078+12	5.5886-02	1.0293+03	5.9045+09	6.0775+12	5.8494-02
8.1186+04	1.8563+07	1.5070+12	5.9855-02	9.6960+02	6.3359+09	6.1433+12	5.9663-02
7.1299+04	1.9054+07	1.3585+12	5.5324-02	9.1124+02	6.5794+09	5.9954+12	5.8319-02
6.2022+04	2.3764+07	1.4739+12	5.5476-02	8.5623+02	7.4460+09	6.3765+12	5.8951-02
5.4444+04	2.8676+07	1.5613+12	5.6186-02	8.0916+02	8.3379+09	6.7467+12	5.9738-02
4.8175+04	3.1554+07	1.5201+12	5.9952-02	7.6169+02	7.8483+09	5.9780+12	5.9532-02
4.2354+04	3.7446+07	1.5860+12	5.4553-02	7.1812+02	9.9806+09	7.167[illegible]12	5.9889-02
3.7025+04	5.0541+07	1.8713+12	5.6044-02	6.8069+02	9.9317+09	6.7404[illegible]12	5.9475-02
3.2642+04	5.3105+07	1.7334+12	5.9484-02	6.4169+02	1.0396+10	6.6[illegible]3+12	5.8373-02
2.8994+04	5.9615+07	1.7285+12	5.7821-02	6.0490+02	1.1412+10	6.903[illegible]	5.9821-02
2.5925+04	7.8725+07	2.0409+12	5.3847-02	5.7212+02	1.2884+10	7.37[illegible]+12	5.8158-02
2.3087+04	7.8543+07	1.8133+12	5.5543-02	5.4194+02	1.3630+10	7.3868+12	5.9395-02
2.0685+04	1.0069+08	2.0826+12	5.3382-02	5.1176+02	1.3622+10	6.9713+12	5.8557-02
1.8500+04	1.1796+08	2.1587+12	5.4329-02	4.8327+02	1.5698+10	[illegible]5865+12	5.9117-02
1.6546+04	1.2612+08	2.0741+12	5.829[illegible]02	4.5909+02	1.7535+10	8.0[illegible]99+12	5.9254-02
1.4861+04	1.4741+08	2.1906+12	5.8376-0[illegible]	4.3548+02	1.7194+10	7.4878+12	5.9253-02
1.3494+04	1.7647+08	2.4083+12	5.6523-02	4.1360+02	2.0548+10	8.4988+12	5.9324-02
1.2218+04	1.7500+08	2.1382+12	5.9125-02	3.9337+02	2.0595+10	8.1014+12	5.7947-02
1.1111+04	2.3158+08	2.5731+12	5.8292-02	3.7119+02	1.9760+10	7.3348+12	5.8649-02
1.0151+04	2.4552+08	2.4923+12	5.7333-02	3.5079+02	2.3709+10	8.[illegible]169+12	5.9387-02
9.1902+03	2.7275+08	2.5066+12	5.5717-02	3.3247+02	2.3652+10	7.8636+12	5.9265-02
8.3069+03	3.2277+08	2.6812+12	5.5156-02	3.1478+02	2.6018+10	8.1899+12	5.9997-02
7.5866+03	3.9941+08	3.0310+12	5.6117-02	2.9744+02	2.5667+10	7.6344+12	5.9761-02
7.0390+03	4.6353+08	3.2628+12	5.9322-02	2.8021+02	2.9513+10	7.9897+12	5.9073-02
6.5133+03	4.5219+08	2.9453+12	5.7031-02	[illegible].6471+02	3.1992+10	8.4636+12	5.8839-02
6.0109+03	6.2904+08	3.7811+12	5.9125-02	2.5101+02	3.4737+10	8.7194+12	5.9924-02
5.5656+03	5.4154+08	3.0142+12	5.9637-02	2.3816+02	3.6775+10	8.7561+12	5.8645-02
5.1426+03	6.2464+08	3.2123+12	5.9164-02	2.2593+02	3.9808+10	8.9939+12	5.9720-02

INFINITE MEDIUM GRAPHITE SPECTRUM

5/26/66 014 P=50.3 24 DEGREES NE226

(COMPUTED 2/15/67)

ENERGY (EV)	N(E)	E*N(E)	DELTA(N)/N	ENERGY (EV)	N(E)	E*N(E)	DELTA(N)/N
1.5301+06	8.2403+05	1.2608+12	3.9842-02	7.2977+03	2.9289+08	2.1375+12	5.9531-02
1.3033+06	8.8401+05	1.1521+12	4.2759-02	6.4549+03	3.3319+08	2.1507+12	5.7142-02
1.1235+06	1.0116+06	1.1366+12	4.4007-02	5.6618+03	4.1768+08	2.3648+12	5.7449-02
9.7846+05	1.2185+06	1.1923+12	4.3840-02	5.0282+03	4.9087+08	2.4682+12	5.9809-02
8.5980+05	1.2680+06	1.0902+12	4.7169-02	4.4977+03	5.4268+08	2.4409+12	5.8467-02
7.6148+05	1.3997+06	1.0659+12	4.9024-02	4.0114+03	6.4729+08	2.5965+12	5.8402-02
6.7911+05	1.4292+06	9.7059+11	5.2967-02	3.5718+03	7.1970+08	2.5706+12	5.8149-02
6.0942+05	1.5381+06	9.3734+11	5.5117-02	3.1756+03	8.5220+08	2.7063+12	5.9350-02
5.4993+05	1.6139+06	8.8755+11	5.9580-02	2.8519+03	1.0644+09	3.0355+12	5.9427-02
4.9675+05	1.9345+06	9.6485+11	5.9992-02	2.5672+03	1.1850+09	3.0422+12	5.8368-02
4.3504+05	2.3493+06	1.0220+12	4.6932-02	2.3003+03	1.3551+09	3.1172+12	5.8669-02
3.8676+05	2.6494+06	9.7168+11	4.7181-02	2.0727+03	1.6795+09	3.4811+12	5.8186-02
3.1339+05	2.7760+06	8.6997+11	5.3668-02	1.8669+03	1.7393+09	3.2470+12	5.9586-02
2.7067+05	3.4689+06	9.3961+11	5.4033-02	1.6759+03	2.0699+09	3.4689+12	5.9709-02
2.3646+05	4.0413+06	9.5560+11	5.6298-02	1.5128+03	2.4550+09	3.7139+12	5.9465-02
2.0821+05	5.1346+06	1.0691+12	5.5250-02	1.3724+03	3.0196+09	4.1441+12	5.7485-02
1.7968+05	5.3073+06	9.5362+11	5.1479-02	1.2391+03	3.0596+09	3.7912+12	5.9290-02
1.5237+05	6.6444+06	1.0124+12	5.5005-02	1.1140+03	3.6248+09	4.0381+12	5.9632-02
1.3025+05	7.5107+06	9.8278+11	5.7367-02	1.0111+03	4.5731+09	4.6239+12	5.8838-02
1.1114+05	9.5239+06	1.0585+12	5.1344-02	9.2205+02	4.9142+09	4.5311+12	5.9460-02
9.3531+04	1.1984+07	1.1208+12	5.5642-02	8.3926+02	5.6305+09	4.7255+12	5.8678-02
7.8359+04	1.3609+07	1.0664+12	5.3794-02	7.6151+02	5.9108+09	4.5012+12	5.9993-02
6.5402+04	1.7588+07	1.1503+12	5.3794-02	6.8791+02	6.6548+09	4.5779+12	5.9781-02
5.5414+04	2.0074+07	1.1124+12	5.8762-02	6.2132+02	7.7680+09	4.8264+12	5.8757-02
4.6887+04	2.5298+07	1.1861+12	5.5430-02	5.6479+02	9.1509+09	5.1683+12	5.9865-02
3.9625+04	3.3109+07	1.3119+12	5.7131-02	5.1494+02	1.0096+10	5.1987+12	5.9122-02
3.3527+04	3.9587+07	1.3272+12	5.9721-02	4.7200+02	1.2664+10	5.9773+12	5.8233-02
2.8396+04	4.4520+07	1.2642+12	5.8780-02	4.3612+02	1.3997+10	6.1044+12	5.8236-02
2.4359+04	5.5931+07	1.3624+12	5.9012-02	4.0308+02	1.4946+10	6.0246+12	5.9834-02
2.0928+04	6.7837+07	1.4197+12	5.7535-02	3.7126+02	1.5746+10	5.8458+12	5.9813-02
1.8161+04	9.2690+07	1.6870+12	5.7365-02	3.4216+02	1.8552+10	6.3476+12	5.9173-02
1.5919+04	9.8577+07	1.5693+12	5.9914-02	3.1527+02	1.9103+10	6.0227+12	5.9648-02
1.3739+04	1.1090+08	1.5236+12	5.8531-02	2.8842+02	2.0700+10	5.9704+12	5.9541-02
1.1881+04	1.4435+08	1.7151+12	5.9536-02	2.6453+02	2.4488+10	6.4777+12	5.9693-02
1.0450+04	1.8196+08	1.9015+12	5.8727-02	2.4302+02	2.5852+10	6.2827+12	5.9846-02
9.2053+03	2.0958+08	1.9293+12	5.8392-02	2.2310+02	3.0081+10	6.7110+12	5.9416-02
8.1672+03	2.6382+08	2.1547+12	5.9165-02				

INFINITE MEDIUM GRAPHITE SPECTRUM

5/24/66 002 R=50.8 37 DEGREES NE226

(COMPUTED 2/15/67)

ENERGY (EV)	N(E)	E*N(E)	DELTA(N)/N	ENERGY (EV)	N(E)	E*N(E)	DELTA(N)/N
1.7961+06	4.7959+05	8.6139+11	5.7901-02	8.4315+03	1.8412+08	1.5524+12	9.7938-02
1.5108+06	5.2676+05	7.9583+11	6.0529-02	7.6543+03	2.1734+08	1.6635+12	9.6589-02
1.2884+06	6.6934+05	8.6237+11	5.8772-02	6.9798+03	2.6229+08	1.8307+12	9.3523-02
1.1117+06	7.5809+05	8.4277+11	6.1752-02	6.3240+03	2.6655+08	1.6857+12	9.4549-02
9.6902+05	9.3282+05	9.0392+11	5.9997-02	5.7249+03	3.4188+08	1.9572+12	9.9387-02
8.5215+05	1.1313+06	9.6400+11	5.9580-02	5.2332+03	3.8289+08	2.0037+12	9.4012-02
7.5521+05	1.1246+06	8.4934+11	6.5762-02	4.7586+03	3.8093+08	1.8127+12	9.6803-02
6.7392+05	1.1914+06	8.0293+11	6.9805-02	4.2880+03	4.1400+08	1.7752+12	9.9408-02
6.0508+05	1.4074+06	8.5159+11	6.8689-02	3.8831+03	5.3905+08	2.0932+12	9.4246-02
5.4027+05	1.4861+06	8.1182+11	7.4268-02	3.5337+03	5.6331+08	1.9906+12	9.9408-02
4.9564+05	1.6187+06	8.0231+11	7.9425-02	3.2167+03	6.7383+08	2.1675+12	9.7474-02
4.5174+05	1.9971+06	9.0218+11	8.3218-02	2.9724+03	9.0835+08	2.7000+12	9.6996-02
4.1342+05	2.3116+06	9.5567+11	8.2683-02	2.7657+03	9.1023+08	2.5174+12	9.7529-02
3.7978+05	1.9475+06	7.3964+11	9.2282-02	2.5449+03	9.5984+08	2.4427+12	9.6423-02
3.5091+05	2.2072+06	7.4362+11	6.8167-02	2.3339+03	1.0907+09	2.5456+12	9.7557-02
2.3975+05	2.4855+06	7.2017+11	7.4361-02	2.1481+03	1.2297+09	2.6415+12	9.8959-02
2.5184+05	2.7684+06	6.9720+11	7.9392-02	1.9778+03	1.3300+09	2.6306+12	9.9380-02
2.2092+05	3.5002+06	7.7327+11	7.8524-02	1.8063+03	1.4549+09	2.6281+12	9.5948-02
1.9536+05	3.6004+06	7.0337+11	8.8587-02	1.6467+03	1.6613+09	2.7357+12	9.9734-02
1.7599+05	5.0178+06	8.7305+11	8.0061-02	1.5153+03	2.0033+09	3.0356+12	9.8579-02
1.5595+05	5.1905+06	8.0945+11	9.2350-02	1.4027+03	2.2415+09	3.1442+12	9.9709-02
1.4057+05	5.4665+06	7.6842+11	9.8491-02	1.3022+03	2.5515+09	3.3225+12	9.8803-02
1.2737+05	6.0769+06	7.7401+11	9.8491-02	1.2149+03	2.9514+09	3.5856+12	9.9849-02
1.1594+05	8.0765+06	9.3639+11	9.2020-02	1.1387+03	3.4815+09	3.9644+12	9.5163-02
1.0598+05	9.6770+06	1.0256+12	8.8885-02	1.0557+03	3.2222+09	3.4017+12	9.6223-02
9.5269+04	1.0415+07	9.9248+11	8.2175-02	9.7494+02	3.8464+09	3.7501+12	9.9269-02
8.4413+04	1.0366+07	8.7505+11	9.6741-02	9.0330+02	3.9478+09	3.5660+12	9.9142-02
7.5299+04	1.1680+07	8.7948+11	9.4716-02	8.3589+02	4.7611+09	3.9797+12	9.5920-02
6.7585+04	1.4157+07	9.5679+11	9.3426-02	7.7724+02	5.1197+09	3.9792+12	9.9500-02
6.0999+04	1.5843+07	9.6640+11	9.6396-02	7.2069+02	5.3473+09	3.8538+12	9.8567-02
5.5331+04	1.8647+07	1.0318+12	9.6054-02	6.7344+02	6.8937+09	4.6425+12	9.9958-02
4.9683+04	2.2595+07	1.1226+12	8.2721-02	6.2881+02	6.4565+09	4.0599+12	9.6327-02
4.4823+04	2.4938+07	1.1178+12	9.9998-02	5.8726+02	8.4118+09	4.9399+12	9.8203-02
4.0140+04	2.5712+07	1.0321+12	8.8833-02	5.5076+02	7.9131+09	4.3582+12	9.8346-02
3.5219+04	3.2426+07	1.1420+12	9.8393-02	5.0970+02	8.1462+09	4.1521+12	9.9048-02
3.1515+04	3.6404+07	1.1473+12	9.8135-02	4.7227+02	9.6263+09	4.5462+12	9.9777-02
2.9024+04	4.7584+07	1.3898+12	9.9250-02	4.3527+02	9.2807+09	4.0396+12	9.9759-02
2.6262+04	3.9642+07	1.0411+12	9.2028-02	4.0013+02	1.1453+10	4.5827+12	9.9596-02
2.3128+04	4.6701+07	1.0801+12	9.4146-02	3.7248+02	1.3399+10	4.9910+12	9.8646-02
2.0524+04	5.3554+07	1.0991+12	9.7856-02	3.4764+02	1.4440+10	5.0200+12	9.8213-02
1.8501+04	7.3173+07	1.3538+12	9.5917-02	3.2556+02	1.6911+10	5.5056+12	9.7503-02
1.6628+04	7.7296+07	1.2953+12	8.8978-02	3.0240+02	1.5432+10	4.6665+12	9.8948-02
1.4057+04	8.2239+07	1.2054+12	9.3523-02	2.7931+02	1.8936+10	5.2891+12	9.7401-02
1.3011+04	9.8422+07	1.2806+12	9.9944-02	2.5992+02	2.0438+10	5.3123+12	9.9110-02
1.1633+04	1.1257+08	1.3095+12	9.6855-02	2.4374+02	2.4617+10	6.0002+12	9.9938-02
1.0398+04	1.3735+08	1.4268+12	9.5282-02	2.2679+02	2.2236+10	5.0429+12	9.8964-02
9.3335+03	1.5850+08	1.4794+12	9.7123-02				

INFINITE MEDIUM GRAPHITE SPECTRUM

5/17/66 002 R=20.3 0 DEGREES NE211

(COMPUTED 2/7/67)

ENERGY (EV)	N(E)	DELTA(N)/N	ENERGY (EV)	N(E)	DELTA(N)/N
2.0236+07	6.7917+04	8.5564-02	1.6701+06	1.5794+08	1.2665-02
1.5152+07	3.1505+05	6.9423-02	1.6004+06	1.5936+08	1.3045-02
1.3361+07	5.8359+05	5.4294-02	1.5349+06	1.5723+08	1.3364-02
1.1869+07	1.0463+06	4.3115-02	1.4734+06	1.5914+08	1.3646-02
1.0615+07	2.2642+06	3.1452-02	1.4156+06	1.5905+08	1.4012-02
9.5488+06	4.0259+06	2.5471-02	1.3610+06	1.5906+08	1.4436-02
8.6358+06	8.1154+06	1.9450-02	1.3096+06	1.5375+08	1.5073-02
7.8478+06	6.9982+06	2.2574-02	1.2610+06	1.5334+08	1.5366-02
7.1630+06	2.0333+07	1.4304-02	1.2151+06	1.5901+08	1.5579-02
6.5640+06	3.5415+07	1.1518-02	1.1716+06	1.5617+08	1.6223-02
6.0372+06	2.9865+07	1.3429-02	1.1305+06	1.5936+08	1.6682-02
5.5713+06	4.2440+07	1.1918-02	1.0914+06	1.5527+08	1.7513-02
5.1573+06	4.8592+07	1.1787-02	1.0544+06	1.5628+08	1.8015-02
4.7879+06	5.0100+07	1.2195-02	1.0192+06	1.6230+08	1.8419-02
4.4567+06	4.0390+07	1.4304-02	9.8571+05	1.5646+08	1.9222-02
4.1588+06	3.1539+07	1.6844-02	9.5387+05	1.5332+08	1.9825-02
3.8898+06	3.3614+07	1.6968-02	9.2355+05	1.5907+08	2.0046-02
3.6460+06	2.3155+07	2.1299-02	8.9465+05	1.6866+08	2.0087-02
3.4245+06	2.2552+07	2.2364-02	8.6708+05	1.6807+08	2.0786-02
3.2226+06	3.4891+07	1.8485-02	8.4078+05	1.7307+08	2.1174-02
3.0380+06	8.7007+07	1.2002-02	8.1565+05	1.7306+08	2.1924-02
2.8688+06	4.6387+07	1.6897-02	7.9163+05	1.7259+08	2.2730-02
2.7134+06	6.9072+07	1.4306-02	7.6865+05	1.7221+08	2.3580-02
2.5703+06	9.9026+07	1.2328-02	7.4667+05	1.7416+08	2.4300-02
2.4382+06	1.1595+08	1.1738-02	7.2561+05	1.7237+08	2.5339-02
2.3160+06	1.2824+08	1.1513-02	7.0543+05	1.7526+08	2.6078-02
2.2028+06	1.3491+08	1.1605-02	6.8608+05	1.7538+08	2.7052-02
2.0977+06	1.2933+08	1.2216-02	6.6752+05	1.7548+08	2.8111-02
2.0000+06	1.3366+08	1.2357-02	6.4970+05	1.8085+08	2.8778-02
1.9089+06	1.5500+08	1.1812-02	6.3258+05	1.7447+08	3.0465-02
1.8239+06	1.5793+08	1.2069-02	6.1613+05	1.8053+08	3.1137-02
1.7444+06	1.5451+08	1.2505-02	6.0032+05	1.9170+08	3.1695-02

INFINITE MEDIUM GRAPHITE SPECTRUM

5/27/66 001 R=20.3 30 DEGREES NE213

(COMPUTED 2/8/67)

ENERGY (EV)	N(E)	E*N(E)	DELTA(N)/N	ENERGY (EV)	N(E)	E*N(E)	DELTA(N)/N
8.6269+06	2.5715+05	2.2184+12	5.5614-02	1.4673+06	3.0446+07	4.4674+13	9.7658-03
7.8378+06	3.7884+05	2.9693+12	3.8538-02	1.4096+06	3.1007+07	4.3707+13	1.0045-02
7.1521+06	6.8147+05	4.8739+12	2.5395-02	1.3552+06	3.3043+07	4.4780+13	1.0112-02
6.5527+06	7.6840+05	5.0351+12	2.3784-02	1.3040+06	3.3854+07	4.4145+13	1.0280-02
6.0256+06	9.8710+05	5.9479+12	2.1286-02	1.2555+06	3.4713+07	4.3592+13	1.0344-02
5.5597+06	1.4575+06	8.1032+12	1.7871-02	1.2098+06	3.7936+07	4.5895+13	1.0285-02
5.1457+06	2.1333+06	1.0977+13	1.5274-02	1.1665+06	3.9257+07	4.5794+13	1.0458-02
4.7764+06	2.7373+06	1.3074+13	1.4045-02	1.1254+06	4.1267+07	4.6442+13	1.0657-02
4.4454+06	3.2624+06	1.4503+13	1.3512-02	1.0865+06	4.2480+07	4.6155+13	1.0848-02
4.1477+06	3.7629+06	1.5607+13	1.3123-02	1.0496+06	4.3663+07	4.5828+13	1.1096-02
3.8789+06	3.6038+06	1.3979+13	1.4038-02	1.0145+06	4.6710+07	4.7387+13	1.1280-02
3.6354+06	3.1314+06	1.1384+13	1.5762-02	9.8120+05	4.7439+07	4.6547+13	1.1412-02
3.4142+06	3.2180+06	1.0987+13	1.6191-02	9.4948+05	4.9732+07	4.7220+13	1.1459-02
3.2125+06	4.4950+06	1.4440+13	1.4187-02	9.1927+05	5.2270+07	4.8051+13	1.1561-02
3.0282+06	6.6398+06	2.0107+13	1.2053-02	8.9048+05	5.3855+07	4.7957+13	1.1807-02
2.8594+06	4.4921+06	1.2845+13	1.5265-02	8.6302+05	5.6199+07	4.8501+13	1.2000-02
2.7042+06	7.4476+06	2.0140+13	1.2274-02	8.3682+05	6.1056+07	5.1093+13	1.1957-02
2.5614+06	9.8646+06	2.5267+13	1.1075-02	8.1179+05	6.2071+07	5.0389+13	1.2323-02
2.4296+06	1.1413+07	2.7729+13	1.0668-02	7.8786+05	6.5591+07	5.1677+13	1.2470-02
2.3077+06	1.2907+07	2.9785+13	1.0422-02	7.6498+05	6.8051+07	5.2058+13	1.2754-02
2.1947+06	1.5279+07	3.3533+13	9.9665-03	7.4308+05	7.2298+07	5.3723+13	1.2893-02
2.0899+06	1.5105+07	3.1569+13	1.0393-02	7.2211+05	7.2593+07	5.2420+13	1.3416-02
1.9923+06	1.9217+07	3.8285+13	9.5553-03	7.0201+05	7.7865+07	5.4662+13	1.3508-02
1.9015+06	2.0402+07	3.8794+13	9.6397-03	6.8274+05	8.0882+07	5.5221+13	1.3835-02
1.8167+06	2.1939+07	3.9857+13	9.6939-03	6.6425+05	8.2010+07	5.4475+13	1.4337-02
1.7375+06	2.3669+07	4.1125+13	9.6353-03	6.4651+05	8.5424+07	5.5227+13	1.4667-02
1.6633+06	2.4735+07	4.1141+13	9.7588-03	6.2946+05	8.6148+07	5.4227+13	1.5204-02
1.5938+06	2.6730+07	4.2603+13	9.8009-03	6.1308+05	8.9678+07	5.4980+13	1.5527-02
1.5286+06	2.8053+07	4.2881+13	9.8155-03				

INFINITE MEDIUM GRAPHITE SPECTRUM

5/17/66 003 R=35.6 0 DEGREES NE211

(COMPUTED 2/7/67)

ENERGY (EV)	N(E)	DELTA(N)/N	ENERGY (EV)	N(E)	DELTA(N)/N
1.9488+07	1.7757+04	9.6082-02	1.6256+06	1.4014+07	2.0538-02
1.4144+07	7.7854+04	7.7044-02	1.5584+06	1.3406+07	2.1482-02
1.2520+07	1.1414+05	6.5787-02	1.4954+06	1.2818+07	2.2429-02
1.1160+07	2.1267+05	5.0232-02	1.4360+06	1.2444+07	2.3320-02
1.0010+07	5.9929+05	3.1723-02	1.3802+06	1.1553+07	2.4808-02
9.0290+06	1.1088+06	2.5178-02	1.3275+06	1.0909+07	2.6372-02
8.1856+06	1.6223+06	2.2292-02	1.2778+06	1.0903+07	2.6708-02
7.4550+06	1.0434+06	3.0310-02	1.2308+06	1.0226+07	2.8376-02
6.8181+06	1.0340+07	1.0202-02	1.1864+06	1.0540+07	2.8809-02
6.2595+06	6.9309+06	1.3235-02	1.1443+06	1.0582+07	2.9645-02
5.7668+06	8.2967+06	1.2938-02	1.1045+06	1.0474+07	3.1160-02
5.3301+06	9.4232+06	1.2810-02	1.0666+06	9.9325+06	3.2740-02
4.9412+06	9.7677+06	1.3241-02	1.0307+06	9.4095+06	3.5052-02
4.5933+06	7.1076+06	1.6286-02	9.9660+05	9.5481+06	3.5831-02
4.2809+06	3.1901+06	2.5476-02	9.6414+05	8.9076+06	3.7799-02
3.9994+06	3.1841+06	2.6480-02	9.3324+05	9.2260+06	3.8155-02
3.7447+06	1.7906+06	3.6796-02	9.0381+05	9.2970+06	3.9166-02
3.5136+06	1.0325+06	5.0514-02	8.7574+05	8.9365+06	4.1242-02
3.3033+06	1.2263+06	4.7775-02	8.4896+05	9.2537+06	4.1852-02
3.1113+06	4.9795+06	2.4139-02	8.2340+05	9.5079+06	4.2682-02
2.9356+06	1.2019+07	1.5886-02	7.9897+05	8.9911+06	4.5458-02
2.7743+06	3.4798+06	3.0564-02	7.7561+05	9.3014+06	4.6278-02
2.6260+06	8.2281+06	2.0448-02	7.5326+05	9.9107+06	4.6377-02
2.4892+06	1.1916+07	1.7478-02	7.3186+05	8.6979+06	5.1370-02
2.3629+06	1.3943+07	1.6601-02	7.1136+05	9.3484+06	5.1438-02
2.2460+06	1.5395+07	1.6313-02	6.9171+05	9.2624+06	5.3609-02
2.1375+06	1.5321+07	1.6789-02	6.7287+05	1.0232+07	5.3003-02
2.0367+06	1.0795+07	2.0577-02	6.5478+05	9.4842+06	5.7169-02
1.9428+06	1.6227+07	1.7221-02	6.3742+05	9.1724+06	6.0525-02
1.8553+06	1.5905+07	1.7909-02	6.2073+05	8.8284+06	6.4151-02
1.7736+06	1.5365+07	1.8690-02	6.0469+05	1.0356+07	6.1782-02
1.6972+06	1.4948+07	1.9324-02			

INFINITE MEDIUM GRAPHITE SPECTRUM

5/20/66 001 R=35.6 0 DEGREES NE213

(COMPUTED 2/8/67)

ENERGY (EV)	N(E)	DELTA(N)/N	ENERGY (EV)	N(E)	DELTA(N)/N
1.1950+07	2.5163+05	9.4567-02	1.5215+06	1.4664+07	2.1663-02
9.5358+06	8.4695+05	3.9450-02	1.4603+06	1.4261+07	2.2588-02
8.6188+06	1.7204+06	2.2897-02	1.4028+06	1.3005+07	2.4297-02
7.8280+06	1.3512+06	2.6964-02	1.3487+06	1.2201+07	2.5916-02
7.1413+06	4.1884+06	1.4471-02	1.2976+06	1.1754+07	2.7008-02
6.5411+06	1.2632+07	8.5232-03	1.2493+06	1.1732+07	2.7651-02
6.0136+06	6.4414+06	1.3009-02	1.2037+06	1.1597+07	2.8760-02
5.5473+06	1.0356+07	1.0821-02	1.1606+06	1.1349+07	3.0042-02
5.1333+06	1.0709+07	1.1316-02	1.1197+06	1.1567+07	3.1174-02
4.7640+06	1.0650+07	1.1995-02	1.0810+06	1.1401+07	3.2376-02
4.4331+06	6.2246+06	1.6631-02	1.0442+06	1.1100+07	3.4159-02
4.1356+06	2.8264+06	2.6048-02	1.0093+06	1.0345+07	3.6910-02
3.8670+06	3.3044+06	2.5098-02	9.7608+05	1.0255+07	3.8068-02
3.6238+06	1.5018+06	3.9184-02	9.4449+05	1.0305+07	3.9221-02
3.4028+06	1.0480+06	4.9066-02	9.1441+05	1.0010+07	4.1236-02
3.2014+06	2.1794+06	3.4870-02	8.8574+05	1.0418+07	4.2030-02
3.0174+06	1.1767+07	1.5427-02	8.5841+05	1.0634+07	4.3229-02
2.8488+06	6.7952+06	2.0858-02	8.3231+05	1.1022+07	4.4189-02
2.6940+06	6.0280+06	2.3093-02	8.0739+05	1.0062+07	4.8215-02
2.5514+06	1.1294+07	1.7409-02	7.8357+05	1.0841+07	4.8440-02
2.4199+06	1.4094+07	1.6057-02	7.6079+05	1.0615+07	5.1150-02
2.2983+06	1.6221+07	1.5507-02	7.3899+05	1.2244+07	4.9618-02
2.1856+06	1.6584+07	1.5877-02	7.1812+05	1.1852+07	5.2761-02
2.0810+06	1.5030+07	1.7216-02	6.9811+05	1.2509+07	5.3664-02
1.9838+06	1.4503+07	1.8128-02	6.7893+05	1.1420+07	5.8893-02
1.8932+06	1.7786+07	1.6901-02	6.6053+05	1.3648+07	5.6141-02
1.8087+06	1.7211+07	1.7923-02	6.4287+05	1.2251+07	6.2213-02
1.7297+06	1.6610+07	1.8615-02	6.2591+05	1.1653+07	6.6750-02
1.6558+06	1.5812+07	1.9684-02	6.0961+05	1.0887+07	7.2446-02
1.5865+06	1.5051+07	2.0939-02			

INFINITE MEDIUM GRAPHITE SPECTRUM

5/27/66 006 R=35.6 17 DEGREES NE213

(COMPUTED 2/8/67)

ENERGY (EV)	N(E)	E*N(E)	DELTA(N)/N	ENERGY (EV)	N(E)	E*N(E)	DELTA(N)/N
9.0169+06	1.0230+05	9.2246+11	5.6100-02	1.6897+06	4.1959+06	7.0898+12	1.2801-02
8.1725+06	1.3519+05	1.1049+12	4.0246-02	1.6183+06	4.4092+06	7.1354+12	1.3000-02
7.4414+06	1.9266+05	1.4337+12	2.9528-02	1.5514+06	4.4852+06	6.9584+12	1.3281-02
6.8041+06	4.2332+05	2.8803+12	1.7509-02	1.4885+06	4.5726+06	6.8063+12	1.3564-02
6.2454+06	3.1063+05	1.9400+12	2.1386-02	1.4294+06	4.7768+06	6.8280+12	1.3749-02
5.7528+06	5.1800+05	2.9800+12	1.6547-02	1.3737+06	5.0511+06	6.9387+12	1.3852-02
5.3162+06	6.9544+05	3.6971+12	1.4677-02	1.3212+06	5.0142+06	6.6247+12	1.4421-02
4.9275+06	8.6167+05	4.2459+12	1.3673-02	1.2717+06	5.1967+06	6.6087+12	1.4397-02
4.5800+06	8.9344+05	4.0920+12	1.4061-02	1.2249+06	5.4113+06	6.6283+12	1.4584-02
4.2679+06	6.9550+05	2.9683+12	1.6773-02	1.1807+06	5.5652+06	6.5708+12	1.4829-02
3.9867+06	7.9191+05	3.1571+12	1.6329-02	1.1388+06	5.6040+06	6.3818+12	1.5328-02
3.7324+06	5.2839+05	1.9721+12	2.1045-02	1.0990+06	5.8302+06	6.4074+12	1.5668-02
3.5017+06	4.0017+05	1.4013+12	2.5301-02	1.0614+06	6.0526+06	6.4243+12	1.5820-02
3.2917+06	5.1975+05	1.7109+12	2.2976-02	1.0256+06	6.2809+06	6.4417+12	1.6215-02
3.1001+06	1.2182+06	3.7766+12	1.5415-02	9.9163+05	6.1246+06	6.0733+12	1.6921-02
2.9247+06	1.0514+06	3.0749+12	1.7167-02	9.5930+05	6.3230+06	6.0657+12	1.7061-02
2.7638+06	9.8492+05	2.7221+12	1.8489-02	9.2853+05	6.4265+06	5.9672+12	1.7472-02
2.6159+06	1.6006+06	4.1870+12	1.5007-02	8.9922+05	6.9915+06	6.2869+12	1.7330-02
2.4795+06	2.0363+06	5.0491+12	1.3778-02	8.7127+05	7.0806+06	6.1691+12	1.7855-02
2.3534+06	2.4452+06	5.7546+12	1.3010-02	8.4461+05	7.1690+06	6.0550+12	1.8416-02
2.2368+06	2.7650+06	6.1847+12	1.2740-02	8.1915+05	7.4028+06	6.0640+12	1.8809-02
2.1286+06	3.0724+06	6.5400+12	1.2516-02	7.9483+05	7.6571+06	6.0861+12	1.9207-02
2.0281+06	3.0027+06	6.0897+12	1.3149-02	7.7157+05	8.3156+06	6.4161+12	1.9171-02
1.9346+06	3.6507+06	7.0625+12	1.2350-02	7.4932+05	8.4021+06	6.2959+12	1.9854-02
1.8473+06	3.8585+06	7.1277+12	1.2511-02	7.2802+05	8.5911+06	6.2545+12	2.0447-02
1.7659+06	3.9863+06	7.0393+12	1.2731-02				

INFINITE MEDIUM GRAPHITE SPECTRUM

5/28/66 011 R=35.6 35 DEGREES NE213

(COMPUTED 2/8/67)

ENERGY (EV)	N(E)	E*N(E)	DELTA(N)/N	ENERGY (EV)	N(E)	E*N(E)	DELTA(N)/N
9.0616+06	1.8893+04	1.7121+11	5.7973-02	1.4966+06	2.9590+06	4.4285+12	1.0993-02
8.2133+06	3.0162+04	2.4773+11	4.1719-02	1.4372+06	3.1972+06	4.5950+12	1.0961-02
7.4787+06	4.7492+04	3.5518+11	3.2484-02	1.3812+06	3.3483+06	4.6246+12	1.1097-02
6.8385+06	1.2032+05	8.2282+11	2.0033-02	1.3284+06	3.5263+06	4.6843+12	1.1244-02
6.2772+06	1.0043+05	6.3039+11	2.3066-02	1.2786+06	3.5908+06	4.5911+12	1.1330-02
5.7822+06	1.6190+05	9.3616+11	1.8850-02	1.2316+06	3.7925+06	4.6708+12	1.1379-02
5.3435+06	2.3145+05	1.2367+12	1.6384-02	1.1871+06	3.9261+06	4.6606+12	1.1568-02
4.9530+06	3.2378+05	1.6037+12	1.4446-02	1.1450+06	4.0605+06	4.6492+12	1.1751-02
4.6037+06	3.8017+05	1.7502+12	1.3969-02	1.1051+06	4.4033+06	4.8661+12	1.1824-02
4.2901+06	3.7149+05	1.5937+12	1.4872-02	1.0672+06	4.5804+06	4.8882+12	1.1892-02
4.0075+06	4.0600+05	1.6271+12	1.4805-02	1.0312+06	4.6162+06	4.7602+12	1.2379-02
3.7520+06	3.0952+05	1.1613+12	1.7822-02	9.9707+05	4.7418+06	4.7279+12	1.2629-02
3.5201+06	2.4480+05	8.6174+11	2.0997-02	9.6457+05	4.7701+06	4.6011+12	1.2893-02
3.3091+06	2.9922+05	9.9014+11	1.9694-02	9.3364+05	5.0589+06	4.7232+12	1.2922-02
3.1165+06	5.4543+05	1.6998+12	1.5011-02	9.0417+05	5.2853+06	4.7788+12	1.3081-02
2.9402+06	4.8712+05	1.4322+12	1.6464-02	8.7607+05	5.5217+06	4.8374+12	1.3270-02
2.7785+06	5.4330+05	1.5096+12	1.6185-02	8.4927+05	5.7993+06	4.9251+12	1.3439-02
2.6298+06	8.4965+05	2.2344+12	1.3397-02	8.2367+05	5.8620+06	4.8284+12	1.3881-02
2.4927+06	1.0662+06	2.6577+12	1.2393-02	7.9922+05	6.1462+06	4.9122+12	1.4084-02
2.3660+06	1.2396+06	2.9330+12	1.1892-02	7.7583+05	6.2839+06	4.8752+12	1.4496-02
2.2488+06	1.4501+06	3.2609+12	1.1448-02	7.5346+05	6.8568+06	5.1663+12	1.4440-02
2.1401+06	1.6389+06	3.5074+12	1.1152-02	7.3205+05	6.8645+06	5.0251+12	1.5039-02
2.0390+06	1.7281+06	3.5235+12	1.1280-02	7.1153+05	7.2420+06	5.1529+12	1.5258-02
1.9450+06	2.0422+06	3.9720+12	1.0744-02	6.9186+05	7.3356+06	5.0752+12	1.5815-02
1.8573+06	2.2246+06	4.1317+12	1.0704-02	6.7300+05	7.8260+06	5.2669+12	1.5971-02
1.7754+06	2.3835+06	4.2317+12	1.0731-02	6.5490+05	7.6728+06	5.0249+12	1.6837-02
1.6988+06	2.5311+06	4.2999+12	1.0736-02	6.3752+05	7.8522+06	5.0060+12	1.7351-02
1.6271+06	2.6823+06	4.3644+12	1.0844-02	6.2082+05	8.0080+06	4.9715+12	1.7875-02
1.5598+06	2.8666+06	4.4713+12	1.0845-02	6.0477+05	8.3574+06	5.0543+12	1.8288-02

INFINITE MEDIUM GRAPHITE SPECTRUM

5/21/66 010 R=35.6 60 DEGREES NE213

(COMPUTED 2/8/67)

ENERGY (EV)	N(E)	E*N(E)	DELTA(N)/N	ENERGY (EV)	N(E)	E*N(E)	DELTA(N)/N
6.4356+06	2.3858+04	1.5354+11	7.0435-02	1.3973+06	2.1146+06	2.9547+12	1.9723-02
5.9221+06	4.1114+04	2.4348+11	5.6260-02	1.3436+06	2.2141+06	2.9749+12	1.9941-02
5.4677+06	6.5341+04	3.5727+11	4.7267-02	1.2930+06	2.2898+06	2.9607+12	2.0025-02
5.0637+06	8.6551+04	4.3827+11	4.3256-02	1.2451+06	2.3663+06	2.9463+12	2.0237-02
4.7028+06	1.3626+05	6.4081+11	3.6269-02	1.1999+06	2.6049+06	3.1257+12	2.0009-02
4.3792+06	1.8149+05	7.9477+11	3.3039-02	1.1571+06	2.7101+06	3.1359+12	2.0142-02
4.0879+06	1.9886+05	8.1293+11	3.3075-02	1.1166+06	2.8254+06	3.1549+12	2.0629-02
3.8248+06	2.2812+05	8.7253+11	3.2290-02	1.0781+06	2.8646+06	3.0884+12	2.1041-02
3.5862+06	1.8173+05	6.5170+11	3.7844-02	1.0416+06	3.1914+06	3.3242+12	2.0776-02
3.3693+06	1.5457+05	5.2114+11	4.2819-02	1.0069+06	3.2312+06	3.2535+12	2.1498-02
3.1715+06	1.7608+05	5.5842+11	4.1402-02	9.7393+05	3.3241+06	3.2375+12	2.1745-02
2.9906+06	2.8079+05	8.3974+11	3.3804-02	9.4255+05	3.5639+06	3.3592+12	2.1704-02
2.8248+06	2.4511+05	6.9238+11	3.7470-02	9.1266+05	3.8858+06	3.5464+12	2.1623-02
2.6723+06	3.7097+05	9.9133+11	3.1449-02	8.8417+05	3.8082+06	3.3671+12	2.2746-02
2.5319+06	4.6823+05	1.1855+12	2.8868-02	8.5699+05	4.0859+06	3.5016+12	2.2900-02
2.4023+06	5.7343+05	1.3776+12	2.6670-02	8.3104+05	4.4576+06	3.7044+12	2.2930-02
2.2824+06	6.7385+05	1.5380+12	2.5483-02	8.0626+05	4.4595+06	3.5955+12	2.3981-02
2.1712+06	8.2215+05	1.7850+12	2.3797-02	7.8257+05	4.5640+06	3.5716+12	2.4582-02
2.0680+06	8.8281+05	1.8257+12	2.3670-02	7.5991+05	4.7893+06	3.6395+12	2.4900-02
1.9720+06	1.0804+06	2.1305+12	2.2050-02	7.3822+05	5.0128+06	3.7006+12	2.5376-02
1.8825+06	1.2048+06	2.2681+12	2.1512-02	7.1744+05	5.0961+06	3.6561+12	2.6390-02
1.7989+06	1.3060+06	2.3493+12	2.1345-02	6.9753+05	5.1771+06	3.6112+12	2.7288-02
1.7208+06	1.4825+06	2.5510+12	2.0568-02	6.7844+05	5.5696+06	3.7786+12	2.7493-02
1.6477+06	1.6083+06	2.6500+12	2.0312-02	6.6012+05	5.9304+06	3.9174+12	2.8017-02
1.5791+06	1.8372+06	2.9011+12	1.9688-02	6.4253+05	5.8253+06	3.7429+12	2.9643-02
1.5148+06	1.8347+06	2.7793+12	2.0093-02	6.2563+05	5.8181+06	3.6400+12	3.0801-02
1.4542+06	2.0722+06	3.0134+12	1.9364-02	6.0940+05	5.9333+06	3.6158+12	3.1765-02

INFINITE MEDIUM GRAPHITE SPECTRUM

5/20/66 004 R=50.8 0 DEGREES NE213

(COMPUTED 2/8/67)

ENERGY (EV)	N(E)	DELTA(N)/N	ENERGY (EV)	N(E)	DELTA(N)/N
7.7599+06	2.3785+05	4.1031-02	1.4480+06	1.3440+06	3.0538-02
7.0793+06	1.3237+06	1.1734-02	1.3910+06	1.2673+06	3.2286-02
6.4845+06	4.1930+06	6.3735-03	1.3373+06	1.2007+06	3.4393-02
5.9616+06	1.5076+06	1.1863-02	1.2866+06	1.1014+06	3.6553-02
5.4995+06	2.4800+06	9.5419-03	1.2388+06	1.1300+06	3.7076-02
5.0891+06	2.4164+06	1.0209-02	1.1936+06	1.0235+06	4.0437-02
4.7230+06	1.9231+06	1.2060-02	1.1508+06	1.0515+06	4.1149-02
4.3950+06	9.3253+05	1.8449-02	1.1103+06	1.0646+06	4.2968-02
4.1001+06	3.1684+05	3.4271-02	1.0719+06	1.0499+06	4.4513-02
3.8339+06	3.1427+05	3.5524-02	1.0354+06	9.9432+05	4.7847-02
3.5928+06	1.3485+05	5.8548-02	1.0008+06	1.0196+06	4.9097-02
3.3737+06	7.1600+04	8.7088-02	9.6787+05	1.0071+06	5.0773-02
3.1741+06	1.7498+05	5.3544-02	9.3655+05	9.5060+05	5.4230-02
2.9917+06	1.9196+06	1.6101-02	9.0672+05	1.0626+06	5.3075-02
2.8245+06	1.1548+06	2.1259-02	8.7830+05	1.1301+06	5.3452-02
2.6710+06	6.0326+05	3.0855-02	8.5119+05	1.1194+06	5.5981-02
2.5297+06	1.3089+06	2.1483-02	8.2532+05	1.1379+06	5.7815-02
2.3993+06	1.8151+06	1.8750-02	8.0061+05	1.1420+06	6.0273-02
2.2788+06	2.0613+06	1.8215-02	7.7699+05	1.3173+06	5.8303-02
2.1671+06	2.1529+06	1.8401-02	7.5441+05	1.1480+06	6.5726-02
2.0634+06	1.8189+06	2.0665-02	7.3279+05	1.1288+06	6.9565-02
1.9670+06	1.7404+06	2.1838-02	7.1209+05	1.1287+06	7.2974-02
1.8771+06	2.0905+06	2.0546-02	6.9226+05	1.2530+06	7.2215-02
1.7934+06	1.9149+06	2.2200-02	6.7324+05	1.2031+06	7.7617-02
1.7150+06	1.7839+06	2.3602-02	6.5499+05	1.3580+06	7.6265-02
1.6417+06	1.7351+06	2.4867-02	6.3748+05	1.3927+06	7.8801-02
1.5731+06	1.5208+06	2.7306-02	6.2066+05	1.3948+06	8.2422-02
1.5086+06	1.4487+06	2.8627-02	6.0450+05	1.3733+06	8.7560-02

INFINITE MEDIUM GRAPHITE SPECTRUM

5/27/66 007 R=50.8 12 DEGREES NE213

(COMPUTED 2/8/67)

ENERGY (EV)	N(E)	E*N(E)	DELTA(N)/N	ENERGY (EV)	N(E)	E*N(E)	DELTA(N)/N
8.1289+06	3.9500+04	3.2109+11	5.9493-02	1.4799+06	7.7221+05	1.1428+12	2.3452-02
7.4014+06	6.6151+04	4.8961+11	3.7530-02	1.4211+06	7.8574+05	1.1166+12	2.4076-02
6.7674+06	1.8095+05	1.2246+12	1.9109-02	1.3658+06	7.7266+05	1.0553+12	2.5172-02
6.2115+06	1.0587+05	6.5764+11	2.6656-02	1.3136+06	7.7843+05	1.0225+12	2.5895-02
5.7214+06	1.6830+05	9.1715+11	2.1570-02	1.2643+06	7.6664+05	9.6926+11	2.6590-02
5.2871+06	2.1068+05	1.1139+12	1.9280-02	1.2178+06	7.9055+05	9.6273+11	2.7092-02
4.9004+06	2.5173+05	1.2336+12	1.8184-02	1.1738+06	8.5490+05	1.0035+12	2.6857-02
4.5547+06	2.1827+05	9.9417+11	2.0529-02	1.1321+06	8.5131+05	9.6377+11	2.7957-02
4.2443+06	1.3131+05	5.5731+11	2.7990-02	1.0927+06	8.7432+05	9.5537+11	2.8589-02
3.9646+06	1.3899+05	5.5106+11	2.8269-02	1.0552+06	8.9990+05	9.4957+11	2.9104-02
3.7116+06	9.0060+04	3.3427+11	3.7211-02	1.0196+06	9.1958+05	9.3760+11	3.0033-02
3.4821+06	6.2818+04	2.1874+11	4.6976-02	9.8584+05	9.9810+05	9.8397+11	2.9597-02
3.2733+06	7.1984+04	2.3563+11	4.5351-02	9.5370+05	1.0137+06	9.6674+11	3.0128-02
3.0827+06	2.3733+05	7.3162+11	2.5141-02	9.2311+05	9.3637+05	8.6438+11	3.2447-02
2.9082+06	2.2704+05	6.6027+11	2.6542-02	8.9396+05	1.0091+06	9.0212+11	3.2345-02
2.7482+06	1.6219+05	4.4574+11	3.2955-02	8.6618+05	1.0482+06	9.0790+11	3.2899-02
2.6010+06	2.8416+05	7.3910+11	2.5602-02	8.3967+05	1.0746+06	9.0234+11	3.3730-02
2.4654+06	3.8310+05	9.4449+11	2.2776-02	8.1436+05	1.0046+06	8.1809+11	3.6292-02
2.3401+06	4.5195+05	1.0576+12	2.1679-02	7.9017+05	1.1936+06	9.4315+11	3.4461-02
2.2241+06	5.1679+05	1.1494+12	2.1078-02	7.6705+05	1.1548+06	8.8581+11	3.6509-02
2.1165+06	5.5767+05	1.1803+12	2.1003-02	7.4493+05	1.2369+06	9.2138+11	3.6729-02
2.0165+06	5.3927+05	1.0874+12	2.2168-02	7.2375+05	1.2097+06	8.7552+11	3.8794-02
1.9235+06	6.5901+05	1.2676+12	2.0744-02	7.0346+05	1.3708+06	9.6429+11	3.7894-02
1.8367+06	6.9337+05	1.2735+12	2.0984-02	6.8401+05	1.2744+06	8.7173+11	4.1110-02
1.7557+06	7.1151+05	1.2492+12	2.1442-02	6.6536+05	1.3155+06	8.7525+11	4.2226-02
1.6800+06	7.1318+05	1.1981+12	2.2129-02	6.4746+05	1.3641+06	8.8321+11	4.3317-02
1.6090+06	7.0715+05	1.1378+12	2.3118-02	6.3027+05	1.3911+06	8.7677+11	4.4717-02
1.5424+06	7.2600+05	1.1198+12	2.3440-02	6.1376+05	1.3786+06	8.4613+11	4.6914-02

INFINITE MEDIUM GRAPHITE SPECTRUM

5/28/66 013 R=50.8 24 DEGREES NE213

(COMPUTED 1/3/67)

ENERGY (EV)	N(E)	E*N(E)	DELTA(N)/N	ENERGY (EV)	N(E)	E*N(E)	DELTA(N)/N
1.2100+07	1.5166+03	1.8350+10	9.7004-02	1.5590+06	6.3408+05	9.8853+11	2.2826-02
1.0201+07	3.7277+03	3.8026+10	8.9659-02	1.4955+06	6.5392+05	9.7794+11	2.3013-02
9.1876+06	5.7200+03	5.2553+10	7.6247-02	1.4359+06	6.9274+05	9.9471+11	2.2946-02
8.3177+06	1.0931+04	9.0917+10	5.7535-02	1.3797+06	6.9307+05	9.5622+11	2.3562-02
7.5057+06	1.2862+04	9.7310+10	5.7535-02	1.3267+06	7.2010+05	9.5535+11	2.3896-02
6.9113+06	5.5465+04	3.8334+11	2.8682-02	1.2768+06	6.9819+05	8.9145+11	2.4623-02
6.3383+06	5.0634+04	3.2094+11	3.2160-02	1.2296+06	7.5283+05	9.2568+11	2.4439-02
5.8537+06	6.6956+04	3.9060+11	3.0060-02	1.1850+06	7.9056+05	9.3682+11	2.4638-02
5.3871+06	9.4585+04	5.0954+11	2.6779-02	1.1428+06	8.0735+05	9.2264+11	2.5235-02
4.9698+06	1.2583+05	6.2785+11	2.4505-02	1.1027+06	8.3137+05	9.1675+11	2.6052-02
4.6350+06	1.2813+05	5.9387+11	2.5663-02	1.0648+06	8.2663+05	8.8020+11	2.6885-02
4.3167+06	9.9876+04	4.3113+11	3.0776-02	1.0288+06	9.1516+05	9.4152+11	2.6693-02
4.0301+06	1.0556+05	4.2544+11	3.1284-02	9.9456+05	9.1606+05	9.1107+11	2.7571-02
3.7711+06	7.7237+04	2.9127+11	3.8566-02	9.6201+05	9.1382+05	8.7910+11	2.8357-02
3.5363+06	5.2765+04	1.8659+11	4.9369-02	9.3104+05	9.6116+05	8.9487+11	2.8611-02
3.3227+06	6.0550+04	2.0119+11	4.7720-02	9.0154+05	9.6961+05	8.7414+11	2.9570-02
3.1280+06	1.1558+05	3.6153+11	3.5070-02	8.7342+05	1.0237+06	8.9410+11	2.9911-02
2.9499+06	1.5667+05	4.6217+11	3.0894-02	8.4659+05	1.1164+06	9.4511+11	2.9752-02
2.7865+06	1.0639+05	2.9646+11	3.9241-02	8.2099+05	1.0395+06	8.5342+11	3.2144-02
2.6364+06	1.8935+05	4.9920+11	3.0114-02	7.9652+05	1.0979+06	8.7452+11	3.2549-02
2.4981+06	2.5966+05	6.4866+11	2.6421-02	7.7314+05	1.1371+06	8.7916+11	3.3372-02
2.3704+06	3.0049+05	7.1229+11	2.5251-02	7.5077+05	1.2747+06	9.5698+11	3.2864-02
2.2522+06	3.7708+05	8.4927+11	2.3304-02	7.2935+05	1.2338+06	8.9987+11	3.4942-02
2.1427+06	4.0483+05	8.6744+11	2.3167-02	7.0884+05	1.2833+06	9.0966+11	3.5803-02
2.0409+06	4.0662+05	8.2987+11	2.3875-02	6.8919+05	1.3176+06	9.0807+11	3.6956-02
1.9463+06	4.9513+05	9.6366+11	2.2243-02	6.7034+05	1.3513+06	9.0586+11	3.8199-02
1.8581+06	5.2165+05	9.6928+11	2.2387-02	6.5225+05	1.4428+06	9.4108+11	3.8623-02
1.7757+06	5.6400+05	1.0015+12	2.2210-02	6.3488+05	1.3879+06	8.8112+11	4.1254-02
1.6987+06	5.7816+05	9.8212+11	2.2495-02	6.1820+05	1.5524+06	9.5967+11	4.0605-02
1.6266+06	6.0148+05	9.7838+11	2.2791-02	6.0217+05	1.4403+06	8.6732+11	4.4331-02

INFINITE MEDIUM GRAPHITE SPECTRUM

5/24/66 003 R=50.8 37 DEGREES NE213

(COMPUTED 2/8/67)

ENERGY (EV)	N(E)	E*N(E)	DELTA(N)/N	ENERGY (EV)	N(E)	E*N(E)	DELTA(N)/N
7.1366+06	7.2503+03	5.1743+10	9.9517-02	1.4014+06	4.4404+05	6.2228+11	3.2782-02
6.5366+06	2.5664+04	1.6775+11	5.0297-02	1.3472+06	4.5902+05	6.1839+11	3.3472-02
6.0093+06	1.9886+04	1.1950+11	6.0768-02	1.2962+06	4.7226+05	6.1214+11	3.3756-02
5.5432+06	2.9749+04	1.6491+11	5.1290-02	1.2480+06	4.8792+05	6.0892+11	3.3989-02
5.1294+06	4.4068+04	2.2604+11	4.3594-02	1.2024+06	5.0201+05	6.0361+11	3.4655-02
4.7602+06	5.7506+04	2.7374+11	3.9735-02	1.1593+06	5.3746+05	6.2307+11	3.4470-02
4.4295+06	6.9102+04	3.0609+11	3.8001-02	1.1185+06	5.7422+05	6.4227+11	3.4823-02
4.1322+06	6.1391+04	2.5368+11	4.2219-02	1.0798+06	5.6906+05	6.1447+11	3.6020-02
3.8637+06	6.6296+04	2.5615+11	4.2557-02	1.0431+06	6.0075+05	6.2664+11	3.6423-02
3.6206+06	4.0365+04	1.4614+11	5.8056-02	1.0082+06	6.5553+05	6.6090+11	3.6184-02
3.3998+06	3.7545+04	1.2765+11	6.3214-02	9.7500+05	6.4810+05	6.3189+11	3.7272-02
3.1986+06	3.8731+04	1.2388+11	6.4629-02	9.4344+05	6.2948+05	5.9388+11	3.8994-02
3.0147+06	7.4399+04	2.2429+11	4.7104-02	9.1339+05	6.7359+05	6.1525+11	3.8896-02
2.8462+06	8.0222+04	2.2833+11	4.6795-02	8.8475+05	6.7628+05	5.9834+11	4.0223-02
2.6915+06	7.9133+04	2.1299+11	4.9095-02	8.5744+05	7.4828+05	6.4161+11	3.9620-02
2.5490+06	1.2212+05	3.1129+11	4.0551-02	8.3137+05	7.9473+05	6.6071+11	3.9870-02
2.4176+06	1.4777+05	3.5726+11	3.7962-02	8.0648+05	8.3246+05	6.7136+11	4.0419-02
2.2961+06	1.8281+05	4.1976+11	3.5318-02	7.8268+05	8.2727+05	6.4749+11	4.2210-02
2.1835+06	1.9903+05	4.3459+11	3.5122-02	7.5993+05	8.7301+05	6.6343+11	4.2745-02
2.0790+06	2.5652+05	5.3331+11	3.1888-02	7.3815+05	9.2054+05	6.7950+11	4.3341-02
1.9818+06	2.4686+05	4.8923+11	3.3737-02	7.1729+05	9.5552+05	6.8538+11	4.4348-02
1.8913+06	2.8995+05	5.4838+11	3.2200-02	6.9731+05	9.4751+05	6.6071+11	4.6491-02
1.8068+06	3.3361+05	6.0276+11	3.1274-02	6.7815+05	1.0700+06	7.2562+11	4.5475-02
1.7279+06	3.3280+05	5.7505+11	3.2134-02	6.5977+05	1.0073+06	6.6462+11	4.9094-02
1.6541+06	3.5268+05	5.8337+11	3.2284-02	6.4212+05	1.0738+06	6.8953+11	4.9633-02
1.5848+06	3.9923+05	6.3270+11	3.1537-02	6.2518+05	1.0658+06	6.6634+11	5.1906-02
1.5199+06	4.0541+05	6.1618+11	3.2035-02	6.0890+05	1.1246+06	6.8475+11	5.2760-02
1.4588+06	4.2229+05	6.1604+11	3.2470-02				

INFINITE MEDIUM GRAPHITE SPECTRUM

5/21/66 005 R=66.0 0 DEGREES NE213

(COMPUTED 2/8/67)

ENERGY (EV)	N(E)	DELTA(N)/N	ENERGY (EV)	N(E)	DELTA(N)/N
8.9309+06	7.3298+04	5.8088-02	1.7411+06	2.6532+05	4.9912-02
8.0914+06	1.3384+05	3.3787-02	1.6659+06	2.5032+05	5.2960-02
7.3649+06	3.7725+04	9.2511-02	1.5954+06	2.3127+05	5.7378-02
6.7321+06	1.4233+06	8.7249-03	1.5293+06	2.1788+05	6.0645-02
6.1774+06	9.4842+05	1.1383-02	1.4672+06	2.0905+05	6.3751-02
5.6886+06	5.8112+05	1.5800-02	1.4089+06	2.0022+05	6.7083-02
5.2556+06	6.3083+05	1.5939-02	1.3539+06	1.7258+05	7.5243-02
4.8702+06	6.3435+05	1.6649-02	1.3021+06	1.8270+05	7.4825-02
4.5257+06	3.0931+05	2.5468-02	1.2532+06	1.7807+05	7.7672-02
4.2165+06	8.3234+04	5.3612-02	1.2070+06	1.6749+05	8.3317-02
3.9380+06	5.4480+04	7.1023-02	1.1634+06	1.6408+05	8.7610-02
3.6281+06	2.5457+04	9.5142-02	1.1220+06	1.8309+05	8.6318-02
3.2047+06	3.5829+04	6.5448-02	1.0828+06	1.6125+05	9.6336-02
2.8867+06	5.3695+05	2.5161-02	1.0457+06	1.7480+05	9.5902-02
2.7276+06	7.5555+04	7.2842-02	1.0019+06	1.7017+05	8.4200-02
2.5812+06	1.3127+05	5.5986-02	9.5288+05	1.5019+05	9.5285-02
2.4463+06	2.4489+05	4.1606-02	9.0734+05	1.8137+05	9.1013-02
2.3218+06	3.1764+05	3.7511-02	8.5831+05	1.7056+05	8.8636-02
2.2065+06	3.2949+05	3.8130-02	8.0690+05	1.8581+05	9.2884-02
2.0996+06	3.1792+05	4.0163-02	7.5997+05	2.1652+05	9.3265-02
2.0002+06	2.1265+05	5.0938-02	7.1198+05	2.3956+05	8.8866-02
1.9078+06	3.0303+05	4.3721-02	6.5926+05	2.2500+05	9.8666-02
1.8216+06	3.0785+05	4.4893-02	6.0807+05	2.9820+05	9.6981-02

UNCLASSIFIED

Security Classification

DOCUMENT CONTROL DATA - R&D

(Security classification of title, body of abstract and indexing annotation must be entered when the overall report is classified)

1. ORIGINATING ACTIVITY (Corporate author)	2a. REPORT SECURITY CLASSIFICATION
General Atomic Division, General Dynamics Corp.	Unclassified
	2b. GROUP

3. REPORT TITLE

Measurements of the Neutron Angular Flux Spectrum in Graphite

4. DESCRIPTIVE NOTES (Type of report and inclusive dates)

Annual Report - October 1, 1965 to September 30, 1966

5. AUTHOR(S) (Last name, first name, initial)

Profio, A. E., Antunez, H. M., Williamson, T. G.

6. REPORT DATE	7a. TOTAL NO. OF PAGES	7b. NO. OF REFS
October 30, 1966	266	28

8a. CONTRACT OR GRANT NO.	9a. ORIGINATOR'S REPORT NUMBER(S)
DA-49-146-XZ-482	
b. PROJECT NO. 543	GA-7470
c.	9b. OTHER REPORT NO(S) (Any other numbers that may be assigned this report)
d.	

10. AVAILABILITY/LIMITATION NOTICES

Reproduction in whole or in part subject to DASA's approval is permitted for any purpose of the United States Government.

11. SUPPLEMENTARY NOTES	12. SPONSORING MILITARY ACTIVITY
	Defense Atomic Support Agency

13. ABSTRACT

Measurements of the neutron angular flux spectrum in graphite have been made to provide a standard of comparison for neutron penetration calculations. The configuration approximated a point, fission-like source in an infinite medium. The spectrum from 0.002 eV to 15 MeV was measured with an accuracy of ±10% to ±20%, and resolution of ≈ 10%, by the pulsed-source, time-of-flight method. The source spectrum and other characteristics were also measured. Spectra were obtained at angles from 0° to 60° and penetrations to 66 cm. In addition, dieaway measurements, indium subcadmium and epicadmium flux traverses, sulfur and aluminum threshold foil traverses, and a threshold foil spectrum measurement were made. Procedures, apparatus, and results are described in detail so that others can evaluate our results and use them to test transport codes and input approximations. Comparison of the time-of-flight data with a preliminary discrete-ordinates calculation indicates fairly good agreement except for detail in the carbon resonance region, where the flux oscillates strongly. Both calculations and experiment indicate the intermediate spectrum for r > 20 cm from the source is not 1/E as usually assumed. Low energy foil activation and time-of-flight results are consistent, but threshold foils give poor results.

DD FORM 1 JAN 64 1473

UNCLASSIFIED

Security Classification

14. KEY WORDS	LINK A		LINK B		LINK C	
	ROLE	WT	ROLE	WT	ROLE	WT

INSTRUCTIONS

1. **ORIGINATING ACTIVITY:** Enter the name and address of the contractor, subcontractor, grantee, Department of Defense activity or other organization *(corporate author)* issuing the report.

2a. **REPORT SECURITY CLASSIFICATION:** Enter the overall security classification of the report. Indicate whether "Restricted Data" is included. Marking is to be in accordance with appropriate security regulations.

2b. **GROUP:** Automatic downgrading is specified in DoD Directive 5200.10 and Armed Forces Industrial Manual. Enter the group number. Also, when applicable, show that optional markings have been used for Group 3 and Group 4 as authorized.

3. **REPORT TITLE:** Enter the complete report title in all capital letters. Titles in all cases should be unclassified. If a meaningful title cannot be selected without classification, show title classification in all capitals in parenthesis immediately following the title.

4. **DESCRIPTIVE NOTES:** If appropriate, enter the type of report, e.g., interim, progress, summary, annual, or final. Give the inclusive dates when a specific reporting period is covered.

5. **AUTHOR(S):** Enter the name(s) of author(s) as shown on or in the report. Enter last name, first name, middle initial. If military, show rank and branch of service. The name of the principal author is an absolute minimum requirement.

6. **REPORT DATE:** Enter the date of the report as day, month, year; or month, year. If more than one date appears on the report, use date of publication.

7a. **TOTAL NUMBER OF PAGES:** The total page count should follow normal pagination procedures, i.e., enter the number of pages containing information.

7b. **NUMBER OF REFERENCES:** Enter the total number of references cited in the report.

8a. **CONTRACT OR GRANT NUMBER:** If appropriate, enter the applicable number of the contract or grant under which the report was written.

8b, 8c, & 8d. **PROJECT NUMBER:** Enter the appropriate military department identification, such as project number, subproject number, system numbers, task number, etc.

9a. **ORIGINATOR'S REPORT NUMBER(S):** Enter the official report number by which the document will be identified and controlled by the originating activity. This number must be unique to this report.

9b. **OTHER REPORT NUMBER(S):** If the report has been assigned any other report numbers *(either by the originator or by the sponsor)*, also enter this number(s).

10. **AVAILABILITY/LIMITATION NOTICES:** Enter any limitations on further dissemination of the report, other than those imposed by security classification, using standard statements such as:

(1) "Qualified requesters may obtain copies of this report from DDC."

(2) "Foreign announcement and dissemination of this report by DDC is not authorized."

(3) "U. S. Government agencies may obtain copies of this report directly from DDC. Other qualified DDC users shall request through _____."

(4) "U. S. military agencies may obtain copies of this report directly from DDC. Other qualified users shall request through _____."

(5) "All distribution of this report is controlled. Qualified DDC users shall request through _____."

If the report has been furnished to the Office of Technical Services, Department of Commerce, for sale to the public, indicate this fact and enter the price, if known.

11. **SUPPLEMENTARY NOTES:** Use for additional explanatory notes.

12. **SPONSORING MILITARY ACTIVITY:** Enter the name of the departmental project office or laboratory sponsoring *(paying for)* the research and development. Include address.

13. **ABSTRACT:** Enter an abstract giving a brief and factual summary of the document indicative of the report, even though it may also appear elsewhere in the body of the technical report. If additional space is required, a continuation sheet shall be attached.

It is highly desirable that the abstract of classified reports be unclassified. Each paragraph of the abstract shall end with an indication of the military security classification of the information in the paragraph, represented as *(TS), (S), (C), or (U)*.

There is no limitation on the length of the abstract. However, the suggested length is from 150 to 225 words.

14. **KEY WORDS:** Key words are technically meaningful terms or short phrases that characterize a report and may be used as index entries for cataloging the report. Key words must be selected so that no security classification is required. Identifiers, such as equipment model designation, trade name, military project code name, geographic location, may be used as key words but will be followed by an indication of technical context. The assignment of links, rules, and weights is optional.

GPO 886-551